



UNIVERSITAT DE  
BARCELONA

**Neurobiological mechanisms involved  
in the antidepressant and psychotomimetic effects of  
NMDA receptor antagonists: role of the GluN2C subunit**

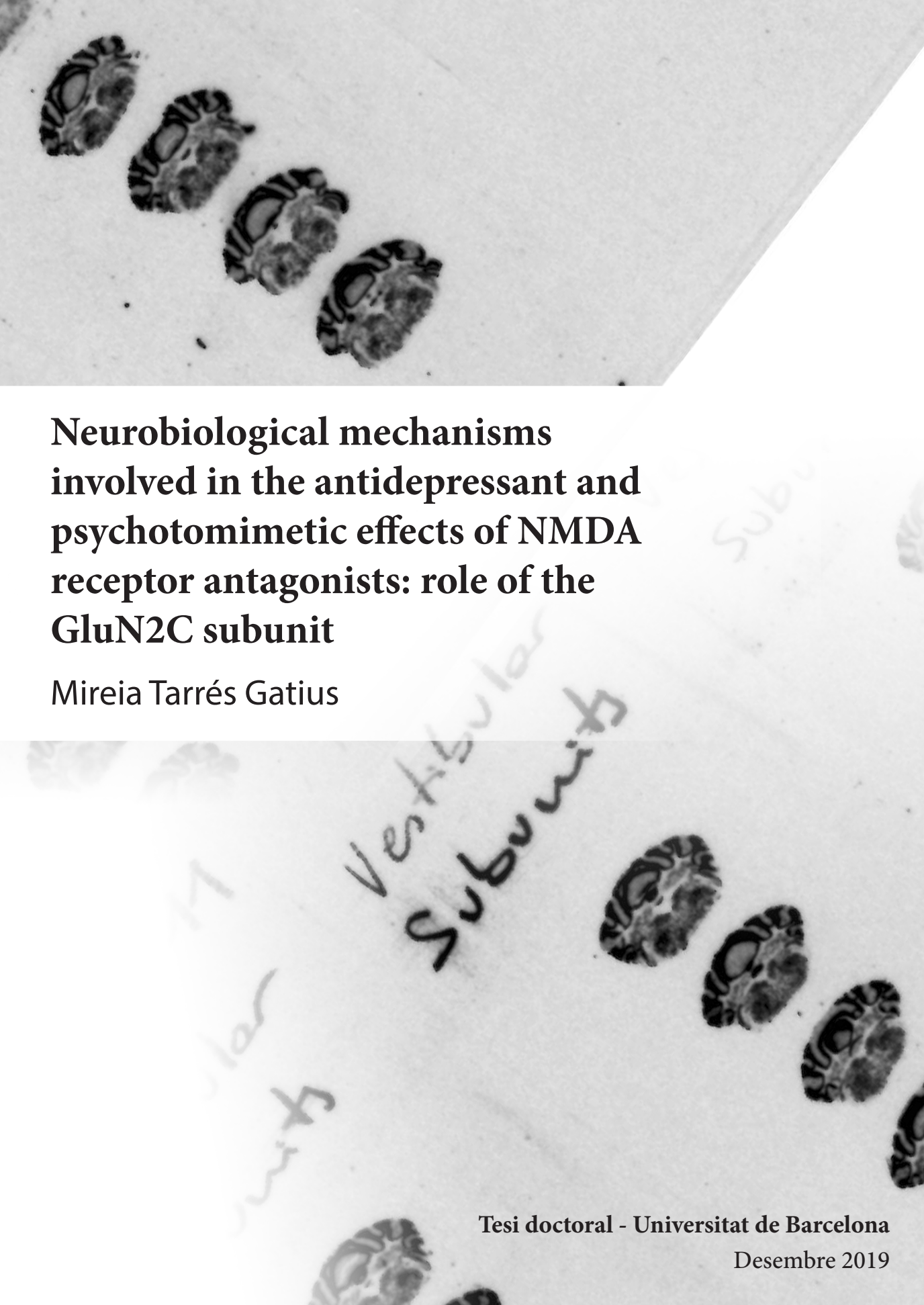
Mireia Tarrés Gatius



Aquesta tesi doctoral està subjecta a la llicència **Reconeixement- NoComercial – SenseObraDerivada 4.0. Espanya de Creative Commons.**

Esta tesis doctoral está sujeta a la licencia **Reconocimiento - NoComercial – SinObraDerivada 4.0. España de Creative Commons.**

This doctoral thesis is licensed under the **Creative Commons Attribution-NonCommercial-NoDerivs 4.0. Spain License.**



**Neurobiological mechanisms  
involved in the antidepressant and  
psychotomimetic effects of NMDA  
receptor antagonists: role of the  
GluN2C subunit**

Mireia Tarrés Gatiús

Tesi doctoral - Universitat de Barcelona

Desembre 2019



Programa de Doctorat en Biomedicina

**Neurobiological mechanisms involved in  
the antidepressant and psychotomimetic  
effects of NMDA receptor antagonists: role  
of the GluN2C subunit**

Tesi doctoral

Directors

**Anna Castañé i Francesc Artigas**

Tutor

**Carles Sindreu**

Doctorand

**Mireia Tarrés Gatius**

Institut d'Investigacions Biomèdiques de Barcelona (IIBB) – Consejo Superior de Investigaciones Científicas (CSIC): Departament de Neuroquímica i Neurofarmacologia, grup de Neurofarmacologia de sistemes

Centro de Investigación Biomédica en Red de Salud Mental (CIBERSAM)

Institut d'Investigacions Biomèdiques August Pi i Sunyer (IDIBAPS)

Universitat de Barcelona (UB)



This doctoral thesis has been financed by the following projects:

1. Alteraciones de la corteza infralímbica en depresión: mecanismo de acción de nuevas estrategias antidepresivas. Code: SAF2015-68346-P. Financed by Ministerio de Economía y Competitividad. Cofinanced by FEDER.
2. Grup d'Investigació consolidat, Neuroquímica i Neurofarmacologia. Code: 2017SGR717. Financed by Generalitat de Catalunya.

And the following fellowship:

Ajuts per a la contractació de personal investigador novell (FI). Code: 2016FI\_B 00285. Financed by Generalitat de Catalunya. Cofinanced by the European Social Fund.

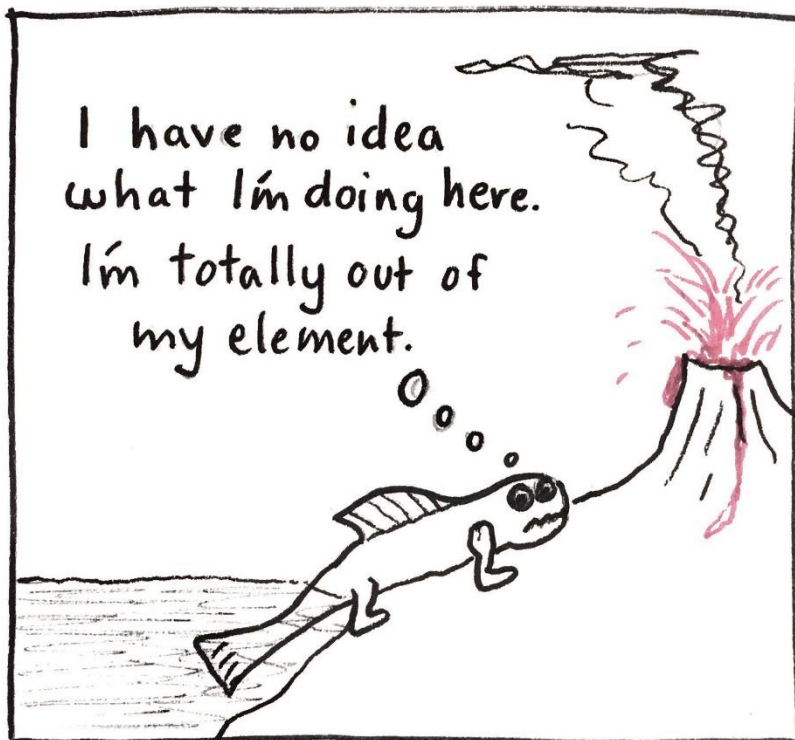
During this doctoral thesis, I have received the following recognitions after sharing my results in poster presentations:

- Best poster award.  
Poster presentation: Tarrés-Gatius M, Scorza MC, López-Hill X, Santana N, Artigas F, Castañé A. The absence of the GluN2C subunit attenuates the psychotomimetic effects induced by ketamine and other NMDA antagonists. V Laboratorio de ideas para jóvenes investigadores CIBERSAM. June 2017. Santander (Spain).
- Invitation to give a presentation at the 31<sup>st</sup> ECNP Congress during the New Findings symposium.  
Poster presentation: Tarrés-Gatius M, Scorza MC, Miquel-Rio L, López-Hill X, Santana N, Artigas F, Castañé A. Involvement of the GluN2C subunit in the behavioural syndrome induced by non-competitive NMDA antagonists. ECNP Workshop on Neuropsychopharmacology for Junior Scientists in Europe 2018. March 2018. Nice (France).

Behavioral studies were a collaboration with Dr. Cecilia Scorza from Instituto de Investigaciones Biológicas Clemente Estable (Montevideo, Uruguay).

The western blot experiments were a collaboration with Dr. Andrés Ozaita's group in the Universitat Pompeu Fabra (Barcelona, Catalunya).





The Birth of Imposter Syndrome  
@redpen blackpen





## Culpabilitzacions

Aquesta tesi era el primer pas cap a una vida idealitzada de felicitat i autorealització a partir de reconeixements científics. Lluny d'això, aquest camí m'ha portat a conèixer-me i adonar-me que la meua felicitat no rau en aconseguir grans fites professionals, sinó que està en compartir el meu temps amb qui també el vol compartir amb mi. Així doncs, aquí cito un seguit de persones que són culpables d'haver-me fet feliç i us vull fer saber que us estic molt agraïda per deixar-me formar part de la vostra vida, per haver-me escollit, per compartir el vostre temps amb mi. Sóc afortunada. Gràcies és una paraula que diem per hàbit, però vull que sapiguen que la dic amb tot el significat. GRÀCIES. De tot cor.

Als meus directors de tesi. **Anna**, gràcies per ser positiva i optimista en els moments en què jo ho veia tot negre entre tant resultat inconsistent i tanta two-way ANOVA significativa sense *post hoc*. Gràcies per ser honesta i per creure que la base de la ciència és la col·laboració i no la competició. **Paco**, gràcies per l'oportunitat de poder fer la tesi al teu grup i per tenir la porta del despatx sempre oberta. Gràcies per la passió que tens per la ciència, que et fa ser tan bon investigador i ens motiva als altres a voler-ho ser.

A la família. **Papà, Mamà, Sylvie, Adrià i Lluís**. Gràcies perquè hi heu estat, hi sou i hi estareu. Què més puc demanar? Estic orgullosa de formar part d'aquesta GRAN família (literalment i figurativament). Us estimo moltíssim i vull seguir aprenent amb vosaltres i de vosaltres, perquè encara que ens coneguem de tota la vida, queda molt a descobrir! **Mamita i Avi**, gràcies per interessar-vos pel que faig i haver seguit les peripècies de la tesi els diumenges a la tarda. **Abuelita**, et tinc present i et trobo a faltar, tan de bo hagués pogut compartir amb tu aquesta etapa de la meua vida, hauries rigut molt.

Als del laboratori i als de la cantina. Gràcies per fer del IIBB un bon lloc on treballar. Per mi és molt important l'ambient a la feina i vosaltres sou un dels

grans motius per tenir ganes de venir a treballar amb un somriure. **Maria**, no sé ni per on començar, gràcies em sembla poc. Companya de feina, companya de pis, companya de viatge... però per sobre de tot això, amiga. Hem compartit moltíssim i el que encara ens queda, segur. Gràcies per adoptar-me i crear l'oportunitat per aquesta preada relació. I'm always gonna be your safe place to land! **Lluís**, gràcies per saber compartir tan bé: des del menjar, passant pel coneixement, fins a l'afició pels horts urbans. Amb tu aprenc molt i m'encanta. Gràcies per tot l'amor que m'has donat, has aconseguit desfer una mica el meu corazón de hielo. **Júlia**, gràcies per acollir-me al grup, per ensenyar-me, per fer-me de mentora i d'exemple a seguir. Però sobretot, gràcies per continuar amb aquesta amistat fora del laboratori i a Lausanne. **Esther**, gràcies per tota l'ajuda i suport. Pels moments de plorar juntes per motius diferents, per les confidències a la sala de microdiàlisi, per pensar de forma oposada i respectar-nos igualment, per Berlin. **Sharon**, thank you for the conversations, the meta-analyses and for picking me up when I was in need of support. **Vero**, gràcies per la xocolata en els moments de necessitat, l'ajuda amb les ISH i per ser una constant d'estabilitat al laboratori. **Rubén**, gràcies per compartir les pors i nervis dels primers congressos i per ser un defensor dels drets de tots a molts nivells. **Neus**, gràcies per deixar-me conèixer-te una mica més fora de l'àmbit científic, vals la pena. **Leti**, gràcies per la rigorositat, per trobar-me sempre un forat a l'HPLC i per tenir una paraula bonica per tothom. Gràcies també a la Raquel, la Laura, en Xavi, l'Elena, en Mau, la Diana, l'Analía i la Pau, amb qui he pogut compartir riures, opinions o feina i també han col·laborat en aquesta tesi.

A la família que tries. Ja us he dit més d'una vegada que sou un gran pilar i sovint la meva brúixola per no perdre el nord i seguir tocant de peus a terra. Perquè m'escolteu, em dieu les coses que no vull sentir i m'abraceu. Gràcies per la incondicionalitat. **Guillem**, gràcies per confiar en què seria una tesi "important" i per servir-me aigua durant el sopar a Vilobí. Fora bromes,

gràcies per la sinceritat, els debats i el recolzament. **Judit**, gràcies pels mil plans genials que organitzes, per les ganes i motivació que transmetes, per tenir la ment oberta i no tenir por. **Sònia**, situ del meu cor, gràcies per aquest vincle tan íntim i proper, per entendre'ns, per ser-hi sempre i en tot moment: tant al fons del pou com al cim d'una muntanya.

**Joan**, gràcies per haver-me acompanyat (i suportat) durant un tros d'aquesta tesi. Per Bulgària, pels congressos de màgia, per ensenyar-me tant i per tot el que hem après, que ha sigut molt. Penso en tu i somric amb nostàlgia per allò perdut, però sóc feliç d'haver-ho viscut.

**Martí**, gràcies per buscar el sentit de la vida, per les reflexions, teories i anàlisis i per compartir part d'aquest camí de creixement personal. I ja saps, racional – emocional! (Espero que ho hagi llegit amb l'entonació adequada!). De res.

**Alba**, recordo amb un gran somriure el dia que per fi ens vam veure la cara a fora de SPF. El millor dels meus experiments de PPI va ser poder-te conèixer! Gràcies pels dinars a la facultat, per la gestió emocional, per compartir mil i una confidències i voler-ne seguir compartint mil i una més. Ets molt cuqui.

**Chiara**, gràcies per compartir la vida d'urbanita per Barcelona i per acompanyar-me a trobar la calma fugint-ne.

**Martí**, gràcies per la confiança que diposites en mi, per la immillorable companyia fent birres, per Ginebra.

Als de la uni, gràcies per seguir compartint la vida més de 10 anys després d'haver-nos conegut i pels retrobaments a cada casament (que no sé d'on heu tret aquesta mania tan poc sana). Especialment, gràcies **Helena, Dani i Joan**.

A tots els que formeu part d'aquestes culpabilitzacions, el meu desig és el de seguir compartint la meua vida amb vosaltres.

I res, només esperar que Déu sigui un gat, que després de tots els sacrificis...



# Index

<b>Abbreviations</b> .....	ix
<b>Introduction</b> .....	1
1. Schizophrenia and major depressive disorder: implication of glutamate neurotransmission .....	3
1.1. Glutamate neurotransmission .....	4
1.2. Schizophrenia .....	5
1.3. Major depressive disorder .....	6
2. NMDA-R: structure, distribution and genetic models .....	8
2.1. Structure of the NMDA-R .....	8
2.2. Distribution of NMDA-R subunits in the brain .....	10
2.3. Genetic models of NMDA-R subunits .....	11
3. Non-competitive NMDA-R antagonists .....	14
3.1. MK-801, PCP and ketamine .....	14
3.2. Psychotomimetic effects of non-competitive NMDA-R antagonists in rodents: a pharmacological model of schizophrenia .....	15
3.3. Non-competitive NMDA-R antagonists and depression .....	17
3.3.1. Antidepressant effects of ketamine .....	17
3.3.2. Importance of sex in depression .....	18
3.4. Mechanism of action of non-competitive NMDA-R antagonists .....	20
3.4.1. Disinhibition hypothesis .....	20
3.4.2. Direct inhibition hypothesis .....	22
4. Cerebellum .....	25
4.1. Functional architecture of the cerebellum .....	25
4.2. Cerebellum and NMDA-R subunits .....	27
4.3. Motor functions and cortico – cerebellar connectivity .....	27
4.4. Non-motor functions of the cerebellum .....	29
<b>Hypothesis and objectives</b> .....	31

<b>Methods</b> .....	35
1. Subjects .....	37
2. Drugs .....	37
3. Effects of non-competitive NMDA-R antagonists in WT and GluN2CKO mice .....	38
3.1. Behavioral studies in mice .....	38
3.2. Intracerebral microdialysis studies in mice.....	41
3.3. Molecular studies in mice .....	42
4. NMDA-R subunit distribution in male WT and GluN2CKO mice .....	43
5. Effects of ketamine in rats.....	44
5.1. Behavioral studies in rats .....	44
5.2. Molecular studies in rats.....	45
6. Statistical analysis .....	48
<b>Results</b> .....	49
1. Involvement of the GluN2C subunit in the mechanism of action of MK-801 and PCP in male mice.....	51
1.1. Behavioral syndrome .....	51
1.2. Rotarod test .....	54
1.3. Pre-pulse inhibition test.....	55
1.4. <i>In vivo</i> intracerebral microdialysis .....	55
1.5. <i>c-fos</i> and <i>zif268</i> mRNA expression.....	57
2. Involvement of the GluN2C subunit in the mechanism of action of ketamine in male and female mice .....	64
2.1. Behavioral syndrome .....	64
2.2. Antidepressant-like effect.....	66
2.3. <i>In vivo</i> intracerebral microdialysis .....	68
2.4. <i>c-fos</i> mRNA expression .....	74
3. GluN1 and GluN2A-D subunit distribution in male WT and GluN2CKO mice .....	84

4. Ketamine’s antidepressant-like effect in rats.....	88
4.1. Antidepressant-like effect.....	88
4.2. Intracellular signaling.....	89
<b>Discussion</b> .....	93
1. GluN2CKO mice are less motor impaired after acute NMDA-R blockade by MK-801 and PCP .....	97
2. Ketamine-induced antidepressant-like effects are preserved in GluN2CKO mice .....	103
3. Compensatory mechanisms in GluN2CKO mice .....	109
4. Acute ketamine administration induces rapid, but not sustained, antidepressant-like effects and activates mTOR pathway in rats .....	111
<b>Conclusions</b> .....	117
<b>Bibliography</b> .....	121
<b>Annex</b> .....	157
Article 1 .....	159
Gasull-Camós, J., <u>Tarrés-Gatius, M.</u> , Artigas, F., Castañé, A., 2017. Glial GLT-1 blockade in infralimbic cortex as a new strategy to evoke rapid antidepressant-like effects in rats. <i>Transl. Psychiatry</i> 7, e1038.	
Article 2 .....	171
Gasull-Camós, J., Martínez-Torres, S., <u>Tarrés-Gatius, M.</u> , Ozaita, A., Artigas, F., Castañé, A., 2018. Serotonergic mechanisms involved in antidepressant-like responses evoked by GLT-1 blockade in rat infralimbic cortex. <i>Neuropharmacology</i> 139, 41–51.	
Article 3 .....	185
Fullana, N., Gasull-Camós, J., <u>Tarrés-Gatius, M.</u> , Bortolozzi, A., Castañé, A., Artigas, F. Astrocyte control of glutamatergic activity: Downstream effects on serotonergic function and emotional behavior. <i>Neuropharmacology</i> (invited review, submitted).	





## Abbreviations

4/5Cb	Lobules 4 and 5 of the cerebellar vermis
5-HT	Serotonin (5-hydroxytryptamine)
aCSF	Artificial cerebrospinal fluid
Amg	Amygdala
AMPA	$\alpha$ -amino-3-hydroxy-5-methyl-4-isoxazolepropionic acid
ANOVA	Analysis of variance
AP	Anterior-posterior
APTS	3-aminopropyltriethoxysilane
BDNF	Brain-derived neurotrophic factor
Ca <sup>2+</sup>	Calcium ion
Cg	Cingulate cortex
CL	Central lateral thalamic nucleus
CM	Centromedial thalamic nucleus
CPu	Caudate-Putamen nuclei
Crus1	Crus1 of the ansiform lobule
DA	Dopamine
DCN	Deep cerebellar nuclei
DEA	Drug Enforcement Administration
Deep M1-M2	Deep layer of primary and secondary motor cortices
dHPC	Dorsal hippocampus
DV	Dorsal-ventral
DR	Dorsal raphe
DSM-5	Diagnostic and Statistical Manual of Mental Disorders 5 <sup>th</sup> edition
EC	Entorhinal cortex
FDA	Food and Drug Administration
FST	Forced swim test
GABA	$\gamma$ -aminobutyric acid
GLT-1	Glial glutamate transporter-1
Glu	Glutamate
GluN1	NMDA-R subunit 1

GluN2A-D	NMDA-R subunit 2A-D
GluN3A-B	NMDA-R subunit 3A-B
Hb	Habenula
HNK	Hydroxynorketamine
HPC	Hippocampus
HPLC	High Performance Liquid Chromatography
IMD	Intermediodorsal thalamic nucleus
I.P.	Intraperitoneal
ISH	<i>In situ</i> hybridization
K <sup>+</sup>	Potassium ion
KD	Knockdown
KO	Knockout
LN	Lateral nucleus
LTD	Long-term depression
LTP	Long-term potentiation
M1-M2	Primary and secondary motor cortices
MD	Mediodorsal thalamic nucleus
MDD	Major depressive disorder
mEPSC	miniature excitatory postsynaptic current
Mg <sup>2+</sup>	Magnesium
MGV	Mean grey values
Mid M1-M2	Intermediate layer of primary and secondary motor cortices
mIPSC	miniature inhibitory postsynaptic currents
MK-801	Dizocilpine
ML	Medial-lateral
mPFC	Medial prefrontal cortex
mTOR	Mammalian target of rapamycin
Na <sup>+</sup>	Sodium ion
NAc	Nucleus accumbens
NBQX	2,3-dihydroxy-6-nitro-7-sulfamoyl-benzo[f]quinoxaline-2,3-dione
NMDA-R	N-methyl-D-aspartate receptor
NR1	Previous nomenclature for NMDA-R subunit 1
NR2A-B	Previous nomenclature for NMDA-R subunit 2A-B

NSFT	Novelty suppressed feeding test
OB	Olfactory bulb
OB(i)	Inner part of the olfactory bulb
OB(o)	Outer part of the olfactory bulb
p70S6K	Ribosomal protein S6 kinase
PC	Paracentral thalamic nucleus
PCP	Phencyclidine
pCPA	Para-chlorophenylalanine
PFC	Prefrontal cortex
Pir	Piriform cortex
PPI	Pre-pulse inhibition
PSD95	Post synaptic density protein 95
PV	Paraventricular thalamic nucleus
qRT-PCR	Quantitative real-time polymerase chain reaction
Re/Rh	Reuniens and rhomboid nuclei of the thalamus
RSC	Retrosplenial cortex
RtN	Reticular nucleus
S.C.	Subcutaneous
S.E.M.	Standard error of the mean
Sim	Cerebellar simple lobule
SNr	Substantia nigra pars reticulata
SSRI	Selective serotonin reuptake inhibitor
TRD	Treatment-resistant depression
TST	Tail suspension test
Upper M1-M2	Upper layer of primary and secondary motor cortices
VA	Ventral anterior thalamic nucleus
Ve	Vestibular nucleus
vHPC	Ventral hippocampus
VL	Ventrolateral thalamic nucleus
WB	Western blotting
WHO	World Health Organization
WT	Wild-type



# **Introduction**



## **1. Schizophrenia and major depressive disorder: implication of glutamate neurotransmission**

The human brain is likely the most complex biological organ. Complex systems have emerging properties that cannot be predicted from the properties of the single components. Hence, complex brain functions not only arise from the properties of individual brain regions, but also from the connectivity among different brain areas (Bullmore & Sporns, 2009). This concept implies that the brain network organization is important for its healthy functioning and that dysfunctions in connectivity may lead to brain disorders. In this regard, mental disorders have been considered as “connectopathies”, with complex pathological mechanisms that apply at the level of circuits and their communication (Bargmann & Lieberman, 2014).

Indeed, psychiatric disorders, including schizophrenia and Major Depressive Disorder (MDD), that are treated as distinct categories in clinical practice, may share a common neural substrate, as it has been suggested by recent genetic and imaging studies (Cross-disorder group of the psychiatric genomics consortium, 2013; Chang et al., 2018; Sambataro et al., 2019; Tu et al., 2018). For instance, schizophrenic and depressed patients exhibited a similar pattern of thalamocortical hypoconnectivity, characterized by a decrease in thalamocortical functional connectivity with the dorsal anterior cingulate, anterior prefrontal cortex (PFC) and inferior parietal cortex (Tu et al., 2018).

Thus, whereas classical theories on schizophrenia and MDD focus on disturbances of the brainstem monoamine systems (serotonin (5-HT), dopamine (DA) and noradrenaline), more recent views suggest that these disorders involve alterations of the glutamatergic excitatory neurotransmission. Indeed, glutamate (Glu) is the main excitatory neurotransmitter in the central nervous system and dysfunction of the glutamatergic system has been implicated in the pathophysiology of

schizophrenia and MDD (Krystal et al., 2003; Réus et al., 2016). Hence, the neocortex is composed by about 80-85 % excitatory pyramidal neurons whose activity is regulated by 15-20 % local inhibitory gamma-aminobutyric acid (GABA) interneurons. Likewise, many subcortical areas, such as the thalamus, the amygdala (Amg) or the hippocampus (HPC) have also a vast majority of glutamatergic excitatory neurons. Moreover, the cerebellum, a brain structure whose role in mental disorders has been typically neglected, contains a vast majority of excitatory neurons (there are 3-4 neurons in the cerebellum to every neuron in the cerebral cortex; Herculano-Houzel, 2010).

### **1.1. Glutamate neurotransmission**

Glu was recognized as a neurotransmitter in the late 1970s and most excitatory synapses in the brain use it to carry impulses in the mammalian central nervous system (Meldrum, 2000). Glu is released into the synaptic cleft, where it binds on postsynaptic and presynaptic neural receptors and on glial cells. Glu receptors comprise the ionotropic and metabotropic receptors. Ionotropic receptors are ion channels that flux cations (calcium ( $\text{Ca}^{2+}$ ), sodium ( $\text{Na}^+$ )) and they undergo conformational changes in response to agonist or antagonist binding. Ionotropic receptors can be subdivided into *N*-methyl-D-aspartate receptors (NMDA-Rs),  $\alpha$ -amino-3-hydroxy-5-methyl-4-isoxazolepropionic acid receptors (AMPA-Rs) and kainate receptors (Traynelis et al., 2010). Metabotropic receptors activate or inhibit second messenger systems via interactions with G-proteins. To date, eight metabotropic Glu receptors have been identified (mGluR1-8) (Kim et al., 2008).

NMDA-Rs have a widespread distribution and have been implicated in neural plasticity (Lau & Zukin, 2007), cognitive function (Collingridge et al., 2013), anti-NMDA-R encephalitis (Dalmau et al., 2008, 2019), as well as in neurodegenerative diseases (Gladding & Raymond, 2011) and psychiatric



disorders, such as schizophrenia (Snyder & Gao, 2013) and MDD (Amidfar et al., 2019). NMDA-Rs are highly permeable to  $\text{Ca}^{2+}$  and they were first studied due to their role in learning and memory (Bliss & Collingridge, 1993; Volianskis et al., 2015). The  $\text{Ca}^{2+}$  influx through NMDA-Rs is essential to up-regulate and down-regulate the strength of synaptic transmission, leading to induction of long-term potentiation (LTP) and long-term depression (LTD), respectively (Lisman, 2017).

## **1.2. Schizophrenia**

Schizophrenia is a chronic psychiatric disorder characterized by positive symptoms (i.e., hallucinations and delusions, disorganized speech, disorganized or catatonic behavior), negative symptoms (i.e., avolition, social withdrawal, blunted affect), and cognitive deficits (i.e., working memory deficits, attentional deficits). This disorder affects nearly 1 % of the population (Perälä et al., 2007) with significant social and economic implications, partly because many patients have a very poor response to standard antipsychotic treatments (Howes et al., 2017).

Current pharmacotherapy of schizophrenia targets the DA system (Miyamoto et al., 2005). It was proposed that hyperactivity in the mesolimbic DA pathway was the mediator of positive symptoms, whereas hypoactivity in the mesocortical DA pathway mediated the negative and cognitive symptoms of schizophrenia (McCutcheon et al., 2019; Meltzer & Stahl, 1976; Weinberger, 1987). However, this model has been challenged by the NMDA-R hypofunction hypothesis of schizophrenia, which proposed that reduced NMDA-R activity might result in a reduced excitation of GABAergic interneurons and, subsequently, in a disinhibition of pyramidal cells, especially in the PFC (Lisman et al., 2008), leading to schizophrenic symptoms. This hypothesis arose from the observation that both acute or repeated

administration of phencyclidine (PCP) or ketamine, two non-competitive NMDA-R antagonists, induced schizophrenia-like symptoms in healthy humans or they exacerbated symptoms in schizophrenic patients (Javitt & Zukin, 1991; Lahti et al., 2001; Malhotra et al., 1996; Xu et al., 2015).

### **1.3. Major depressive disorder**

According to the *Diagnostic and Statistical Manual of Mental Disorders* (5<sup>th</sup> ed.; DSM-5), the diagnosis of MDD requires a series of symptoms including depressed mood, loss of interest or pleasure in activities, irritability, lack of energy, dysregulated sleep or appetite, inability to concentrate, feelings of guilt or worthlessness, and suicidal ideation (American Psychiatric Association, 2013). The World Health Organization (WHO, 2017) estimates to affect 322 million people, a 4.4 % worldwide prevalence, and it is more common among females (5.1 %) than males (3.6 %). MDD is predicted to be the second leading cause of illness by 2030 (Mathers & Loncar, 2006) and it has a very high socioeconomic impact (Kessler, 2012; Trautmann et al., 2016), since mood disorders are estimated to cost 113 € billion to European countries (Gustavsson et al., 2011). The public health impact of depression is partially attributable to the lack of optimal treatments.

Current standard pharmacological treatments for MDD are monoaminergic, based on the serendipitous discovery that drugs inhibiting the reuptake or metabolism of monoaminergic neurotransmitters elicited antidepressant effects (Kuhn, 1958; Wong et al., 1974). The therapeutic efficacy of these agents is limited by a delayed onset of action and low remission rates (Insel & Wang, 2009). Approximately one-third of depressed subjects are considered to have treatment-resistant depression (TRD), described as an inadequate response to adequate antidepressant therapy (Fava, 2003) or as failure to respond to one or more antidepressant treatments. However, compelling

evidence has stated the glutamatergic system as a mediator in MDD since a single administration of a sub-anesthetic dose of ketamine has been found to elicit fast-acting (within hours) and sustained (lasting up to 7 days) antidepressant effects in patients with TRD (Zarate et al., 2006a).

## 2. NMDA-R: structure, distribution and genetic models

### 2.1. Structure of the NMDA-R

NMDA-Rs are ligand-gated cation channels permeable to  $\text{Na}^+$ , potassium ( $\text{K}^+$ ) and  $\text{Ca}^{2+}$ . They were first identified in 1981 (Watkins & Evans, 1981), and they mediate excitatory signaling in the presence of glycine and Glu. NMDA-Rs exhibit particular properties that differentiate them from other ligand-gated ionotropic receptors, namely voltage-dependent blockade by magnesium ( $\text{Mg}^{2+}$ ) ions and high permeability to  $\text{Ca}^{2+}$  ions. At resting membrane potential, the pore of the NMDA-R channel is blocked by physiological levels of extracellular  $\text{Mg}^{2+}$ , which reduces  $\text{Ca}^{2+}$  influx. A depolarization of sufficient amplitude and duration is required to release the  $\text{Mg}^{2+}$  ions from the pore, thereby allowing NMDA-Rs activation. They are called coincidence detectors (Nowak et al., 1984; Tabone & Ramaswami; 2012), meaning that they need the simultaneous stimulation of presynaptic and postsynaptic neurons. Therefore, NMDA-R activation requires depolarization of the postsynaptic neuron, which allows removal of  $\text{Mg}^{2+}$ , and Glu release from the presynaptic neuron. A third element is needed, which is the presence of glycine or D-serine.

NMDA-Rs are tetrameric complexes (Figure 1) composed of two GluN1 subunits with either two GluN2 subunits (i.e., GluN2A, GluN2B, GluN2C, and GluN2D) or a combination of GluN2 and GluN3 subunits (i.e., GluN3A or GluN3B) (Ulbrich & Isacoff, 2008). A single gene encodes the GluN1 subunit (GRIN1), whereas GluN2 subunits are encoded by four different genes (GRIN2A-D) and GluN3 subunits by two different genes (GRIN3A-B). Typically, NMDA-Rs are di-heteromers comprising two GluN1 subunits and two GluN2 or GluN3 subunits. However, they can also assemble as tri-heteromers, such as GluN1/GluN2A/GluN2B or GluN1/GluN2A/GluN2C. Combinations of these subunits results in channels with unique pharmacological and biological

properties (Cull-Candy & Leszkiewicz, 2004). GluN1 and GluN3 subunits contain an agonist-binding domain that binds glycine or D-serine (Labrie & Roder, 2010) while Glu binds to the GluN2 subunit (Furukawa et al., 2005). Therefore, the activation of NMDA-Rs composed of GluN1/GluN2 subunits requires two molecules of glycine and two molecules of glutamate, while NMDA-Rs composed of GluN1/GluN3 subunits only require glycine. Most of glycine binding sites are naturally occupied because glycine is present in the extracellular environment of the nervous system (cerebrospinal fluid contains glycine; Iijima et al., 1978). On the other hand, Glu is the major excitatory neurotransmitter of the mammalian brain and it is released from presynaptic terminals of glutamatergic synapses, which make up about 90 % of cortical synapses (Santuy et al., 2018).

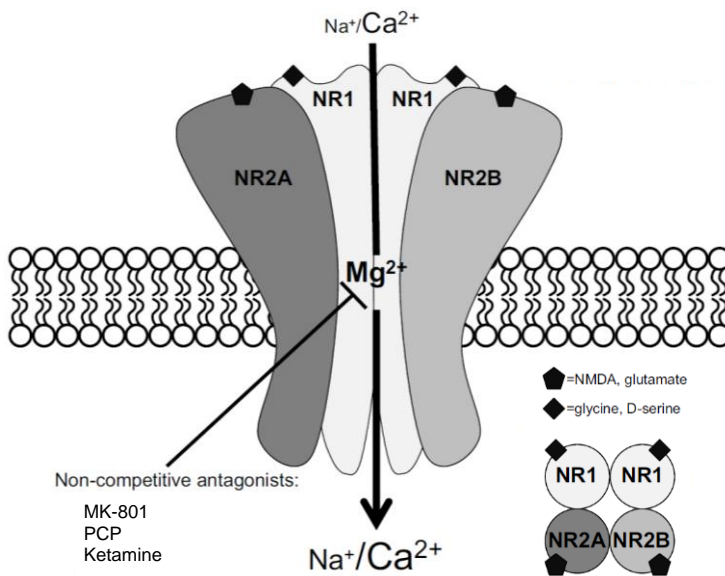


**Figure 1. NMDA receptor.** Tetramer composed of two GluN1 subunits (NR1) and two GluN2 subunits (NR2A and NR2B). At resting membrane potential, the pore is blocked by  $Mg^{2+}$ . Activation of the receptor requires two molecules of glycine that bind to GluN1 and two molecules of Glu that bind to GluN2. Within the channel, there is the PCP binding site, an allosteric site where non-competitive NMDA-R antagonists bind. Modified from Jaso et al., 2017.

## **2.2. Distribution of NMDA-R subunits in the brain**

Given that the GluN1 subunit is essential for the formation of the NMDA-R, its expression is ubiquitous throughout the central nervous system and at every developmental stage. However, GluN2 and GluN3 subunits show distinct region- and age-dependent expression patterns (Pachernegg et al., 2012; Pérez-Otaño et al., 2016; Sanz-Clemente et al., 2013).

During prenatal development, GluN2B and GluN2D are the predominant subunits, while GluN2A and GluN2C expression is more abundant after birth. In the adult brain, GluN2A and GluN2B are highly expressed in PFC and HPC and they are involved in learning and memory via regulation of LTP and LTD (Baez et al., 2018; McQuail et al., 2016). It has been reported that GluN2A is more abundant at synapses compared to extra-synaptic locations, while GluN2B is enriched at extra-synaptic locations (Groc et al., 2006). The GluN2C subunit is highly expressed in the cerebellum (Farrant et al., 1994; Karavanova et al., 2007; Monyer et al., 1994; Wenzel et al., 1997), specifically in cerebellar granule neurons (Scherzer et al., 1997; Bhattacharya et al., 2018), and in the olfactory bulb (OB) (Wenzel et al., 1997). It is also found in thalamus, including the reticular nucleus (RtN) (Hillman et al., 2011; Ravikrishnan et al., 2018; Zhang et al., 2009; Zhang et al., 2012) and in the retrosplenial cortex (RSC), pontine and vestibular (Ve) nuclei (Karavanova et al., 2007). Studies have also reported GluN2C expression in layer 4 of the somatosensory cortex (Binshtok et al., 2006) and in parvalbumin-positive neurons in globus pallidus and substantia nigra (Ravikrishnan et al., 2018). In cortex, striatum, HPC and Amg, GluN2C-expressing cells did not co-localize with parvalbumin-positive neurons, but with astrocytes (Ravikrishnan et al., 2018). In contrast, a study reported GluN2C expression in GABAergic interneurons of the PFC (Xi et al., 2009). Furthermore, the GluN2C subunit is also expressed in oligodendrocytes in the white matter of the cerebellum (Káradóttir et al., 2005). The GluN2D

subunit is highly expressed in diencephalon, mesencephalon and spinal cord (Monyer et al., 1994).

In rodents, GluN3 is abundantly expressed during neonatal stage and its expression declines during adulthood (Al-Hallaq et al., 2002; Ciabarra et al., 1995). Prenatally, GluN3A is expressed in spinal cord, medulla, pons, tegmentum, hypothalamus and thalamus, and postnatally is also found in OB, HPC, Amg, cerebral cortex and cerebellum (Ciabarra et al., 1995; Wong et al., 2002). On the other hand, GluN3B subunit is found in motoneurons of the brain stem and spinal cord (Chatterton et al., 2002; Nishi et al., 2001) and it is also expressed at low levels in forebrain regions, such as the HPC, cerebral cortex, striatum, nucleus accumbens (NAc) and cerebellum (Wee et al., 2008).

GluN2A and GluN2B subunits have high sensitivity to  $Mg^{2+}$  block, while GluN2C and GluN2D subunits display low conductance openings and weaker NMDA-R inhibition by  $Mg^{2+}$  (Cull-Candy & Leszkiewicz, 2004). GluN2C-containing receptors show relatively unique channel properties, such as low conductance levels, reduced permeability of  $Ca^{2+}$  ions and less sensitivity to extracellular  $Mg^{2+}$  blockade compared with GluN2A and GluN2B subunits (Traynelis et al., 2010). This relatively low sensitivity to  $Mg^{2+}$  block would allow the GluN2C-containing receptors to be activated by ambient Glu because they would be able to open without a depolarization (Cull-Candy et al., 2001).

### **2.3. Genetic models of NMDA-R subunits**

The development of subunit-selective drugs would facilitate the investigation of the role of NMDA-R subunits in animal behavior, however to date only GluN2B subunit-selective antagonists like ifenprodil (Carter et al., 1989) or Ro 25-6981 have been developed. Therefore, genetic models have provided current data on the role of GluN1, GluN2A, GluN2C and GluN2D subunits.

Null mutation of GRIN1 is lethal (Forrest et al., 1994). Therefore, a genetic model for the GluN1 subunit is the GluN1 knockdown (GluN1KD), which is used to reproduce the NMDA-R hypofunction hypothesis of schizophrenia (Ramsey, 2009). GluN1KD mice presented deficient sensory processing measured in the pre-pulse inhibition (PPI) paradigm, no deficits on locomotor coordination and altered social behavior (Duncan et al., 2004). Moreover, GluN1KD mice exhibited age-dependent striatal spine density deficits (Ramsey et al., 2011) and reductions in white matter volumes in substantia nigra and striatum (Intson et al., 2019).

GluN2A knockout (GluN2AKO) mice resulted in an anxiolytic- and antidepressant-like profile with normal sensory functions, as shown by a normal PPI of the startle response (Boyce-Rustay & Holmes, 2006). These mice presented impaired spatial working memory (Bannerman et al., 2008) and enhanced brain monoaminergic activity (Petrenko et al., 2013). On the other hand, GluN2A deletion decreased dendritic length and dendritic complexity in dentate granule neurons located in the inner granular zone (Kannangara et al., 2014).

Regarding the GluN2B subunit, its genetic ablation was associated with perinatal lethality, likely because of abnormal suckling behavior (Kutsuwada et al., 1996).

Studies using mice lacking the GluN2C subunit have found that this subunit plays an important role in the acquisition of conditioned fear and working memory (Hillman et al., 2011), but not in motor coordination (Kadotani et al., 1996). These mice did not exhibit deficits in PPI, though they had a significantly higher startle response (Gupta et al., 2016). Regarding oscillations of pyramidal neurons in the medial PFC (mPFC), GluN2CKO mice presented reduced miniature excitatory postsynaptic current (mEPSC) frequency and dendritic spine density and higher frequency of miniature inhibitory



postsynaptic currents (mIPSC) (Gupta et al., 2016). Likewise, GluN2CKO mice have allowed determining that burst firing in reticular thalamic neurons is controlled by NMDA-Rs containing the GluN2C subunit (Liu et al., 2019).

Concerning the GluN2D subunit, GluN2DKO mice displayed anhedonia and a depressive-like state (Yamamoto et al., 2017). The administration of ketamine did not increase locomotor activity in these mice, while wild-type (WT) mice exhibited hyperlocomotion under the same conditions (Sapkota et al., 2016). Moreover, GluN2DKO mice were less sensitive to the motor impairment induced by PCP (Yamamoto et al., 2013).

Finally, young GluN3AKO mice exhibited increased spine densities, suggesting a role of this subunit in synaptic development and neural plasticity (Das et al., 1998).

### **3. Non-competitive NMDA-R antagonists**

#### **3.1. MK-801, PCP and ketamine**

Dizocilpine (MK-801), PCP and ketamine are non-competitive NMDA-R antagonists. They bind to an allosteric site on the receptor, known as the PCP binding site (Temme et al., 2018), which is found within the ion channel (Figure 1). An allosteric site allows a molecule to activate or inhibit the receptor without competing with the endogenous ligand. Since the NMDA-R is blocked by a  $Mg^{2+}$  ion and the allosteric site is within the channel, MK-801, PCP and ketamine can only block the channel once the receptor is open. All three drugs share the ability to produce anesthesia through the blockade of NMDA-Rs (Daniell, 1990). Moreover, their pharmacological potency to elicit anesthesia parallels their affinity for the PCP binding site, which is: MK-801 > PCP > ketamine.

MK-801 was originally described as a potent anticonvulsant agent (Clineschmidt et al., 1982). Nowadays, it is mainly used as a research tool because it showed neurotoxic-like effects, called Olney's lesions, in certain brain regions of rats (Kuroda et al., 2015; Olney et al., 1989).

PCP (formerly known as CI-395) was synthesized in 1956 at the pharmaceutical company Park Davis as a surgical anesthetic. In humans, it was considered a safe compound until some patients experienced adverse effects during recovery, such as prolonged post-surgery delirium. This fact prompted its abandonment except in veterinary medicine. In the 1960s and 70s it became popularized as a recreational drug (currently classified as Schedule II hallucinogen) under the street names of angel dust, hog or belladonna among others (Bertron et al., 2018).

Ketamine is a chemical derivative of PCP and its effects on humans as a dissociative anesthetic were first described in 1965 (Domino et al., 1965).

Actually, ketamine replaced PCP in the clinical practice and is currently used as an anesthetic and analgesic (Elia & Tramèr, 2005; Hocking & Cousins, 2003). During the Vietnam War, ketamine became a widely used treatment for American troops. In 1999, because of its emergence as a club drug due to its hallucinogenic properties, the Drug Enforcement Administration (DEA) of the United States of America classified ketamine under schedule III of the Controlled Substance Use Act, a category designated for substances with a moderate to low potential for physical and psychological dependence. Later on, the antidepressant effects of ketamine were discovered and in 2000 the first placebo-controlled, double-blinded clinical trial reporting antidepressant actions was published (Berman et al., 2000).

### **3.2. Psychotomimetic effects of non-competitive NMDA-R antagonists in rodents: a pharmacological model of schizophrenia**

The administration of non-competitive NMDA-R antagonists, typically PCP but also MK-801 and ketamine, mimic some of the symptoms of schizophrenia in experimental animals, such as rodents (Lee & Zhou, 2019) and nonhuman primates (Elsworth et al., 2015), and have served as pharmacological models of this disorder. These models are intended to assess specific endophenotypes (behavioral traits) instead of modeling the disease as a whole. Moreover, they are aimed at providing tools with high predictive validity.

In rodents, the psychotomimetic effects of NMDA-R antagonists are potentially related to the positive symptoms of schizophrenia, as they are prevented or reversed by antipsychotic medications (Adell et al., 2012; Krystal et al., 2003; Moghaddam & Jackson, 2003;). In addition, non-competitive NMDA-R antagonists also produce negative and cognitive deficits of relevance to schizophrenia (Neill et al., 2010). Behaviors associated with negative

symptoms are social withdrawal and anhedonia, assessed by social interaction and sucrose preference tests. Regarding cognitive impairments, deficits in working memory, attention, visual learning and memory, reasoning and problem solving as well as social cognition have been identified using a variety of behavioral tests, such as novel object recognition test, attentional set-shifting task, Y-maze, T-maze or Morris water maze among others. Moreover, deficits in sensorimotor gating found in schizophrenics can be assessed in rodents using the PPI test (Geyer et al., 2001; Powell et al., 2012).

The effects of acute and repeated treatments have been assessed on a large number of variables, with long-term exposure to non-competitive NMDA-R antagonists more likely resembling the core symptoms of the illness. The acute administration of non-competitive NMDA-R antagonists in rodents produces psychotomimetic effects, characterized by increased locomotor activity, ataxia signs, stereotypies, as well as disorganization in the locomotor pattern and a decrease in the exploratory activity (Andiné et al., 1999; Carlsson & Carlsson, 1990; Geyer & Ellenbroek, 2003; Nilsson et al., 2001, 2006; Scorza et al., 2008; Tricklebank et al., 1989). Moreover, NMDA-R blockade produces deficits in PPI (Leung & Ma, 2017), memory (Rogóz & Kaminska, 2016; Wiescholleck & Manahan-Vaughan, 2012) and social interaction (Rung et al., 2005). When given subchronically, non-competitive NMDA-R antagonists induce a sensitization of acute locomotor effects and prolonged impairments in cognitive function, including novel object recognition, an analog of human declarative memory (Castañé et al., 2015; Meltzer et al., 2013; Szlachta et al., 2017). In addition, chronic administration also leads to decreased social interaction and PPI (Matsuoka et al., 2005; Unal et al., 2018).

In order to incorporate a neurodevelopmental element in the pathophysiology of schizophrenia (Fatemi & Folsom, 2009), non-competitive NMDA-R antagonists can also be subchronically administered during early

development, generally on the first two weeks of postnatal life. During this critical period of neurodevelopment, chronic NMDA-R blockade leads to structural, neurochemical and functional alterations in the brain that last up to adulthood. Neonatal models have been shown to cause decreased exploratory behavior and slower spatial learning (Latysheva & Rayevsky, 2003), attentional deficits (Redrobe et al., 2012) and retarded PPI (Wang et al., 2001).

### **3.3. Non-competitive NMDA-R antagonists and depression**

#### **3.3.1. Antidepressant effects of ketamine**

It has been shown that a single intravenous infusion of ketamine (0.5 mg/kg) reduces depression severity and suicidality within 4 hours in patients with TRD and this effect can last up to 1 week (Berman et al., 2000; Xu et al., 2016; Zarate et al., 2006a). Moreover, some clinical trials assessing the effectivity of intranasal esketamine ((S)-ketamine, one of ketamine's enantiomers) have revealed that it also exhibited a rapid and sustained antidepressant effect in patients with TRD (Daly et al., 2018) and it improved depressive symptoms and suicidal ideation in depressed patients at imminent risk for suicide (Canuso et al., 2018). As a result, on March 5, 2019, the United States Food and Drug Administration (FDA) approved Janssen Pharmaceutical Company (S)-ketamine nasal spray for the treatment of patients with MDD resistant to conventional antidepressant drugs (FDA, 2019). A previous study had demonstrated the efficacy of intranasal ketamine in TRD, a much more convenient administration route than intravenous infusion (Lapidus et al., 2014). However, ketamine administration was also shown to elicit transient perceptual disturbances, such as mild depersonalization (detachment from the body and self), derealization (detachment from the environment and reality), altered body and time perception, euphoria, anxiety... Moreover, it

also caused physical side effects, like dizziness, nausea, and mild increases in blood pressure and heart rate (Loo et al., 2016; Romeo et al., 2015). These adverse effects decline within a few minutes of stopping ketamine infusion and fully disappear within 2 h.

Preclinical studies have reported that ketamine produced behavioral antidepressant-like effects, initiated protein synthesis and its action was mediated by AMPA-Rs (Autry et al., 2011; Koike et al., 2011; Li et al., 2010; Maeng et al., 2008; Zhou et al., 2014). In these studies, a single intraperitoneal injection of ketamine (2.5-30 mg/kg) elicited rapid antidepressant-like effects in adult male rodents, demonstrated by a reduction in forced swim test (FST) or tail suspension test (TST) immobility time. Specifically, ketamine was found to promote rapid synthesis of brain-derived neurotrophic factor (BDNF) in HPC (Autry et al., 2011). Ketamine also rapidly activated the mammalian target of rapamycin (mTOR) pathway, resulting in rapid and sustained increase of synapse-associated proteins and spine number in PFC (Li et al., 2010). Moreover, ketamine's antidepressant-like effects were mediated by AMPA-Rs since 2,3-dihydroxy-6-nitro-7-sulfamoyl-benzo[f]quinoxaline-2,3-dione (NBQX), an AMPA-R antagonist, prevented them (Koike et al., 2011; Maeng et al., 2008). These results were replicated and extended by Zhou et al. (2014), who observed that the levels of mTOR in rat HPC and PFC were modulated by NBQX and CX546 (an AMPA receptor agonist), further supporting the idea that AMPA-Rs mediate ketamine-induced antidepressant effects and mTOR activation.

### **3.3.2. Importance of sex in depression**

Understanding how sex influences physiological and behavioral responses is essential to develop appropriate treatments, especially in the field of neuropsychopharmacology, which seeks to design therapeutics for disorders

that exhibit sex bias in the frequency, severity or response to treatment. Biomedical research in female animals -particularly in the field of mental health- has been largely neglected until recently, despite the fact that lifetime prevalence of MDD is twice as much in women than in men (Albert, 2015). Therefore, it would seem adequate to use subjects of both sexes in all experiments in preclinical research. Among the different reasons that advocate for not including female rodents in experiments, one is the fear that due to their estrous cycle, female rodents would increase variability and the testing of more subjects would be needed (Mogil, 2016). In a meta-analysis, behavioral, morphological, physiological and molecular traits were monitored in male and in female mice tested without considering the estrous cycle stage. They found that variability was not significantly greater in females than males and concluded that the use of female mice in neuroscience experiments does not require monitoring of the estrous cycle (Prendergast et al., 2014). Another study evaluating the effect of sex on the open field and the water-maze concluded that not tracking the estrus cyclicity of female mice did not cause a relevant increase of data variability (Fritz et al., 2017).

In 2013, the first study exhibiting different sensitivities to ketamine's antidepressant action between male and female rats was published (Carrier & Kabbaj, 2013). They reported that a low dose of ketamine (2.5 mg/kg) elicited antidepressant-like effects in female rodents, while it was not effective in their male counterparts. Moreover, they found that this sensitivity depended on estrogen and progesterone, since this low dose of ketamine did not induce antidepressant-like effects in ovariectomized female rats. In mice, the same results were replicated using a higher dose (3 mg/kg) in the FST (Franceschelli et al., 2015) and it was also suggested that this higher sensitivity could be mediated by estradiol, an ovarian hormone (Dossat et al., 2018).

### **3.4. Mechanism of action of non-competitive NMDA-R antagonists**

The administration of MK-801, PCP or ketamine increases Glu release and disorganizes the firing of cortical neurons (Homayoun et al., 2005; Lorrain et al., 2003; Moghaddam & Adams, 1998). Considering that NMDA-Rs are ubiquitously expressed in the central nervous system, it is of relevance to know if they preferentially act on specific NMDA-Rs subunits or on particular neurons or brain regions expressing NMDA-Rs. However, there is still uncertainty concerning their exact mechanism of action. For PCP and MK-801, the prevailing view is that they may block tonically active NMDA-Rs on GABAergic interneurons, suppressing their inhibitory effect. For ketamine, there are different hypothesis, not mutually exclusive, to explain its effects.

#### **3.4.1. Disinhibition hypothesis**

The disinhibition hypothesis proposes that non-competitive NMDA-R antagonists would preferentially act on NMDA-Rs expressed on GABAergic interneurons (Tsai & Coyle, 2002) (Figure 2). Under normal conditions, the activity of pyramidal neurons is under the control of GABAergic interneurons. Without this GABAergic inhibition, excitatory inputs onto pyramidal neurons would lead to an ever-increasing activation. It was suggested that GABA interneurons sense pyramidal cell activity through NMDA-Rs and, by modulating their inhibitory effect, they would stabilize overall pyramidal cell firing. However, the action of non-competitive NMDA-R antagonists would be interpreted as decreased pyramidal cell activity. Consequently, GABAergic interneurons would reduce their inhibitory output in order to compensate for the apparent inactivity. Therefore, non-competitive NMDA-R antagonists, by selectively reducing the excitation of interneurons, would increase pyramidal cell firing and induce schizophrenia-like symptoms.



This hypothesis presumes that interneurons may have a lower threshold for action potential generation compared with pyramidal cells, which is something that was suggested to occur in the HPC, where GABAergic interneurons were 10-fold more sensitive to NMDA-R antagonists than the pyramidal neurons (Grunze et al., 1996). This would mean that interneurons would be more depolarized, implying a higher amount of opened NMDA-Rs, since they are voltage gated. Given this situation, non-competitive NMDA-R antagonists would preferentially block NMDA-Rs in GABAergic interneurons because they are already activated.

Previous studies of our group showed that PCP may act primarily on the GABAergic cells of the RtN of the thalamus, (Kargieman et al., 2007; Santana et al., 2011; Troyano-Rodriguez et al., 2014). GABA neurons in RtN, exert a tonic, feed-forward inhibitory effect on the rest of thalamic excitatory nuclei. Therefore, blockade of NMDA-Rs in RtN neurons led to disinhibition of excitatory thalamocortical neurons and a subsequent increase of pyramidal neuron discharge in mPFC. MK-801, in turn, appeared to act preferentially on GABAergic interneurons of the PFC (Homayoun & Moghaddam, 2007), since MK-801 administration decreased the firing rate of fast-spiking cells (putative interneurons) and increased the firing rate of regular-spiking cells (putative pyramidal neurons) in the PFC. In the case of ketamine, this hypothesis is supported by a study showing an increase in overall activity in the PFC in healthy volunteers after ketamine administration (Breier et al., 1997). In rodent studies, ketamine was also found to increase extracellular Glu levels in the PFC (Moghaddam et al., 1997). In another study, ketamine administration led to a reduction in the firing rate of putative interneurons, but, on average, did not produce any change on the firing rate of putative pyramidal neurons (Quirk et al., 2009). More recently, the effects of ketamine have been assessed in anesthetized and awake rats. Using exactly the same experimental conditions as for the PCP experiments in anesthetized rats (Kargieman et al.,

2007; Santana et al., 2011; Troyano-Rodríguez et al., 2014), ketamine also inhibited the activity of RtN neurons, but unlike PCP, this effect did not translate into a disinhibition of thalamic and cortical neurons, which were equally inhibited by ketamine (Amat-Foraster et al., 2018). However, in awake rats, ketamine and PCP induced a comparable –and moderate– excitatory effect of thalamic and cortical neurons (Amat-Foraster et al., 2019). Interestingly, the latter study showed that both pyramidal neurons and GABA interneurons in mPFC were excited by PCP and ketamine, which allows to exclude the cortical disinhibition as a mechanism of action for both drugs. The remarkable differences of ketamine’s effects in awake and anesthetized rats cast doubts on previous ketamine studies using anesthesia.

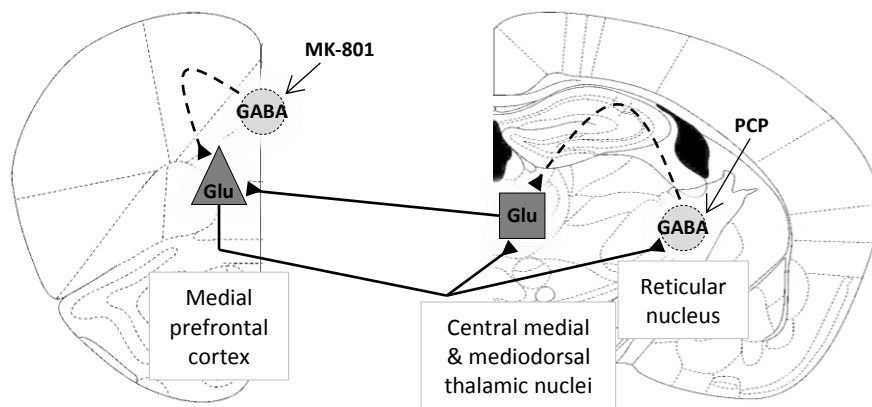


**Figure 2. Disinhibition hypothesis.** Activation of thalamocortical circuits by the action of non-competitive NMDA-R antagonist on GABAergic interneurons. Redrawn from Troyano-Rodríguez et al., 2014.

### 3.4.2. Direct inhibition hypothesis

The direct inhibition hypothesis proposes that ketamine would inhibit extra-synaptic NMDA-Rs (Figure 3). Under normal conditions, there are extra-synaptic NMDA-Rs, not located in the post-synaptic density (Hardingham &

Bading, 2010), and mainly formed by the GluN2B subunit (Groc et al., 2006). These extra-synaptic GluN2B-containing NMDA-Rs are tonically activated by low levels of ambient glutamate, which are directly regulated by Glu transporters expressed by astroglial cells (Rothstein et al., 1996). Moreover, these receptors, through the mTOR signaling pathway, limit protein synthesis and regulate excitatory synaptic plasticity (Miller et al., 2014; Wang et al., 2011; Wang et al., 2013). Therefore, ketamine is hypothesized to specifically block the extra-synaptic GluN2B-containing NMDA-Rs, preventing their tonic activation and enabling protein synthesis.

This hypothesis is supported by studies showing that GluN2B-selective NMDA-R antagonists induce antidepressant effects. In humans, intravenous administration of CP-101,606 (traxoprodil), a GluN2B-selective NMDA-R antagonist, induced antidepressant effects in patients with MDD refractory to treatment with selective serotonin reuptake inhibitor (SSRI) therapy, though this effect was not rapid but appeared 5 days after treatment (Preskorn et al., 2008). There have been no further studies replicating these results. In rodents, Ro 25-6981, a GluN2B-selective antagonist, transiently activated mTOR signaling in PFC, increasing levels of synaptic proteins and producing antidepressant-like responses in the FST and the novelty suppressed feeding test (NSFT) (Li et al., 2010). Moreover, microinfusion of Ro 25-6981 into mPFC was sufficient to mimic the antidepressant-like effect of systemic Ro 25-6981 administration in the FST (Kiselycznyk et al., 2015). In mice lacking the GluN2B subunit, specifically in NMDA-Rs localized in pyramidal neurons, ketamine injection did not further decrease behavioral despair (Miller et al., 2014).

It must be taken into consideration that studies have reported that ketamine has greater selectivity for GluN2C- and/or GluN2D-containing NMDA-Rs compared with GluN2B- and GluN2A-containing receptors (Khlestova et al., 2016; Kotermanski & Johnson, 2009). Therefore, it is uncertain how ketamine

would preferentially act on GluN2B-containing receptors to elicit its antidepressant actions.

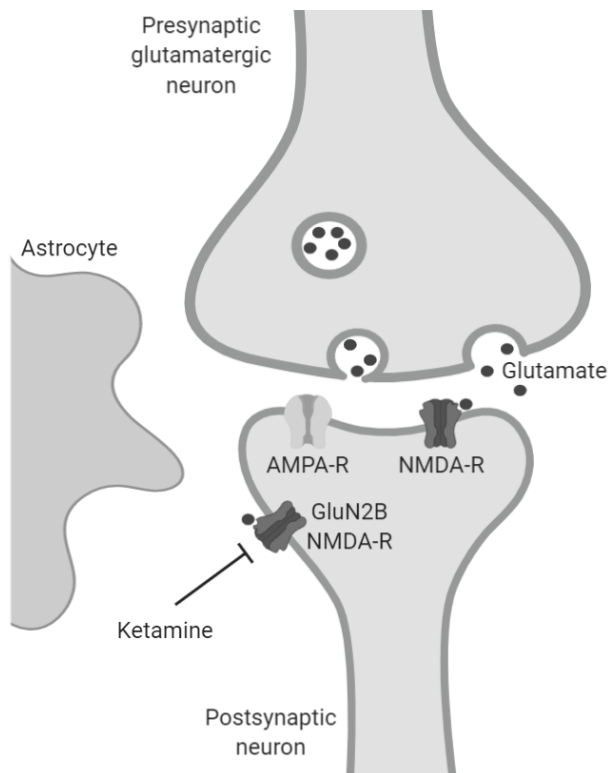


**Figure 3. Direct inhibition hypothesis.** Ketamine would antagonize NMDA-Rs at excitatory synapses onto pyramidal neurons that are tonically activated by ambient glutamate. Created using BioRender.

While inconclusive, discrepancies between these hypotheses could be explained by distinct preference for NMDA-R subunits, brain areas and/or by different sub-populations of interneurons being affected by non-competitive NMDA-R antagonists.

## **4. Cerebellum**

As mentioned above, the cerebellum has been a neglected brain structure in mental disorders. Over the years, research in this field has mainly focused on cortical and limbic areas, leaving aside the cerebellum, which –together with basal ganglia circuits– plays a major role in motor behavior. However, a few researchers in schizophrenia (mainly Nancy C. Andreasen) have stressed the role of cerebellum in schizophrenia (Andreasen et al., 1998, 1999) and recent studies suggest a key role of the cerebellum in higher brain functions, including cognition (Koziol et al., 2014; Sokolov et al., 2017). For this reason, and given the relevance of cerebellar GluN2C-containing NMDA-Rs found in the present Thesis, here I summarize some relevant aspects about the functional architecture of the cerebellum.

### **4.1. Functional architecture of the cerebellum**

The cerebellar cortex is composed of three different layers and each layer has distinct cell types (Figure 4). The granular layer is the innermost layer and it contains millions of small granule cells (the most numerous cell type in the brain), in addition to excitatory Golgi cells, Lugaro cells, mossy fibers, and unipolar brush cells. The middle layer is called the Purkinje cell layer because it primarily contains Purkinje cell somas, apart from candelabrum interneurons and astrocytes called Bergmann glia. The superficial layer, called molecular layer, is made up primarily of the large dendrites of Purkinje cells as well as granule cells axons, referred to as parallel fibers, but also contains stellate and basket cell inhibitory interneurons and climbing fibers.

Climbing fibers and mossy fibers constitute the majority of the afferents entering the cerebellum. Climbing fibers terminate within the molecular layer and each one of them forms several synaptic contacts with the dendrites of a

single Purkinje cell (each Purkinje cell is innervated by one climbing fiber). Mossy fibers terminate within the granular layer, where they deliver excitatory signals to granule cells. Granule neurons are excitatory and convey the information providing a single ascending axon that bifurcates into a parallel fiber and synapses with the dendrites of Purkinje cells. Purkinje cells are inhibitory and deliver the output of the cerebellar cortex to the deep cerebellar nuclei (DCN), which send projections back to the brainstem, or to the cerebral cortex via the thalamus.

Below the three layers, embedded in the white matter, there are the DCN. These three bilateral pairs of cerebellar nuclei, called fastigial, interposed and lateral nucleus (LN), transmit the output of the cerebellum to the rest of the brain and spinal cord (Sillitoe & Joyner, 2007).

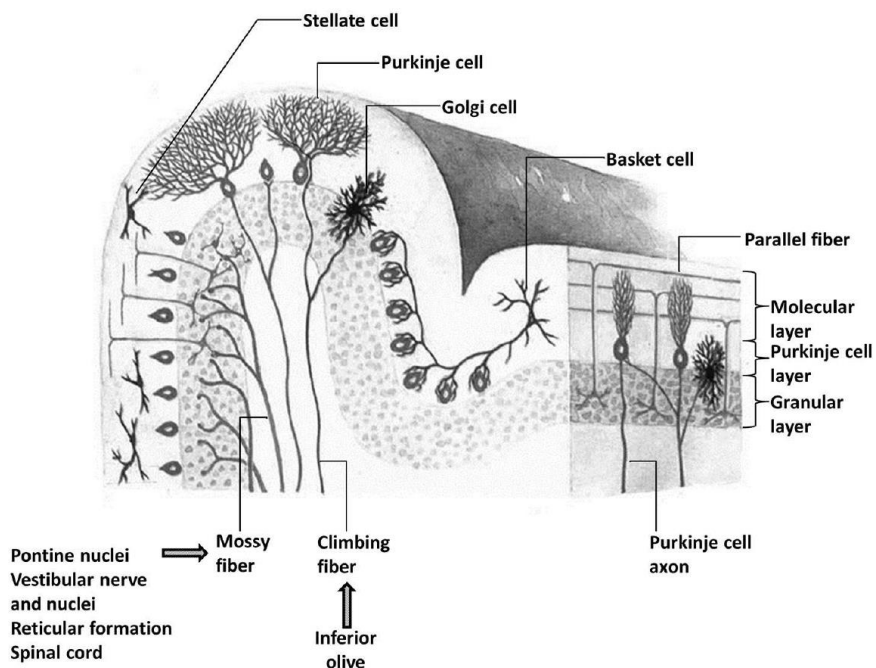


**Figure 4. Structural organization of the cerebellar cortex.** There are three different layers with distinct cell types. The afferents to the cerebellar cortex are the climbing fibers and the mossy fibers. Copied from Mosconi et al., 2015.

## **4.2. Cerebellum and NMDA-R subunits**

In the adult cerebellum, each layer and cellular type exhibits a different GluN subunit profile. Purkinje neurons mostly express GluN2A subunit, followed by GluN2D and low levels of GluN2C, while granule cells show high levels of GluN2C subunit and moderate levels of GluN2A and GluN2D subunits (Scherzer et al., 1997). Moreover, GluN3A and GluN3B expression has been described in the three layers of the cerebellar cortex, with GluN3A being especially expressed in granule neurons (Wong et al., 2002) and GluN3B in Purkinje cells (Wee et al., 2008).

Granule cells show changes in the expression of the different GluN2 subunits during development. The GluN2B subunit is expressed during migration and after arrival in the internal granular layer, but its expression disappears in adulthood (Monyer et al., 1994). In contrast, GluN2A subunit expression begins postnatally during migration. Conversely, the GluN2C subunit is not detected in the internal granular layer of the immature brain, but it is heavily expressed during synaptic pruning (Monyer et al., 1994).

## **4.3. Motor functions and cortico – cerebellar connectivity**

The cerebellum has long been regarded as contributing to the planning, learning and execution of movement (Clarac, 2008). The hallmark of cerebellar damage is not loss of movement, but loss of sensorimotor coordination or impaired timing (Bareš et al, 2010). In fact, it acts as a coordination center, using sensory inputs from the periphery to fine-tune movement and balance. The cerebellum receives a copy of the motor commands and, based on this information and exteroceptive and proprioceptive inputs, it predicts the sensory outcome of that motor act (Blakemore et al., 2001). A sensory discrepancy between the intended

movement and the actual movement allows for rapid adjustments in the motor output, essential for learning and refine coordination. The extremely high discharge rate of granule and Purkinje cells (up to 200 Hz for granule cells in certain experimental conditions) allows for these fast adjustments in a feed-forward manner.

The cerebellum is reciprocally connected with the neocortex and the basal ganglia and these connections are mediated by different nuclei of the thalamus (Figure 5) (Bostan et al., 2013, 2018). The motor cortex projects via the pons to granule cells in the cerebellar cortex (Kelly & Strick, 2003) and it also projects to the striatum in the basal ganglia (Bolam et al., 2000). Studies have suggested that regions of the cerebellar cortex that receive input from the motor cortex are the same as those that project to the motor cortex (Kelly & Strick, 2003). Efferents from the DCN, being the LN (or dentate nucleus in humans) the major output nucleus of the cerebellum, project to multiple subdivisions of the thalamus (Percheron et al., 1996). One of these subdivisions is the motor thalamus, which includes the ventrolateral (VL) and ventral anterior (VA) nuclei and receives massive afferents from the cerebellum and basal ganglia, conveying the information to motor cortical areas (Kuramoto et al., 2009). In addition, the motor thalamus and the central lateral (CL) thalamic nucleus receive GABAergic afferents from the RtN (Kuramoto et al., 2011; Lam & Sherman, 2015; Sawyer et al., 1991). The VL receives glutamatergic projections from the LN (Dum & Strick, 2003; Kuramoto et al., 2011; Tanaka et al., 2018) and the VA receives GABAergic projections from the basal ganglia, specifically from the substantia nigra pars reticulata (SNr) (Kuramoto et al., 2011; Tanaka et al., 2018). It is unlikely that the motor thalamus integrates information from cerebellum and basal ganglia because projections from both areas do not converge at the neuronal level or within a territory (Bosch-Bouju et al., 2013). The cerebellum and basal ganglia are also directly linked, since the LN projects to the striatum through the CL



(Ichinohe et al., 2000) and the basal ganglia, through the subthalamic nucleus, project to the cerebellar cortex (Jwair et al., 2017; Moers-Hornikx et al., 2011). The motor cortex is reciprocally connected to VL and VA (Dum & Strick, 2003; Haber & Calzavara, 2009; Tlamsa & Brumberg, 2010) and it contains neurons that receive from and/or project to specific areas of the brain in a layer-specific manner. Thalamocortical inputs from VL and VA are mainly glutamatergic and target layers I, II and V of the motor cortex (Hooks et al., 2013; McFarland & Haber, 2002). Specifically, the part of the motor thalamus that receives basal ganglia output mainly projects to layer I, while the part that receives cerebellum output projects to layers II to V in the motor cortex (Kuramoto et al., 2009; Shigematsu et al., 2016; Tanaka et al., 2018). On the other hand, corticothalamic neurons project from layers V and VI to VL and VA (Na et al., 1997).

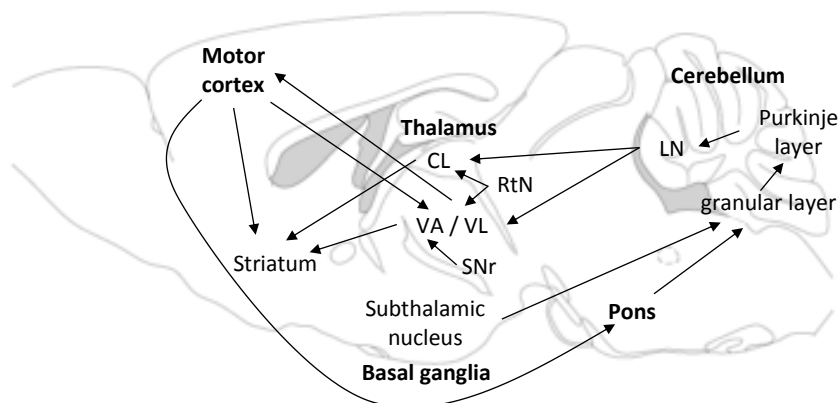


**Figure 5. Cortico – cerebellar connectivity.** The motor cortex projects to the cerebellum through the pons and the cerebellum projects back to the motor cortex through the thalamus. CL: central lateral thalamic nucleus; LN: lateral nucleus; RtN: reticular nucleus of the thalamus; SNr: substantia nigra pars reticulata; VA/VL: ventral anterior and ventrolateral nuclei of the thalamus.

#### 4.4. Non-motor functions of the cerebellum

Apart from the motor functions, the cerebellum has also been implicated in non-motor functions, such as cognition, language, emotion and reward

(Adamaszek et al., 2017; Kim et al., 1994; Koziol et al., 2014; Mariën et al., 2014; Sokolov et al., 2017; Wagner et al., 2017). Tract-tracing studies have proved that the cerebellum, linked through the pons and thalamus, is connected to motor and non-motor cortical regions, such as the PFC (Dum & Strick, 2003; Kelly & Strick, 2003; Middleton & Strick, 1994), creating the potential for the cerebellum to influence cognition. Regarding its implication in mental illnesses, there has been accumulating evidence about cerebellar abnormalities in schizophrenia and mood disorders such as MDD (Dutta et al., 2014; Heath et al., 1979; Lupo et al., 2019; Picard et al., 2008). On a connectivity level, schizophrenic and depressed patients had a higher causal out-inflow (net flow) from the cerebellum to the mPFC compared to healthy controls (Jiang et al., 2019), meaning they had an increased effective connectivity. Another study also found an increased causal connectivity in the prefrontal-thalamic-cerebellar circuit in schizophrenic patients, which was suggested to be a compensatory mechanism for the structural deficits (Guo et al., 2015). In addition, this altered connectivity between the cerebellum and the PFC, specifically the right dorsolateral part, was associated with negative symptom severity (Brady et al., 2019). In medication-free depressed patients, there was a reduced fractional anisotropy (a measure of water diffusion that, when it is decreased, is associated with abnormalities in the cellular microstructure (i.e., the integrity of white matter pathways)) in the white matter of the right cerebellum hemispheric lobule (Jiang et al., 2017). Moreover, MDD patients exhibited in the left cerebellum a significantly decreased regional homogeneity (Liu et al., 2010), an “index of network centrality for characterizing the importance of the node in the human functional connectome” (Jiang & Zuo, 2016). Finally, a reduction in cerebellar volume was found in patients with MDD (Escalona et al., 1993), further supporting the role of the cerebellum in MDD.

# **Hypothesis and objectives**



The main objective of my PhD has been to study the involvement of GluN2C-containing NMDA-Rs in the psychotomimetic actions of non-competitive NMDA-R antagonists as well as in the antidepressant effects of ketamine. Given that one of the sites of action of non-competitive NMDA-R antagonists is the RtN and that the GluN2C subunit is expressed in this nucleus, our working hypothesis was that the psychotomimetic and the antidepressant-like effects induced by non-competitive NMDA-R antagonists would be partly attenuated in absence of the GluN2C subunit. In order to examine this hypothesis, we have used mice lacking the GluN2C subunit.

In addition, we have studied the intracellular signaling pathways of the antidepressant-like effect of ketamine in rats.

The specific objectives have been:

1. To evaluate the psychotomimetic effects induced by MK-801 and PCP in WT and GluN2CKO mice.
2. To characterize the brain circuits involved in the effects of MK-801 and PCP using *c-fos* mRNA expression in WT and GluN2CKO mice.
3. To examine the effects of sex in the psychotomimetic and antidepressant actions of ketamine -including neurochemical effects- in WT and GluN2CKO mice.
4. To characterize the brain circuits involved in the effects of ketamine using *c-fos* mRNA expression in male and female WT and GluN2CKO mice.
5. To characterize NMDA-R subunits distribution in WT and GluN2CKO mice.
6. To assess ketamine's antidepressant-like effect in rats and its relationship to intracellular signaling pathways.



# Methods





## 1. Subjects

Male and female WT and GluN2CKO mice backcrossed onto a C57BL/6J genetic background (achieving >99%) and male Wistar rats (weighing 275–350g) purchased from Charles River Laboratories (France) were used. In mice, behavioral tests were conducted at 8 to 12 weeks-of-age. Rats were daily handled for at least 5 days before any test. All animals were maintained in the animal facilities of the School of Medicine in the University of Barcelona, in a controlled environment (12-h light/dark cycle,  $22 \pm 1$  °C room temperature) with *ad libitum* access to food and water. All experimental procedures were conducted in accordance with national (Royal Decree 53/2013) and European legislation (Directive 2010/63/EU, on the protection of animals used for scientific purposes, 22 September 2010), and were approved by the Institutional Animal Care and Use Committee of the University of Barcelona.

## 2. Drugs

MK-801, PCP (Sigma-Aldrich, MA) and ketamine (Ketolar®, Pfizer) were dissolved in saline. PCP had its pH adjusted to 6.0-7.0 with sodium bicarbonate. MK-801 (0.25 mg/kg) and ketamine (10-30 mg/kg) were injected intraperitoneally (i.p.), while PCP (5 mg/kg) was injected by subcutaneous route (s.c.). Doses of MK-801 and PCP were selected in order to effectively produce the behavioral motor syndrome as previously described (Castañé et al., 2015; Scorza et al., 2010). Doses of ketamine were chosen in order to elicit antidepressant-like effects (Fukumoto et al., 2016; Yang et al., 2013). Doses are expressed as free base. The volume of injection was 4 ml/kg in mice and 1 ml/kg in rats.

### **3. Effects of NMDA-R antagonists in WT and GluN2CKO mice**

#### **3.1. Behavioral studies in mice**

Open field test. Mice were placed in a dimly lighted (20-30 lux) arena (35 x 35 cm) during a 30-min trial. The test started 30 min after MK-801 or saline, 15 min after PCP or saline or immediately after ketamine or saline administration. Male mice were used in MK-801 and PCP experiments, where distance moved (cm) and meandering (the change in direction of movement of the animal relative to the distance moved; °/cm) were automatically recorded by a camera mounted above the open field and connected to a computer equipped with a video-tracking software (Ethovision XT-12.0, Noldus, The Netherlands). In ketamine experiments, male and female mice were used and distanced moved was analyzed using the SMART 3.0 video tracking software (Panlab/Harvard apparatus, USA). In addition, behavioral signs such as number of rearings and falls (during horizontal displacement or by loss of balance while performing rearings), as well as the intensity of hindlimb abduction and circling were observed and scored using a graded scale (0, absent; 1, equivocal; 2, present; and 3, intense) as previously published (Scorza et al., 2010; Spanos & Yamamoto, 1989). All behaviors were recorded by a trained experimenter blind to mice genotype as previously described (Scorza et al., 2010). After recording the animal behavior, the open field was cleaned with alcohol 30 % before placing the following animal. Mice were naive to the open field and were used only once.

Rotarod test. Two different protocols were used in male mice in order to assess motor coordination under drug administration and motor learning under basal conditions. The apparatus consisted of a black striated rod (3 cm in diameter) supported 20 cm above the floor (Rota-rod/RS, Leticia Scientific Instruments, Spain). For motor coordination, mice were first trained to stay in the rod at 4 rpm for 1 min and at 8 rpm for 2 min. Animals that achieved 2 min

in the rod at 8 rpm in three or less training sessions (training criteria) performed the test. On the testing day, drug free mice were retrained on the rod at 8 rpm as before. Afterwards, animals were tested 2.5 h or 2 h after MK-801 or PCP administration respectively, with the apparatus revolving at 8 rpm. Latency to fall was recorded until criteria (2 min) or three trials elapsed, whatever occurred first. Motor learning was assessed using an accelerating protocol in which the rotarod accelerated from 4 to 40 rpm over a 5-min period. Mice were placed on the rotating drum and the acceleration started after a couple of seconds. The latency to fall was measured automatically. Mice were trained for four consecutive days, with one daily session consisting of 4 trials and a 300-s inter-trial interval.

Pre-pulse inhibition (PPI) test. Male mice were individually tested in an acoustic startle chamber (Panlab/Harvard apparatus, Spain) and PackWin software controlled the delivery of all stimuli to the animals and recorded the response. During four previous days to testing, mice were habituated for 15 min to the chamber at background noise levels (60 dB). At the testing day, the experiment started 25 min after administration of MK-801 or 10 min after administration of PCP, with a 5-min adaptation period during which the animals were exposed to 60-dB background white noise that lasted throughout the test. Afterward, a basal startle reflex was measured by administering 10 repeated pulse stimuli (115 dB, 8 kHz, 40-ms duration each). Then, animals were exposed to 4 different trial types randomly presented: 10 pulse alone trials (115 dB, 8 kHz, 40 ms), 10 pre-pulse alone trials (80 dB, 10 kHz, 20 ms), 10 pre-pulse and pulse trials (100 ms prepulse onset to pulse onset) and 10 no-stimuli trials during which only background noise was present. The startle reflex was measured for 1 s after the administration of the stimulus; the inter-trial interval was 29 s and the test lasted 30 min in total. Pre-pulse inhibition was calculated as the percent inhibition of the startle

amplitude evoked by the pulse alone: % PPI = [(magnitude on pulse alone trial – magnitude on pre-pulse + pulse trial) / magnitude on pulse alone trial] x 100.

Tail suspension test (TST). Male and female mice were tested 30 min after ketamine administration. They were suspended 30 cm above the floor by adhesive tape placed approximately 1 cm from the tip of the tail. Clear hollow cylinders (2.1 cm length, 1.5 cm outside diameter, 1.1 cm inside diameter, 2.1 grams) were placed around the tails of mice to prevent tail climbing behavior. Sessions were videotaped for 6 min and the immobility time was determined by an experimenter blind to mice genotype and treatment.

Forced swim test (FST). Male mice were tested 30 min after ketamine administration. They were forced to swim in a clear methacrylate cylinder (15 cm diameter x 30 cm height) containing 20 cm of water maintained at  $24 \pm 1^\circ\text{C}$ , as described by Porsolt et al. (1978). The cylinder was filled with fresh water for every single animal. Mice were given a single trial that lasted 6 min and it was recorded using a video camera system. In a posterior analysis, the time the animal spent immobile during the last 4 min of the test was quantified by an experimenter blind to treatment and genotype.

Novelty suppressed feeding test (NSFT). The testing apparatus consisted of a box (35 cm x 35 cm) with the floor covered with 1 cm of wooden bedding. Two food pellets were placed in the highly illuminated center of the arena (600 lx) on a white circular paper (8 cm in diameter). Male mice underwent a 24-h food deprivation in order to motivate food consumption behavior during test. 30 min after ketamine administration, each mouse was placed in the corner of the testing arena. During a 10-min test, the latency to feed was measured, only sniffing was not considered. Immediately after the animal began to eat the chow, the mouse was placed alone and food consumption in the homecage was measured for 5 min.

### 3.2. Intracerebral microdialysis studies in mice

Extracellular DA, 5-HT or Glu concentration were measured by *in vivo* intracerebral microdialysis in freely moving mice as previously described (Castañé et al., 2008; López-Gil et al., 2009). Briefly, one concentric dialysis probe (1 mm membrane length for NAc, 2 mm membrane length for mPFC) was previously implanted in the NAc of anaesthetized male mice (coordinates in mm: AP: +1.5; ML: -0.65; DV: -5) or in the mPFC of male and female anaesthetized mice (coordinates in mm: AP: +2.2; ML: -0.2; DV: -3.4). The coordinates were taken from bregma and top of skull and experiments were performed 24-48 h after surgery. Mice were continuously perfused with artificial cerebrospinal fluid (aCSF) enriched with calcium (in mM: 125 NaCl, 2.5 KCl, 2.52 CaCl<sub>2</sub>, 1.18 MgCl<sub>2</sub>) at a rate of 1.65 µl/min with a syringe pump (WPI model sp220i, Aston, UK) attached to an overhead liquid swivel (Instech, Plymouth Meeting, PA, USA). For DA measurements in NAc, aCSF contained 10 µM nomifensine and 20-min samples were collected in vials containing 5 µL of 10 mM HClO<sub>4</sub> after a stabilization period of 1 h. For 5-HT and Glu measurements in mPFC, aCSF contained 1 µM citalopram and 30-min samples were collected after a stabilization period of 3 h. Neurotransmitter concentrations were determined by High Performance Liquid Chromatography (HPLC). 5-HT and DA levels were measured by electrochemical detection (+ 0.7 V, Waters 2465, Waters Cromatografía, Spain). Samples were injected in a Waters 717 plus autosampler (Waters Cromatografía, Spain) and a Waters 515 pump and a 2.6 µm particle size C18 column (75x4.6 mm, Kinetex, Phenomenex, Spain) were used. In both cases, the detection limit was 3 fmol. For DA, the mobile phase consisted of 0.15 M Na<sub>2</sub>HPO<sub>4</sub>, 0.9 mM PICB8, 0.5 mM Na<sub>2</sub>-EDTA (pH adjusted to 2.8 with phosphoric acid), and 10 % methanol, it was pumped at 0.8 ml/min and the total sample analysis time lasted 5 min. For 5-HT, the mobile phase consisted of 0.15 M NaH<sub>2</sub>PO<sub>4</sub>·H<sub>2</sub>O, 1.7 mM PICB8, 0.2 mM Na<sub>2</sub>-EDTA (pH adjusted to 2.8

with phosphoric acid), and 16 % methanol, it was pumped at 1 ml/min and the total sample analysis time lasted 5 min. For Glu measurements, a fluorimetric detector (Waters 2475, Waters Cromatografía, Spain) set at 360 nm excitation and 450 nm emission wavelengths was used. The detection limit was 0.3 pmol. Dialysate samples were precolumn derivatized with OPA reagent. The mobile phase consisted of two components: solution A (0.05 M Na<sub>2</sub>HPO<sub>4</sub>, pH adjusted to 5.6 with phosphoric acid, and 28 % methanol), and solution B (methanol/H<sub>2</sub>O at an 8:2 ratio). The mobile phase was pumped at 0.8 ml/min (Waters 600 HPLC Pump, Waters Cromatografía, Spain) and a gradient was established going from 100 % of solution A to 100 % of solution B, and returning to initial conditions in a 20 min run time. Glu was separated in a 5 µm particle size XBridge Shield RP18 Waters column (100x3 mm, Waters Cromatografía, Spain). Baseline neurotransmitter levels were calculated as the average of the four pre-drug samples. At the end of the experiments, mice were sacrificed and a Fast Green solution was perfused through the dialysis probe to stain the surrounding tissue for subsequent histological examination. Brains were removed and histologically processed in order to confirm the localization of the dialysis probes. Only data obtained from animals with histologically correct probe placements were used for subsequent statistical analysis.

### **3.3. Molecular studies in mice**

*In situ* hybridization (ISH). Male and female mice were sacrificed 1 h after treatment and brains were rapidly removed, frozen on dry ice and stored at -30 °C until processed. Brain coronal sections (14 µm) were cut using a microtome-cryostat (HM500-OM, Microm, Germany), thaw-mounted onto APTS (3-aminopropyltriethoxysilane, Sigma, MO, USA)-coated slides, kept at

-30 °C and fixed in 4 % paraformaldehyde. The following primer sequences of mRNAs were used:

- *c-fos*, gene ID: NM\_022197.1  
sense, 5'-GACCATGATGTTCTCGGGTTTCAACGCGGACTACGAGGCGTCATCCTC-3'
- *zif268*, gene ID: M22326.1  
sense, 5'-GCATCATCTCCTCCAGTTGGGGTAGTTGCCATGGTGGGTGAGT-3'

The oligonucleotides were labeled with [33P]-dATP (42500 Ci mmol<sup>-1</sup>; DuPont-NEN, MA, USA) with terminal deoxynucleotidyltransferase (Calbiochem, CA, USA) and purified with ProbeQuant G-50 Micro Columns (GE Healthcare UK Limited, UK), as described previously (Santana et al., 2004). Hybridized sections were exposed (*zif268*: 2 days; *c-fos*: 7 days) to Biomax MR film (Kodak, Sigma-Aldrich, Spain) with intensifying screens. Relative mean grey values (MGV) (arbitrary units) were measured with an image analyzer (Fiji, Madison, WI, USA). Two consecutive brain sections at any level of interest (AP coordinates from atlas Franklin & Paxinos, 2007) were analyzed for each mouse and averaged to obtain individual values.

#### 4. NMDA-R subunit distribution in male WT and GluN2CKO mice

*In situ* hybridization (ISH). Male mice were sacrificed and brains were rapidly removed, frozen on dry ice and stored at -30 °C until processed. Brain coronal sections (14 µm) were cut using a microtome-cryostat (HM500-OM, Microm, Germany), thaw-mounted onto APTS (3-aminopropyltriethoxysilane, Sigma, MO, USA)-coated slides, kept at -30 °C and fixed in 4 % paraformaldehyde. The following primer sequences of mRNAs were used:

- GluN1, gene ID: 14810Grin1  
sense, 5'-GGGCGAATGTCAGCAGGTGCATGGTGCTCATGAGCTCCGGGCACA-3'
- GluN2A, gene ID: 14811Grin2a  
sense, 5'-AAGTTCGCGTTCTGTACGTCGTGGCTGTGACCCAGCAGCACCGC-3'

- GluN2B, gene ID: 14812Grin2b  
sense, 5'-AAGTGCCACGAGGATGACAGCGATGCCGATGCTGGGGGGGCTCT-3'
- GluN2C, gene ID: 14813Grin2c  
sense, 5'-TCCCTGCCTGCGCCAGCCTTGCCCAAGCACCAAGGAGTGAAGT-3'
- GluN2D, gene ID: 14814Grin2d  
sense, 5'-TGGCGCACGCCAGCGCCAGCAGCAGCAGCATCTTAGCGGGGCCCC-3'

The oligonucleotides were labeled with [<sup>33</sup>P]-dATP (42500 Ci mmol<sup>-1</sup>; DuPont-NEN, MA, USA) with terminal deoxynucleotidyltransferase (Calbiochem, CA, USA) and purified with ProbeQuant G-50 Micro Columns (GE Healthcare UK Limited, UK), as described previously (Santana et al., 2004). Hybridized sections were exposed (GluN1: 1 day; GluN2A: 4 days; GluN2B: 7 days; GluN2C and GluN2D: 15 days) to Biomax MR film (Kodak, Sigma-Aldrich, Spain) with intensifying screens. Relative MGv (arbitrary units) were measured with an image analyzer (Fiji, Madison, WI, USA). Two consecutive brain sections at any level of interest (AP coordinates from atlas Franklin & Paxinos, 2007) were analyzed for each mouse and averaged to obtain individual values.

## 5. Effects of ketamine in rats

### 5.1. Behavioral studies in rats

Open field test. Rats were placed in a dimly lighted (20-30 lux) arena (35 x 35 cm) during a 30-min trial. The test started 30 min after ketamine (10-20 mg/kg) or saline injection. Distance moved (cm) was automatically recorded by a camera mounted above the open field and connected to a computer equipped with a video-tracking software (VideoTrack View Point software, France). After recording the animal behavior, the open field was cleaned with alcohol 30 % before placing the following animal. Rats were naive to the open field and were used only once.



Forced swim test (FST). Rats were forced to swim in a clear methacrylate cylinder (20 x 46 cm) filled with water ( $24 \pm 1$  °C) to a depth of 30 cm, and from which they could not escape (Porsolt et al., 1978). Animals were subjected to a pretest session lasting 15 min and 24-hours later, 30 min after ketamine treatment (10-20 mg/kg), a 5-min test was performed and recorded, as previously reported (Slattery & Cryan, 2012). The cylinders were filled with fresh water for every single animal. In a posterior analysis, the time the animal spent immobile during the test was quantified by an experimenter blind to treatment.

Novelty suppressed feeding test (NSFT). The testing apparatus consisted of a box (90 x 90 x 40 cm) with the floor covered with 1 cm of wooden bedding. Two food pellets were placed in the highly illuminated center of the arena (600 lx) on a black circular paper (10 cm in diameter). Rats underwent a food restriction protocol (18 g per day for 3 days + 24 h deprivation) in order to motivate food consumption behavior during test. 30 min after ketamine administration (10-15 mg/kg), each rat was placed in the corner of the testing arena. During a 10-min test, the latency to feed was measured, only sniffing was not considered. As a control, food consumption in the homecage was measured at 5 min and 24 h after the test.

## **5.2. Molecular studies in rats**

Synaptosome preparation and western blotting (WB). The activation of mTOR and the ribosomal protein S6 kinase (p70S6K) was assessed 30 min after ketamine (15 mg/kg) administration. Immediately after decapitation, brains were removed and placed on an ice-cold plate. Brain sections were dissected out, quickly frozen on dry ice and stored at -80 °C. Tissue was dounce-homogenized by 10 strokes with a loose pestle and 10 strokes with a tight pestle in 30 volumes of ice-cold synaptosome lysis buffer (in mM: 2.5 CaCl<sub>2</sub>,

124 NaCl, 3.2 KCl, 1.06 KH<sub>2</sub>PO<sub>4</sub>, 26 NaHCO<sub>3</sub>, 1.3 MgCl<sub>2</sub>, 10 Glucose, 320 Sucrose, 20 HEPES/NaOH pH7.4) including phosphatase inhibitors (in mM: 5 NaPyro, 100 NaF, 1 NaOrth, 40 beta-glycer-olphosphate) and protease inhibitors (1 µg/mL leupeptin, 10 µg/mL aprotinin, 1 µg/ml pepstatin and 1 mM phenylmethylsulfonyl fluoride). This crude homogenate was centrifuged for 1 min at 2000 ×g, 4 °C, the supernatant was recovered (S1) and the pellet resuspended in 1 mL of synaptosome lysis buffer for further centrifugation (1 min at 2000 ×g, 4 °C). This second supernatant (S2) was recovered and combined with S1. Total supernatant (S1 + S2) was passed through a 10 µm nitrocellulose filter and centrifuged for 1 min at 4000 ×g, 4 °C to attain the supernatant (S3). S3 was transferred to a new tube and centrifuged for 4 min at 14000 ×g, 4 °C. This final supernatant (S4) was discarded and the pellet was used as the synaptosomal fraction. Samples with equal amounts of total protein (20 µg per well) were separated in 8% sodium dodecyl sulfate-polyacrylamide gel before electrophoretic transfer onto nitrocellulose membrane (Bio-Rad, Spain). Membranes were blocked for 1 h at 21 ± 1 °C in Tris-buffered saline (100 mmol/L NaCl, 10 mmol/L Tris, pH 7.4) with 0.1% Tween-20 and 3% bovine serum albumin. Afterwards, membranes were incubated for 2 h with the primary antibodies: anti-phospho-mTOR (rabbit, 1:300, Ser2448), anti-phospho-p70S6K (rabbit, 1:300, Thr389) (Cell Signaling Technology), anti-β-actin (mouse, 1:15000, MAB1501, MerckMillipore). Bound antibodies were detected with horseradish peroxidase-conjugated anti-rabbit or anti-mouse antibodies and visualized by enhanced chemiluminescence detection (SuperSignal, Pierce, Spain). Digital images were acquired on a ChemiDoc XRS System (Bio-Rad) and quantified by The Quantity One software v4.6.3 (Bio-Rad). Optical density values for target proteins were normalized to β-actin as loading control in the same sample and expressed as a percentage of control group (saline).

Quantitative real-time polymerase chain reaction (qRT-PCR). The genic expression of post synaptic density protein 95 (PSD95) and synapsin I was evaluated 6 h after ketamine (15 mg/kg) administration. The following primers specific for rat were used:

- *PSD95*  
sense, 5'-GGATCACAGGGTCGAGAAGA-3'  
antisense, 5'-TGATGATGGGACGAGCATAG-3'
- *Synapsin I*  
sense, 5'-GGACGGAAGGGATCACATTA-3'  
antisense, 5'-TGGTGATCCCCAATGAGTG-3'
- *$\beta$ -actin*  
sense, 5'-GGAGATTACTGCCCTGGCTCCTA-3'  
antisense, 5'-GACTCATCGTACTCCTGCTTGCTG-3'

Total RNA was isolated from tissues with Trizol solution (Sigma-Aldrich) and was digested using TURBO DNA-free™ kit (Life technologies) to eliminate the genomic DNA. Complementary DNA synthesis was performed using iScript™ cDNA synthesis kit (Biorad). qRT-PCR (7900HT Fast Real-Time PCR System, Applied Biosystems) was performed using GoTaq® qPCR Master Mix (Promega) in 20  $\mu$ l of reaction mix. Quantification was performed by using the comparative CT Method ( $\Delta\Delta$ CT Method). All the samples were tested in duplicate and the relative expression values were normalized to the expression value of  *$\beta$ -actin* cDNA. Results were expressed as the unitary ratio vs saline controls.

## 6. Statistical analysis

The number of animals used for each test is reported in the figure legends. The sample sizes were determined based on power analysis and common practice in behavioral ( $\approx 10$  animals per group) and molecular studies ( $\approx 5$  animals per group). The data are expressed as mean  $\pm$  S.E.M.. Statistical analysis was carried out using unpaired *t*-test, one-way analysis of variance (ANOVA) followed by Bonferroni *post hoc* comparisons, two-way ANOVA followed by Newman-Keuls *post hoc* comparisons, two-way repeated measures ANOVA followed by Bonferroni *post hoc* comparisons and three-way ANOVA followed by Newman-Keuls *post hoc* comparisons. In all cases, the level of significance was set at  $p < 0.05$ .

# Results



## 1. Involvement of the GluN2C subunit in the mechanism of action of MK-801 and PCP in male mice

### 1.1. Behavioral syndrome

The acute administration of MK-801 (0.25 mg/kg) or PCP (5 mg/kg) significantly enhanced locomotor activity in GluN2CKO compared to WT mice (Figure 6a). For MK-801, two-way ANOVA showed a main effect of treatment ( $F_{1,32}=24.33$ ;  $p<0.0001$ ) and genotype ( $F_{1,32}=4.98$ ;  $p<0.05$ ). *Post hoc* comparisons indicated a significant hyperlocomotion in GluN2CKO mice after MK-801 treatment ( $p<0.01$ ) and a significant difference between MK-801-treated WT and GluN2CKO mice ( $p<0.01$ ). For PCP, two-way ANOVA showed a significant main effect of treatment ( $F_{1,28}=34.70$ ;  $p<0.0001$ ), genotype ( $F_{1,28}=11.61$ ;  $p<0.01$ ) and interaction ( $F_{1,28}=4.90$ ;  $p<0.05$ ). *Post hoc* comparisons showed a significant increase in locomotor activity in treated animals ( $p<0.05$  for WT,  $p<0.01$  for GluN2CKO) and a significant difference between PCP-treated WT and GluN2CKO mice ( $p<0.01$ ).

The two NMDA-R antagonists increased meandering in both genotypes (Figure 6b). Two-way ANOVA showed a significant effect of treatment in the MK-801 study ( $F_{1,32}=35.03$ ;  $p<0.0001$ ) and a significant effect of treatment ( $F_{1,28}=50.30$ ;  $p<0.0001$ ) and interaction ( $F_{1,28}=4.69$ ;  $p<0.05$ ) in the PCP study. *Post hoc* comparisons indicated a significant increase in meandering after MK-801 or PCP administration in both genotypes ( $p<0.01$ , all cases). However, no differences between genotypes were obtained in drug-treated mice, although a tendency to reduced meandering in GluN2CKO compared to WT mice was noted.

Both drugs dramatically reduced the number of rearings in WT and GluN2CKO mice (Figure 6c), even though this decrease was significantly less marked in GluN2CKO mice treated with PCP. Thus, for MK-801 two-way ANOVA showed

a main effect of treatment ( $F_{1,33}=300.90$ ;  $p<0.0001$ ). *Post hoc* comparisons indicated a significant decrease in rearings in both genotypes ( $p<0.01$ , all cases). For PCP, two-way ANOVA showed a main effect of treatment ( $F_{1,27}=56.50$ ;  $p<0.0001$ ) and genotype ( $F_{1,27}=7.91$ ;  $p<0.01$ ). *Post hoc* comparisons showed a significant reduction in rearings in both genotypes ( $p<0.01$ , all cases) and a significant difference between PCP-treated WT and GluN2CKO mice ( $p<0.05$ ).

Moreover, acute administration of MK-801 and PCP enhanced the number of falls, hindlimb abduction and the circling behavior in both genotypes, and these effects were dramatically less marked in GluN2CKO mice, particularly for the number of spontaneous falls and the circling behavior (Figure 7a-c).

For the number of falls, two-way ANOVA revealed a main effect of treatment ( $F_{1,34}=63.68$ ;  $p<0.0001$ ), genotype ( $F_{1,34}=45.77$ ;  $p<0.0001$ ) and interaction ( $F_{1,34}=45.77$ ;  $p<0.0001$ ) in mice treated with MK-801. For PCP, there was a main effect of treatment ( $F_{1,27}=26.92$ ;  $p<0.0001$ ), genotype ( $F_{1,27}=23.61$ ;  $p<0.0001$ ) and interaction ( $F_{1,27}=23.61$ ;  $p<0.0001$ ). *Post hoc* comparisons showed a significant increase in the number of falls in WT mice after MK-801 or PCP treatment ( $p<0.01$ , all cases) and significant differences between WT and GluN2CKO mice treated with both drugs ( $p<0.01$ , all cases) (Figure 7a).

Regarding hindlimb abduction, two-way ANOVA indicated a main effect of treatment ( $F_{1,35}=192.40$ ;  $p<0.0001$ ), genotype ( $F_{1,35}=7.09$ ;  $p<0.05$ ) and interaction ( $F_{1,35}=7.09$ ;  $p<0.05$ ) for MK-801. For PCP, there was a main effect of treatment ( $F_{1,27}=65.61$ ;  $p<0.0001$ ), genotype ( $F_{1,27}=9.90$ ;  $p<0.01$ ) and interaction ( $F_{1,27}=9.90$ ;  $p<0.01$ ). *Post hoc* comparisons indicated a significant increase in hindlimb abduction in both genotypes after both drugs ( $p<0.01$ , all cases) and significant differences between WT and GluN2CKO mice treated with MK-801 or PCP ( $p<0.01$ , all cases) (Figure 7b).



For circling behavior, two-way ANOVA indicated a main effect of treatment ( $F_{1,35}=12.70$ ;  $p<0.01$ ), genotype ( $F_{1,35}=4.30$ ;  $p<0.05$ ) and interaction ( $F_{1,35}=4.30$ ;  $p<0.05$ ) in mice treated with MK-801. For PCP, there was a main effect of treatment ( $F_{1,27}=17.45$ ;  $p<0.001$ ), genotype ( $F_{1,27}=17.45$ ;  $p<0.001$ ) and interaction ( $F_{1,27}=17.45$ ;  $p<0.001$ ). *Post hoc* comparisons showed a significant increase in circling behavior in WT mice after both drugs ( $p<0.01$ , all cases) and significant differences between WT and GluN2CKO mice treated with MK-801 or PCP ( $p<0.01$ , all cases) (Figure 7c).

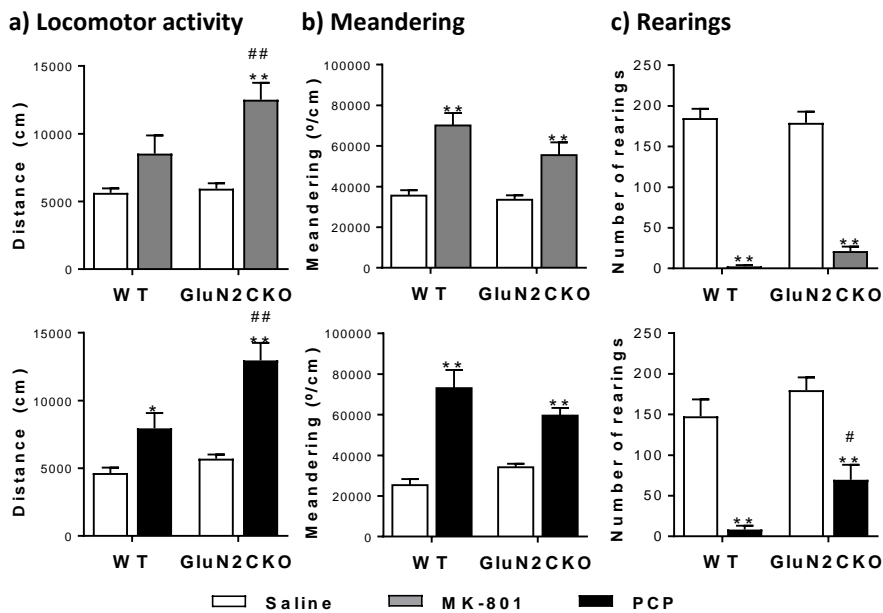


**Figure 6.** Effects of MK-801 (0.25 mg/kg;  $n=8-10$ /group) and PCP (5 mg/kg;  $n=7-8$ /group) in male WT and GluN2CKO mice on a) Locomotor activity, b) Meandering and c) Rearings. \* $p<0.05$ , \*\* $p<0.01$  vs saline; # $p<0.05$ , ## $p<0.01$  vs WT (Newman-Keuls *post hoc* test)

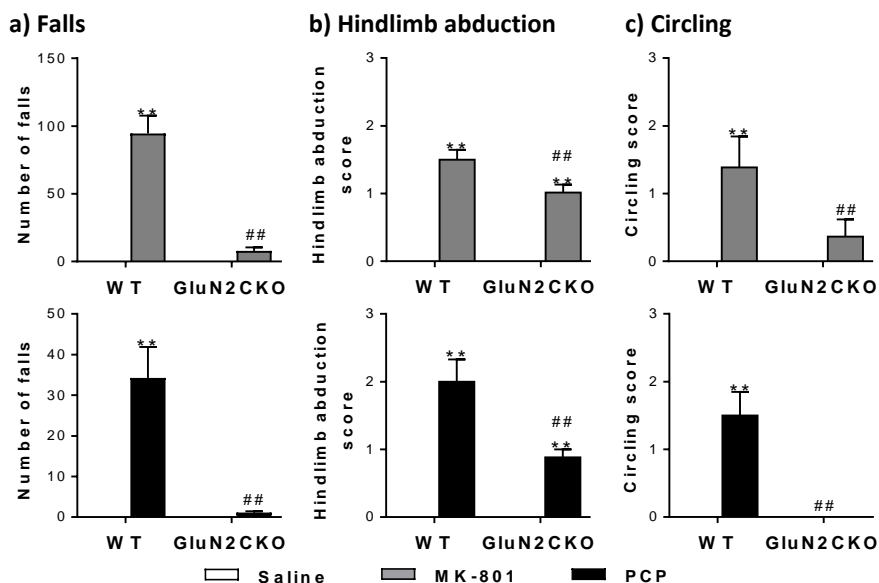


**Figure 7.** Effects of MK-801 (0.25 mg/kg; n=8-10/group) and PCP (5 mg/kg; n=7-8/group) in male WT and GluN2CKO mice on a) Falls, b) Hindlimb abduction and c) Circling. \*\*p<0.01 vs saline; ##p<0.01 vs WT (Newman-Keuls *post hoc* test)

## 1.2. Rotarod test

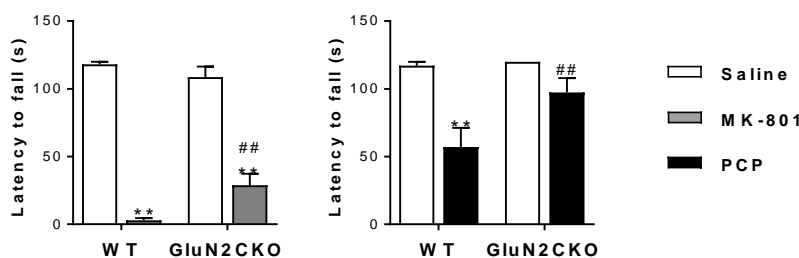
The administration of MK-801 (0.25 mg/kg) significantly decreased the latency to fall (s) after drug injection in both genotypes, and this effect was significantly attenuated in GluN2CKO mice. Two-way ANOVA showed a main effect of treatment ( $F_{1,36}=250.90$ ;  $p<0.0001$ ) and interaction ( $F_{1,36}=8.22$ ;  $p<0.01$ ). *Post hoc* comparisons showed a significant reduction in the latency to fall in WT and GluN2CKO mice after treatment ( $p<0.01$ , all cases) and a significant difference between MK-801-treated WT and GluN2CKO mice ( $p<0.01$ ) (Figure 8a). Likewise, acute treatment with PCP (5 mg/kg) significantly reduced the latency to fall in WT but not GluN2CKO mice. Thus, two-way ANOVA showed a main effect of treatment ( $F_{1,25}=18.59$ ;  $p<0.001$ ) and genotype ( $F_{1,25}=5.06$ ;  $p<0.05$ ). *Post hoc* comparisons indicated a significant decrease in the latency to fall in WT mice after treatment ( $p<0.01$ ) and a significant difference between PCP-treated WT and GluN2CKO mice

( $p < 0.01$ ) (Figure 8a). Moreover, there was no significant difference in motor learning (latency to fall) between both genotypes (Figure 8b).

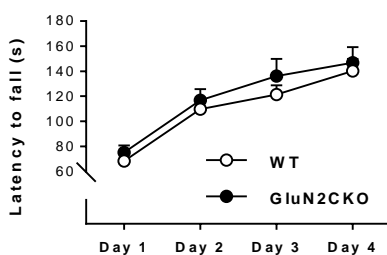
### 1.3. Pre-pulse inhibition test

Acute treatment with MK-801 (0.25 mg/kg) and PCP (5 mg/kg) similarly reduced the startle reflex in response to the pre-pulse plus pulse trials in both genotypes, though there were no differences in the amplitude of the startle response (data not shown). Thus, two-way ANOVA showed a main effect of treatment ( $F_{2,54} = 24.05$ ;  $p < 0.0001$ ), but not of genotype or the treatment  $\times$  genotype interaction. *Post hoc* comparisons showed a significant decrease of % PPI in drug-treated vs saline-treated mice ( $p < 0.01$ , all cases) (Figure 8c).

#### a) Motor coordination



#### b) Motor learning



#### c) Pre-pulse inhibition

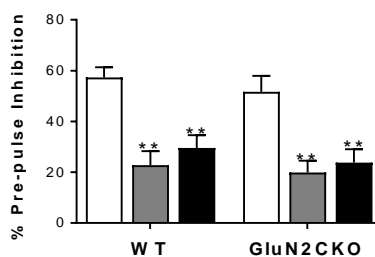


**Figure 8.** a) Latency to fall in the rotarod test after MK-801 (0.25 mg/kg;  $n = 9-11$ /group) or PCP (5 mg/kg;  $n = 7-8$ /group) administration. b) Latency to fall in the rotarod test in basal conditions ( $n = 10$ /group). c) Percentage (%) of pre-pulse inhibition after MK-801 (0.25 mg/kg) or PCP (5 mg/kg) administration ( $n = 10$ /group). \*\* $p < 0.01$  vs saline; ## $p < 0.01$  vs WT (Newman-Keuls *post hoc* test)

### 1.4. *In vivo* intracerebral microdialysis

Baseline extracellular concentrations of DA in NAC in WT and GluN2CKO mice were  $8 \pm 1$  fmol/30 $\mu$ l ( $n = 12$ ) and  $9 \pm 2$  fmol/30 $\mu$ l ( $n = 11$ ), respectively.

## Results

Unpaired *t*-test revealed no significant differences between genotypes. Saline injections did not alter dialysate DA values (Figure 9a) whereas MK-801 induced a moderate elevation (Figure 9b). Two-way repeated measures ANOVA showed a significant effect of time ( $F_{15,210}=2.51$ ;  $p<0.01$ ) but not of genotype or time x genotype interaction.

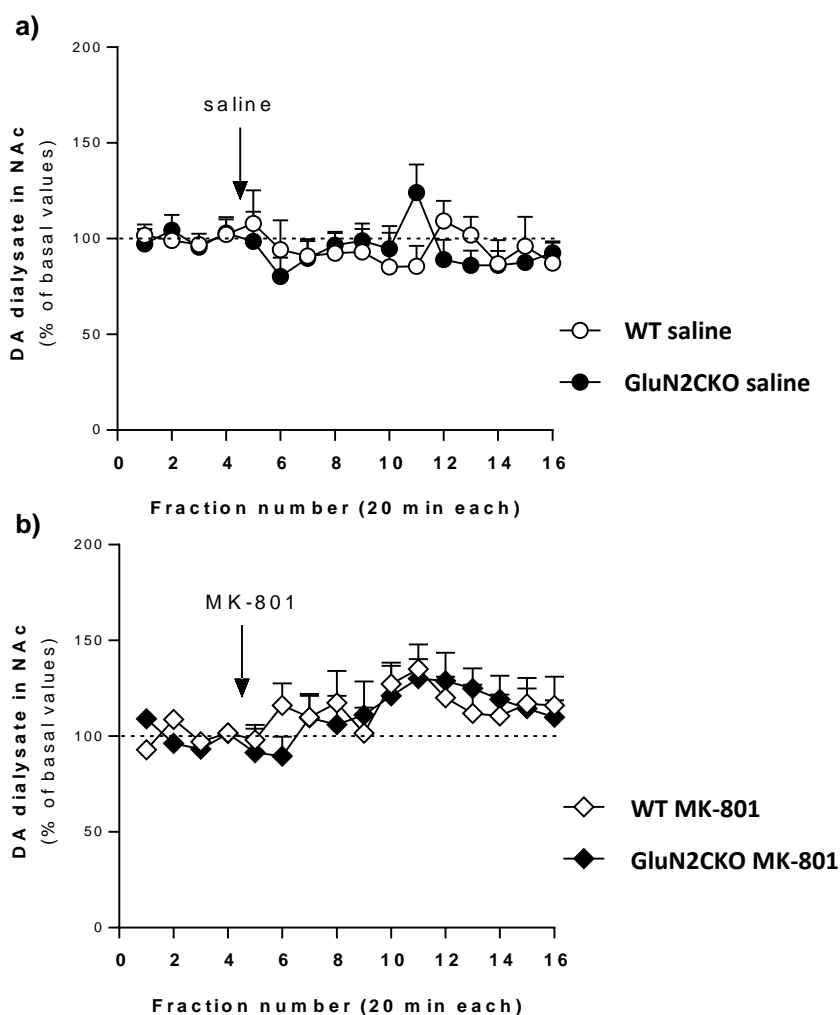


**Figure 9.** Time course of extracellular levels of DA in the NAc after a) Saline administration ( $n=7-8$ /group) or b) MK-801 administration ( $0.25$  mg/kg;  $n=7-9$ /group) in male WT and GluN2CKO mice. Microdialysis data are expressed as percentages of four basal values (fractions 1-4). The values are expressed as mean  $\pm$  S.E.M. The arrow represents the time of IP injection of saline or MK-801. Dialysate fractions were 20 min each.

### 1.5. *c-fos* and *zif268* mRNA expression

The effects of MK-801 and PCP on *c-fos* mRNA expression are shown following an anatomical anteroposterior order (Figures 10, 11 and 12). A detailed statistical analysis (two-way ANOVA) is shown in Table 1.

In WT mice, MK-801 (0.25 mg/kg) significantly enhanced *c-fos* mRNA expression in mPFC, cingulate cortex (Cg), NAc ( $p < 0.01$ , all cases) and piriform cortex (Pir) ( $p < 0.05$ ) and significantly decreased its expression in upper and deep layers of primary and secondary motor cortices (Upper M1-M2, Deep M1-M2) ( $p < 0.01$ , all cases). In GluN2CKO mice, MK-801 significantly increased *c-fos* expression in mPFC, NAc ( $p < 0.01$ , all cases) and Pir ( $p < 0.05$ ) and significantly reduced its expression in Upper M1-M2 ( $p < 0.05$ ). Significant differences between WT and GluN2CKO mice treated with MK-801 were found in mPFC, Cg, caudate-putamen nuclei (CPu) and NAc ( $p < 0.01$ , all cases). In WT mice, PCP (5 mg/kg) significantly enhanced *c-fos* mRNA expression in mPFC, Cg, CPu, NAc and Pir ( $p < 0.01$ , all cases) and significantly decreased its expression in Upper M1-M2 ( $p < 0.01$ ). In GluN2CKO mice, PCP significantly increased *c-fos* expression in mPFC, NAc ( $p < 0.01$ , all cases) and Pir ( $p < 0.05$ ) and significantly reduced its expression in Upper M1-M2, Deep M1-M2 and CPu ( $p < 0.01$ , all cases). Significant differences between WT and GluN2CKO mice treated with PCP were found in Cg, CPu and NAc ( $p < 0.01$ , all cases) (Figure 10).

In WT mice, MK-801 (0.25 mg/kg) significantly enhanced *c-fos* mRNA expression in RSC, HPC, habenula (Hb) and different thalamic nuclei (paraventricular thalamic nucleus, PV; mediodorsal thalamic nucleus, MD; intermediodorsal thalamic nucleus, IMD; centromedial thalamic nucleus, CM; paracentral thalamic nucleus, PC; VL; and reuniens and rhomboid nuclei of the thalamus, Re/Rh) ( $p < 0.01$ , all cases). In GluN2CKO mice, MK-801 significantly increased *c-fos* expression in RSC, HPC, Hb, different thalamic nuclei (PV, MD,

IMD, CM, Re/Rh) ( $p < 0.01$ , all cases) and PC ( $p < 0.05$ ). Significant differences between WT and GluN2CKO mice treated with MK-801 were found in PC and VL ( $p < 0.01$ , all cases). In WT mice, PCP (5 mg/kg) significantly enhanced *c-fos* mRNA expression in RSC, HPC and different thalamic nuclei (PV, MD, IMD, CM, PC, VL, Re/Rh) ( $p < 0.01$ , all cases). In GluN2CKO mice, PCP significantly increased *c-fos* expression in different thalamic nuclei (PV, MD, IMD, CM, PC, VL, Re/Rh) ( $p < 0.01$ , all cases). Significant differences between WT and GluN2CKO mice treated with PCP were found in RSC ( $p < 0.01$ ) and HPC ( $p < 0.05$ ) (Figure 11).

In WT mice, MK-801 (0.25 mg/kg) significantly enhanced *c-fos* mRNA expression in Amg, entorhinal cortex (EC) and dorsal raphe (DR) ( $p < 0.01$ , all cases) and significantly decreased its expression in Crus1 of the ansiform lobule (Crus1) and cerebellar simple lobule (Sim) ( $p < 0.01$ , all cases). In GluN2CKO mice, MK-801 significantly increased *c-fos* expression in Amg, EC, DR ( $p < 0.01$ , all cases) and Ve ( $p < 0.05$ ) and significantly reduced its expression in Sim ( $p < 0.01$ ). Significant differences between WT and GluN2CKO mice treated with MK-801 were found in Amg, lobules 4 and 5 of the cerebellar vermis (4/5Cb) ( $p < 0.05$ , all cases) and Crus1 ( $p < 0.01$ ). In WT mice, PCP (5 mg/kg) significantly enhanced *c-fos* mRNA expression in EC ( $p < 0.01$ ) and significantly decreased its expression in Crus1 and Sim ( $p < 0.01$ , all cases). In GluN2CKO mice, PCP significantly increased *c-fos* expression in Ve ( $p < 0.01$ ) and significantly decreased its expression in Sim ( $p < 0.01$ ). Significant differences between WT and GluN2CKO mice treated with PCP were found in EC, Crus1 ( $p < 0.01$ , all cases) and Ve ( $p < 0.05$ ) (Figure 12).

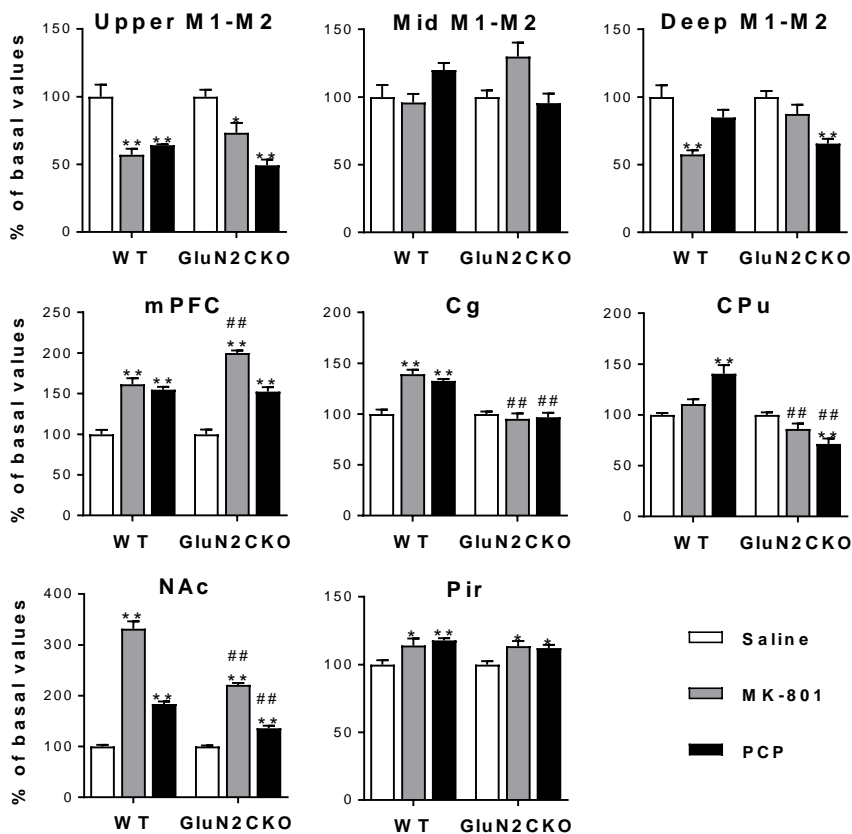


**Figure 10.** *C-fos* mRNA expression for male WT and GluN2CKO mice after MK-801 (0.25 mg/kg) or PCP (5 mg/kg) administration in upper, intermediate and deep layers of primary and secondary motor cortices (Upper M1-M2, Mid M1-M2 and Deep M1-M2, AP: +2.10), medial prefrontal cortex (mPFC, AP: +2.10), cingulate cortex (Cg, AP: +1.18), caudate-putamen nuclei (CPu, AP: +1.18), nucleus accumbens (NAc, AP: +1.18) and piriform cortex (Pir, AP: +1.18) (n=8-10/group in saline groups; n=4-5/group in treated groups). \*p<0.05, \*\*p<0.01 vs saline; ##p<0.01 vs WT (Newman-Keuls *post hoc* test)

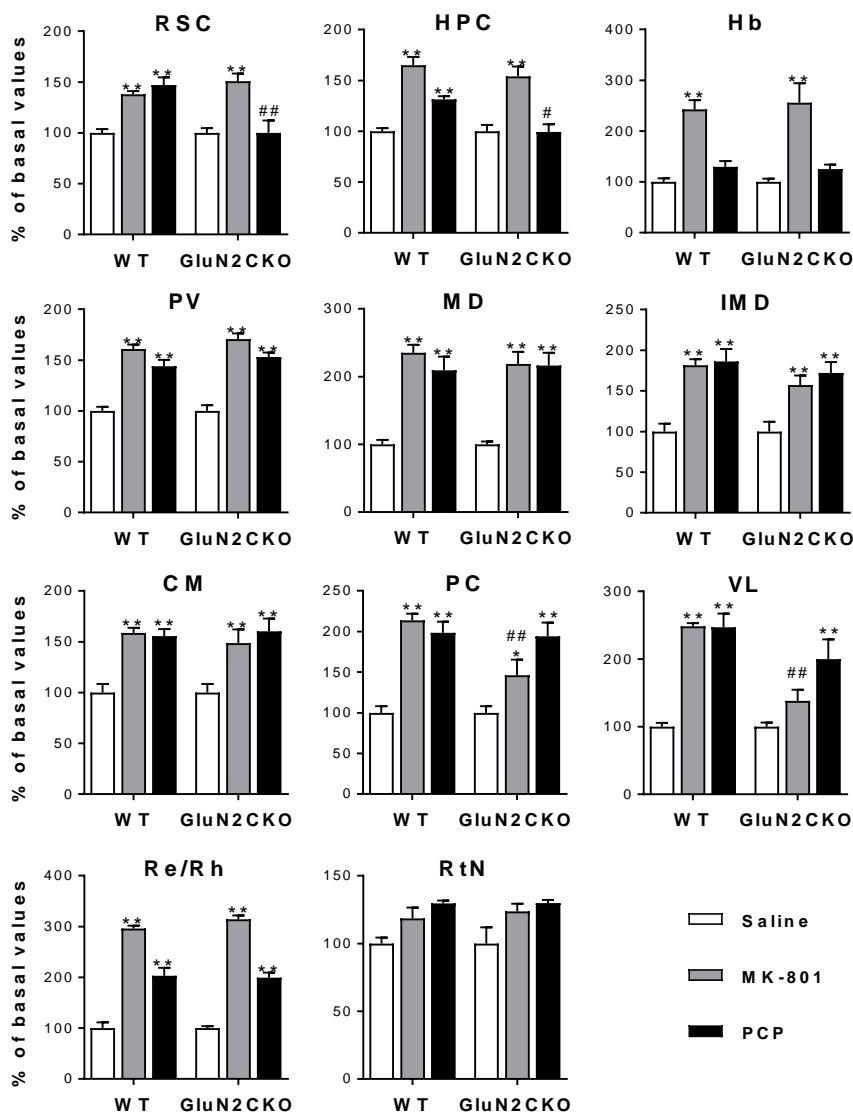


**Figure 11.** *C-fos* mRNA expression for male WT and GluN2CKO mice after MK-801 (0.25 mg/kg) or PCP (5 mg/kg) administration in retrosplenial cortex (RSC, AP: -1.70), hippocampus (HPC, AP: -1.70), habenula (Hb, AP: -1.70), paraventricular thalamic nucleus (PV, AP: -1.70), mediodorsal thalamic nucleus (MD, AP: -1.70), intermediodorsal thalamic nucleus (IMD, AP: -1.70), centromedial thalamic nucleus (CM, AP: -1.70), paracentral thalamic nucleus (PC, AP: -1.70), ventrolateral thalamic nucleus (VL, AP: -1.70), reuniens and rhomboid nuclei of the thalamus (Re/Rh, AP: -1.70) and reticular nucleus (RtN, AP: -1.70) (n=8-10/group in saline groups; n=4-5/group in treated groups). \*p<0.05, \*\*p<0.01 vs saline; #p<0.05, ##p<0.01 vs WT (Newman-Keuls *post hoc* test)



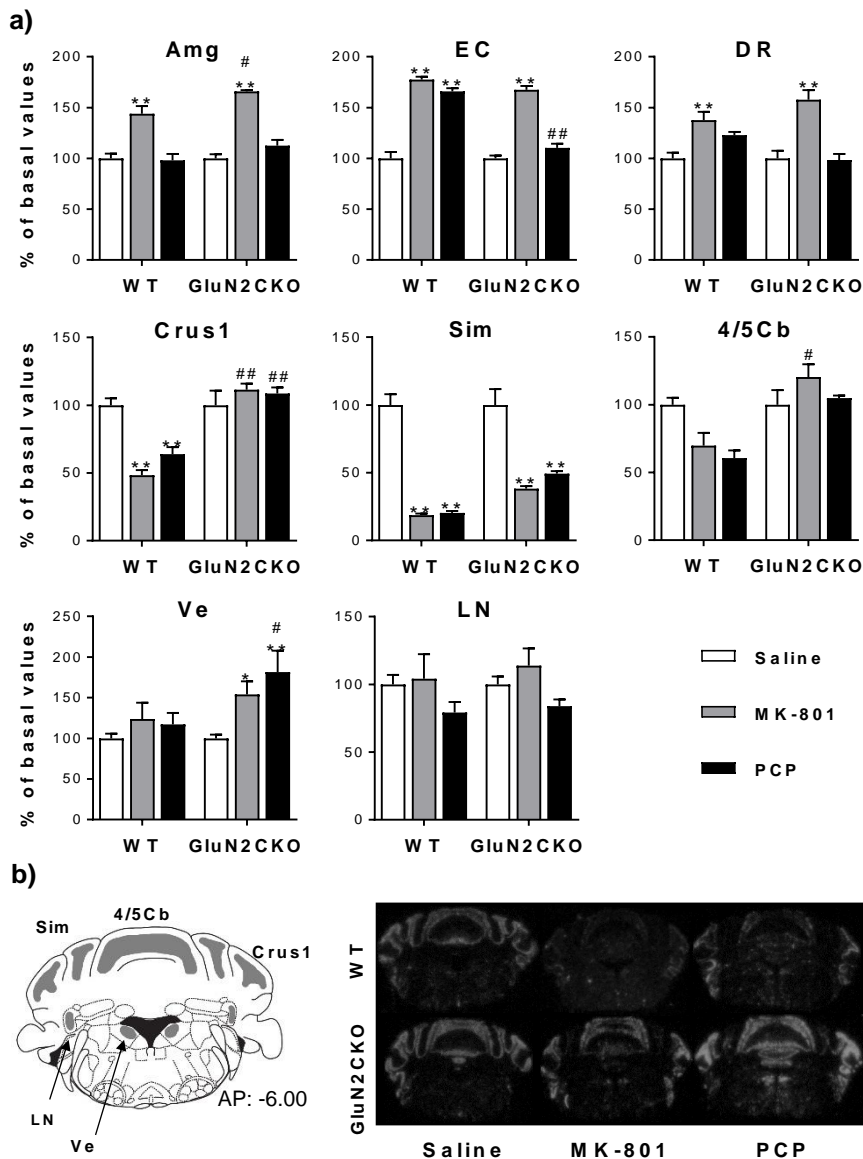


**Figure 12.** a) *C-fos* mRNA expression for male WT and GluN2CKO mice after MK-801 (0.25 mg/kg) or PCP (5 mg/kg) administration in amygdala (Amg, AP: -3.40), entorhinal cortex (EC, AP: -3.40), dorsal raphe (DR, AP: -4.60), crus 1 of the ansiform lobule (Crus1, AP: -6.00), cerebellar simple lobule (Sim, AP: -6.00), lobules 4 and 5 of the cerebellar vermis (4/5Cb, AP: -6.00), vestibular nucleus (Ve, AP: -6.00), and lateral nucleus (LN, AP: -6.00). (n=8-10/group in saline groups; n=4-5/group in treated groups). b) On the left, analyzed regions of the cerebellum from the Franklin & Paxinos mouse atlas; on the right, representative film images of *c-fos* mRNA expression in the different experimental groups. \* $p < 0.05$ , \*\* $p < 0.01$  vs saline; # $p < 0.05$ , ## $p < 0.01$  vs WT (Newman-Keuls *post hoc* test)

## Results

	Treatment (T)		Genotype (G)		T x G		Figure
Upper M1-M2	$F_{2,33}=21.91$	$p<0.0001$	$F_{1,33}=0.01$	n.s.	$F_{2,33}=1.68$	n.s.	10
Mid M1-M2	$F_{2,34}=1.48$	n.s.	$F_{1,34}=0.22$	n.s.	$F_{2,34}=5.37$	$p<0.01$	10
Deep M1-M2	$F_{2,33}=10.80$	$p<0.001$	$F_{1,33}=0.36$	n.s.	$F_{2,33}=5.04$	$p<0.05$	10
mPFC	$F_{2,34}=110.80$	$p<0.0001$	$F_{1,34}=5.86$	$p<0.05$	$F_{2,34}=6.52$	$p<0.01$	10
Cg	$F_{2,34}=12.40$	$p<0.0001$	$F_{1,34}=59.92$	$p<0.0001$	$F_{2,34}=19.12$	$p<0.0001$	10
CPu	$F_{2,33}=1.48$	n.s.	$F_{1,33}=75.25$	$p<0.0001$	$F_{2,33}=33.78$	$p<0.0001$	10
NAc	$F_{2,34}=507.40$	$p<0.0001$	$F_{1,34}=121.90$	$p<0.0001$	$F_{2,34}=50.11$	$p<0.0001$	10
Pir	$F_{2,33}=14.56$	$p<0.0001$	$F_{1,33}=0.52$	n.s.	$F_{2,33}=0.41$	n.s.	10
RSC	$F_{2,34}=26.99$	$p<0.0001$	$F_{1,34}=4.57$	$p<0.05$	$F_{2,34}=10.17$	$p<0.001$	11
HPC	$F_{2,33}=44.05$	$p<0.0001$	$F_{1,33}=6.81$	$p<0.05$	$F_{2,33}=3.13$	n.s.	11
Hb	$F_{2,34}=54.20$	$p<0.0001$	$F_{1,34}=0.06$	n.s.	$F_{2,34}=0.15$	n.s.	11
PV	$F_{2,34}=90.98$	$p<0.0001$	$F_{1,34}=1.92$	n.s.	$F_{2,34}=0.60$	n.s.	11
MD	$F_{2,31}=80.70$	$p<0.0001$	$F_{1,31}=0.10$	n.s.	$F_{2,31}=0.42$	n.s.	11
IMD	$F_{2,32}=27.92$	$p<0.0001$	$F_{1,32}=1.48$	n.s.	$F_{2,32}=0.55$	n.s.	11
CM	$F_{2,34}=25.75$	$p<0.0001$	$F_{1,34}=0.05$	n.s.	$F_{2,34}=0.24$	n.s.	11
PC	$F_{2,32}=43.54$	$p<0.0001$	$F_{1,32}=5.68$	$p<0.05$	$F_{2,32}=4.72$	$p<0.05$	11
VL	$F_{2,32}=54.41$	$p<0.0001$	$F_{1,32}=22.36$	$p<0.0001$	$F_{2,32}=9.59$	$p<0.001$	11
Re/Rh	$F_{2,33}=244.20$	$p<0.0001$	$F_{1,33}=0.36$	n.s.	$F_{2,33}=0.64$	n.s.	11
RtN	$F_{2,33}=6.49$	$p<0.01$	$F_{1,33}=0.05$	n.s.	$F_{2,33}=0.04$	n.s.	11
Amg	$F_{2,33}=61.06$	$p<0.0001$	$F_{1,33}=7.61$	$p<0.01$	$F_{2,33}=2.55$	n.s.	12
EC	$F_{2,33}=121.20$	$p<0.0001$	$F_{1,33}=27.17$	$p<0.0001$	$F_{2,33}=16.02$	$p<0.0001$	12
DR	$F_{2,32}=21.52$	$p<0.0001$	$F_{1,32}=0.05$	n.s.	$F_{2,32}=3.35$	$p<0.05$	12
Crus1	$F_{2,32}=4.45$	$p<0.05$	$F_{1,32}=35.42$	$p<0.0001$	$F_{2,32}=11.33$	$p<0.001$	12
Sim	$F_{2,33}=47.41$	$p<0.0001$	$F_{1,33}=4.81$	$p<0.05$	$F_{2,33}=1.60$	n.s.	12
4/5Cb	$F_{2,32}=1.73$	n.s.	$F_{1,32}=16.28$	$p<0.001$	$F_{2,32}=5.19$	$p<0.05$	12
Ve	$F_{2,33}=9.78$	$p<0.001$	$F_{1,33}=8.42$	$p<0.01$	$F_{2,33}=3.47$	$p<0.05$	12
LN	$F_{2,34}=3.60$	$p<0.05$	$F_{1,34}=0.38$	n.s.	$F_{2,34}=0.15$	n.s.	12

**Table 1.** Two-way ANOVA (treatment (T) and genotype (G) as factors) for *c-fos* expression data in male WT and GluN2CKO mice in upper, intermediate and deep layers of primary and secondary motor cortices (Upper M1-M2, Mid M1-M2 and Deep M1-M2, AP: +2.10), medial prefrontal cortex (mPFC, AP: +2.10), cingulate cortex (Cg, AP: +1.18), caudate-putamen nuclei (CPu, AP: +1.18), nucleus accumbens (NAc, AP: +1.18), piriform cortex (Pir, AP: +1.18), retrosplenial cortex (RSC, AP: -1.70), hippocampus (HPC, AP: -1.70), habenula (Hb, AP: -1.70), paraventricular thalamic nucleus (PV, AP: -1.70), mediodorsal thalamic nucleus (MD, AP: -1.70), intermediodorsal thalamic nucleus (IMD, AP: -1.70), centromedial thalamic nucleus (CM, AP: -1.70), paracentral thalamic nucleus (PC, AP: -1.70), ventrolateral thalamic nucleus (VL, AP: -1.70), reuniens and rhomboid nuclei of the thalamus (Re/Rh, AP: -1.70), reticular nucleus (RtN, AP: -1.70), amygdala (Amg, AP: -3.40), entorhinal cortex (EC, AP: -3.40), dorsal raphe (DR, AP: -4.60), crus 1 of the ansiform lobule (Crus1, AP: -6.00), cerebellar simple lobule (Sim, AP: -6.00), lobules 4 and 5 of the cerebellar vermis (4/5Cb, AP: -6.00), vestibular nucleus (Ve, AP: -6.00), and lateral nucleus (LN, AP: -6.00).

The effects of MK-801 and PCP on *zif268* expression are shown in Figure 13. In Crus1, two-way ANOVA showed a main effect of genotype ( $F_{1,23}=12.47$ ;  $p<0.01$ ). *Post hoc* comparisons showed significant differences between WT and GluN2CKO mice treated with MK-801 or PCP ( $p<0.05$ , all cases). In Sim, two-way ANOVA indicated a main effect of treatment ( $F_{2,23}=3.73$ ;  $p<0.05$ ), genotype ( $F_{1,23}=21.50$ ;  $p<0.001$ ) and treatment x genotype interaction ( $F_{2,23}=5.17$ ;  $p<0.05$ ). *Post hoc* comparisons showed a reduction in *zif268* expression after MK-801 administration in WT mice ( $p<0.05$ ) and significant differences between WT and GluN2CKO mice treated with MK-801 or PCP ( $p<0.01$ , all cases). In 4/5Cb, two-way ANOVA showed a main effect of treatment ( $F_{2,20}=7.44$ ;  $p<0.01$ ), genotype ( $F_{1,20}=16.52$ ;  $p<0.001$ ) and treatment x genotype interaction ( $F_{2,20}=4.80$ ;  $p<0.05$ ). *Post hoc* comparisons showed increased *zif268* expression in GluN2CKO mice after MK-801 ( $p<0.05$ ) or PCP ( $p<0.01$ ) treatment and significant differences between WT and GluN2CKO mice treated with MK-801 ( $p<0.01$ ) or PCP ( $p<0.05$ ).

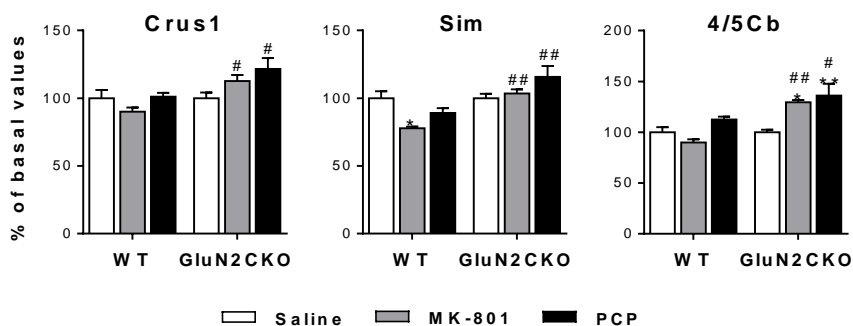


**Figure 13.** *Zif268* mRNA expression for male WT and GluN2CKO mice after MK-801 (0.25 mg/kg) or PCP (5 mg/kg) administration in crus 1 of the ansiform lobule (Crus1, AP: -6.00), cerebellar simple lobule (Sim, AP: -6.00) and lobules 4 and 5 of the cerebellar vermis (4/5Cb, AP: -6.00) ( $n=4-5$ /group). \* $p<0.05$ , \*\* $p<0.01$  vs saline; # $p<0.05$ , ## $p<0.01$  vs WT (Newman-Keuls *post hoc* test)

## 2. Involvement of the GluN2C subunit in the mechanism of action of ketamine in male and female mice

### 2.1. Behavioral syndrome

The acute administration of ketamine (10 and 30 mg/kg) significantly increased locomotor activity in male and female GluN2CKO mice (Figure 14). For male mice, two-way ANOVA showed a main effect of treatment ( $F_{2,59}=25.32$ ;  $p<0.0001$ ), genotype ( $F_{1,59}=17.57$ ;  $p<0.0001$ ) and interaction ( $F_{2,59}=5.49$ ;  $p<0.01$ ). *Post hoc* comparisons indicated a significant increase in locomotor activity in male GluN2CKO mice after ketamine administration ( $p<0.01$ , all cases) and a significant difference between male WT and GluN2CKO mice treated with ketamine ( $p<0.01$ , all cases). For female mice, two-way ANOVA showed a main effect of treatment ( $F_{2,63}=24.47$ ;  $p<0.0001$ ), genotype ( $F_{1,63}=11.93$ ;  $p<0.01$ ) and interaction ( $F_{2,63}=6.98$ ;  $p<0.01$ ). *Post hoc* comparisons revealed a significant increase in locomotor activity in female WT mice after the high dose of ketamine ( $p<0.01$ ) and in female GluN2CKO mice after both doses of ketamine ( $p<0.01$ , all cases). Moreover, a significant difference between female WT and GluN2CKO mice treated with ketamine (10 mg/kg;  $p<0.01$ ) was also found.

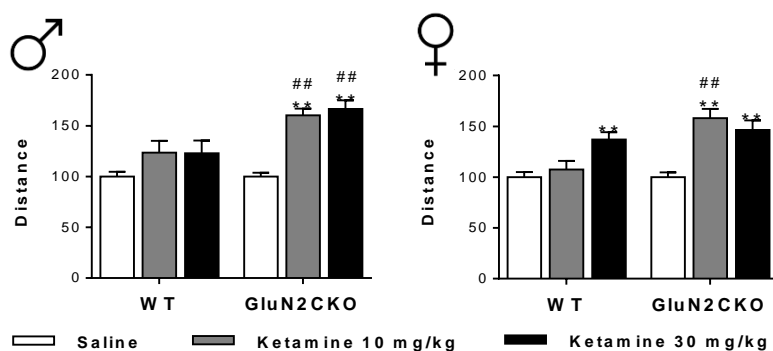


**Figure 14.** Effects of ketamine (10 and 30 mg/kg) in male and female WT and GluN2CKO mice on locomotor activity (percentage of distance from saline-treated mice) ( $n=15-18$ /group in saline groups;  $n=8-10$ /group in treated groups). \*\* $p<0.01$  vs saline; ## $p<0.01$  vs WT (Newman-Keuls *post hoc* test)

Ketamine (10 and 30 mg/kg) reduced the number of rearings in male and female WT and GluN2CKO mice (Figure 15a). For male mice, two-way ANOVA showed a main effect of treatment ( $F_{2,59}=65.99$ ;  $p<0.0001$ ) and genotype ( $F_{1,59}=5.95$ ;  $p<0.05$ ). *Post hoc* comparisons indicated a significant reduction in the number of rearings in both genotypes after ketamine treatment ( $p<0.01$ , all cases). For female mice, two-way ANOVA showed a main effect of treatment ( $F_{2,63}=74.64$ ;  $p<0.0001$ ) and genotype ( $F_{1,63}=5.40$ ;  $p<0.05$ ). *Post hoc* comparisons revealed a significant reduction in the number of rearings in both genotypes after ketamine treatment ( $p<0.01$  in all cases, except in GluN2CKO mice after the low dose of ketamine,  $p<0.05$ ) and a significant difference between female WT and GluN2CKO mice after ketamine 10 mg/kg ( $p<0.01$ ).

Ketamine (30 mg/kg) significantly increased the number of falls in male and female WT mice (Figure 15b). For male mice, two-way ANOVA showed a main effect of treatment ( $F_{2,59}=20.38$ ;  $p<0.0001$ ). *Post hoc* comparisons indicated a significant increase in the number of falls in male WT mice ( $p<0.01$ ). For female mice, two-way ANOVA showed a main effect of treatment ( $F_{2,63}=31.35$ ;  $p<0.0001$ ), genotype ( $F_{1,63}=29.48$ ;  $p<0.0001$ ) and interaction ( $F_{2,63}=24.73$ ;  $p<0.0001$ ). *Post hoc* comparisons revealed a significant increase in the number of falls in female WT mice ( $p<0.01$ ) and a significant difference between female WT and GluN2CKO mice treated with ketamine 30 mg/kg ( $p<0.01$ ).

Regarding hindlimb abduction, ketamine (10 and 30 mg/kg) increased this ataxic behavior in both genotypes and sexes (Figure 15c). For male mice, two-way ANOVA showed a main effect of treatment ( $F_{2,59}=159.40$ ;  $p<0.0001$ ), genotype ( $F_{1,59}=24.39$ ;  $p<0.0001$ ) and interaction ( $F_{2,59}=12.82$ ;  $p<0.01$ ). *Post hoc* comparisons indicated a significant increase in hindlimb abduction after ketamine in both genotypes ( $p<0.01$ , all cases) and a significant difference between male WT and GluN2CKO mice treated with the high dose of ketamine ( $p<0.01$ ). For female mice, two-way ANOVA showed a main effect of treatment ( $F_{2,63}=110.50$ ;  $p<0.0001$ ), genotype ( $F_{1,63}=7.39$ ;  $p<0.01$ ) and

interaction ( $F_{2,63}=3.87$ ;  $p<0.05$ ). *Post hoc* comparisons revealed a significant increase in hindlimb abduction in both genotypes after ketamine ( $p<0.01$  in all cases, except in GluN2CKO mice after the low dose of ketamine,  $p<0.05$ ) and a significant difference between female WT and GluN2CKO mice after ketamine 30 mg/kg ( $p<0.01$ ).

Ketamine (30 mg/kg) increased circling behavior in male and female WT mice (Figure 15d). For male mice, two-way ANOVA showed a main effect of treatment ( $F_{2,59}=74.50$ ;  $p<0.0001$ ), genotype ( $F_{1,59}=96.96$ ;  $p<0.0001$ ) and interaction ( $F_{2,59}=72.06$ ;  $p<0.0001$ ). For female mice, two-way ANOVA showed a main effect of treatment ( $F_{2,63}=29.41$ ;  $p<0.0001$ ), genotype ( $F_{1,63}=23.59$ ;  $p<0.0001$ ) and interaction ( $F_{2,63}=20.80$ ;  $p<0.0001$ ). In both sexes, *post hoc* comparisons indicated a significant increase in circling behavior in WT after the high dose of ketamine ( $p<0.01$ , all cases) and a significant difference between WT and GluN2CKO mice after ketamine 30 mg/kg ( $p<0.01$ , all cases).

### **2.2. Antidepressant-like effect**

Acute administration of ketamine (10 mg/kg) in male mice did not produce changes in the latency to feed in the NSFT (Figure 16a). In the FST, two-way ANOVA showed a main effect of treatment ( $F_{1,36}=5.28$ ;  $p<0.05$ ) (Figure 16b).

Ketamine (30 mg/kg) decreased the immobility time in the TST in male and female WT and GluN2CKO mice (Figure 16c). For male mice, two-way ANOVA showed a main effect of treatment ( $F_{2,54}=86.36$ ;  $p<0.0001$ ). *Post hoc* comparisons indicated a significant reduction in immobility in male WT mice after ketamine 10 mg/kg ( $p<0.05$ ) and in male WT and GluN2CKO mice after ketamine 30 mg/kg ( $p<0.01$ , all cases). For female mice, two-way ANOVA showed a main effect of treatment ( $F_{2,67}=22.70$ ;  $p<0.0001$ ). *Post hoc* comparisons revealed a significant decrease in immobility in female WT and GluN2CKO mice after ketamine 30 mg/kg ( $p<0.01$ , all cases).

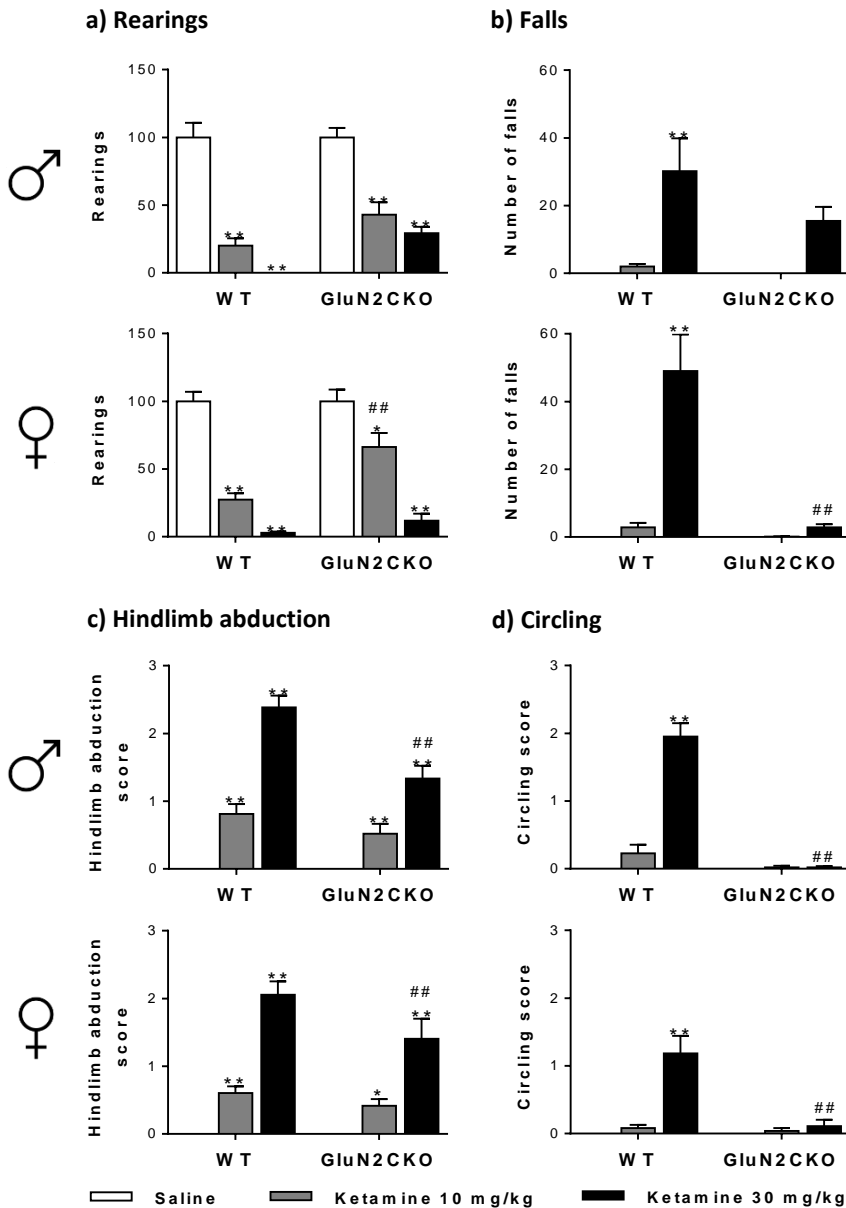


**Figure 15.** Effects of ketamine (10 and 30 mg/kg) in male and female WT and GluN2CKO mice on a) Rearings (percentage from saline-treated mice), b) Falls, c) Hindlimb abduction and d) Circling (n=15-18/group in saline groups; n=8-10/group in treated groups). \*p<0.05, \*\*p<0.01 vs saline; ##p<0.01 vs WT (Newman-Keuls *post hoc* test)

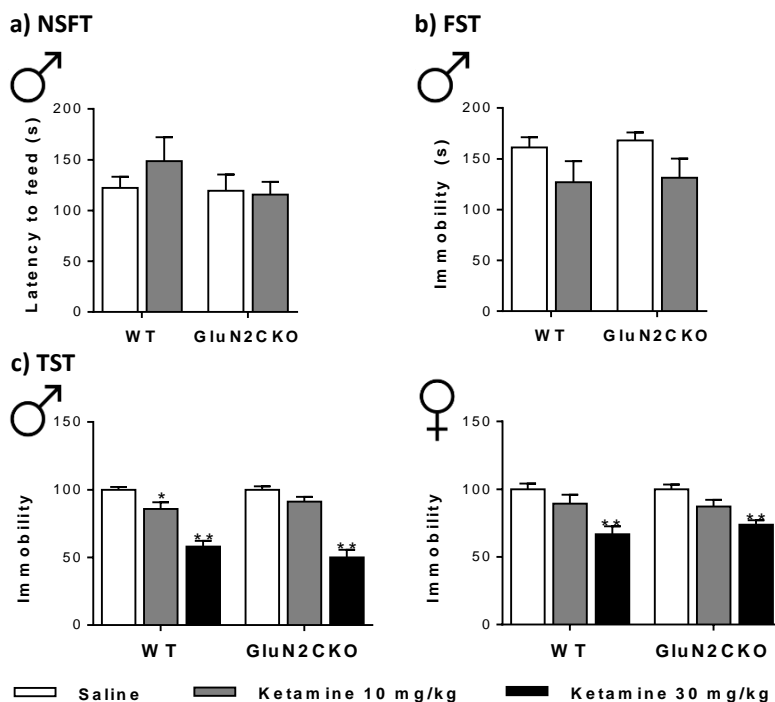


**Figure 16.** Effects of 10 mg/kg ketamine in male mice on a) NSFT (n=9) and b) FST (n=10). c) Percentage of immobility from saline-treated mice in the TST after ketamine (10 and 30 mg/kg) in male (n=14-15 in saline groups; n=7-8 in treated groups) and female (n=16-18 in saline groups; n=7-12 in treated groups) WT and GluN2CKO mice. \*p<0.05, \*\*p<0.01 vs saline (Newman-Keuls *post hoc* test)

### 2.3. *In vivo* intracerebral microdialysis

Baseline extracellular concentrations of 5-HT in mPFC in male WT and GluN2CKO mice were  $17 \pm 2$  fmol/50 $\mu$ l (n=19) and  $14 \pm 2$  fmol/50 $\mu$ l (n=17), respectively. Unpaired *t*-test revealed no significant differences between genotypes. Baseline extracellular concentrations of Glu in mPFC in male WT and GluN2CKO mice were  $11 \pm 1$  pmol/50 $\mu$ l (n=19) and  $9 \pm 1$  pmol/50 $\mu$ l (n=17), respectively. Unpaired *t*-test revealed no significant differences between genotypes. Baseline extracellular concentrations of 5-HT in mPFC in female WT and GluN2CKO mice were  $21 \pm 4$  fmol/50 $\mu$ l (n=13) and  $18 \pm 4$  fmol/50 $\mu$ l



(n=14), respectively. Unpaired *t*-test revealed no significant differences between genotypes. Baseline extracellular concentrations of Glu in mPFC in female WT and GluN2CKO mice were  $7 \pm 1$  pmol/50 $\mu$ l (n=12) and  $7 \pm 1$  pmol/50 $\mu$ l (n=14), respectively. Unpaired *t*-test revealed no significant differences between genotypes.

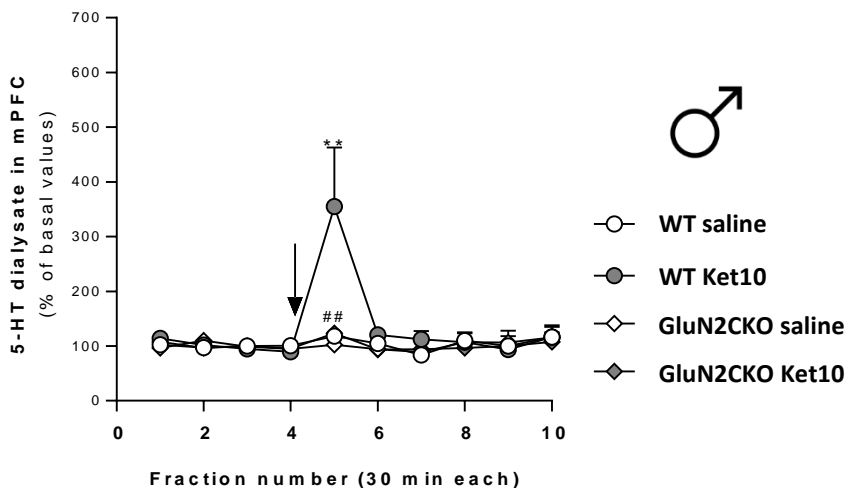
Ketamine (10 mg/kg) significantly increased 5-HT and Glu release in mPFC of male WT mice (Figure 17). For 5-HT, three-way ANOVA showed a main effect of time ( $F_{9,279}=5.46$ ;  $p<0.000001$ ), treatment x time interaction ( $F_{9,279}=4.14$ ;  $p<0.0001$ ), genotype x time interaction ( $F_{9,279}=3.66$ ;  $p<0.001$ ) and treatment x genotype x time interaction ( $F_{9,279}=2.74$ ;  $p<0.01$ ). For Glu, three-way ANOVA showed a main effect of treatment ( $F_{1,31}=8.96$ ;  $p<0.01$ ), time ( $F_{9,279}=2.72$ ;  $p<0.01$ ) and treatment x genotype x time interaction ( $F_{9,279}=2.62$ ;  $p<0.01$ ). In both cases, *post hoc* comparisons indicated a significant increase of 5-HT and Glu release in ketamine-treated WT mice vs controls ( $p<0.01$ , all cases) and a significant difference between WT and GluN2CKO mice treated with ketamine ( $p<0.01$ , all cases) in fraction 5.

Ketamine (30 mg/kg) significantly enhanced 5-HT and Glu release in mPFC in male mice (Figure 18). For 5-HT, three-way ANOVA showed a main effect of treatment ( $F_{1,31}=19.17$ ;  $p<0.0001$ ), genotype ( $F_{1,31}=12.01$ ;  $p<0.01$ ), time ( $F_{9,279}=8.33$ ;  $p<0.0000$ ), treatment x genotype interaction ( $F_{1,31}=11.81$ ;  $p<0.01$ ), treatment x time interaction ( $F_{9,279}=7.57$ ;  $p<0.0000$ ), genotype x time interaction ( $F_{9,279}=3.37$ ;  $p<0.001$ ) and treatment x genotype x time interaction ( $F_{9,279}=3.11$ ;  $p<0.01$ ). *Post hoc* comparisons indicated a significant increase of 5-HT release in ketamine-treated WT mice compared to controls in fraction 5 ( $p<0.01$ ) and fraction 6 ( $p<0.05$ ) and a significant difference between WT and GluN2CKO mice treated with ketamine in fraction 5 ( $p<0.01$ ) and fraction 6 ( $p<0.05$ ). For Glu, three-way ANOVA showed a main effect of treatment ( $F_{1,32}=16.69$ ;  $p<0.001$ ), time ( $F_{9,288}=5.44$ ;  $p<0.0000$ ), treatment x time interaction ( $F_{9,288}=4.71$ ;  $p<0.0000$ ) and treatment x genotype x time

interaction ( $F_{9,288}=2.01$ ;  $p<0.05$ ). *Post hoc* comparisons indicated a significant increase of Glu release in ketamine-treated WT ( $p<0.05$ ) and GluN2CKO ( $p<0.01$ ) mice compared to controls in fraction 5. *Post hoc* comparisons also revealed a significant increase of Glu release in ketamine-treated WT mice ( $p<0.01$ ) and a significant difference between WT and GluN2CKO mice treated with ketamine ( $p<0.01$ ) in fraction 10.

In female mice, ketamine (30 mg/kg) significantly increased 5-HT and Glu release in mPFC (Figure 19). For 5-HT, three-way ANOVA showed a main effect of treatment ( $F_{1,46}=8.18$ ;  $p<0.01$ ), time ( $F_{9,414}=7.74$ ;  $p<0.0000$ ) and treatment x time interaction ( $F_{9,414}=5.55$ ;  $p<0.0000$ ). *Post hoc* comparisons indicated a significant increase of 5-HT release in WT and GluN2CKO female mice ( $p<0.01$ , all cases) and a significant difference between WT and GluN2CKO mice treated with ketamine ( $p<0.01$ ) in fraction 5. For Glu, three-way ANOVA showed a main effect of treatment ( $F_{1,46}=11.41$ ;  $p<0.01$ ), time ( $F_{9,414}=5.00$ ;  $p<0.0000$ ) and treatment x time interaction ( $F_{9,414}=4.24$ ;  $p<0.0000$ ). *Post hoc* comparisons indicated a significant increase of Glu release in GluN2CKO mice in fractions 9 and 10 ( $p<0.01$ , all cases) and a significant difference between WT and GluN2CKO mice treated with ketamine ( $p<0.01$ ) in fraction 9.

## a) Serotonin



## b) Glutamate

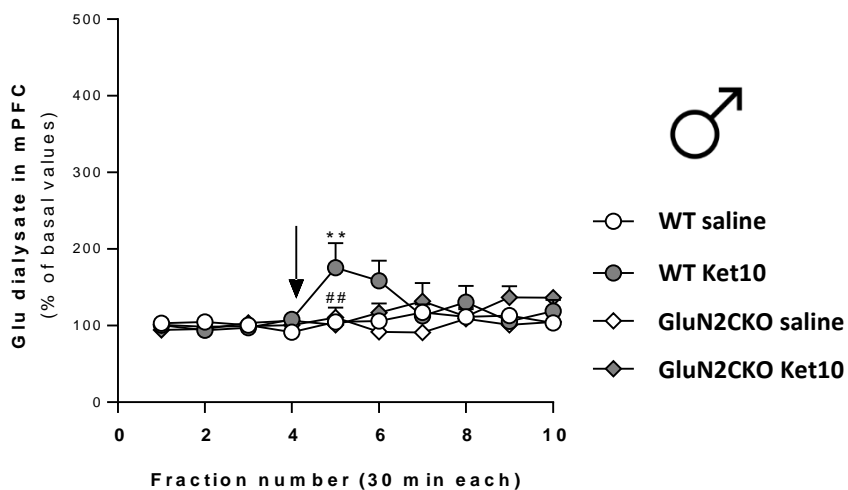
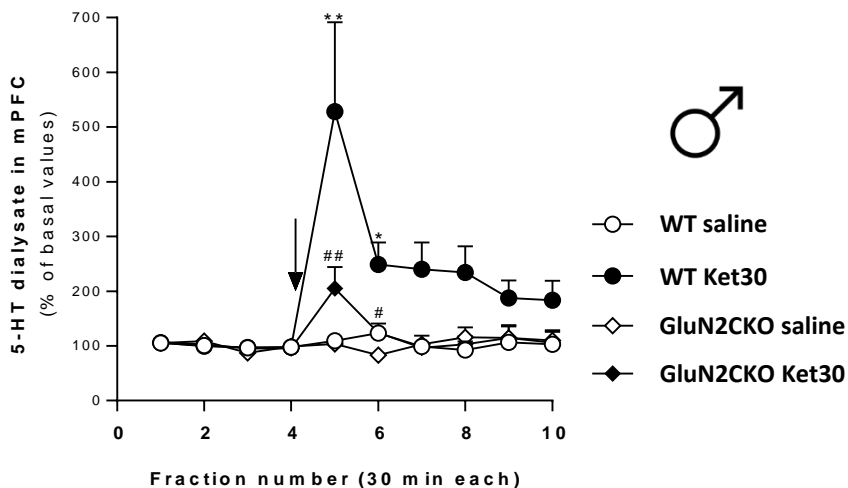


**Figure 17.** Time course of extracellular levels of a) Serotonin and b) Glutamate in mPFC after saline (n=7-8/group) or ketamine (Ket10; 10 mg/kg; n=8-9/group) administration in male WT and GluN2CKO mice. Microdialysis data are expressed as percentages of four basal values (fractions 1-4). The values are expressed as mean  $\pm$  S.E.M. The arrow represents the time of IP injection of saline or ketamine. Dialysate fractions were 30 min each. \*\*p<0.01 vs saline; ##p<0.01 vs WT (Newman-Keuls *post hoc* test)

a) Serotonin



b) Glutamate

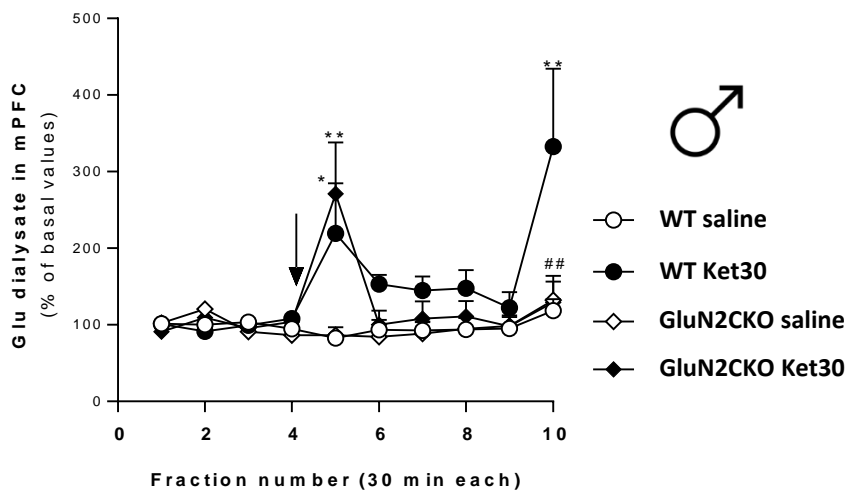
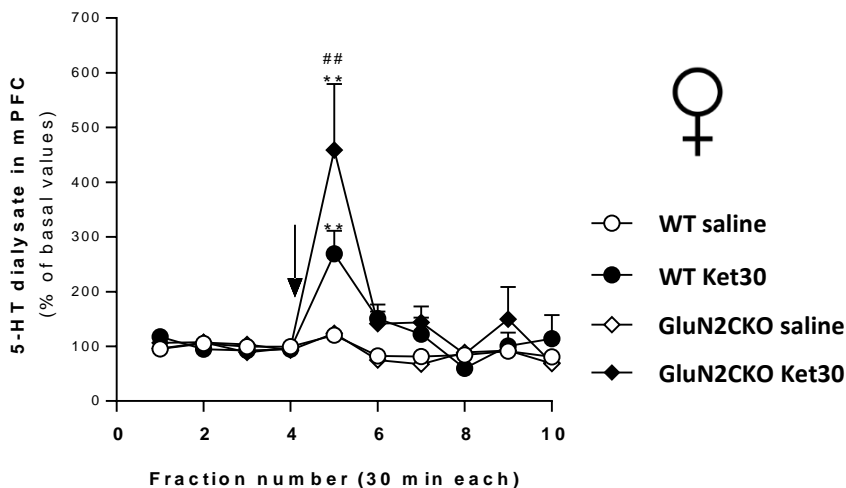


**Figure 18.** Time course of extracellular levels of a) Serotonin and b) Glutamate in mPFC after saline (n=9/group) or ketamine (Ket30; 30 mg/kg; n=8-9/group) administration in male WT and GluN2CKO mice. Microdialysis data are expressed as percentages of four basal values (fractions 1-4). The values are expressed as mean  $\pm$  S.E.M. The arrow represents the time of IP injection of saline or ketamine. Dialysate fractions were 30 min each. \*p<0.05, \*\*p<0.01 vs saline; #p<0.05, ##p<0.01 vs WT (Newman-Keuls *post hoc* test)

## a) Serotonin



## b) Glutamate

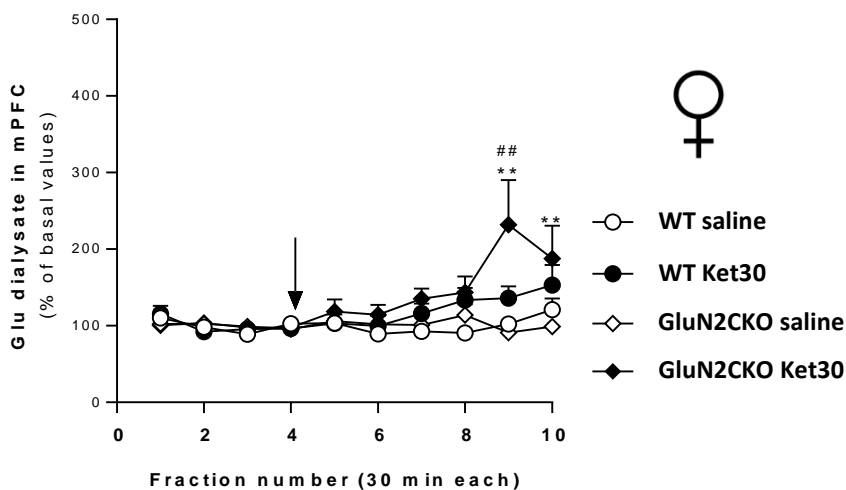


**Figure 19.** Time course of extracellular levels of a) Serotonin and b) Glutamate in mPFC after saline (n=13-14/group) or ketamine (Ket30; 30 mg/kg; n=11/group) administration in female WT and GluN2CKO mice. Microdialysis data are expressed as percentages of four basal values (fractions 1-4). The values are expressed as mean  $\pm$  S.E.M. The arrow represents the time of IP injection of saline or ketamine. Dialysate fractions were 30 min each. \*\*p<0.01 vs saline; ##p<0.01 vs WT (Newman-Keuls *post hoc* test)

## 2.4. *c-fos* mRNA expression

The effects of ketamine on *c-fos* mRNA expression in male mice are shown following an anatomical anteroposterior order (Figures 20, 21 and 22). A detailed statistical analysis (two-way ANOVA) is shown in Table 2.

In male WT mice, ketamine (30 mg/kg) significantly enhanced *c-fos* mRNA expression in intermediate layer of primary and secondary motor cortices (Mid M1-M2), mPFC and Cg ( $p < 0.01$ , all cases). In male GluN2CKO mice, ketamine significantly increased *c-fos* expression in Mid M1-M2, Deep M1-M2, mPFC, NAc ( $p < 0.01$ , all cases) and Cg ( $p < 0.05$ ). Significant differences between male WT and GluN2CKO mice treated with ketamine were found in Mid M1-M2, Deep M1-M2 ( $p < 0.01$ , all cases) and CPu ( $p < 0.05$ ) (Figure 20).

In male WT mice, ketamine (30 mg/kg) significantly enhanced *c-fos* mRNA expression in RSC ( $p < 0.05$ ) and PV ( $p < 0.01$ ). In male GluN2CKO mice, ketamine significantly increased *c-fos* expression in PV and IMD ( $p < 0.01$ , all cases) and significantly reduced its expression in HPC ( $p < 0.01$ ). Significant differences between male WT and GluN2CKO mice treated with ketamine were found in HPC ( $p < 0.05$ ), Hb, PV and IMD ( $p < 0.01$ , all cases) (Figure 21).

In male WT mice, ketamine (30 mg/kg) significantly decreased *c-fos* mRNA expression in Crus1, Sim, 4/5Cb and Ve ( $p < 0.01$ , all cases). In male GluN2CKO mice, ketamine significantly reduced *c-fos* expression in Crus1, Sim ( $p < 0.01$ , all cases) and 4/5Cb ( $p < 0.05$ ). No significant differences were found between male WT and GluN2CKO mice (Figure 22).

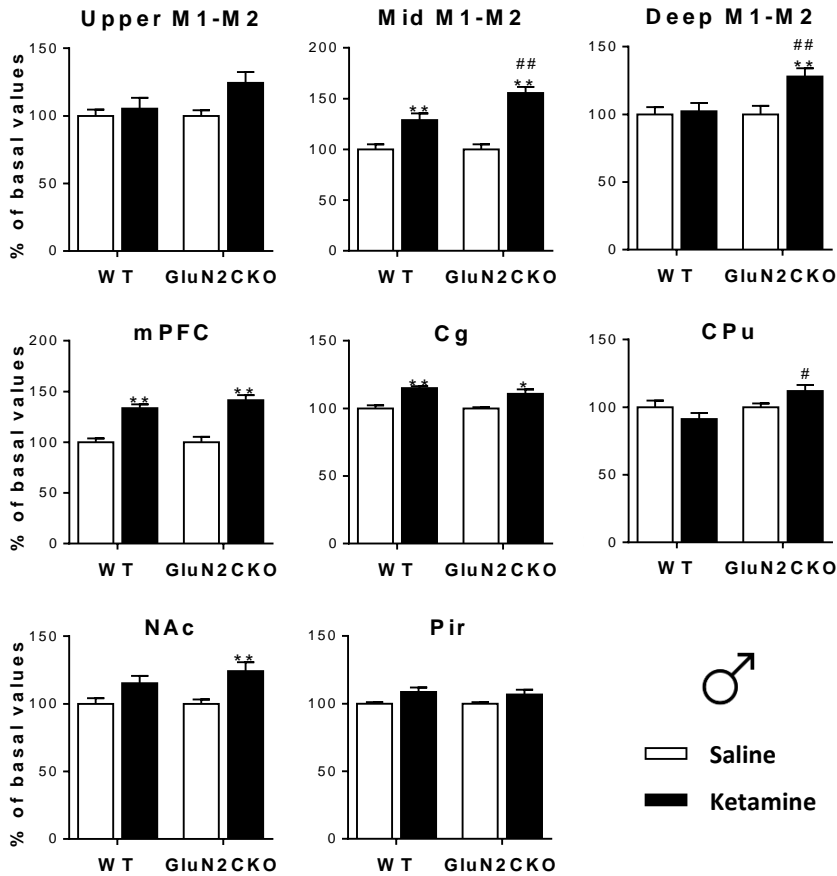


**Figure 20.** *C-fos* mRNA expression for male WT and GluN2CKO mice after ketamine (30 mg/kg) administration in upper, intermediate and deep layers of primary and secondary motor cortices (Upper M1-M2, Mid M1-M2 and Deep M1-M2, AP: +2.10), medial prefrontal cortex (mPFC, AP: +2.10), cingulate cortex (Cg, AP: +1.18), caudate-putamen nuclei (CPu, AP: +1.18), nucleus accumbens (NAc, AP: +1.18) and piriform cortex (Pir, AP: +1.18) (n=4-5/group). \* $p < 0.05$ , \*\* $p < 0.01$  vs saline; # $p < 0.05$ , ## $p < 0.01$  vs WT (Newman-Keuls *post hoc* test)

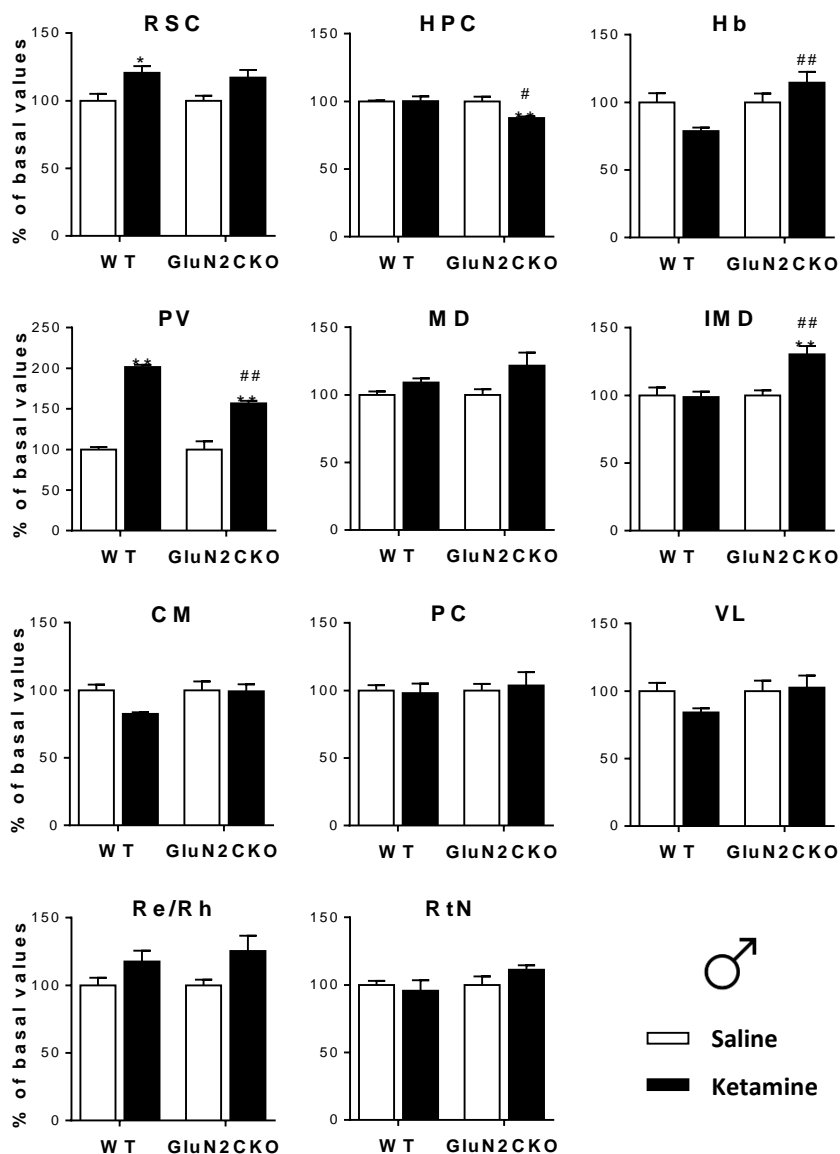


**Figure 21.** *C-fos* mRNA expression for male WT and GluN2CKO mice after ketamine (30 mg/kg) administration in retrosplenial cortex (RSC, AP: -1.70), hippocampus (HPC, AP: -1.70), habenula (Hb, AP: -1.70), paraventricular thalamic nucleus (PV, AP: -1.70), mediodorsal thalamic nucleus (MD, AP: -1.70), intermediodorsal thalamic nucleus (IMD, AP: -1.70), centromedial thalamic nucleus (CM, AP: -1.70), paracentral thalamic nucleus (PC, AP: -1.70), ventrolateral thalamic nucleus (VL, AP: -1.70), reuniens and rhomboid nuclei of the thalamus (Re/Rh, AP: -1.70) and reticular nucleus (RtN, AP: -1.70) (n=4-5/group). \*p<0.05, \*\*p<0.01 vs saline; #p<0.05, ##p<0.01 vs WT (Newman-Keuls *post hoc* test)



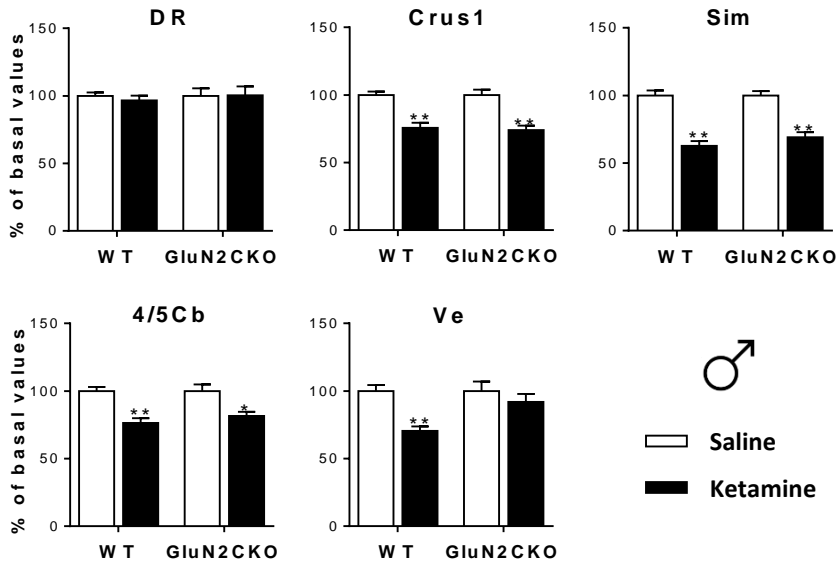


**Figure 22.** *C-fos* mRNA expression for male WT and GluN2CKO mice after ketamine (30 mg/kg) administration in dorsal raphe (DR, AP: -4.60), crus 1 of the ansiform lobule (Crus1, AP: -6.00), cerebellar simple lobule (Sim, AP: -6.00), lobules 4 and 5 of the cerebellar vermis (4/5Cb, AP: -6.00) and vestibular nucleus (Ve, AP: -6.00) (n=4-5/group). \*p<0.05, \*\*p<0.01 vs saline (Newman-Keuls *post hoc* test)

## Results

	Treatment (T)		Genotype (G)		T x G		Figure
Upper M1-M2	$F_{1,16}=5.43$	$p<0.05$	$F_{1,16}=2.20$	n.s.	$F_{1,16}=2.20$	n.s.	20
Mid M1-M2	$F_{1,16}=55.48$	$p<0.0001$	$F_{1,16}=5.52$	$p<0.05$	$F_{1,16}=5.52$	$p<0.05$	20
Deep M1-M2	$F_{1,16}=6.62$	$p<0.05$	$F_{1,16}=4.70$	$p<0.05$	$F_{1,16}=4.70$	$p<0.05$	20
mPFC	$F_{1,16}=67.81$	$p<0.0001$	$F_{1,16}=0.71$	n.s.	$F_{1,16}=0.71$	n.s.	20
Cg	$F_{1,15}=31.27$	$p<0.0001$	$F_{1,15}=0.91$	n.s.	$F_{1,15}=0.91$	n.s.	20
CPu	$F_{1,16}=0.71$	n.s.	$F_{1,16}=5.93$	$p<0.05$	$F_{1,16}=5.93$	$p<0.05$	20
NAC	$F_{1,16}=15.60$	$p<0.01$	$F_{1,16}=0.81$	n.s.	$F_{1,16}=0.81$	n.s.	20
Pir	$F_{1,16}=8.48$	$p<0.05$	$F_{1,16}=0.13$	n.s.	$F_{1,16}=0.13$	n.s.	20
RSC	$F_{1,16}=14.54$	$p<0.01$	$F_{1,16}=0.13$	n.s.	$F_{1,16}=0.13$	n.s.	21
HPC	$F_{1,16}=5.47$	$p<0.05$	$F_{1,16}=5.95$	$p<0.05$	$F_{1,16}=5.95$	$p<0.05$	21
Hb	$F_{1,16}=0.29$	n.s.	$F_{1,16}=7.98$	$p<0.05$	$F_{1,16}=7.98$	$p<0.05$	21
PV	$F_{1,16}=187.30$	$p<0.0001$	$F_{1,16}=15.04$	$p<0.01$	$F_{1,16}=15.04$	$p<0.01$	21
MD	$F_{1,16}=7.39$	$p<0.05$	$F_{1,16}=1.23$	n.s.	$F_{1,16}=1.23$	n.s.	21
IMD	$F_{1,15}=8.02$	$p<0.05$	$F_{1,15}=9.48$	$p<0.01$	$F_{1,15}=9.48$	$p<0.01$	21
CM	$F_{1,15}=3.33$	n.s.	$F_{1,15}=2.74$	n.s.	$F_{1,15}=2.74$	n.s.	21
PC	$F_{1,16}=0.02$	n.s.	$F_{1,16}=0.18$	n.s.	$F_{1,16}=0.18$	n.s.	21
VL	$F_{1,16}=0.93$	n.s.	$F_{1,16}=1.84$	n.s.	$F_{1,16}=1.84$	n.s.	21
Re/Rh	$F_{1,16}=7.57$	$p<0.05$	$F_{1,16}=0.24$	n.s.	$F_{1,16}=0.24$	n.s.	21
RtN	$F_{1,16}=0.39$	n.s.	$F_{1,16}=2.03$	n.s.	$F_{1,16}=2.03$	n.s.	21
DR	$F_{1,16}=0.09$	n.s.	$F_{1,16}=0.14$	n.s.	$F_{1,16}=0.14$	n.s.	22
Crus1	$F_{1,15}=54.79$	$p<0.0001$	$F_{1,15}=0.05$	n.s.	$F_{1,15}=0.05$	n.s.	22
Sim	$F_{1,15}=91.17$	$p<0.0001$	$F_{1,15}=0.80$	n.s.	$F_{1,15}=0.80$	n.s.	22
4/5Cb	$F_{1,15}=30.77$	$p<0.0001$	$F_{1,15}=0.49$	n.s.	$F_{1,15}=0.49$	n.s.	22
Ve	$F_{1,15}=11.44$	$p<0.01$	$F_{1,15}=3.72$	n.s.	$F_{1,15}=3.72$	n.s.	22

**Table 2.** Two-way ANOVA (treatment (T) and genotype (G) as factors) for *c-fos* expression data in male WT and GluN2CKO mice in upper, intermediate and deep layers of primary and secondary motor cortices (Upper M1-M2, Mid M1-M2 and Deep M1-M2, AP: +2.10), medial prefrontal cortex (mPFC, AP: +2.10), cingulate cortex (Cg, AP: +1.18), caudate-putamen nuclei (CPu, AP: +1.18), nucleus accumbens (NAC, AP: +1.18), piriform cortex (Pir, AP: +1.18), retrosplenial cortex (RSC, AP: -1.70), hippocampus (HPC, AP: -1.70), habenula (Hb, AP: -1.70), paraventricular thalamic nucleus (PV, AP: -1.70), mediodorsal thalamic nucleus (MD, AP: -1.70), intermediodorsal thalamic nucleus (IMD, AP: -1.70), centromedial thalamic nucleus (CM, AP: -1.70), paracentral thalamic nucleus (PC, AP: -1.70), ventrolateral thalamic nucleus (VL, AP: -1.70), reuniens and rhomboid nuclei of the thalamus (Re/Rh, AP: -1.70), reticular nucleus (RtN, AP: -1.70), dorsal raphe (DR, AP: -4.60), crus 1 of the ansiform lobule (Crus1, AP: -6.00), cerebellar simple lobule (Sim, AP: -6.00), lobules 4 and 5 of the cerebellar vermis (4/5Cb, AP: -6.00) and vestibular nucleus (Ve, AP: -6.00).

The effects of ketamine on *c-fos* mRNA expression in female mice are shown following an anatomical anteroposterior order (Figures 23, 24 and 25). A detailed statistical analysis (two-way ANOVA) is shown in Table 3.

In female WT mice, ketamine (30 mg/kg) significantly enhanced *c-fos* mRNA expression in Upper M1-M2 and Pir ( $p < 0.05$ , all cases) and in Mid M1-M2, Deep M1-M2, mPFC, Cg and NAc ( $p < 0.01$ , all cases). In female GluN2CKO mice, ketamine significantly increased *c-fos* expression in Mid M1-M2 ( $p < 0.05$ ) and in CPu, NAc and Pir ( $p < 0.01$ , all cases). Significant differences between female WT and GluN2CKO mice treated with ketamine were found in Mid M1-M2 and Cg ( $p < 0.01$ , all cases) (Figure 23).

In female WT mice, ketamine (30 mg/kg) significantly enhanced *c-fos* mRNA expression in RSC, PV, MD, IMD, PC, VL, Re/Rh, RtN ( $p < 0.01$ , all cases) and CM ( $p < 0.05$ ). In female GluN2CKO mice, ketamine significantly increased *c-fos* expression in PV, MD, IMD, PC, Re/Rh ( $p < 0.01$ , all cases) and CM ( $p < 0.05$ ). Significant differences between female WT and GluN2CKO mice treated with ketamine were found in PV ( $p < 0.01$ ) (Figure 24).

In female mice, ketamine (30 mg/kg) did not produce any changes in *c-fos* mRNA expression in DR, Crus1, Sim, 4/5Cb and Ve (Figure 25).

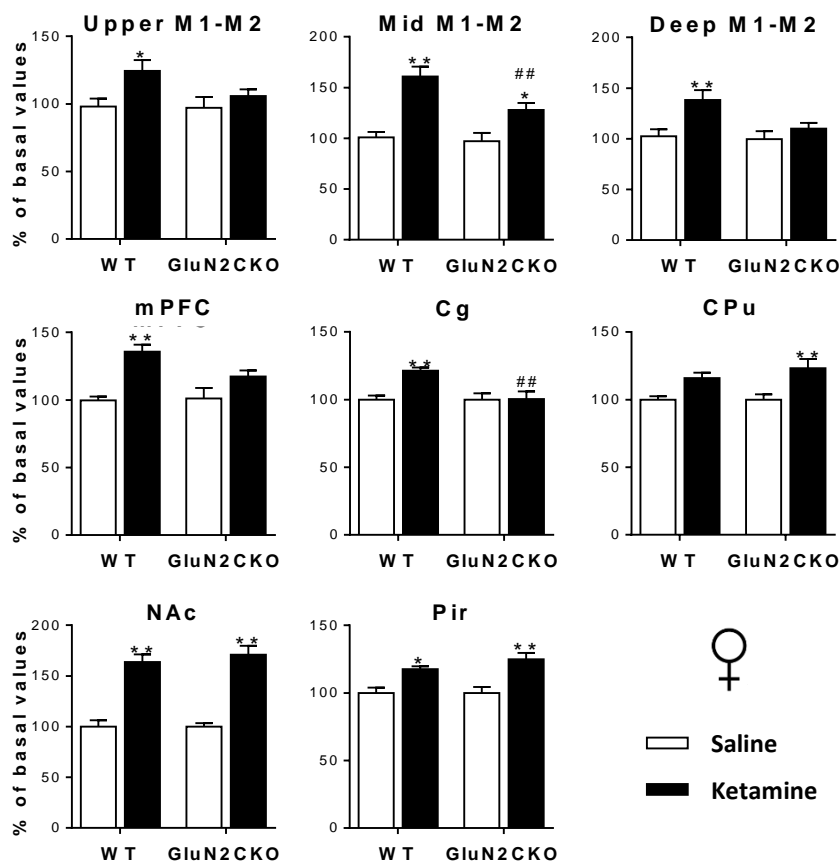


**Figure 23.** *C-fos* mRNA expression for female WT and GluN2CKO mice after ketamine (30 mg/kg) administration in upper, intermediate and deep layers of primary and secondary motor cortices (Upper M1-M2, Mid M1-M2 and Deep M1-M2, AP: +2.10), medial prefrontal cortex (mPFC, AP: +2.10), cingulate cortex (Cg, AP: +1.18), caudate-putamen nuclei (CPu, AP: +1.18), nucleus accumbens (NAc, AP: +1.18) and piriform cortex (Pir, AP: +1.18) (n=5-6/group). \* $p < 0.05$ , \*\* $p < 0.01$  vs saline; ## $p < 0.01$  vs WT (Newman-Keuls *post hoc* test)

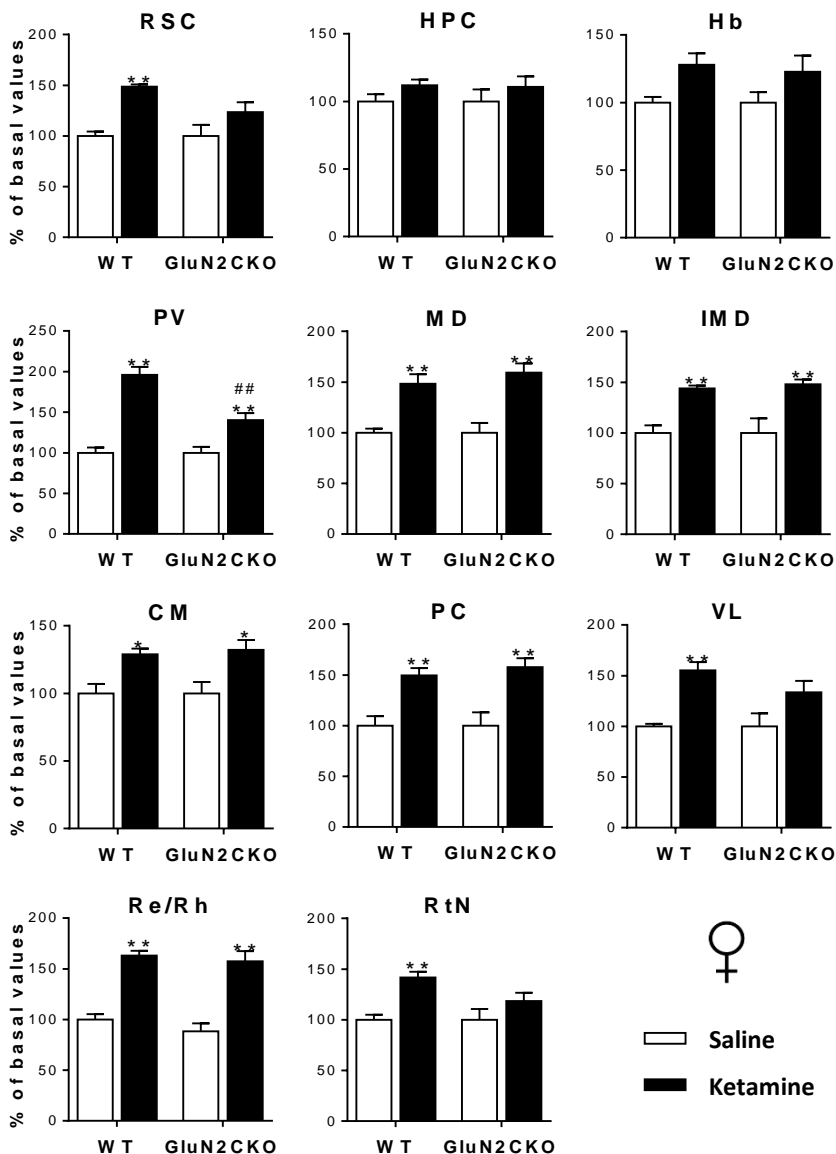


**Figure 24.** *C-fos* mRNA expression for female WT and GluN2CKO mice after ketamine (30 mg/kg) administration in retrosplenial cortex (RSC, AP: -1.70), hippocampus (HPC, AP: -1.70), habenula (Hb, AP: -1.70), paraventricular thalamic nucleus (PV, AP: -1.70), mediodorsal thalamic nucleus (MD, AP: -1.70), intermediodorsal thalamic nucleus (IMD, AP: -1.70), centromedial thalamic nucleus (CM, AP: -1.70), paracentral thalamic nucleus (PC, AP: -1.70), ventrolateral thalamic nucleus (VL, AP: -1.70), reuniens and rhomboid nuclei of the thalamus (Re/Rh, AP: -1.70) and reticular nucleus (RtN, AP: -1.70) (n=5-6/group). \*p<0.05, \*\*p<0.01 vs saline; ##p<0.01 vs WT (Newman-Keuls *post hoc* test)

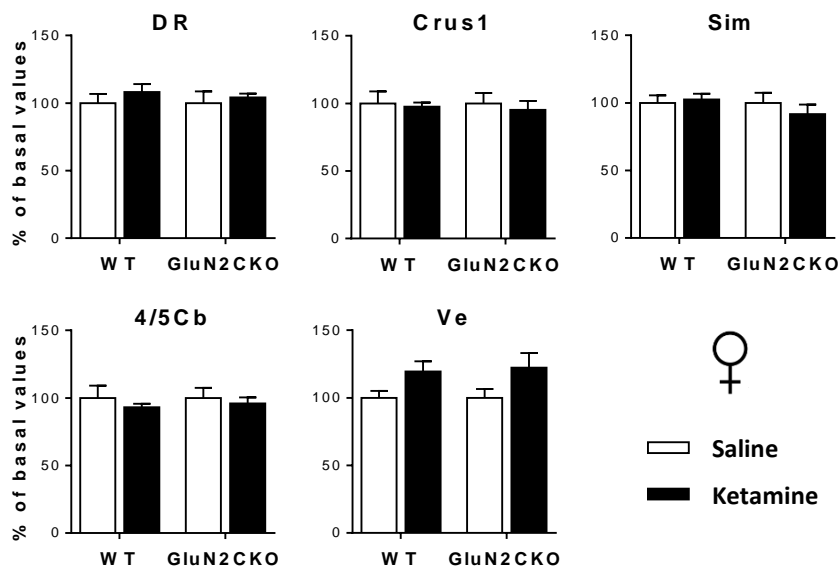


**Figure 25.** *C-fos* mRNA expression for female WT and GluN2CKO mice after ketamine (30 mg/kg) administration in dorsal raphe (DR, AP: -4.60), crus 1 of the ansiform lobule (Crus1, AP: -6.00), cerebellar simple lobule (Sim, AP: -6.00), lobules 4 and 5 of the cerebellar vermis (4/5Cb, AP: -6.00) and vestibular nucleus (Ve, AP: -6.00) (n=5-6/group)

	Treatment (T)		Genotype (G)		T x G		Figure
Upper M1-M2	$F_{1,20}=6.69$	$p<0.05$	$F_{1,20}=2.07$	n.s.	$F_{1,20}=1.69$	n.s.	23
Mid M1-M2	$F_{1,20}=34.84$	$p<0.0001$	$F_{1,20}=5.63$	$p<0.05$	$F_{1,20}=3.64$	n.s.	23
Deep M1-M2	$F_{1,20}=9.14$	$p<0.01$	$F_{1,20}=4.07$	n.s.	$F_{1,20}=2.75$	n.s.	23
mPFC	$F_{1,20}=23.62$	$p<0.0001$	$F_{1,20}=2.47$	n.s.	$F_{1,20}=3.32$	n.s.	23
Cg	$F_{1,19}=7.44$	$p<0.05$	$F_{1,19}=6.77$	$p<0.05$	$F_{1,19}=6.77$	$p<0.05$	23
CPu	$F_{1,20}=17.98$	$p<0.001$	$F_{1,20}=0.61$	n.s.	$F_{1,20}=0.61$	n.s.	23
NAc	$F_{1,20}=97.84$	$p<0.0001$	$F_{1,20}=0.27$	n.s.	$F_{1,20}=0.27$	n.s.	23
Pir	$F_{1,20}=28.70$	$p<0.0001$	$F_{1,20}=0.80$	n.s.	$F_{1,20}=0.80$	n.s.	23
RSC	$F_{1,19}=19.91$	$p<0.001$	$F_{1,19}=2.40$	n.s.	$F_{1,19}=2.40$	n.s.	24
HPC	$F_{1,20}=2.88$	n.s.	$F_{1,20}=0.01$	n.s.	$F_{1,20}=0.01$	n.s.	24
Hb	$F_{1,20}=8.68$	$p<0.01$	$F_{1,20}=0.09$	n.s.	$F_{1,20}=0.09$	n.s.	24
PV	$F_{1,20}=69.96$	$p<0.0001$	$F_{1,20}=11.69$	$p<0.01$	$F_{1,20}=11.69$	$p<0.01$	24
MD	$F_{1,20}=40.03$	$p<0.0001$	$F_{1,20}=0.41$	n.s.	$F_{1,20}=0.41$	n.s.	24
IMD	$F_{1,18}=24.34$	$p<0.0001$	$F_{1,18}=0.05$	n.s.	$F_{1,18}=0.05$	n.s.	24
CM	$F_{1,19}=18.25$	$p<0.001$	$F_{1,19}=0.05$	n.s.	$F_{1,19}=0.05$	n.s.	24
PC	$F_{1,20}=29.22$	$p<0.0001$	$F_{1,20}=0.18$	n.s.	$F_{1,20}=0.18$	n.s.	24
VL	$F_{1,20}=21.91$	$p<0.001$	$F_{1,20}=1.29$	n.s.	$F_{1,20}=1.29$	n.s.	24
Re/Rh	$F_{1,18}=76.42$	$p<0.0001$	$F_{1,18}=1.30$	n.s.	$F_{1,18}=0.15$	n.s.	24
RtN	$F_{1,19}=14.36$	$p<0.01$	$F_{1,19}=2.10$	n.s.	$F_{1,19}=2.10$	n.s.	24
DR	$F_{1,20}=0.92$	n.s.	$F_{1,20}=0.10$	n.s.	$F_{1,20}=0.10$	n.s.	25
Crus1	$F_{1,17}=0.27$	n.s.	$F_{1,17}=0.03$	n.s.	$F_{1,17}=0.03$	n.s.	25
Sim	$F_{1,16}=0.19$	n.s.	$F_{1,16}=0.72$	n.s.	$F_{1,16}=0.72$	n.s.	25
4/5Cb	$F_{1,15}=0.68$	n.s.	$F_{1,15}=0.05$	n.s.	$F_{1,15}=0.05$	n.s.	25
Ve	$F_{1,17}=7.85$	$p<0.05$	$F_{1,17}=0.04$	n.s.	$F_{1,17}=0.04$	n.s.	25

**Table 3.** Two-way ANOVA (treatment (T) and genotype (G) as factors) for *c-fos* expression data in female WT and GluN2CKO mice in upper, intermediate and deep layers of primary and secondary motor cortices (Upper M1-M2, Mid M1-M2 and Deep M1-M2, AP: +2.10), medial prefrontal cortex (mPFC, AP: +2.10), cingulate cortex (Cg, AP: +1.18), caudate-putamen nuclei (CPu, AP: +1.18), nucleus accumbens (NAc, AP: +1.18), piriform cortex (Pir, AP: +1.18), retrosplenial cortex (RSC, AP: -1.70), hippocampus (HPC, AP: -1.70), habenula (Hb, AP: -1.70), paraventricular thalamic nucleus (PV, AP: -1.70), mediodorsal thalamic nucleus (MD, AP: -1.70), intermediodorsal thalamic nucleus (IMD, AP: -1.70), centromedial thalamic nucleus (CM, AP: -1.70), paracentral thalamic nucleus (PC, AP: -1.70), ventrolateral thalamic nucleus (VL, AP: -1.70), reuniens and rhomboid nuclei of the thalamus (Re/Rh, AP: -1.70), reticular nucleus (RtN, AP: -1.70), dorsal raphe (DR, AP: -4.60), crus 1 of the ansiform lobule (Crus1, AP: -6.00), cerebellar simple lobule (Sim, AP: -6.00), lobules 4 and 5 of the cerebellar vermis (4/5Cb, AP: -6.00) and vestibular nucleus (Ve, AP: -6.00).

### **3. GluN1 and GluN2A-D subunit distribution in male WT and GluN2CKO mice**

Deletion of the GluN2C subunit produced remarkable changes in the mRNA expression of GluN1 subunit (Table 4, Figure 26). There were significant decreases in the expression of the GluN1 subunit in the outer part of the OB (OB(o)) and Crus1 ( $p < 0.05$ , all cases) and in the inner part of the OB (OB(i)), mPFC, Sim, and 4/5Cb ( $p < 0.01$ , all cases). It also caused increases of the GluN1 subunit in thalamic nuclei (PV, IMD, CM, and Re/Rh) and HPC ( $p < 0.05$ , all cases) and in RSC, Hb, and MD ( $p < 0.01$ , all cases).

Deletion of the GluN2C subunit produced minor changes in the mRNA expression of GluN2A, GluN2B and GluN2D subunits (Table 4). For the GluN2A subunit, there was an increase in its expression in DR ( $p < 0.05$ ). Regarding the GluN2B subunit, an increase in MD ( $p < 0.05$ ) and a decrease in Ve ( $p < 0.05$ ) was found. For the GluN2D subunit, there was a decline in its expression in OB(i) ( $p < 0.05$ ).

In WT mice, GluN2C subunit mRNA (Figure 27) was detected in OB(o), OB(i), Crus1, Sim, 4/5Cb, Ve, MD, CM, IMD, Pir, Re/Rh, PV, Hb, RSC, NAc, HPC, mPFC, Amg, CPu, Cg, and DR (areas are listed in descending order of GluN2C expression). No signal above background levels was detected in GluN2CKO mice.



	GluN1		GluN2A		GluN2B		GluN2D	
	WT	GluN2CKO	WT	GluN2CKO	WT	GluN2CKO	WT	GluN2CKO
OB(i)	112.7±4	99.1±6 <sup>#</sup>	113.9±7	105.0±17	140.4±10	141.0±11	79.8±7	67.3±9 <sup>#</sup>
OB(o)	56.2±5	47.1±8 <sup>#</sup>	62.2±8	62.3±15	75.5±8	70.6±14	170.4±12	156.6±8
mPFC	86.2±8	72.5±5 <sup>#</sup>	126.2±10	116.1±11	129.7±3	131.0±9	50.8±6	49.2±10
Cg	80.5±15	81.2±11	114.5±15	122.8±7	120.6±9	118.0±6	23.3±2	22.4±1
CPu	67.6±10	69.6±8	73.4±6	75.6±11	85.3±6	89.4±6	11.8±1	13.3±3
NAC	65.9±6	66.4±8	78.6±14	78.3±13	105.4±4	101.0±7	14.6±3	16.1±3
Pir	121.6±9	122.7±12	141.1±13	154.6±13	163.1±8	164.1±5	14.0±2	17.6±4
RSC	67.8±9	84.4±9 <sup>#</sup>	114.1±4	110.9±13	77.1±5	77.1±7	46.8±4	49.2±5
HPC	133.7±14	153.6±8 <sup>#</sup>	161.4±8	163.9±6	173.9±4	173.0±18	31.7±2	29.6±2
Hb	57.0±6	68.3±5 <sup>#</sup>	119.5±9	121.9±9	54.6±10	59.6±13	29.4±3	30.8±4
PV	43.7±6	52.9±6 <sup>#</sup>	58.6±6	62.1±12	59.9±11	57.0±14	173.4±12	171.0±10
MD	43.9±5	54.3±6 <sup>#</sup>	60.8±6	63.6±16	74.2±6	88.1±9 <sup>#</sup>	127.8±10	134.1±10
IMD	40.2±6	50.2±8 <sup>#</sup>	60.9±5	64.6±14	62.9±3	69.7±18	158.6±13	162.9±12
Re/Rh	45.3±7	56.7±10 <sup>#</sup>	52.9±7	58.8±7	65.4±3	61.3±16	166.8±12	166.5±15
Amg	58.7±5	67.2±11	54.6±8	57.8±13	85.6±6	74.6±17	82.2±6	87.2±7
DR	63.2±14	62.7±11	51.2±11	65.2±5 <sup>#</sup>	51.9±15	46.5±5	132.2±19	128.2±19
Crus1	114.4±4	89.9±23 <sup>#</sup>	137.6±11	140.4±6	22.1±6	20.2±4	41.5±3	42.4±10
Sim	114.3±3	97.0±4 <sup>#</sup>	141.6±7	138.6±6	21.0±4	19.0±4	33.8±2	36.8±6
4/5Cb	108.3±7	87.8±5 <sup>#</sup>	128.7±20	139.0±8	19.1±3	15.9±2	37.2±5	35.0±5
Ve	50.9±3	42.2±9	43.3±5	41.4±8	28.5±5	20.8±5 <sup>#</sup>	126.4±13	120.4±16

**Table 4.** GluN1, GluN2A, GluN2B and GluN2D mRNA expression in male WT and GluN2CKO mice and results from unpaired *t*-test in inner and outer part of the olfactory bulb (OB(i) and OB(o)), AP: +3.92), medial prefrontal cortex (mPFC, AP: +2.10), cingulate cortex (Cg, AP: +1.18), caudate-putamen nuclei (CPu, AP: +1.18), nucleus accumbens (NAC, AP: +1.18), piriform cortex (Pir, AP: +1.18), retrosplenial cortex (RSC, AP: -1.70), hippocampus (HPC, AP: -1.70), habenula (Hb, AP: -1.70), paraventricular thalamic nucleus (PV, AP: -1.70), mediodorsal thalamic nucleus (MD, AP: -1.70), intermediodorsal thalamic nucleus (IMD, AP: -1.70), centromedial thalamic nucleus (CM, AP: -1.70), reuniens and rhomboid nuclei of the thalamus (Re/Rh, AP: -1.70), amygdala (Amg, AP: -3.40), dorsal raphe (DR, AP: -4.60), crus 1 of the ansiform lobule (Crus1, AP: -6.00), cerebellar simple lobule (Sim, AP: -6.00), lobules 4 and 5 of the cerebellar vermis (4/5Cb, AP: -6.00), and vestibular nucleus (Ve, AP: -6.00). #*p*<0.05, ##*p*<0.01 vs WT

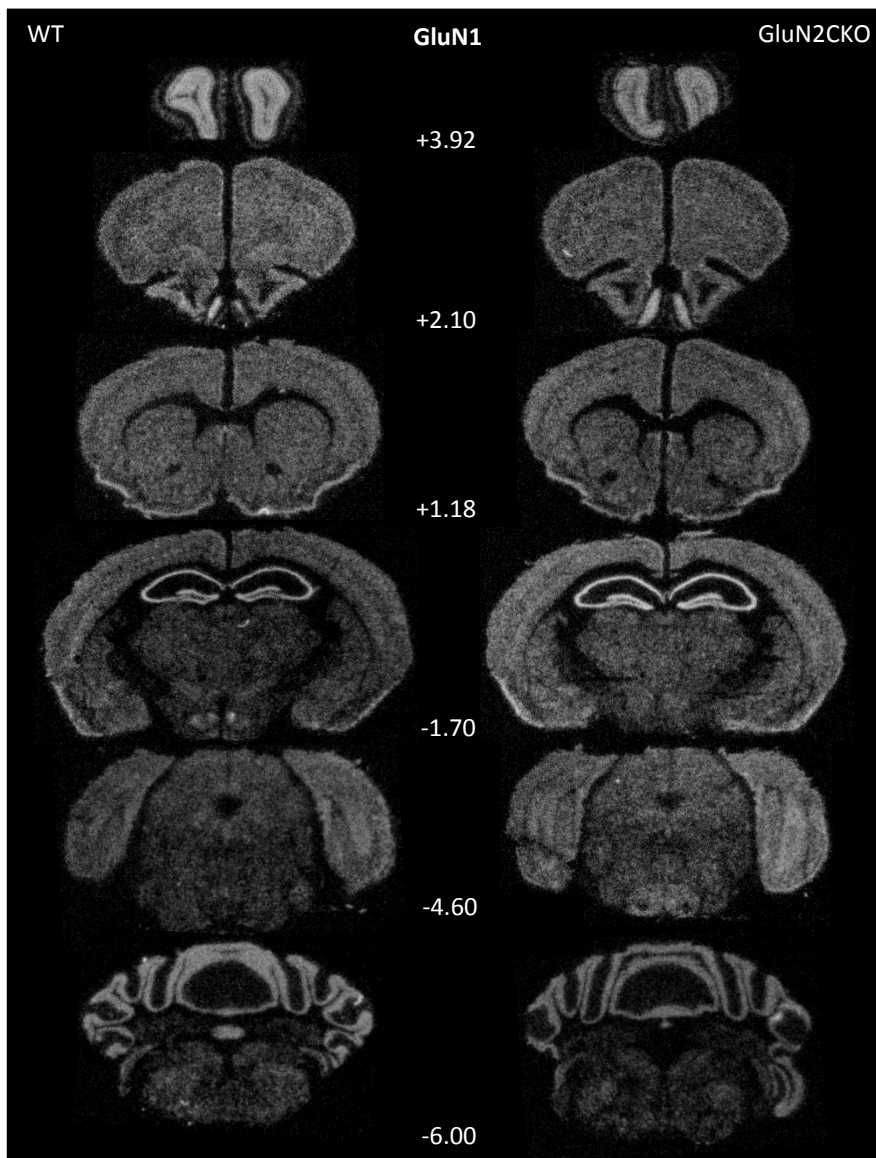


**Figure 26.** Representative film images of GluN1 mRNA expression in coronal sections of male WT and GluN2CKO mice in different anteroposterior coordinates from the Franklin & Paxinos mouse atlas.

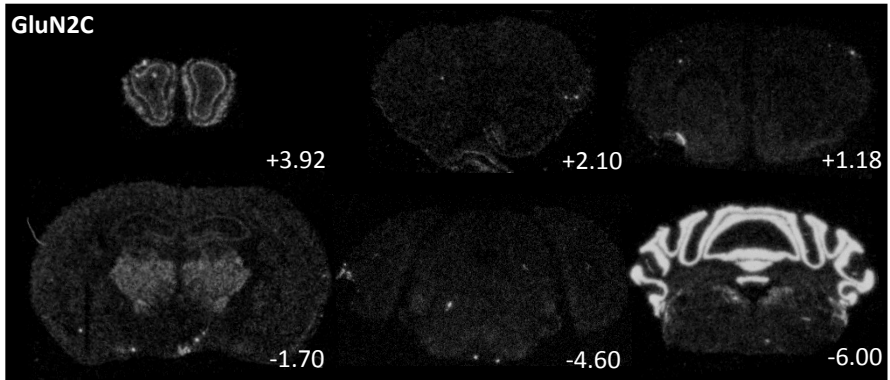


**Figure 27.** Representative film images of GluN2C mRNA expression in coronal sections of male WT mice in different anteroposterior coordinates from the Franklin & Paxinos mouse atlas.

## 4. Ketamine's antidepressant-like effect in rats

### 4.1. Antidepressant-like effect

Ketamine (10, 15 and 20 mg/kg), injected 30 min prior to the test, induced antidepressant-like responses in the FST (Figure 28a). One-way ANOVA showed a main effect of treatment ( $F_{3,32}=7.61$ ;  $p<0.001$ ). *Post hoc* comparisons indicated that all three doses of ketamine significantly reduced the immobility time ( $p<0.05$  for ketamine 10 mg/kg,  $p<0.01$  for ketamine 15 and 20 mg/kg). Nevertheless, ketamine (10 and 15 mg/kg) did not reduce the immobility time when administered 1 h prior to the test (Figure 28b). Ketamine (10 and 15 mg/kg), injected 30 min prior to the test, did not induce an anxiolytic-like behavior in the NSFT (Figure 28c). One-way ANOVA showed a main effect of treatment ( $F_{2,18}=18.83$ ;  $p<0.0001$ ). *Post hoc* comparisons indicated that both doses of ketamine significantly increased the latency to feed. Ketamine (10, 15 and 20 mg/kg) significantly reduced locomotor activity in the open field (Figure 28d). One-way ANOVA showed a main effect of treatment ( $F_{3,14}=12.59$ ;  $p<0.001$ ). *Post hoc* comparisons indicated that all three doses of ketamine significantly produced hypolocomotion ( $p<0.05$  for ketamine 10 mg/kg,  $p<0.01$  for ketamine 15 and 20 mg/kg).

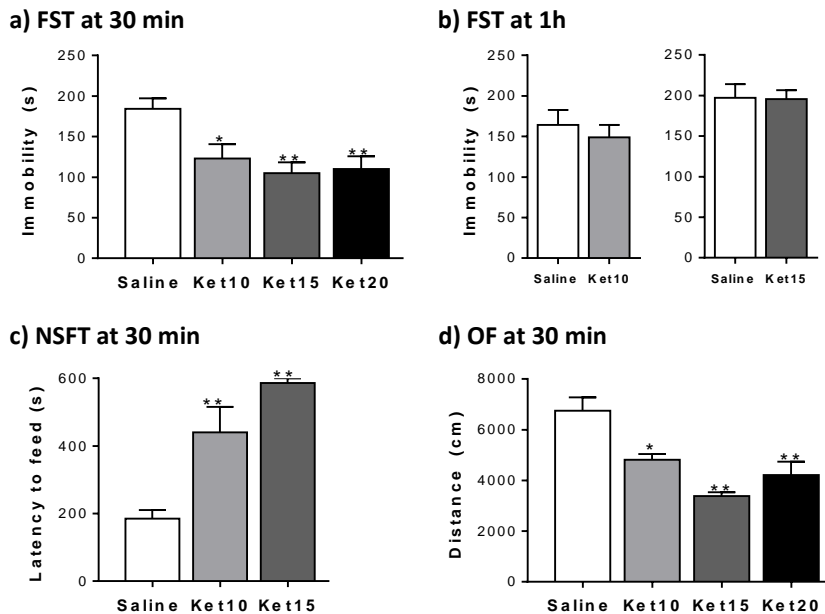


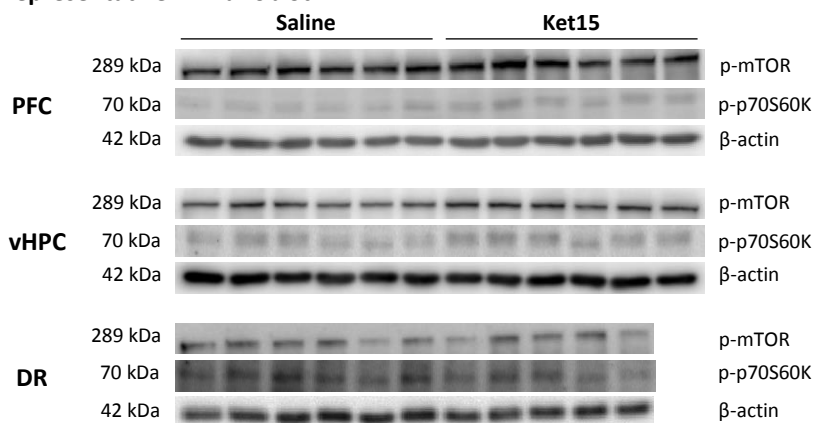
**Figure 28.** Effects of ketamine (Ket10, Ket15 and Ket20 for ketamine 10, 15 or 20 mg/kg respectively) in the a) FST at 30 min (n=13 in saline group, n=7-9 in treated groups), b) FST at 1 h (n=8-10/group), c) NSFT at 30 min (n=7/group) and d) OF (n=4-5/group). \* $p < 0.05$ ; \*\* $p < 0.01$  vs saline (Bonferroni *post hoc* test or Student's *t*-test)

## 4.2. Intracellular signaling

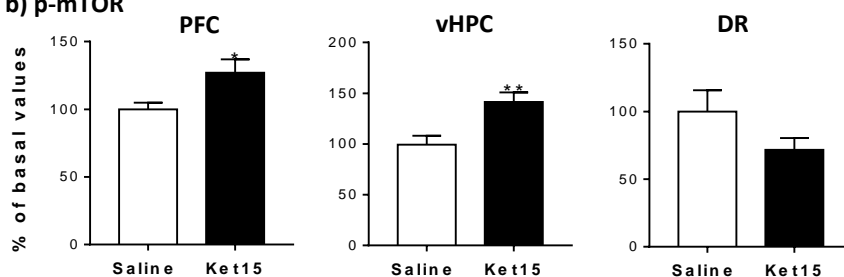
Ketamine (15 mg/kg) significantly activated mTOR in PFC ( $t_{(9)}=2.29$ ;  $p < 0.05$ ) and ventral HPC (vHPC) ( $t_{(10)}=3.27$ ;  $p < 0.01$ ) and it significantly enhanced phospho-p70S6K in PFC ( $t_{(10)}=6.11$ ;  $p < 0.0001$ ) and vHPC ( $t_{(10)}=2.44$ ;  $p < 0.05$ ) (Figure 29).

Ketamine (15 mg/kg) significantly increased mRNA levels of PSD95 in DR ( $t_{(8)}=3.11$ ;  $p < 0.05$ ) and synapsin I in PFC ( $t_{(8)}=2.31$ ;  $p < 0.05$ ), dorsal HPC (dHPC) ( $t_{(8)}=2.34$ ;  $p < 0.05$ ), vHPC ( $t_{(8)}=2.62$ ;  $p < 0.05$ ) and DR ( $t_{(8)}=3.26$ ;  $p < 0.05$ ) (Figure 30).

## a) Representative immunoblot



## b) p-mTOR



## c) p-p70S6K

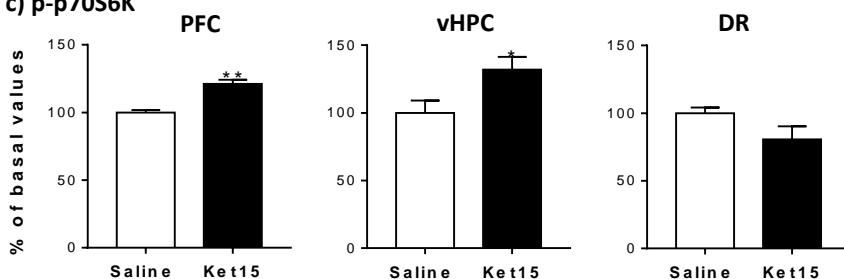


**Figure 29.** a) Representative immunoblot of p-mTOR (Ser2448), p-p70S6K (Thr389) and  $\beta$ -actin. Optical density quantification of b) p-mTOR and c) p-p70S6K 30 min after ketamine (15 mg/kg) administration in prefrontal cortex (PFC), ventral hippocampus (vHPC) and dorsal raphe (DR) (n=5-6/group). \*p<0.05; \*\*p<0.01 vs saline (Student's t-test)

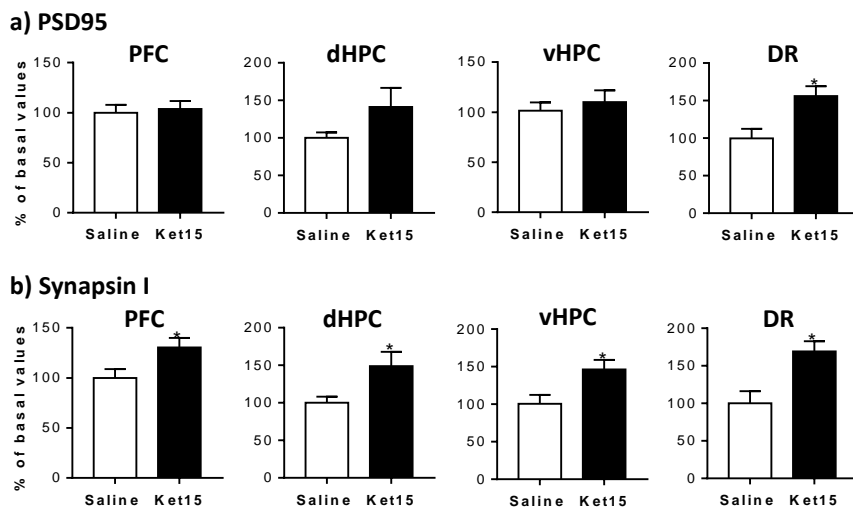


**Figure 30.** a) PSD95 and b) Synapsin I expression 6 h after ketamine (15 mg/kg) administration in prefrontal cortex (PFC), dorsal hippocampus (dHPC), ventral hippocampus (vHPC) and dorsal raphe (DR) (n=5/group). \*p<0.05 vs saline (Student's *t*-test)





# Discussion



Compelling evidence supports the hypothesis that dysfunction of the glutamatergic system mediates the pathophysiology of schizophrenia (Krystal et al., 2003) and MDD (Réus et al., 2016). In schizophrenia, the involvement of Glu neurotransmission mainly arises from findings that blockade of the NMDA-R by non-competitive NMDA-R antagonists induced symptoms that mimicked those of schizophrenia in healthy humans and they aggravated symptoms in schizophrenic patients (Javitt & Zukin, 1991; Lahti et al., 2001; Malhotra et al., 1996; Xu et al., 2015). More recently, it has been found that a single subanaesthetic dose of the non-competitive NMDA-R antagonist ketamine elicits rapid and sustained antidepressant effects in patients with TRD (see Xu et al., 2016 for a review). Starting from these observations, PCP, MK-801 and ketamine have been used to attempt to develop a pharmacological rodent model of schizophrenia (Lee & Zhou, 2019) and ketamine has also been studied in rodents in order to identify the neurobiological basis of its fast antidepressant actions (Browne & Lucki, 2013). Nevertheless, the exact mechanism of action by which MK-801, PCP and ketamine exert these effects is yet to be fully elucidated.

It has been hypothesized that non-competitive NMDA-R antagonists preferentially block NMDA-Rs on cortical GABAergic interneurons (Homayoun & Moghaddam, 2007) or GABAergic projection neurons such as RtN neurons (Kargieman et al., 2007; Santana et al., 2011; Troyano-Rodriguez et al., 2014), consequently increasing thalamo-cortical activity in PFC, RSC, EC, CM and MD, among other areas (Celada et al., 2013). Given that the GluN2C subunit is expressed in thalamic areas including the RtN (Karavanova et al., 2007; Ravikrishnan et al., 2018; Wenzel et al., 1997; Zhang et al., 2012), and modulates burst firing in RtN neurons (Liu et al., 2019), in the present thesis, we investigated the involvement of the GluN2C subunit in the mechanism of action of non-competitive NMDA-R antagonists to produce psychotomimetic

and/or antidepressant effects, under the working hypothesis that these effects would be partly attenuated in absence of the GluN2C subunit.

The data from the present thesis show that the GluN2C subunit appears to be strongly involved in motor components of the behavioral syndrome induced by non-competitive NMDA-R antagonists, while the antidepressant-like effects of ketamine are preserved. The differential role of the GluN2C subunit in mediating the psychotomimetic and antidepressant effects of ketamine identifies this subunit as a potential target for preventing the emergence of pro-psychotic effects while keeping a full antidepressant action.

## **1. GluN2CKO mice show less motor impairment after acute NMDA-R blockade by MK-801 and PCP**

Typically, non-competitive NMDA-R antagonists induce a behavioral syndrome, resembling that of a psychotic state, that in animals is defined by hyperlocomotion, ataxia signs (falls, hindlimb abduction) and stereotypies (circling), as well as other behavioral responses like abnormal locomotor pattern and a decrease in the exploratory activity (rearrings) (Andiné et al., 1999; Carlsson & Carlsson, 1990; Geyer & Ellenbroek, 2003; Nilsson et al., 2001; Nilsson et al., 2006; Scorza et al., 2008; Tricklebank et al., 1989). Accordingly, in the present study, MK-801 and PCP induced robust psychotomimetic effects in WT mice. However, in GluN2CKO mice, some motor components of the behavioral syndrome induced by both drugs were dramatically attenuated. Specifically, the circling score, the number of falls, and the hindlimb abduction score were extremely reduced in GluN2CKO mice, suggesting a better motor coordination in the absence of the GluN2C subunit. In support of this hypothesis, GluN2CKO mice spent more time on the rotarod compared to WT mice after acute MK-801 or PCP treatment, despite showing the same ability for motor learning, motor coordination and spontaneous activity in basal conditions (Hillman et al., 2011; Kadotani et al., 1996; Shelkar et al., 2019). Moreover, a better motor coordination due to reduced stereotypies and ataxia in GluN2CKO mice could explain the significant increase in the distance moved in the mutant animals, since stereotypies and hyperlocomotion have been considered competitive behaviors (Wu et al., 2005).

DA projections to the NAc have been associated with PCP-induced hyperlocomotion (McCullough & Salamone, 1992) and depletion of DA in NAc attenuated the locomotor stimulating effects of PCP (Steinpreis & Salamone, 1993). Given that GluN2CKO mice exhibited a higher locomotor

activity and much better coordination than WT mice after NMDA-R blockade, we evaluated DA release in NAc after MK-801 treatment. The present results show that MK-801 elevated DA release in the NAc similarly in both genotypes, indicating that the greater locomotor activity in GluN2CKO mice did not depend on a differential activity of mesolimbic DA pathways. These results are in agreement with previous studies suggesting that activation of DA neurotransmission in NAc is not sufficient to sustain the locomotor activity effects of NMDA-R antagonists (Moghaddam & Adams, 1998; Ouagazzal et al., 1994) and further support the hypothesis that the better motor coordination of GluN2CKO mice would be due to a differential NMDA-R blockade.

The GluN2C subunit (present study) seems not the unique NMDA-R subunit involved in the impaired locomotor and coordination induced by non-competitive NMDA-R antagonists. Indeed, PCP administration led to a reduced motor impairment in the rotarod test in GluN2DKO mice (Yamamoto et al., 2013) and no hyperlocomotion was observed in these animals after PCP or ketamine treatment (Hagino et al., 2010; Ikeda et al., 1995; Sapkota et al., 2016; Yamamoto et al., 2016). However, the very high abundance of the GluN2C subunit in the cerebellum and the involvement of this brain structure in motor coordination suggest that GluN2C subunits may play a critical role in the motor actions of MK-801 and PCP.

In order to investigate the neurobiological basis of the described motor differences between WT and GluN2CKO mice, we used *c-fos* expression as a surrogate marker of neuronal activity, given its direct relationship with neuronal discharge (Dragunow & Faull, 1989; Konkle & Bielajew, 2004; Kovács, 2008; Lladó-Pelfort et al., 2012). In general, MK-801 and PCP administration evoked a very similar pattern of increased *c-fos* expression, as it has already been reported (Castañé et al., 2015; Inta et al., 2009). Thus, acute NMDA-R blockade elicited significant increases in *c-fos* mRNA

expression 1 h post-treatment in many brain areas, such as mPFC, NAc, Pir, RSC, HPC, thalamic nuclei, and EC. As expected, MK-801 and PCP increased *c-fos* mRNA expression in areas that have been described to exhibit structural alterations in schizophrenic patients, such as Cg, HPC, thalamus and Amg (Shepherd et al., 2012). In the present study, we found significant decreases of *c-fos* mRNA expression in upper and deep layers of the motor cortices as well as in the cerebellar areas Crus1 and Sim (4/5Cb marginally significant) after MK-801 or PCP administration. Previous studies have also reported decreases in *c-fos* expression in brain areas with high basal activity (Mineur et al., 2007; Mineur et al., 2016). Therefore, the decrease in *c-fos* expression, at least in the cerebellum, likely reflects the very high activity and discharge rates of granule cells, which can show bursts that consist of tens of spikes at instantaneous frequencies over 800 Hz upon sensory stimulation (Beugen et al., 2013). Hence, unlike in forebrain, where non-competitive NMDA-R antagonist may increase the activity of principal neurons via disinhibition (see above), their action in cerebellar granule cells appears to be mainly inhibitory, likely blocking NMDA-Rs that contribute to maintain these very high rates of neuronal activity.

Interestingly, genotype differences on *c-fos* expression were found in cerebellar areas Crus1, 4/5Cb and Ve, mostly showing a lessened effect of non-competitive NMDA-R antagonists in the GluN2CKO mice.

In agreement, genotype differences among cerebellar areas Crus1, Sim and 4/5Cb were also found using *zif268*, although the effects were less robust probably because we sacrificed the animals 1 h after treatment and not 30 min after the injection, when *zif268* expression shows a high expression in C57BL/6J mice (Ziółkowska et al., 2015). Although the decreased activity of motor cortices probably contribute to motor dysfunction after NMDA-R blockade, genotype differences in motor coordination would be more likely attributable to cerebellum activity. It is known that the cerebellum does not

initiate movement, but it contributes to coordination, precision, and accurate timing. It receives input from motor areas, sensory systems of the spinal cord and from other parts of the brain and integrates these inputs to refine motor activity. In agreement, cerebellar dysfunction deeply alters fine movement, equilibrium, posture, and motor learning. Moreover, we cannot exclude that other motor-related areas such the basal ganglia or the motor thalamus may also contribute to the behavioral variances between WT and GluN2CKO mice, since genotype differences in these areas were also observed. Concretely, MK-801 and PCP increased *c-fos* expression in CPu and NAc (MK-801's effect in CPu did not reach statistical significance), but this increase was significantly attenuated in GluN2CKO mice. In the VL nucleus of the thalamus, MK-801 only increased *c-fos* expression in WT mice, not in GluN2CKO mice, while PCP increased *c-fos* in both genotypes.

Remarkably, MK-801 and PCP have been reported to produce neuronal damage in Cg and RSC, which are brain regions suggested to be related to the psychotomimetic effects (Nishizawa et al., 2000; Olney et al., 1989; Tomitaka et al., 2000). As anticipated, both drugs increased *c-fos* expression in Cg and RSC of WT mice. Nevertheless, there were differences between WT and GluN2CKO mice in both areas, since MK-801 and PCP did not increase *c-fos* expression in Cg and neither did PCP in RSC of GluN2CKO mice. These genotype differences further support the hypothesis that the Cg and RSC are involved in the psychotic-like effects of non-competitive NMDA-R antagonists because GluN2CKO mice, which exhibited less psychotomimetic effects, were less affected by MK-801 and PCP.

Overall, our results support that both MK-801 and PCP partly evoke their motor actions by interacting with GluN2C-containing NMDA-Rs, possibly located in the cerebellum, since it is a brain structure strongly involved in motor coordination and it contains, by large, the highest density of GluN2C subunits in brain (Monyer et al., 1994; Lin et al., 1996; Wenzel et al., 1997),



particularly in cerebellar granule neurons (Scherzer et al., 1997; Bhattacharya et al., 2018).

Besides the positive symptomatology, another relevant aspect in schizophrenia is the impairment in sensorimotor gating, which can be assessed using the PPI test. The PPI reflex is a measure of the suppression of irrelevant information (Braff & Geyer, 1990) and clinical studies have demonstrated that patients with schizophrenia showed impairments in automatically filtering irrelevant thoughts and sensory stimuli (Dissanayake et al., 2013). In agreement with previous studies, PCP and MK-801 produced deficits in PPI in WT mice (Ishii et al., 2010; Long et al., 2006; Shirai et al., 2012; Spooen et al., 2004). However, in contrast to the above differences in motor activity and coordination, mice from both genotypes exhibited identical responses (startle amplitude, % of PPI) to PCP and MK-801, suggesting that the GluN2C subunit is not involved in the expression of sensorimotor gating deficits after NMDA-R blockade. Recently, Shelkar and colleagues (Shelkar et al., 2019) showed similar results regarding MK-801-induced PPI deficits in WT and GluN2CKO mice. However, in this study authors suggest that the GluN2C subunit is important for the rescue of MK-801-induced deficits by the GluN2C/2D potentiator CIQ, as CIQ attenuated MK-801-induced impairment in PPI in WT mice (Suryavanshi et al., 2014), but not in GluN2CKO mice (Shelkar et al., 2019).

Moreover, no significant differences were observed between drug-free WT and GluN2CKO mice in the PPI response, as it had already been reported (Gupta et al., 2016; Shelkar et al., 2019). To date, other NMDA-R subunits have been involved in sensory gating in basal conditions, since reduction of GluN1 (Duncan et al., 2004) or block of the GluN2B subunit in GluN2AKO mice led to disruptions in PPI (Spooen et al., 2004), though GluN2AKO mice exhibit a normal PPI response (Boyce-Rustay & Holmes, 2006; Spooen et al., 2004). More recently, a reduction of the PPI was also found in GluN2D

heterozygotes and GluN2DKO mice, together with increased startle amplitude (Shelkar et al., 2019).

The brain circuitry responsible for the PPI of the startle response involves mainly the limbic cortex, basal ganglia structures and the pontine tegmentum (Swerdlow et al., 2001). Therefore, the absence of genotype differences between WT and GluN2CKO mice in the PPI test agrees with the poor expression of GluN2C subunits in the above brain structures (Monyer et al., 1994; Lin et al., 1996; Wenzel et al., 1997).

In summary, GluN2C-containing NMDA-Rs in the cerebellum may be involved in the motor components of the psychotomimetic action of MK-801 and PCP, but not in the impairment in sensorimotor gating produced by these two non-competitive NMDA-R antagonists. Even though the cerebellum is not typically considered a brain area of interest in schizophrenia, Andreasen and colleagues have postulated that a dysfunction in cortico-thalamic-cerebellar circuitry may account for the cognitive deficits in this disorder (Andreasen et al., 1998). Moreover, Hillman et al. (2011) have reported working memory deficits in GluN2CKO mice, despite having intact reference memory, suggesting the participation of the GluN2C subunit in cognition. Therefore, it would be interesting to further study the role of the cerebellum and the GluN2C subunit in other cognitive tests under the challenge of a non-competitive NMDA-R antagonist.

## **2. Ketamine-induced antidepressant-like effects are preserved in GluN2CKO mice**

Ketamine, as well as MK-801 and PCP, is a non-competitive NMDA-R antagonist that not only elicits psychotomimetic effects, but also exerts antidepressant responses. Therefore, we evaluated the involvement of the GluN2C subunit in both actions. Since MDD is a psychiatric disorder with a higher prevalence among females than males (WHO, 2017), we assessed ketamine's effects in both sexes.

Ketamine induced psychotomimetic effects in male and female WT and GluN2CKO mice. The stereotypes (circling) and ataxic behavior (falls, hindlimb abduction) were dramatically reduced in GluN2CKO mice of both sexes. These results are similar to the ones reported by MK-801 and PCP, where the absence of the GluN2C subunit led to a better motor coordination, and further support the involvement of the GluN2C subunit in the motor components of the psychotomimetic effects induced by non-competitive NMDA-R antagonists. Of the three NMDA-R antagonists used in the present thesis, MK-801 is the one eliciting a greater behavioral syndrome, followed by PCP and ketamine, and its effects on increased locomotor activity, ataxia and stereotypes lasted longer than those of PCP or ketamine (data not shown). Concerning the psychotomimetic effects of ketamine on both sexes, we did not statistically compare both male and female results because they underwent behavioral testing on alternating weeks, but it seems that there are no relevant differences between males and females as similar dose-dependent effects of ketamine were found. These results may be in contrast with previous studies that reported that female rats were more sensitive to NMDA-R blockade by MK-801 than males, showing an increased and long-lasting recumbency (Hur et al.,

1999), locomotor activity, ataxia and head weaving (Hönack & Löscher, 1993) after 5 mg/kg or 0.1-0.3 mg/kg of MK-801, respectively.

We did not evaluate PPI in WT and GluN2CKO mice after ketamine administration since experiments with MK-801 and PCP had already proved that the GluN2C is not involved in sensorimotor gating. Moreover, other research groups have already studied the deficits in PPI caused by 30 mg/kg of ketamine in mice (Lin et al., 2016; Zanos et al., 2017).

Regarding the antidepressant action of ketamine, we found that 30 mg/kg but not 10 mg/kg of the drug elicited antidepressant-like effects in mice of both sexes and genotypes, as seen by the reduction in the immobility time in the TST. These results clearly suggest that the GluN2C subunit is not involved in the antidepressant-like effects of ketamine. While some studies have described antidepressant-like effects after 10 mg/kg or lower doses of ketamine 30 min (Franceschelli et al., 2015; Mantovani et al., 2003), 45 min (Ghasemi et al., 2009) or 1 h (Zanos et al., 2016) before the TST or FST in male WT mice, others have only found significant responses at higher doses (Cruz et al., 2009; Koike et al., 2011; Nguyen & Matsumoto, 2015). In our study, GluN2CKO mice did not exhibit a depressive-like phenotype in the TST nor FST as previously reported (Hillman et al., 2011). However, a recent study that also used GluN2CKO mice found basal differences in the FST (Shelkar et al., 2019). These discrepancies could be explained by strain differences on anxiety-like behaviors and immobility between C57BL/6N (Shelkar et al., 2019) and C57BL/6J mice (present study), as C57BL/6N exhibited a higher anxiety-like behavior (Matsuo et al., 2010; Simon et al., 2013).

Regarding the contribution of sex to the antidepressant-like effects of ketamine, there is evidence showing that female rats are more sensitive to the rapid antidepressant-like effects of ketamine, since they usually

respond to lower doses of ketamine (i.e. 2.5 or 3 mg/kg) that are not effective to their male counterparts (Carrier & Kabbaj, 2013; Sarkar & Kabbaj, 2016). In mice, ketamine exhibited controverted results in freely cycling females, with studies supporting this higher sensitivity (Franceschelli et al., 2015; Zanos et al., 2016) and others reporting no differences between males and females (Dossat et al., 2018), as the present study.

In addition to the glutamatergic system, serotonergic neurotransmission might also be involved in the antidepressant actions of ketamine (du Jardin et al., 2016). Studies of our group have reported that an acute increase of glutamatergic neurotransmission in the infralimbic cortex (ventral subdivision of the mPFC), produced by blockade of the glial Glu transporter-1 (GLT-1), evoked antidepressant-like effects associated with an increase of serotonergic activity (Gasull-Camós et al., 2017, 2018, see publications in the annex section). Other studies supporting the contribution of the serotonergic system have shown that depletion of 5-HT by *para*-chlorophenylalanine (pCPA, a 5-HT synthesis inhibitor) attenuated the antidepressant-like effects of ketamine 30 min (Fukumoto et al., 2016) and 24 h (Gigliucci et al., 2013; Pham et al., 2017) after its administration, suggesting a key role of 5-HT in the antidepressant-like action of ketamine. Thus, we evaluated the contribution of the serotonergic and glutamatergic systems using *in vivo* microdialysis in mPFC in male and female mice, since, to our knowledge, sex differences in the neurochemical effects of ketamine have been poorly addressed.

An increase of extracellular levels of 5-HT were found in mPFC in WT and GluN2CKO mice of both sexes after an antidepressant-like effective dose of ketamine (30 mg/kg). Although some genotype differences exist, our results suggest that 5-HT may be contributing to the observed antidepressant response. Results regarding Glu neurotransmission do not

parallel the antidepressant response, since no rapid increases of Glu were found in either WT or GluN2CKO female mice after ketamine administration. We are not the first to describe sex-differentiated effects of ketamine, since a study had previously indicated that repeated ketamine treatment induced different neurochemical and molecular effects depending on sex (Thelen et al., 2016).

Interestingly, the increases in 5-HT or Glu (when found) were transient, reaching a maximum within the first 30 min after the administration of ketamine and then returning to basal levels. This matches the fast pharmacokinetic profile of ketamine in male C57BL/6, which its half-life has been reported to be approximately of 13 min (Maxwell et al., 2006) or between 30 to 40 min (Sato et al., 2004). Unexpectedly, Glu levels in mPFC peaked at 2-3 h after ketamine (30 mg/kg) treatment in some experimental groups, which would not be a direct effect of ketamine, given its faster pharmacokinetic profile.

Previous microdialysis studies have shown that ketamine increased the extracellular levels of 5-HT in the PFC of male rats (Amargós-Bosch et al., 2006; Kinoshita et al., 2018; López-Gil et al., 2012, 2019) and so did each of its enantiomers in male mice (Ago et al., 2019). However, there are controverted results regarding Glu release in this area, with studies showing increases of Glu (Moghaddam et al., 1997; Lorrain et al., 2003) or no effects (López-Gil et al., 2019). Moreover, Glu increases in rats were long-lasting (Moghaddam et al., 1997; Lorrain et al., 2003) after ketamine administration.

Altogether, our results suggest that an increase in serotonergic -but not glutamatergic- transmission may be involved in the acute antidepressant-like response of ketamine. Nevertheless, the neurochemical basis of the

antidepressant response of ketamine in male and female WT and GluN2CKO mice deserves further attention.

In order to identify brain areas responding to ketamine's treatment, we used ISH studies to investigate the expression of the immediate early gene *c-fos*. In WT mice, ketamine increased *c-fos* expression in Mid M1-M2, mPFC, Cg, and PV in both sexes. Moreover, ketamine induced *c-fos* expression in RSC of male and female WT mice, as it had been described after a dose of 10 mg/kg (Inta et al., 2009) or 50 mg/kg (Nakao et al., 2002; Nishizawa et al., 2000). Remarkably, the DR was not activated in male nor female mice after ketamine treatment, which would have been expected given that ketamine enhanced 5-HT neurotransmission and a previous study had reported a significantly increased *c-fos* immunoreactivity in DR after systemic 30 mg/kg ketamine administration (Fukumoto et al., 2016). Surprisingly, ketamine did not systematically activate thalamic nuclei in male mice, as it would have been expected since MK-801 and PCP increased *c-fos* expression in thalamus. Nevertheless, female mice did exhibit an increased activity in all thalamic nuclei analyzed after ketamine treatment. On the other hand, small reductions in *c-fos* expression were only found in cerebellar areas of male mice, while no decreases in *c-fos* were found in female mice. Overall, even though there were no differences between males and females in the behavioral variables analyzed, we did find a differential brain activation after ketamine treatment between sexes.

In comparison with MK-801 and PCP, ketamine did not evoke a general pattern of *c-fos* activation. Unexpectedly, we did not replicate the cerebellar genotype differences found after MK-801 or PCP administration. However, the magnitude of *c-fos* change observed in most brain areas after ketamine was more moderate than after MK-801 or PCP administration, which would complicate the appreciation of genotype differences.

A possible explanation for the behavioral and molecular differences among the three non-competitive NMDA-R antagonists could be their affinity for the PCP binding site. The order of affinity (MK-801 > PCP > ketamine; Temme et al., 2018) is the same as their order of potency with which these drugs induced psychotomimetic effects (Tricklebank et al., 1987). Therefore, ketamine activated *c-fos* activation in a lower number of brain areas than MK-801 or PCP because it has a weaker effect on NMDA-Rs. Another reason could be the subunit preference of each drug. On one hand, it has been described that sensitivity to MK-801 is greater for GluN2A and GluN2B-containing receptors than GluN2C or GluN2D-containing receptors (Bresink et al., 1996; Dravid et al., 2007). Further, it was suggested that ketamine would preferentially act on GluN2C and/or GluN2D subunits (Kotermanski & Johnson, 2009). Moreover, based on this previous study, it was hypothesized that, at a concentration at which ketamine produces psychosis in humans, this drug would selectively block a substantial fraction of GluN2C-containing NMDA-Rs, with less effect on other subunits (Khlestova et al., 2016). However, there are two important facts that must be taken into consideration. First, this conclusion was reached using diheteromeric receptors. Therefore, ketamine's preference for GluN2C-containing triheteromeric receptors remains unknown. Second, ketamine's preference for the GluN2C subunit might not be due to a higher affinity for this subunit, but due to the differential capacity of GluN2C for Mg<sup>2+</sup> block, meaning that ketamine may block distinct NMDA-R subunits depending on local Mg<sup>2+</sup> concentrations.



### 3. Compensatory mechanisms in GluN2CKO mice

One of the limitations of studies using constitutive knockout mice is that compensatory mechanisms may exist during brain development. In order to investigate this issue we performed ISH studies to investigate whether GluN2C had been replaced with other NMDA-R subunits in the brain of GluN2CKO mice.

In WT mice, we found that the GluN2C subunit was highly expressed in cerebellum and olfactory bulb, and moderately in different thalamic nuclei, as previously reported (Farrant et al., 1994; Karavanova et al., 2007; Monyer et al., 1994; Wenzel et al., 1997). Our data extended these earlier studies by also showing GluN2C expression in other brain areas, such as Pir, Hb, NAc, HPC, mPFC, Amg, CPu, Cg and DR.

The NMDA-R is a tetramer that requires two GluN1 subunits with either two GluN2 subunits or a combination of GluN2 and GluN3 subunits (Cull-Candy et al., 2001). Therefore, it would be expected that in the GluN2CKO mice, the GluN2C subunit would be replaced by another GluN2 subunit or by a GluN3 subunit. Contrary to this expectation, the present results suggest that the GluN2C subunit was not systematically replaced by any other GluN2 subunit. However, complete deletion of the GluN2C led to significant changes in GluN1 expression. On one hand, the GluN1 subunit was significantly decreased in olfactory bulb, mPFC and cerebellar cortex (Crus1, Sim and 4/5Cb). Furthermore, its expression was increased in RSC, HPC, Hb and thalamus (PV, MD, IMD, CM and Re/Rh). These results partially replicate those of another study, which reported significant reductions in the expression of GluN1, GluN2A and GluN2B subunits in the whole cerebellum from postnatal day 21 GluN2CKO mice (Lu et al., 2006).

Reductions in GluN1 subunit expression may suggest a downregulation of NMDA-Rs in the olfactory bulb and cerebellum. Moreover, the fact that we

did not find reductions in any GluN2 subunits may suggest that only diheteromeric GluN1-GluN2C NMDA-Rs disappeared. In contrast, increases of GluN1 subunit are more difficult to explain, and we can speculate that a substitution of GluN2C with the GluN1 may occur in triheteromeric receptors. Nevertheless, no definite conclusion can be drawn about the possible compensatory mechanisms in GluN2CKO mice until evaluation of GluN3A and GluN3B mRNA expression (in progress) and/or receptor binding studies are performed in order to determine the density of NMDA-Rs in WT and GluN2CKO mice.

Overall, deletion of GluN2C subunit produced minor changes on the expression of GluN2A, GluN2B and GluN2D subunits, yet a significant reduction of GluN1 subunit expression in cerebellar areas. Therefore, the reported behavioral differences observed in the GluN2CKO mice, and in particular, the reduced motor incoordination induced by non-competitive NMDA-R antagonists may not only be attributable to the lack of the GluN2C subunit, but also to the compensatory changes in other subunits ensuing genetic manipulation. Another shortcoming of this study is that we did not assess GluN subunits distribution in female WT and GluN2CKO mice.

#### **4. Acute ketamine administration induces rapid, but not sustained, antidepressant-like effects and activates mTOR pathway in rats**

Ketamine is presently considered a revolutionary treatment in psychiatry because a single administration of this drug produces fast and sustained antidepressant actions in patients with TRD (see Xu et al., 2016 for a review). However, some aspects of these clinical findings are difficult to replicate in experimental animals, in particular, the presence of long-lasting antidepressant-like effects at times exceeding the actual presence of the drug.

Here we found that an acute administration of ketamine in a range of doses between 10 and 20 mg/kg induced rapid antidepressant-like responses in the FST. In particular, we observed a significant decrease of the immobility time 30 min after ketamine administration, in agreement with previously published reports (Wang et al., 2014; Yang et al., 2013), and this effect was obtained in the absence of drug-induced psychomotor stimulation. Interestingly, the temporal course of the behavioral effect follows the pharmacokinetics of (*S*)-ketamine in Wistar rats, whose brain concentration rises sharply, reaching a maximal concentration 15 min after subcutaneous administration (Gastambide et al., 2013). Despite some studies reported longer lasting effects (1 h after administration) (Wang et al., 2011), in our experimental conditions we did not find any significant effect of ketamine at this time point, as already described with a dose of 10 mg/kg ketamine (Gigliucci et al., 2013). Therefore, we were not able to reproduce the sustained antidepressant-like effects of ketamine in rats. To date, few studies have shown long-lasting antidepressant-like effects after acute ketamine administration, such as at 24 h in rats and mice (Burgdorf et al.,

2013; Gigliucci et al., 2013; Li et al., 2010; Pham et al., 2017; Zanos et al., 2016) or even at 1 week in mice (Autry et al., 2011).

In the NSFT, ketamine did not elicit an anxiolytic-like behavior, which is contrary to other studies where ketamine reduced the latency to feed (Carrier & Kabbaj, 2013; Wang et al., 2014). Remarkably, ketamine elicited hypolocomotion, in agreement with another study (Gigliucci et al., 2013) but in contrast with other reports that did not find any effects of ketamine on locomotor activity (Wang et al., 2014; Yang et al., 2013). Therefore, the increased latency to feed in the NSFT could be attributed to hypolocomotion and not to an anxiogenic effect of ketamine.

Overall, the present data support the view that acute ketamine administration induces rapid antidepressant-like responses in the FST within a short time window, paralleling its pharmacokinetics. Temporal differences between the present study and other reports may be explained by experimental conditions such as rat strain (Burke et al., 2016; Tizabi et al., 2012) or sex (Carrier & Kabbaj, 2013; Franceschelli et al., 2015). Moreover, previous exposure to stressful environments may also mediate in the antidepressant-like response of ketamine (Fitzgerald et al., 2019). In addition, sex of the human experimenter should be taken into consideration, since male scent was found necessary to elicit ketamine's antidepressant effects under specific conditions (Georgiou et al., 2018). Another variable could be the source of ketamine, although no systematic evidence associates the supplier of ketamine with the behavioral outcome of rodent experiments (Browne & Lucki, 2013). Altogether, these experimental conditions may affect replicability and should be considered when comparing studies.

It has been hypothesized that the antidepressant response of ketamine is mediated by induction of mTOR signaling and subsequent synaptogenesis

after stimulation of Glu transmission and AMPA-Rs activation (Duman et al., 2012). Moreover, a dysregulation in mTOR signaling is associated with MDD (Jernigan et al., 2011; Karolewicz et al., 2011) and post-mortem studies have described lower levels of mTOR and p70S6K in the PFC of depressed patients (Jernigan et al., 2011).

We found increased levels of the phosphorylated form of mTOR in a preparation enriched in synaptoneurosomes in the PFC and vHPC. Evidence of mTOR activation was supported by increased phosphorylation of the downstream protein p70S6K in both areas. These results are in agreement with previous data showing that activation of mTOR signaling occurs in the PFC and HPC at low but not high anesthetic doses of ketamine, which in turn produce rapid antidepressant behavioral actions (Li et al., 2010; Yang et al., 2013). Interestingly, a partial agonist at the glycine binding site of the NMDA-R, rapastinel (formerly GLYX-13), has been found to induce rapid (Burgdorf et al., 2013) but not sustained (Yang et al., 2016) antidepressant-like effects in rats, which are paralleled by increased mTOR signaling in the mPFC (Liu et al., 2017).

Taking into account that activation of mTOR and p70S6K has been functionally linked with synaptic plasticity (Hoeffler & Klann, 2010), initiation of protein translation and cell growth (Fenton & Gout, 2011; Tavares et al., 2015), we investigated the mRNA levels of two synaptic proteins: PSD95 and synapsin I. On one hand, PSD95 is a scaffolding protein located at excitatory synapses and it is involved in the stabilization, recruitment and trafficking of NMDA-Rs and AMPA-Rs to the postsynaptic membrane (Chen et al., 2000; Kornau et al., 1995). On the other hand, synapsin I plays an important role in synapse formation and modulates neurotransmitter release (Mirza & Zahid, 2018; Song & Augustine, 2015). Previous work has reported significant increased levels of PSD95 and synapsin I in PFC (Li et al., 2010), and we further extended these results

describing increased levels of PSD95 in DR and synapsin I in HPC and DR. Overall, these molecular changes reinforce the idea that the antidepressant effects of ketamine could be prompted by activation of the mTOR signaling pathway.

However, other mechanisms than NMDA-R blockade may be involved in the action of ketamine, either in the acute or sustained antidepressant effects. First, of the three non-competitive NMDA-R antagonists studied, MK-801 also elicited antidepressant-like effects in rodents (Maeng et al., 2008; Rosa et al., 2003; Skolnick et al., 2015) and activated mTOR signaling (Yoon et al., 2008), while PCP did not (Turgeon et al., 2007). Moreover, memantine, another non-competitive NMDA-R antagonist with the same affinity for the NMDA-R than ketamine, did not exhibit antidepressant effects in two double-blinded, placebo-controlled studies (Lenze et al., 2012; Zarate et al., 2006b). In addition, while the NMDA-R hypothesis of ketamine action would predict greater efficacy of (*S*)-ketamine since it shows more affinity at the NMDA-R site than (*R*)-ketamine (Domino, 2010), studies have demonstrated greater and longer antidepressant-like effects of (*R*)-ketamine (Chang et al., 2019; Fukumoto et al., 2017; Yang et al., 2015; Zanos et al., 2016; Zhang et al., 2014). This discrepancy between affinity and potency also suggests that ketamine's antidepressant effects may not entirely depend on NMDA-R antagonism. For instance, ketamine exhibited binding affinity for the dopamine D<sub>2</sub> and serotonin 5-HT<sub>2</sub> receptors (Kapur & Seeman, 2002; Tsukada et al., 2000). In addition, ketamine inhibited monoamine (norepinephrine, DA and 5-HT) transporters (Nishimura et al., 1998) and also modulated subtypes of the GABA<sub>A</sub> receptor in granular neurons within the cerebellum (Hevers et al., 2008). Therefore, it would be interesting to study the contribution of these other targets on the antidepressant effects of ketamine. Finally, in 2016, it was hypothesized that (*2S,6S;2R,6R*)-hydroxynorketamine (HNK), a metabolite of ketamine, was necessary for its long-lasting antidepressant

action in rodent tests, which involved the activation of AMPA-Rs and did not depend on NMDA-R inhibition (Zanos et al., 2016). Since then, other researchers have replicated and extended this finding (Chou et al., 2018; Fukumoto et al., 2019; Pham et al., 2018).





# Conclusions



The main conclusions of the present work can be summarized as follows:

- The GluN2C subunit is strongly involved in motor components of the psychotomimetic syndrome induced by non-competitive NMDA-R antagonists, but not in sensorimotor gating deficits. Its genetic deletion results in an improved motor coordination after NMDA-R blockade.
- The GluN2C subunit plays a role in the differential neural activation of motor areas induced by MK-801 or PCP administration, such as the cerebellum and the basal ganglia. These results allow to identify the cerebellum, where the GluN2C subunit is highly expressed, as a key regional target in the action of these non-competitive NMDA-R antagonists.
- The GluN2C subunit does not contribute to the antidepressant-like effects induced by ketamine in both sexes. These effects likely involve different networks than those involved in the psychotomimetic effects and probably depend on increased 5-HT neurotransmission in mPFC.
- Deletion of the GluN2C subunit produces remarkable changes in the expression of the GluN1 subunit in cerebellar and thalamic areas, which may contribute to the behavioral and molecular differences between both genotypes.
- Acute ketamine treatment induces rapid but not sustained antidepressant-like responses in rats. It activates the mTOR signaling pathway and the expression of synaptic proteins in PFC, HPC and DR.



# **Bibliography**



- Adamaszek, M., D'Agata, F., Ferrucci, R., Habas, C., Keulen, S., Kirkby, K.C., Leggio, M., Mariën, P., Molinari, M., Moulton, E., Orsi, L., Van Overwalle, F., Papadelis, C., Priori, A., Sacchetti, B., Schutter, D.J., Styliadis, C., Verhoeven, J., 2017. Consensus Paper: Cerebellum and Emotion. *Cerebellum* 16, 552–576. <https://doi.org/10.1007/s12311-016-0815-8>
- Adell, A., Jiménez-Sánchez, L., López-Gil, X., Romón, T., 2012. Is the acute NMDA receptor hypofunction a valid model of schizophrenia? *Schizophr. Bull.* 38, 9–14. <https://doi.org/10.1093/schbul/sbr133>
- Ago, Y., Tanabe, W., Higuchi, M., Tsukada, S., Tanaka, T., Yamaguchi, T., Igarashi, H., Yokoyama, R., Seiriki, K., Kasai, A., Nakazawa, T., Nakagawa, S., Hashimoto, K., Hashimoto, H., 2019. (R)-ketamine induces a greater increase in prefrontal 5-HT release than (S)-ketamine and ketamine metabolites via an AMPA receptor-independent mechanism. *Int. J. Neuropsychopharmacol.* <https://doi.org/https://doi.org/10.1093/ijnp/pyz041>
- Al-Hallaq, R.A., Jarabek, B.R., Fu, Z., Vicini, S., Wolfe, B.B., Yasuda, R.P., 2002. Association of NR3A with the N-methyl-D-aspartate receptor NR1 and NR2 subunits. *Mol. Pharmacol.* 62, 1119–1127. <https://doi.org/10.1124/mol.62.5.1119>
- Albert, P.R., 2015. Why is depression more prevalent in women? *J. Psychiatry Neurosci.* 40, 219–221. <https://doi.org/10.1503/jpn.150205>
- Amargós-Bosch, M., López-Gil, X., Artigas, F., Adell, A., 2006. Clozapine and olanzapine, but not haloperidol, suppress serotonin efflux in the medial prefrontal cortex elicited by phencyclidine and ketamine. *Int. J. Neuropsychopharmacol.* 9, 565–573. <https://doi.org/10.1017/S1461145705005900>
- Amat-Foraster, M., Celada, P., Richter, U., Jensen, A.A., Plath, N., Artigas, F., Herrik, K.F., 2019. Modulation of thalamo-cortical activity by the NMDA receptor antagonists ketamine and phencyclidine in the awake freely-moving rat. *Neuropharmacology* 158, 107745. <https://doi.org/10.1016/j.neuropharm.2019.107745>
- Amat-Foraster, M., Jensen, A.A., Plath, N., Herrik, K.F., Celada, P., Artigas, F., 2018. Temporally dissociable effects of ketamine on neuronal discharge and gamma oscillations in rat thalamo-cortical networks. *Neuropharmacology* 137, 13–23. <https://doi.org/10.1016/j.neuropharm.2018.04.022>
- American Psychiatric Association, 2013. Diagnostic and statistical manual of mental disorders, fifth edition.
- Amidfar, M., Woelfer, M., Réus, G.Z., Quevedo, J., Walter, M., Kim, Y.K., 2019. The role of NMDA receptor in neurobiology and treatment of major depressive disorder: Evidence from translational research. *Prog. Neuropsychopharmacol. Biol. Psychiatry* 94, 109668. <https://doi.org/10.1016/j.pnpbp.2019.109668>
- Andiné, P., Widermark, N., Axelsson, R., Nyberg, G., Olofsson, U., Mårtensson, E.,

- Sandberg, M., 1999. Characterization of MK-801-induced behavior as a putative rat model of psychosis. *J. Pharmacol. Exp. Ther.* 290, 1393–408.
- Andreasen, N.C., Nopoulos, P., O’Leary, D.S., Miller, D.D., Wassink, T., Flaum, M., 1999. Defining the phenotype of schizophrenia: Cognitive dysmetria and its neural mechanisms. *Biol. Psychiatry* 46, 908–920. [https://doi.org/10.1016/S0006-3223\(99\)00152-3](https://doi.org/10.1016/S0006-3223(99)00152-3)
- Andreasen, N.C., Paradiso, S., O’Leary, D.S., 1998. “Cognitive dysmetria” as an integrative theory of schizophrenia: A dysfunction in cortical-subcortical-cerebellar circuitry? *Schizophr. Bull.* <https://doi.org/10.1093/oxfordjournals.schbul.a033321>
- Autry, A.E., Adachi, M., Nosyreva, E., Na, E.S., Los, M.F., Cheng, P.F., Kavalali, E.T., Monteggia, L.M., 2011. NMDA receptor blockade at rest triggers rapid behavioural antidepressant responses. *Nature* 475, 91–96. <https://doi.org/10.1038/nature10130>
- Baez, M.V., Cercato, M.C., Jerusalinsky, D.A., 2018. NMDA receptor subunits change after synaptic plasticity induction and learning and memory acquisition. *Neural Plast.* 2018, 5093048. <https://doi.org/10.1155/2018/5093048>
- Bannerman, D.M., Niewoehner, B., Lyon, L., Romberg, C., Schmitt, W.B., Taylor, A., Sanderson, D.J., Cottam, J., Sprengel, R., Seeburg, P.H., Köhr, G., Rawlins, J.N.P., 2008. NMDA receptor subunit NR2A is required for rapidly acquired spatial working memory but not incremental spatial reference memory. *J. Neurosci.* 28, 3623–3630. <https://doi.org/10.1523/JNEUROSCI.3639-07.2008>
- Bareš, M., Lungu, O. V., Husárová, I., Gescheidt, T., 2010. Predictive motor timing performance dissociates between early diseases of the cerebellum and parkinson’s disease. *Cerebellum* 9, 124–135. <https://doi.org/10.1007/s12311-009-0133-5>
- Bargmann, C.I., Lieberman, J.A., 2014. What the BRAIN initiative means for psychiatry. *Am. J. Psychiatry* 171, 1038–1040. <https://doi.org/10.1176/appi.ajp.2014.14081029>
- Benes, F.M., Berretta, S., 2001. GABAergic interneurons: Implications for understanding schizophrenia and bipolar disorder. *Neuropsychopharmacology* 25, 1–27. [https://doi.org/10.1016/S0893-133X\(01\)00225-1](https://doi.org/10.1016/S0893-133X(01)00225-1)
- Berman, R.M., Cappiello, A., Anand, A., Oren, D.A., Heninger, G.R., Charney, D.S., Krystal, J.H., 2000. Antidepressant effects of ketamine in depressed patients. *Biol. Psychiatry* 47, 351–354. [https://doi.org/10.1016/S0006-3223\(99\)00230-9](https://doi.org/10.1016/S0006-3223(99)00230-9)
- Bertron, J.L., Seto, M., Lindsley, C.W., 2018. DARK Classics in Chemical Neuroscience: Phencyclidine (PCP). *ACS Chem. Neurosci.* 9, 2459–2474. <https://doi.org/10.1021/acscchemneuro.8b00266>
- Bhattacharya, S., Khatri, A., Swanger, S.A., DiRaddo, J.O., Yi, F., Hansen, K.B., Yuan, H., Traynelis, S.F., 2018. Triheteromeric GluN1/GluN2A/GluN2C NMDARs with Unique Single-Channel Properties Are the Dominant Receptor Population in



- Cerebellar Granule Cells. *Neuron* 99, 315–328.  
<https://doi.org/10.1016/j.neuron.2018.06.010>
- Binshtok, A.M., Fleidervish, I.A., Sprengel, R., Gutnick, M.J., 2006. NMDA receptors in layer 4 spiny stellate cells of the mouse barrel cortex contain the NR2C subunit. *J. Neurosci.* 26, 708–715.  
<https://doi.org/10.1523/JNEUROSCI.4409-05.2006>
- Blakemore, S.J., Frith, C.D., Wolpert, D.M., 2001. The cerebellum is involved in predicting the sensory consequences of action. *Neuroreport* 12, 1879–1884.  
<https://doi.org/10.1097/00001756-200107030-00023>
- Bliss, T.V.P., Collingridge, G.L., 1993. A synaptic model of memory: Long-term potentiation in the hippocampus. *Nature* 361, 31–39.  
<https://doi.org/10.1038/361031a0>
- Bloch, R.G., Dooneief, A.S., Buchberg, A.S., Spellman, S., 1954. The Clinical Effect of Isoniazid and Iproniazid in the Treatment of Pulmonary Tuberculosis. *Ann. Intern. Med.* 40, 881–900. <https://doi.org/10.7326/0003-4819-40-5-881>
- Bolam, J., Hanley, J., Booth, P., Bevan, M., 2000. Synaptic organisation of the basal ganglia. *J. Anat.* 196, 527–542.
- Bosch-Bouju, C., Hyland, B.I., Parr-Brownlie, L.C., 2013. Motor thalamus integration of cortical, cerebellar and basal ganglia information: Implications for normal and parkinsonian conditions. *Front. Comput. Neurosci.* 7, 163.  
<https://doi.org/10.3389/fncom.2013.00163>
- Bostan, A.C., Dum, R.P., Strick, P.L., 2018. Functional Anatomy of Basal Ganglia Circuits with the Cerebral Cortex and the Cerebellum. *Prog. Neurol. Surg.* 33, 50–61. <https://doi.org/10.1159/000480748>
- Bostan, A.C., Dum, R.P., Strick, P.L., 2013. Cerebellar networks with the cerebral cortex and basal ganglia. *Trends Cogn. Sci.* 17, 241–254.  
<https://doi.org/10.1016/j.tics.2013.03.003>
- Boyce-Rustay, J.M., Holmes, A., 2006. Genetic inactivation of the NMDA receptor NR2A subunit has anxiolytic- and antidepressant-like effects in mice. *Neuropsychopharmacology* 31, 2405–2414.  
<https://doi.org/10.1038/sj.npp.1301039>
- Brady, R.O., Gonsalvez, I., Lee, I., Öngür, D., Seidman, L.J., Schmahmann, J.D., Eack, S.M., Keshavan, M.S., Pascual-Leone, A., Halko, M.A., 2019. Cerebellar-Prefrontal Network Connectivity and Negative Symptoms in Schizophrenia. *Am. J. Psychiatry* 176, 512–520. <https://doi.org/10.1176/appi.ajp.2018.18040429>
- Braff, D.L., 1990. Sensorimotor Gating and Schizophrenia. *Arch. Gen. Psychiatry* 47, 181. <https://doi.org/10.1001/archpsyc.1990.01810140081011>
- Breier, A., Malhotra, A.K., Pinals, D.A., Weisenfeld, N.I., Pickar, D., 1997. Association of ketamine-induced psychosis with focal activation of the prefrontal cortex in healthy volunteers. *Am. J. Psychiatry* 154, 805–811.

<https://doi.org/10.1176/ajp.154.6.805>

Bresink, I., Benke, T., Collett, V., Seal, A., Parsons, C., Henley, J., Collingridge, G.L., 1996. Effects of memantine on recombinant rat NMDA receptors expressed in HEK 293 cells. *Br. J. Pharmacol.* 119, 195–204. <https://doi.org/10.1111/j.1530-0277.1999.tb04122>

Browne, C.A., Lucki, I., 2013. Antidepressant effects of ketamine: Mechanisms underlying fast-acting novel antidepressants. *Front. Pharmacol.* 4, 161. <https://doi.org/10.3389/fphar.2013.00161>

Bullmore, E., Sporns, O., 2009. Complex brain networks: Graph theoretical analysis of structural and functional systems. *Nat. Rev. Neurosci.* 10, 186–198. <https://doi.org/10.1038/nrn2575>

Burgdorf, J., Zhang, X.L., Nicholson, K.L., Balster, R.L., David Leander, J., Stanton, P.K., Gross, A.L., Kroes, R.A., Moskal, J.R., 2013a. GLYX-13, a NMDA receptor glycine-site functional partial agonist, induces antidepressant-like effects without ketamine-like side effects. *Neuropsychopharmacology* 38, 729–742. <https://doi.org/10.1038/npp.2012.246>

Burgdorf, J., Zhang, X.L., Nicholson, K.L., Balster, R.L., David Leander, J., Stanton, P.K., Gross, A.L., Kroes, R.A., Moskal, J.R., 2013b. GLYX-13, a NMDA receptor glycine-site functional partial agonist, induces antidepressant-like effects without ketamine-like side effects. *Neuropsychopharmacology* 38, 729–742. <https://doi.org/10.1038/npp.2012.246>

Burke, N.N., Coppinger, J., Deaver, D.R., Roche, M., Finn, D.P., Kelly, J., 2016. Sex differences and similarities in depressive- and anxiety-like behaviour in the Wistar-Kyoto rat. *Physiol. Behav.* 167, 28–34. <https://doi.org/10.1016/j.physbeh.2016.08.031>

Canuso, C.M., Singh, J.B., Fedgchin, M., Alphas, L., Lane, R., Lim, P., Pinter, C., Hough, D., Sanacora, G., Manji, H., Drevets, W.C., 2018. Efficacy and safety of intranasal esketamine for the rapid reduction of symptoms of depression and suicidality in patients at imminent risk for suicide: Results of a double-blind, randomized, placebo-controlled study. *Am. J. Psychiatry* 175, 620–630. <https://doi.org/10.1176/appi.ajp.2018.17060720>

Carlsson, M., Carlsson, A., 1990. Interactions between glutamatergic and monoaminergic systems within the basal ganglia-implications for schizophrenia and Parkinson's disease. *Trends Neurosci.* [https://doi.org/10.1016/0166-2236\(90\)90108-M](https://doi.org/10.1016/0166-2236(90)90108-M)

Carrier, N., Kabbaj, M., 2013. Sex differences in the antidepressant-like effects of ketamine. *Neuropharmacology* 70, 27–34. <https://doi.org/10.1016/j.neuropharm.2012.12.009>

Carter, C., Rivy, J.P., Scatton, B., 1989. Ifenprodil and SL 82.0715 are antagonists at the polyamine site of the N-methyl-D-aspartate (NMDA) receptor. *Eur. J. Pharmacol.* 164, 611–612. [https://doi.org/10.1016/0014-2999\(89\)90275-6](https://doi.org/10.1016/0014-2999(89)90275-6)

- Castañé, A., Artigas, F., Bortolozzi, A., 2008. The absence of 5-HT<sub>1A</sub> receptors has minor effects on dopamine but not serotonin release evoked by MK-801 in mice prefrontal cortex. *Psychopharmacology (Berl)*. 200, 281–290.  
<https://doi.org/10.1007/s00213-008-1205-9>
- Castañé, A., Santana, N., Artigas, F., 2015. PCP-based mice models of schizophrenia: Differential behavioral, neurochemical and cellular effects of acute and subchronic treatments. *Psychopharmacology (Berl)*. 232, 4085–4097.  
<https://doi.org/10.1007/s00213-015-3946-6>
- Catts, V.S., Lai, Y.L., Weickert, C.S., Weickert, T.W., Catts, S. V., 2016. A quantitative review of the postmortem evidence for decreased cortical N-methyl-d-aspartate receptor expression levels in schizophrenia: How can we link molecular abnormalities to mismatch negativity deficits? *Biol. Psychol.* 116, 57–67. <https://doi.org/10.1016/j.biopsycho.2015.10.013>
- Celada, P., Lladó-Pelfort, L., Santana, N., Kargieman, L., Troyano-Rodriguez, E., Riga, M.S., Artigas, F., 2013. Disruption of thalamocortical activity in schizophrenia models: Relevance to antipsychotic drug action. *Int. J. Neuropsychopharmacol.* 16, 2145–2163.  
<https://doi.org/10.1017/S1461145713000643>
- Chang, L., Zhang, K., Pu, Y., Qu, Y., Wang, S. ming, Xiong, Z., Ren, Q., Dong, C., Fujita, Y., Hashimoto, K., 2019. Comparison of antidepressant and side effects in mice after intranasal administration of (R,S)-ketamine, (R)-ketamine, and (S)-ketamine. *Pharmacol. Biochem. Behav.* 181, 53–59.  
<https://doi.org/10.1016/j.pbb.2019.04.008>
- Chang, M., Womer, F.Y., Edmiston, E.K., Bai, C., Zhou, Q., Jiang, X., Wei, S., Wei, Y., Ye, Y., Huang, H., He, Y., Xu, K., Tang, Y., Wang, F., 2018. Neurobiological Commonalities and Distinctions among Three Major Psychiatric Diagnostic Categories: A Structural MRI Study. *Schizophr. Bull.* 44, 65–74.  
<https://doi.org/10.1093/schbul/sbx028>
- Chatterton, J.E., Awobuluyi, M., Premkumar, L.S., Takahashi, H., Talantova, M., Shin, Y., Cul, J., Tu, S., Sevarino, K.A., Nakanishi, N., Tong, G., Lipton, S.A., Zhang, D., 2002. Excitatory glycine receptors containing the NR3 family of NMDA receptor subunits. *Nature* 415, 793–798. <https://doi.org/10.1038/nature715>
- Chen, L., Chetkovich, D.M., Petralia, R.S., Sweeney, N.T., Kawasaki, Y., Wenthold, R.J., Brecht, D.S., Nicoll, R.A., 2000. Stargazin regulates synaptic targeting of AMPA receptors by two distinct mechanisms. *Nature* 408, 936–943.  
<https://doi.org/10.1038/35050030>
- Chou, D., Peng, H.Y., Lin, T. Bin, Lai, C.Y., Hsieh, M.C., Wen, Y.C., Lee, A.S., Wang, H.H., Yang, P.S., Chen, G. Den, Ho, Y.C., 2018. (2R,6R)-hydroxynorketamine rescues chronic stress-induced depression-like behavior through its actions in the midbrain periaqueductal gray. *Neuropharmacology* 139, 1–12.  
<https://doi.org/10.1016/j.neuropharm.2018.06.033>
- Ciabarra, A.M., Sullivan, J.M., Gahn, L.G., Pecht, G., Heinemann, S., Sevarino,

K.A., 1995. Cloning and characterization of  $\alpha$ -1: A developmentally regulated member of a novel class of the ionotropic glutamate receptor family. *J. Neurosci.* 15, 6498–6508.

Clarac, F., 2008. Some historical reflections on the neural control of locomotion. *Brain Res. Rev.* 57, 13–21. <https://doi.org/10.1016/j.brainresrev.2007.07.015>

Clineschmidt, B. V., Martin, G.E., Bunting, P.R., 1982. Anticonvulsant activity of (+)-5-methyl-10, 11-dihydro-5H-dibenzo[a, d]cyclohepten-5, 10-imine (MK-801), a substance with potent anticonvulsant, central sympathomimetic, and apparent anxiolytic properties. *Drug Dev. Res.* 2, 123–134.

Collingridge, G.L., Volianskis, A., Bannister, N., France, G., Hanna, L., Mercier, M., Tidball, P., Fang, G., Irvine, M.W., Costa, B.M., Monaghan, D.T., Bortolotto, Z.A., Molnár, E., Lodge, D., Jane, D.E., 2013. The NMDA receptor as a target for cognitive enhancement. *Neuropharmacology* 64, 13–26. <https://doi.org/10.1038/nature13527>

Cross-Disorder Group of the Psychiatric Genomics Consortium, 2003. Identification of risk loci with shared effects on five major psychiatric disorders: a genome-wide analysis. *Lancet* 381, 1371–1379. <https://doi.org/10.1038/jid.2014.371>

Cruz, S.L., Soberanes-Chávez, P., Páez-Martínez, N., López-Rubalcava, C., 2009. Toluene has antidepressant-like actions in two animal models used for the screening of antidepressant drugs. *Psychopharmacology (Berl)*. 204, 279–286. <https://doi.org/10.1007/s00213-009-1462-2>

Cull-Candy, S.G., Brickley, S., Farrant, M., 2001. NMDA receptor subunits: diversity, development and disease. *Curr. Opin. Neurobiol.* 11, 327–335.

Cull-Candy, S.G., Leszkiewicz, D.N., 2004. Role of Distinct NMDA Receptor Subtypes at Central Synapses. *Sci. STKE* 2004, re16. <https://doi.org/10.1126/stke.2552004re16>

Dalmau, J., Armangué, T., Planagumà, J., Radosevic, M., Mannara, F., Leypoldt, F., Geis, C., Lancaster, E., Titulaer, M.J., Rosenfeld, M.R., Graus, F., 2019. An update on anti-NMDA receptor encephalitis for neurologists and psychiatrists: mechanisms and models. *Lancet Neurol.* [https://doi.org/10.1016/s1474-4422\(19\)30244-3](https://doi.org/10.1016/s1474-4422(19)30244-3)

Dalmau, J., Gleichman, A.J., Hughes, E.G., Rossi, J.E., Peng, X., Dessain, S.K., Rosenfeld, M.R., Balice-gordon, R., Lynch, D.R., 2009. Anti-NMDA-receptor encephalitis: case series and analysis of the effects of antibodies. *Lancet Neurol.* 7, 1091–1098. [https://doi.org/10.1016/S1474-4422\(08\)70224-2](https://doi.org/10.1016/S1474-4422(08)70224-2)

Daly, E.J., Singh, J.B., Fedgchin, M., Cooper, K., Lim, P., Shelton, R.C., Thase, M.E., Winokur, A., Van Nueten, L., Manji, H., Drevets, W.C., 2018. Efficacy and safety of intranasal esketamine adjunctive to oral antidepressant therapy in treatment-resistant depression: A randomized clinical trial. *JAMA Psychiatry* 75, 139–148. <https://doi.org/10.1001/jamapsychiatry.2017.3739>

- Daniell, L.C., 1990. The noncompetitive N-methyl-D-aspartate antagonists, MK-801, phencyclidine and ketamine, increase the potency of general anesthetics. *Pharmacol. Biochem. Behav.* 36, 111–115. [https://doi.org/10.1016/0091-3057\(90\)90134-4](https://doi.org/10.1016/0091-3057(90)90134-4)
- Das, S., Sasaki, Y.F., Rothe, T., Premkumar, L.S., Takasu, M., Crandalli, J.E., Dikkes, P., Conner, D.A., Rayudu, P. V., Cheung, W., Vincent, C., Lipton, S.A., Nakanish, N., 1998. Increased NMDA current and spine density in mice lacking the NMDA receptor subunit NR3A. *Nature* 393, 377–381. <https://doi.org/10.1038/30748>
- Dissanayake, D.W.N., Mason, R., Marsden, C.A., 2013. Sensory gating, Cannabinoids and Schizophrenia. *Neuropharmacology* 67, 66–77. <https://doi.org/10.1016/j.neuropharm.2012.10.011>
- Domino, E.F., 2010. Taming the ketamine tiger. *Anesthesiology* 113, 678–684. <https://doi.org/10.1097/ALN.0b013e3181ed09a2>
- Domino, E.F., Chodoff, P., Corssen, G., 1965. Pharmacologic effects of CI-581, a new dissociative anesthetic, in man. *Clin. Pharmacol. Ther.* 6, 279–291. <https://doi.org/10.1002/cpt196563279>
- Dossat, A.M., Wright, K.N., Strong, C.E., Kabbaj, M., 2018. Behavioral and biochemical sensitivity to low doses of ketamine: Influence of estrous cycle in C57BL/6 mice. *Neuropharmacology* 130, 30–41. <https://doi.org/10.1016/j.neuropharm.2017.11.022>
- Dragunow, M., Faull, R., 1989. The use of c-fos as a metabolic marker in neuronal pathway tracing. *J. Neurosci. Methods* 29, 261–265.
- Dravid, S.M., Erreger, K., Yuan, H., Nicholson, K., Le, P., Lyuboslavsky, P., Almonte, A., Murray, E., Mosely, C., Barber, J., French, A., Balster, R., Murray, T.F., Traynelis, S.F., 2007. Subunit-specific mechanisms and proton sensitivity of NMDA receptor channel block. *J. Physiol.* 581, 107–128. <https://doi.org/10.1113/jphysiol.2006.124958>
- du Jardin, K.G., Müller, H.K., Elfving, B., Dale, E., Wegener, G., Sanchez, C., 2016. Potential involvement of serotonergic signaling in ketamine's antidepressant actions: A critical review. *Prog. Neuro-Psychopharmacology Biol. Psychiatry* 71, 27–38. <https://doi.org/10.1016/j.pnpbp.2016.05.007>
- Dum, R.P., Strick, P.L., 2003. An unfolded map of the cerebellar dentate nucleus and its projections to the cerebral cortex. *J. Neurophysiol.* 89, 634–639.
- Duman, R.S., Li, N., Liu, R.-J., Duric, V., Aghajanian, G., 2012. Signaling pathways underlying the rapid antidepressant actions of ketamine. *Neuropharmacology* 62, 35–41. <https://doi.org/10.1038/jid.2014.371>
- Duncan, G.E., Moy, S.S., Perez, A., Eddy, D.M., Zinzow, W.M., Lieberman, J.A., Snouwaert, J.N., Koller, B.H., 2004. Deficits in sensorimotor gating and tests of social behavior in a genetic model of reduced NMDA receptor function. *Behav. Brain Res.* 153, 507–519. <https://doi.org/10.1016/j.bbr.2004.01.008>

- Durand, G., Kovalchuk, Y., Konnerth, A., 1996. Long-term potentiation and functional synapse induction in developing hippocampus. *Nature* 381, 71–75.
- Dutta, A., McKie, S., Deakin, J.F.W., 2014. Resting state networks in major depressive disorder. *Psychiatry Res. - Neuroimaging* 224, 139–151. <https://doi.org/10.1016/j.pscychresns.2014.10.003>
- Elia, N., Tramèr, M.R., 2005. Ketamine and postoperative pain - A quantitative systematic review of randomised trials. *Pain* 113, 61–70. <https://doi.org/10.1016/j.pain.2004.09.036>
- Elsworth, J.D., Groman, S.M., Jentsch, J.D., Leranath, C., Eugene Redmond, D., Kim, J.D., Diano, S., Roth, R.H., 2015. Primate phencyclidine model of schizophrenia: Sex-specific effects on cognition, brain derived neurotrophic factor, spine synapses, and dopamine turnover in prefrontal cortex. *Int. J. Neuropsychopharmacol.* 18, 1–10. <https://doi.org/10.1093/ijnp/pyu048>
- Escalona, P.R., Early, B., McDonald, W.M., Doraiswamy, P.M., Shah, S.A., Husain, M.M., Boyko, O.B., Figiel, G.S., Ellinwood, E.H., Nemeroff, C.B., Krishnan, K.R.R., 1993. Reduction of cerebellar volume in major depression: A controlled MRI study. *Depression* 1, 156–158. <https://doi.org/10.1002/depr.3050010307>
- Farrant, M., Feldmeyer, D., Takahashi, T., Cull-Candy, S.G., 1994. NMDA-receptor channel diversity in the developing cerebellum. *Nature* 368, 335–339. <https://doi.org/10.1038/368335a0>
- Fatemi, S.H., Folsom, T.D., 2009. The neurodevelopmental hypothesis of schizophrenia, revisited. *Schizophr. Bull.* 35, 528–548. <https://doi.org/10.1093/schbul/sbn187>
- Fava, M., 2003. Diagnosis and definition of treatment-resistant depression. *Biol. Psychiatry* 53, 649–659. [https://doi.org/10.1016/S0006-3223\(03\)00231-2](https://doi.org/10.1016/S0006-3223(03)00231-2)
- FDA News Release on March 5, 2019. FDA Approves New Nasal Spray Medication for Treatment-resistant Depression; Available Only at a Certified Doctor's Office or Clinic. <https://www.fda.gov/NewsEvents/Newsroom/PressAnnouncements/ucm632761.htm>
- Fenton, T.R., Gout, I.T., 2011. Functions and regulation of the 70 kDa ribosomal S6 kinases. *Int. J. Biochem. Cell Biol.* 43, 47–59. <https://doi.org/10.1016/j.biocel.2010.09.018>
- Fitzgerald, P.J., Yen, J.Y., Watson, B.O., 2019. Stress-sensitive antidepressant-like effects of ketamine in the mouse forced swim test. *PLoS One* 14, 1–17. <https://doi.org/10.1371/journal.pone.0215554>
- Forrest, D., Yuzaki, M., Soares, H.D., Ng, L., Luk, D.C., Sheng, M., Stewart, C.L., Morgan, J.I., Connor, J.A., Curran, T., 1994. Targeted disruption of NMDA receptor 1 gene abolishes NMDA response and results in neonatal death. *Neuron* 13, 325–338. [https://doi.org/10.1016/0896-6273\(94\)90350-6](https://doi.org/10.1016/0896-6273(94)90350-6)

- Franceschelli, A., Sens, J., Herchick, S., Thelen, C., Pitychoutis, P.M., 2015. Sex differences in the rapid and the sustained antidepressant-like effects of ketamine in stress-naïve and “depressed” mice exposed to chronic mild stress. *Neuroscience* 290, 49–60. <https://doi.org/10.1016/j.neuroscience.2015.01.008>
- Franklin, K.B.J., Paxinos, G., 2007. *The mouse brain in stereotaxi coordinates*, third ed. Elsevier Academic Press, London.
- Fritz, A.K., Amrein, I., Wolfer, D.P., 2017. Similar reliability and equivalent performance of female and male mice in the open field and water-maze place navigation task. *Am. J. Med. Genet.* 175, 1–12. <https://doi.org/10.1002/ajmg.c.31565>
- Fukumoto, K., Fogaça, M. V., Liu, R.J., Duman, C., Kato, T., Li, X.Y., Duman, R.S., 2019. Activity-dependent brain-derived neurotrophic factor signaling is required for the antidepressant actions of (2R,6R)-hydroxynorketamine. *Proc. Natl. Acad. Sci. U. S. A.* 116, 297–302. <https://doi.org/10.1073/pnas.1814709116>
- Fukumoto, K., Iijima, M., Chaki, S., 2016. The Antidepressant Effects of an mGlu2/3 Receptor Antagonist and Ketamine Require AMPA Receptor Stimulation in the mPFC and Subsequent Activation of the 5-HT Neurons in the DRN. *Neuropsychopharmacology* 41, 1046–1056. <https://doi.org/10.1038/npp.2015.233>
- Fukumoto, K., Toki, H., Iijima, M., Hashihayata, T., Yamaguchi, J.I., Hashimoto, K., Chaki, S., 2017. Antidepressant potential of (R)-ketamine in rodent models: Comparison with (S)-ketamine. *J. Pharmacol. Exp. Ther.* 361, 9–16. <https://doi.org/10.1124/jpet.116.239228>
- Furukawa, H., Singh, S.K., Mancusso, R., Gouaux, E., 2005. Subunit arrangement and function in NMDA receptors. *Nature* 438, 185–192. <https://doi.org/10.1038/nature04089>
- Gastambide, F., Mitchell, S.N., Robbins, T.W., Tricklebank, M.D., Gilmour, G., 2013. Temporally distinct cognitive effects following acute administration of ketamine and phencyclidine in the rat. *Eur. Neuropsychopharmacol.* 23, 1414–1422. <https://doi.org/10.1016/j.euroneuro.2013.03.002>
- Gasull-Camós, J., Martínez-Torres, S., Tarrés-Gatius, M., Ozaita, A., Artigas, F., Castañé, A., 2018. Serotonergic mechanisms involved in antidepressant-like responses evoked by GLT-1 blockade in rat infralimbic cortex. *Neuropharmacology* 139, 41–51. <https://doi.org/10.1016/j.neuropharm.2018.06.029>
- Gasull-Camós, J., Tarrés-Gatius, M., Artigas, F., Castañé, A., 2017. Glial GLT-1 blockade in infralimbic cortex as a new strategy to evoke rapid antidepressant-like effects in rats. *Transl. Psychiatry* 7, e1038. <https://doi.org/10.1038/tp.2017.7>
- Georgiou, P., Zanos, P., Highland, J., Jenne, C., Stewart, B., Gerhard, D., Duman, R., Gould, T., 2018. Human experimenter sex modulates mouse behavioral

- responses to stress and to the antidepressant ketamine. *Neuropsychopharmacology* (Abstract: ACNP 57th annual meeting, poster session I). <https://doi.org/10.1038/s41386-018-0266-7>
- Geyer, M.A., Ellenbroek, B., 2003. Animal behavior models of the mechanisms underlying antipsychotic atypicality. *Prog. Neuro-Psychopharmacology Biol. Psychiatry* 27, 1071–1079. <https://doi.org/10.1016/j.pnpbp.2003.09.003>
- Geyer, M.A., Krebs-Thomson, K., Braff, D.L., Swerdlow, N.R., 2001. Pharmacological studies of prepulse inhibition models of sensorimotor gating deficits in schizophrenia: A decade in review, *Psychopharmacology*. <https://doi.org/10.1007/s002130100811>
- Ghasemi, M., Raza, M., Dehpour, A.R., 2010. NMDA receptor antagonists augment antidepressant-like effects of lithium in the mouse forced swimming test. *J. Psychopharmacol.* 24, 585–594. <https://doi.org/10.1177/0269881109104845>
- Gigliucci, V., O’Dowd, G., Casey, S., Egan, D., Gibney, S., Harkin, A., 2013. Ketamine elicits sustained antidepressant-like activity via a serotonin-dependent mechanism. *Psychopharmacology (Berl)*. 228, 157–166. <https://doi.org/10.1007/s00213-013-3024-x>
- Gladding, C.M., Raymond, L.A., 2011. Mechanisms underlying NMDA receptor synaptic/extrasynaptic distribution and function. *Mol. Cell. Neurosci.* 48, 308–320. <https://doi.org/10.1016/j.mcn.2011.05.001>
- Gonzalez-Burgos, G., Lewis, D.A., 2012. NMDA receptor hypofunction, parvalbumin-positive neurons, and cortical gamma oscillations in schizophrenia. *Schizophr. Bull.* 38, 950–957. <https://doi.org/10.1093/schbul/sbs010>
- Groc, L., Heine, M., Cousins, S.L., Stephenson, F.A., Lounis, B., Cognet, L., Choquet, D., 2006. NMDA receptor surface mobility depends on NR2A-2B subunits. *Proc. Natl. Acad. Sci. U. S. A.* 103, 18769–18774. <https://doi.org/10.1073/pnas.0605238103>
- Grunze, H.C.R., Rainnie, D.G., Hasselmo, M.E., Barkai, E., Hearn, E., McCarley, R.W., Greene, R.W., 1996. NMDA-dependent modulation of CA1 local circuit inhibition. *J. Neurosci.* 16, 2034–2043.
- Guo, W., Liu, F., Liu, J., Yu, L., Zhang, J., Zhang, Z., Xiao, C., Zhai, J., Zhao, J., 2015. Abnormal causal connectivity by structural deficits in first-episode, drug-naive schizophrenia at rest. *Schizophr. Bull.* 41, 57–65. <https://doi.org/10.1093/schbul/sbu126>
- Gupta, S.C., Ravikrishnan, A., Liu, J., Mao, Z., Pavuluri, R., Hillman, B.G., Gandhi, P.J., Stairs, D.J., Li, M., Ugale, R.R., Monaghan, D.T., Dravid, S.M., 2016. The NMDA receptor GluN2C subunit controls cortical excitatory-inhibitory balance, neuronal oscillations and cognitive function. *Sci. Rep.* 6, 38321. <https://doi.org/10.1038/srep38321>
- Gustavsson, A., Svensson, M., Jacobi, F., Allgulander, C., Alonso, J., Beghi, E.,



- Dodel, R., Ekman, M., Faravelli, C., Fratiglioni, L., Gannon, B., Jones, D.H., Jennum, P., Jordanova, A., Jönsson, L., Karampampa, K., Knapp, M., Kobelt, G., Kurth, T., Lieb, R., Linde, M., Ljungcrantz, C., Maercker, A., Melin, B., Moscarelli, M., Musayev, A., Norwood, F., Preisig, M., Pugliatti, M., Rehm, J., Salvador-Carulla, L., Schlehofer, B., Simon, R., Steinhausen, H.C., Stovner, L.J., Vallat, J.M., den Bergh, P. Van, van Os, J., Vos, P., Xu, W., Wittchen, H.U., Jönsson, B., Olesen, J., 2011. Cost of disorders of the brain in Europe 2010. *Eur. Neuropsychopharmacol.* 21, 718–779.  
<https://doi.org/10.1016/j.euroneuro.2011.08.008>
- Haber, S.N., Calzavara, R., 2009. The cortico-basal ganglia integrative network: The role of the thalamus. *Brain Res. Bull.* 78, 69–74.  
<https://doi.org/10.1016/j.brainresbull.2008.09.013>
- Häfner, H., Maurer, K., Trendler, G., An Der Heiden, W., Schmidt, M., Könnecke, R., 2005. Schizophrenia and depression: Challenging the paradigm of two separate diseases - A controlled study of schizophrenia, depression and healthy controls. *Schizophr. Res.* 77, 11–24.  
<https://doi.org/10.1016/j.schres.2005.01.004>
- Hagino, Y., Kasai, S., Han, W., Yamamoto, H., Nabeshima, T., Mishina, M., Ikeda, K., 2010. Essential role of NMDA receptor channel  $\epsilon 4$  subunit (GluN2D) in the effects of hencyclidine, but not methamphetamine. *PLoS One* 5, e13722.  
<https://doi.org/10.1371/journal.pone.0013722>
- Hardingham, G.E., Bading, H., 2010. Synaptic versus extrasynaptic NMDA receptor signalling: Implications for neurodegenerative disorders. *Nat. Rev. Neurosci.* 11, 682–696. <https://doi.org/10.1038/nrn2911>
- Heath, R.G., Franklin, D.E., Shraberg, D., 1974. Gross pathology of the cerebellum in patients diagnosed and treated as functional psychiatric disorders. *J. Nerv. Ment. Dis.* 167, 585–592.
- Herculano-Houzel, S., 2010. Coordinated scaling of cortical and cerebellar numbers of neurons. *Front. Neuroanat.* 4, 1–8.  
<https://doi.org/10.3389/fnana.2010.00012>
- Hevers, W., Hadley, S.H., Lüddens, H., Amin, J., 2008. Ketamine, but not phencyclidine, selectively modulates cerebellar GABAA receptors containing  $\alpha 6$  and  $\delta$  subunits. *J. Neurosci.* 28, 5383–5393.  
<https://doi.org/10.1523/JNEUROSCI.5443-07.2008>
- Hillman, B.G., Gupta, S.C., Stairs, D.J., Buonanno, A., Dravid, S.M., 2011. Behavioral analysis of NR2C knockout mouse reveals deficit in acquisition of conditioned fear and working memory. *Neurobiol. Learn. Mem.* 95, 404–414.  
<https://doi.org/10.1016/j.nlm.2011.01.008>
- Hocking, G., Cousins, M.J., 2003. Ketamine in Chronic Pain Management: An Evidence-Based Review. *Anesth. Analg.* 97, 1730–1739.  
<https://doi.org/10.1213/01.ANE.0000086618.28845.9B>

- Hoeffler, C., Klann, E., 2010. mTOR signaling: At the crossroads of plasticity, memory, and disease. *Trends Neurosci.* 33, 67. <https://doi.org/10.1038/jid.2014.371>
- Homayoun, H., Jackson, M.E., Moghaddam, B., 2005. Activation of metabotropic glutamate 2/3 receptors reverses the effects of NMDA receptor hypofunction on prefrontal cortex unit activity in awake rats. *J. Neurophysiol.* 93, 1989–2001. <https://doi.org/10.1152/jn.00875.2004>
- Homayoun, H., Moghaddam, B., 2007. NMDA Receptor Hypofunction Produces Opposite Effects on Prefrontal Cortex Interneurons and Pyramidal Neurons. *J. Neurosci.* 27, 11496–11500. <https://doi.org/10.1523/jneurosci.2213-07.2007>
- Hönack, D., Löscher, W., 1993. Sex differences in NMDA receptor mediated responses in rats. *Brain Res.* 620, 167–170. [https://doi.org/10.1016/0006-8993\(93\)90287-W](https://doi.org/10.1016/0006-8993(93)90287-W)
- Hooks, B.M., Mao, T., Gutnisky, D.A., Yamawaki, N., Svoboda, K., Shepherd, G.M.G., 2013. Organization of cortical and thalamic input to pyramidal neurons in mouse motor cortex. *J. Neurosci.* 33, 748–760. <https://doi.org/10.1016/j.pestbp.2011.02.012>
- Howes, O.D., McCutcheon, R.A., Agid, O., de Bartolomeis, A., van Beveren, N.J.M., Birnbaum, M.L., Bloomfield, M.A.P., Bressan, R.A., Buchanan, R.W., Carpenter, W.T., Castle, D.J., Citrome, L., Daskalakis, Z.J., Davidson, M., Drake, R.J., Dursun, S., Ebdrup, B.H., Elkis, H., Falkai, P., Fleischacker, W., Gadelha, A., Gaughran, F., Glenthøj, B.Y., Graff-Guerrero, A., Hallak, J.E.C., Honer, W.G., Kennedy, J., Kinon, B.J., Lawrie, S.M., Lee, J., Leweke, F.M., MacCabe, J.H., McNabb, C.B., Meltzer, H.Y., Möller, H.-J., Nakajima, S., Pantelis, C., Marques, T.R., Remington, G., Rossell, S.L., Russell, B.R., Siu, C.O., Suzuki, T., Sommer, I.E., Taylor, D., Thomas, N., Umbricht, D., Walters, J.T.R., Kane, J., Correll, C.U., 2017. Treatment resistant schizophrenia: Treatment Response and Resistance in Psychosis (TRRIP) working group consensus guidelines on diagnosis and terminology. *Am. J. Psychiatry* 174, 216–229. <https://doi.org/10.1176/appi.ajp.2016.16050503>
- Hur, G.H., Son, W.C., Shin, S., Kang, J.K., Kim, Y.B., 1999. Sex differences in dizocilpine (MK-801) neurotoxicity in rats. *Environ. Toxicol. Pharmacol.* 7, 143–146. [https://doi.org/10.1016/S1382-6689\(99\)00003-4](https://doi.org/10.1016/S1382-6689(99)00003-4)
- Ichinohe, N., Mori, F., Shoumura, K., 2000. A di-synaptic projection from the lateral cerebellar nucleus to the laterodorsal part of the striatum via the central lateral nucleus of the thalamus in the rat. *Brain Res.* 880, 191–197. [https://doi.org/10.1016/S0168-0102\(00\)80980-3](https://doi.org/10.1016/S0168-0102(00)80980-3)
- Iijima, K., Takase, S., Tsumuraya, K., Endo, M., Itahara, K., 1978. Changes in free amino acids of cerebrospinal fluid and plasma in various neurological diseases. *Tohoku J Exp Med* 136, 133–150.
- Ikeda, K., Araki, K., Takayama, C., Inoue, Y., Yagi, T., Aizawa, S., Mishina, M., 1995. Reduced spontaneous activity of mice defective in the  $\epsilon 4$  subunit of the

- NMDA receptor channel. *Mol. Brain Res.* 33, 61–71.  
[https://doi.org/10.1016/0169-328X\(95\)00107-4](https://doi.org/10.1016/0169-328X(95)00107-4)
- Insel, T., Wang, P.S., 2009. The STAR\*D trial: revealing the need for better treatments. *Psychiatr. Serv.* 60, 1466–1467.
- Inta, D., Trusel, M., Riva, M.A., Sprengel, R., Gass, P., 2009. Differential c-Fos induction by different NMDA receptor antagonists with antidepressant efficacy: Potential clinical implications. *Int. J. Neuropsychopharmacol.* 12, 1133–1136.  
<https://doi.org/10.1017/S1461145709990319>
- Intson, K., van Eede, M.C., Islam, R., Milenkovic, M., Yan, Y., Salahpour, A., Henkelman, R.M., Ramsey, A.J., 2019. Progressive neuroanatomical changes caused by *Grin1* loss-of-function mutation. *Neurobiol. Dis.* 104527.  
<https://doi.org/10.1016/j.nbd.2019.104527>
- Ishii, D., Matsuzawa, D., Kanahara, N., Matsuda, S., Sutoh, C., Ohtsuka, H., Nakazawa, K., Kohno, M., Hashimoto, K., Iyo, M., Shimizu, E., 2010. Effects of aripiprazole on MK-801-induced prepulse inhibition deficits and mitogen-activated protein kinase signal transduction pathway. *Neurosci. Lett.* 471, 53–57.  
<https://doi.org/10.1016/j.neulet.2010.01.010>
- Jaso, B., Niciu, M., Iadarola, N., Lally, N., Richards, E., Park, M., Ballard, E., Nugent, A., Machado-Vieira, R., Zarate, C., 2017. Therapeutic Modulation of Glutamate Receptors in Major Depressive Disorder. *Curr. Neuropharmacol.* 15, 57–70. <https://doi.org/10.2174/1570159x14666160321123221>
- Javitt, D.C., Zukin, S.R., 1991. Recent advances in the phencyclidine model of schizophrenia. *Am. J. Psychiatry* 148, 1301–1308.
- Jernigan, C., Goswami, D., Austin, M., Iyo, A., Chandran, A., Stockmeier, C., Karolewicz, B., 2011. The mTOR signaling pathway in the prefrontal cortex is compromised in major depressive disorder. *Prog. Neuro-Psychopharmacology Biol. Psychiatry* 35, 1774–1779. <https://doi.org/10.1016/j.pnpbp.2011.05.010>
- Jiang, L., Zuo, X.N., 2016. Regional Homogeneity: A Multimodal, Multiscale Neuroimaging Marker of the Human Connectome. *Neuroscientist* 22, 486–505.  
<https://doi.org/10.1177/1073858415595004>
- Jiang, Y., Duan, M., Chen, X., Zhang, X., Gong, J., Dong, D., Li, H., Yi, Q., Wang, S., Wang, J., Luo, C., Yao, D., 2019a. Aberrant Prefrontal-Thalamic-Cerebellar Circuit in Schizophrenia and Depression: Evidence from a Possible Causal Connectivity. *Int. J. Neural Syst.* 29, 1850032. <https://doi.org/10.1142/S0129065718500326>
- Jiang, Y., Luo, C., Li, X., Li, Y., Yang, H., Li, J., Chang, X., Li, H., Yang, H., Huanghao, Wang, J., Duan, M., Yao, D., 2019b. White-matter functional networks changes in patients with schizophrenia. *Neuroimage* 190, 172–181.  
<https://doi.org/10.1016/j.neuroimage.2018.04.018>
- Jwair, S., Coulon, P., Ruigrok, T.J.H., 2017. Disynaptic subthalamic input to the posterior cerebellum in rat. *Front. Neuroanat.* 11, 1–11.  
<https://doi.org/10.3389/fnana.2017.00013>

- Kadotani, H., Hirano, T., Masugi, M., Nakamura, K., Nakao, K., Katsuki, M., Nakanishi, S., 1996. Motor discoordination results from combined gene disruption of the NMDA receptor NR2A and NR2C subunits, but not from single disruption of the NR2A or NR2C subunit. *J. Neurosci.* 16, 7859–7867.
- Kannangara, T.S., Bostrom, C.A., Ratzlaff, A., Thompson, L., Cater, R.M., Gil-Mohapel, J., Christie, B.R., 2014. Deletion of the NMDA receptor GluN2A subunit significantly decreases dendritic growth in maturing dentate granule neurons. *PLoS One* 9, e103155. <https://doi.org/10.1371/journal.pone.0103155>
- Kapur, S., Seeman, P., 2002. NMDA receptor antagonists ketamine and PCP have direct effects on the dopamine D2 and serotonin 5-HT2 receptors - Implications for models of schizophrenia. *Mol. Psychiatry* 7, 837–844. <https://doi.org/10.1038/sj.mp.4001093>
- Káradóttir, R., Cavelier, P., Bergersen, L.H., Attwell, D., 2005. NMDA receptors are expressed in oligodendrocytes and activated in ischaemia. *Nature* 438, 1162–1166. <https://doi.org/10.1038/nature04302>
- Karavanova, I., Vasudevan, K., Cheng, J., Buonanno, A., 2007. Novel regional and developmental NMDA receptor expression patterns uncovered in NR2C subunit- $\beta$ -galactosidase knock-in mice. *Mol. Cell. Neurosci.* 34, 468–480. <https://doi.org/10.1016/j.mcn.2006.12.001>
- Kargieman, L., Santana, N., Mengod, G., Celada, P., Artigas, F., 2007. Antipsychotic drugs reverse the disruption in prefrontal cortex function produced by NMDA receptor blockade with phencyclidine. *Proc. Natl. Acad. Sci.* 104, 14843–14848. <https://doi.org/10.1073/pnas.0704848104>
- Karolewicz, B., Cetin, M., Aricioglu, F., 2011. Beyond the glutamate N-methyl D-aspartate receptor in major depressive disorder: the mTOR signaling pathway. *Bull. Clin. Psychopharmacol.* 21, 1–6. <https://doi.org/10.5350/kpb-bcp201121101>
- Kelly, R.M., Strick, P.L., 2003. Cerebellar loops with motor cortex and prefrontal cortex of a nonhuman primate. *J. Neurosci.* 23, 8432–8444.
- Kessler, R.C., 2012. The Costs of Depression. *Psychiatr. Clin. North Am.* 35, 1–14. <https://doi.org/10.1016/j.psc.2011.11.005>
- Khlestova, E., Johnson, J.W., Krysta, J.H., Lisman, J., 2016. The role of GluN2C-containing NMDA receptors in ketamine's psychotogenic action and in schizophrenia models. *J. Neurosci.* 36, 11151–11157. <https://doi.org/10.1523/JNEUROSCI.1203-16.2016>
- Kim, C.H., Lee, J., Lee, J.Y., Roche, K.W., 2008. Metabotropic glutamate receptors: Phosphorylation and receptor signaling. *J. Neurosci. Res.* 86, 1–10. <https://doi.org/10.1002/jnr.21437>
- Kim, S.G., Uğurbil, K., Strick, P.L., 1994. Activation of a cerebellar output nucleus during cognitive processing. *Science* (80- ). 265, 949–951. <https://doi.org/10.1126/science.8052851>

- Kinoshita, H., Nishitani, N., Nagai, Y., Andoh, C., Asaoka, N., Kawai, H., Shibui, N., Nagayasu, K., Shirakawa, H., Nakagawa, T., Kaneko, S., 2018. Ketamine-induced prefrontal serotonin release is mediated by cholinergic neurons in the pedunculopontine tegmental nucleus. *Int. J. Neuropsychopharmacol.* 21, 305–310. <https://doi.org/10.1093/ijnp/pyy007>
- Kirino, E., Hayakawa, Y., Inami, R., Inoue, R., Aoki, S., 2019. Simultaneous fMRI-EEG-DTI recording of MMN in patients with schizophrenia. *PLoS One* 14, e0215023. <https://doi.org/10.1371/journal.pone.0215023>
- Kiselycznyk, C., Jury, N.J., Halladay, L.R., Nakazawa, K., Mishina, M., Sprengel, R., Grant, S.G.N., Svenningsson, P., Holmes, A., 2015. NMDA receptor subunits and associated signaling molecules mediating antidepressant-related effects of NMDA-GluN2B antagonism. *Behav. Brain Res.* 287, 89–95. <https://doi.org/10.1016/j.bbr.2015.03.023>
- Koike, H., Iijima, M., Chaki, S., 2011. Involvement of AMPA receptor in both the rapid and sustained antidepressant-like effects of ketamine in animal models of depression. *Behav. Brain Res.* 224, 107–111. <https://doi.org/10.1016/j.bbr.2011.05.035>
- Konkle, A.T.M., Bielajew, C., 2004. Tracing the neuroanatomical profiles of reward pathways with markers of neuronal activation. *Rev. Neurosci.* 15, 383–414. <https://doi.org/10.1515/REVNEURO.2004.15.6.383>
- Kornau, H., Schenker, L.T., Kennedy, M.B., Seeburg, P.H., 1995. Domain interaction between NMDA receptor subunits and the postsynaptic density protein PSD-95. *Science* (80- ). 269, 1737–1740.
- Kotermanski, S.E., Johnson, J.W., 2009. Mg<sup>2+</sup> imparts NMDA receptor subtype selectivity to the Alzheimer's drug memantine. *J. Neurosci.* 29, 2774–2779. <https://doi.org/10.1038/jid.2014.371>
- Kovács, K.J., 2008. Measurement of immediate-early gene activation- c-fos and beyond. *J. Neuroendocrinol.* 20, 665–672. <https://doi.org/10.1111/j.1365-2826.2008.01734>
- Koziol, L.F., Budding, D., Andreasen, N., D'Arrigo, S., Bulgheroni, S., Imamizu, H., Ito, M., Manto, M., Marvel, C., Parker, K., Pezzulo, G., Ramnani, N., Riva, D., Schmahmann, J., Vandervort, L., Yamazaki, T., 2014. Consensus paper: The cerebellum's role in movement and cognition. *Cerebellum* 13, 151–177. <https://doi.org/10.1007/s12311-013-0511-x>
- Krystal, J.H., D'Souza, D.C., Mathalon, D., Perry, E., Belger, A., Hoffman, R., 2003. NMDA receptor antagonist effects, cortical glutamatergic function, and schizophrenia: Toward a paradigm shift in medication development. *Psychopharmacology (Berl.)* 169, 215–233. <https://doi.org/10.1007/s00213-003-1582-z>
- Kuhn, R., 1958. The treatment of depressive states with G 22355 (imipramine hydrochloride). *Am. J. Psychiatry* 115, 459–464.

- Kuramoto, E., Fujiyama, F., Nakamura, K.C., Tanaka, Y., Hioki, H., Kaneko, T., 2011. Complementary distribution of glutamatergic cerebellar and GABAergic basal ganglia afferents to the rat motor thalamic nuclei. *Eur. J. Neurosci.* 33, 95–109. <https://doi.org/10.1111/j.1460-9568.2010.07481.x>
- Kuramoto, E., Furuta, T., Nakamura, K.C., Unzai, T., Hioki, H., Kaneko, T., 2009. Two types of thalamocortical projections from the motor thalamic nuclei of the rat: A single neuron-tracing study using viral vectors. *Cereb. Cortex* 19, 2065–2077. <https://doi.org/10.1093/cercor/bhn231>
- Kuroda, K., Suzumura, K., Shirakawa, T., Hiraishi, T., Nakahara, Y., Fushiki, H., Honda, S., Naraoka, H., Miyoshi, S., Aoki, Y., 2015. Investigation of mechanisms for MK-801-induced neurotoxicity utilizing metabolomic approach. *Toxicol. Sci.* 146, 344–353. <https://doi.org/10.1093/toxsci/kfv100>
- Kutsuwada, T., Sakimura, K., Manabe, T., Takayama, C., Katakura, N., Kushiya, E., Natsume, R., Watanabe, M., Inoue, Y., Yagi, T., Aizawa, S., Arakawa, M., Takahashi, T., Nakamura, Y., Mori, H., Mishina, M., 1996. Impairment of suckling response, trigeminal neuronal pattern formation, and hippocampal LTD in NMDA receptor  $\epsilon 2$  subunit mutant mice. *Neuron* 16, 333–344. [https://doi.org/10.1016/S0896-6273\(00\)80051-3](https://doi.org/10.1016/S0896-6273(00)80051-3)
- Labrie, V., Roder, J.C., 2010. The involvement of the NMDA receptor d-serine/glycine site in the pathophysiology and treatment of schizophrenia. *Neurosci. Biobehav. Rev.* 34, 351–372. <https://doi.org/10.1016/j.neubiorev.2009.08.002>
- Lahti, A.C., Weiler, M.A., Michaelidis, T., Parwani, A., Tamminga, C.A., 2001. Effects of Ketamine in Normal and Schizophrenic Volunteers. *Neuropsychopharmacology* 25, 455–467.
- Lam, Y.W., Murray Sherman, S., 2015. Functional topographic organization of the motor reticulothalamic pathway. *J. Neurophysiol.* 113, 3090–3097. <https://doi.org/10.1152/jn.00847.2014>
- Lapidus, K.A.B., Levitch, C.F., Perez, A.M., Brallier, J.W., Parides, M.K., Soleimani, L., Feder, A., Iosifescu, D. V., Charney, D.S., Murrough, J.W., 2014. A randomized controlled trial of intranasal ketamine in major depressive disorder. *Biol. Psychiatry* 76, 970–976. <https://doi.org/10.1016/j.biopsych.2014.03.026>
- Latysheva, N. V., Rayevsky, K.S., 2003. Chronic neonatal N-methyl-D-aspartate receptor blockade induces learning deficits and transient hypoactivity in young rats. *Prog. Neuro-Psychopharmacology Biol. Psychiatry* 27, 787–794. [https://doi.org/10.1016/S0278-5846\(03\)00110-6](https://doi.org/10.1016/S0278-5846(03)00110-6)
- Lau, C.G., Zukin, R.S., 2007. NMDA receptor trafficking in synaptic plasticity and neuropsychiatric disorders. *Nat. Rev. Neurosci.* 8, 413–426. <https://doi.org/10.1038/nrn2153>
- Lee, G., Zhou, Y., 2019. NMDAR Hypofunction Animal Models of Schizophrenia. *Front. Mol. Neurosci.* 12, 1–26. <https://doi.org/10.3389/fnmol.2019.00185>

- Lenze, E.J., Skidmore, E.R., Begley, A.E., Newcomer, J.W., Butters, M.A., Whyte, E.M., 2012. Memantine for late-life depression and apathy after a disabling medical event: A 12-week, double-blind placebo-controlled pilot study. *Int. J. Geriatr. Psychiatry* 27, 974–980. <https://doi.org/10.1002/gps.2813>
- Leung, L.S., Ma, J., 2017. Medial septum modulates hippocampal gamma activity and prepulse inhibition in an N-methyl-D-aspartate receptor antagonist model of schizophrenia. *Schizophr. Res.* 198, 36–44. <https://doi.org/10.1016/j.schres.2017.07.053>
- Lewis, D.A., Hashimoto, T., Volk, D.W., 2005. Cortical inhibitory neurons and schizophrenia. *Nat. Rev. Neurosci.* 6, 312–324. <https://doi.org/10.1038/nrn1648>
- Li, N., Lee, B., Liu, R.-J., Banasr, M., Dwyer, J.M., Iwata, M., Li, X.-Y., Aghajanian, G., Duman, R.S., 2010. mTOR-Dependent Synapse Formation Underlies the Rapid Antidepressant Effects of NMDA Antagonists. *Science* (80- ). 329, 959–964. <https://doi.org/10.1126/science.1189072>
- Lin, J.C., Lee, M.Y., Chan, M.H., Chen, Y.C., Chen, H.H., 2016. Betaine enhances antidepressant-like, but blocks psychotomimetic effects of ketamine in mice. *Psychopharmacology (Berl)*. 233, 3223–3235. <https://doi.org/10.1007/s00213-016-4359-x>
- Lin, Y.J., Bovezzo, S., Carver, J.M., Giordano, T., 1996. Cloning of the cDNA for the human NMDA receptor NR2C subunit and its expression in the central nervous system and periphery. *Mol. Brain Res.* 43, 57–64. [https://doi.org/10.1016/S0169-328X\(96\)00146-5](https://doi.org/10.1016/S0169-328X(96)00146-5)
- Lisman, J., 2017. Glutamatergic synapses are structurally and biochemically complex because of multiple plasticity processes: Long-term potentiation, long-term depression, short-term potentiation and scaling. *Philos. Trans. R. Soc. B Biol. Sci.* 372, 20160260. <https://doi.org/10.1098/rstb.2016.0260>
- Lisman, J.E., Coyle, J.T., Green, R.W., Javitt, D.C., Benes, F.M., Heckers, S., Grace, A.A., 2008. Circuit-based framework for understanding neurotransmitter and risk gene interactions in schizophrenia. *Trends Neurosci.* 31, 234–242. <https://doi.org/10.1016/j.tins.2008.02.005>
- Liu, F., G. Paule, M., Ali, S., Wang, C., 2011. Ketamine-Induced Neurotoxicity and Changes in Gene Expression in the Developing Rat Brain. *Curr. Neuropharmacol.* 9, 256–261. <https://doi.org/10.2174/157015911795017155>
- Liu, J., Shelkar, G.P., Zhao, F., Clausen, R.P., Dravid, S.M., 2019. Modulation of Burst Firing of Neurons in Nucleus Reticularis of the Thalamus by GluN2C-Containing NMDA Receptors. *Mol. Pharmacol.* 96, 193–203. <https://doi.org/10.1124/mol.119.116780>
- Liu, R.J., Duman, C., Kato, T., Hare, B., Lopresto, D., Bang, E., Burgdorf, J., Moskal, J., Taylor, J., Aghajanian, G., Duman, R.S., 2017. GLYX-13 Produces Rapid Antidepressant Responses with Key Synaptic and Behavioral Effects Distinct from Ketamine. *Neuropsychopharmacology* 42, 1231–1242.

<https://doi.org/10.1038/npp.2016.202>

Liu, Z., Xu, C., Xu, Y., Wang, Y., Zhao, B., Lv, Y., Cao, X., Zhang, K., Du, C., 2010. Decreased regional homogeneity in insula and cerebellum: A resting-state fMRI study in patients with major depression and subjects at high risk for major depression. *Psychiatry Res. - Neuroimaging* 182, 211–215.

<https://doi.org/10.1016/j.pscychresns.2010.03.004>

Lladó-Pelfort, L., Santana, N., Ghisi, V., Artigas, F., Celada, P., 2012. 5-HT1A Receptor agonists enhance pyramidal cell firing in prefrontal cortex through a preferential action on GABA interneurons. *Cereb. Cortex* 22, 1487–1497.

<https://doi.org/10.1093/cercor/bhr220>

Long, L.E., Malone, D.T., Taylor, D.A., 2006. Cannabidiol reverses MK-801-induced disruption of prepulse inhibition in mice. *Neuropsychopharmacology* 31, 795–803. <https://doi.org/10.1038/sj.npp.1300838>

Loo, C.K., Gálvez, V., O'Keefe, E., Mitchell, P.B., Hadzi-Pavlovic, D., Leyden, J., Harper, S., Somogyi, A.A., Lai, R., Weickert, C.S., Glue, P., 2016. Placebo-controlled pilot trial testing dose titration and intravenous, intramuscular and subcutaneous routes for ketamine in depression. *Acta Psychiatr. Scand.* 134, 48–56. <https://doi.org/10.1111/acps.12572>

López-Gil, X., Artigas, F., Adell, A., 2009. Role of different monoamine receptors controlling MK-801-induced release of serotonin and glutamate in the medial prefrontal cortex: Relevance for antipsychotic action. *Int. J. Neuropsychopharmacol.* 12, 487–499.

<https://doi.org/10.1017/S1461145708009267>

López-Gil, X., Jiménez-Sánchez, L., Campa, L., Castro, E., Frago, C., Adell, A., 2019. Role of Serotonin and Noradrenaline in the Rapid Antidepressant Action of Ketamine. *ACS Chem. Neurosci.* 10, 3318–3326.

<https://doi.org/10.1021/acchemneuro.9b00288>

López-Gil, X., Jiménez-Sánchez, L., Romón, T., Campa, L., Artigas, F., Adell, A., 2012. Importance of inter-hemispheric prefrontal connection in the effects of non-competitive NMDA receptor antagonists. *Int. J. Neuropsychopharmacol.* 15, 945–956. <https://doi.org/10.1017/S1461145711001064>

Lorrain, D.S., Baccei, C.S., Bristow, L.J., Anderson, J.J., Varney, M.A., 2003. Effects of ketamine and N-methyl-D-aspartate on glutamate and dopamine release in the rat prefrontal cortex: Modulation by a group II selective metabotropic glutamate receptor agonist LY379268. *Neuroscience* 117, 697–706.

[https://doi.org/10.1016/S0306-4522\(02\)00652-8](https://doi.org/10.1016/S0306-4522(02)00652-8)

Lu, C., Fu, Z., Karavanov, I., Yasuda, R.P., Wolfe, B.B., Buonanno, A., Vicini, S., 2006. NMDA receptor subtypes at autaptic synapses of cerebellar granule neurons. *J. Neurophysiol.* 96, 2282–2294.

<https://doi.org/10.1152/jn.00078.2006>

Lupo, M., Siciliano, L., Leggio, M., 2019. From cerebellar alterations to mood



- disorders: A systematic review. *Neurosci. Biobehav. Rev.* 103, 21–28.  
<https://doi.org/10.1016/j.neubiorev.2019.06.008>
- Maeng, S., Zarate, C.A., Du, J., Schloesser, R.J., McCammon, J., Chen, G., Manji, H.K., 2008. Cellular Mechanisms Underlying the Antidepressant Effects of Ketamine: Role of  $\alpha$ -Amino-3-Hydroxy-5-Methylisoxazole-4-Propionic Acid Receptors. *Biol. Psychiatry* 63, 349–352.  
<https://doi.org/10.1016/j.biopsych.2007.05.028>
- Malhotra, A.K., Pinals, D.A., Weingartner, H., Sirocco, K., Missar, C.D., Pickar, D., Breier, A., 1996. NMDA receptor function and human cognition: The effects of ketamine in healthy volunteers. *Neuropsychopharmacology* 14, 301–307.  
[https://doi.org/10.1016/0893-133X\(95\)00137-3](https://doi.org/10.1016/0893-133X(95)00137-3)
- Manto, M., Bower, J., Conforto, A., Delgado-García, J., da Guarda, S., Gerwig, M., Habas, C., Hagura, N., Ivry, R., Mariën, P., Molinari, M., Naito, E., Nowak, D., Oulad Ben Taib, N., Pelisson, D., Tesche, C., Tilikete, C., Timmann, D., 2012. Consensus Paper: Roles of the Cerebellum in Motor Control— The Diversity of Ideas on Cerebellar Involvement in Movement. *Cerebellum* 11, 457–487.  
<https://doi.org/10.1111/mec.13536>
- Mantovani, M., Pértile, R., Calixto, J.B., Santos, A.R.S., Rodrigues, A.L.S., 2003. Melatonin exerts an antidepressant-like effect in the tail suspension test in mice: Evidence for involvement of N-methyl-D-aspartate receptors and the L-arginine-nitric oxide pathway. *Neurosci. Lett.* 343, 1–4. [https://doi.org/10.1016/S0304-3940\(03\)00306-9](https://doi.org/10.1016/S0304-3940(03)00306-9)
- Mariën, P., Ackermann, H., Adamaszek, M., Barwood, C.H.S., Beaton, A., Desmond, J., De Witte, E., Fawcett, A.J., Hertrich, I., Küper, M., Leggio, M., Marvel, C., Molinari, M., Murdoch, B.E., Nicolson, R.I., Schmähmann, J.D., Stoodley, C.J., Thürling, M., Timmann, D., Wouters, E., Ziegler, W., 2014. Consensus paper: Language and the cerebellum: An ongoing enigma. *Cerebellum* 13, 386–410. <https://doi.org/10.1007/s12311-013-0540-5>
- Mathers, C.D., Loncar, D., 2006. Projections of global mortality and burden of disease from 2002 to 2030. *PLoS Med.* 3, e442.  
<https://doi.org/10.1371/journal.pmed.0030442>
- Matsuo, N., Takao, K., Nakanishi, K., Yamasaki, N., Tanda, K., Miyakawa, T., 2010. Behavioral profiles of three C57BL/6 substrains. *Front. Behav. Neurosci.* 4, 29.  
<https://doi.org/10.3389/fnbeh.2010.00029>
- Matsuoka, T., Sumiyoshi, T., Tanaka, K., Tsunoda, M., Uehara, T., Itoh, H., Kurachi, M., 2005. NC-1900, an arginine-vasopressin analogue, ameliorates social behavior deficits and hyperlocomotion in MK-801-treated rats: Therapeutic implications for schizophrenia. *Brain Res.* 1053, 131–136.  
<https://doi.org/10.1016/j.brainres.2005.06.035>
- Maxwell, C.R., Ehrlichman, R.S., Liang, Y., Trief, D., Kanes, S.J., Karp, J., Siegel, S.J., 2006. Ketamine produces lasting disruptions in encoding of sensory stimuli. *J. Pharmacol. Exp. Ther.* 316, 315–324. <https://doi.org/10.1124/jpet.105.091199>

- McCullough, L.D., Salamone, J.D., 1992. Increases in extracellular dopamine levels and locomotor activity after direct infusion of phencyclidine into the nucleus accumbens. *Brain Res.* 577, 1–9. [https://doi.org/10.1016/0006-8993\(92\)90530-M](https://doi.org/10.1016/0006-8993(92)90530-M)
- McCutcheon, R.A., Abi-Dargham, A., Howes, O.D., 2019. Schizophrenia, Dopamine and the Striatum: From Biology to Symptoms. *Trends Neurosci.* 42, 205–220. <https://doi.org/10.1016/j.tins.2018.12.004>
- McFarland, N.R., Haber, S.N., 2002. Thalamic relay nuclei of the basal ganglia form both reciprocal and nonreciprocal cortical connections, linking multiple frontal cortical areas. *J. Neurosci.* 22, 8117–8132.
- McQuail, J.A., Beas, B.S., Kelly, K.B., Simpson, K.L., Frazier, C.J., Setlow, B., Bizon, J.L., 2016. NR2A-containing NMDARs in the prefrontal cortex are required for working memory and associated with age-related cognitive decline. *J. Neurosci.* 36, 12537–12548. <https://doi.org/10.1523/JNEUROSCI.2332-16.2016>
- Meldrum, B.S., 2000. Glutamate and Glutamine in the Brain Glutamate as a Neurotransmitter in the Brain : Review of Physiology and Pathology. *J. Nutr.* 130, 1007–1015.
- Meltzer, H.Y., Rajagopal, L., Huang, M., Oyamada, Y., Kwon, S., Horiguchi, M., 2013. Translating the N-methyl-d-aspartate receptor antagonist model of schizophrenia to treatments for cognitive impairment in schizophrenia. *Int. J. Neuropsychopharmacol.* 16, 2181–2194. <https://doi.org/10.1017/S1461145713000928>
- Meltzer, H.Y., Stahl, S.M., 1976. The Dopamine Hypothesis of Schizophrenia: a review. *Schizophr. Bull.* 2, 19–76. <https://doi.org/10.1111/j.1744-6163.1990.tb00312>
- Merritt, K., Egerton, A., Kempton, M.J., Taylor, M.J., McGuire, P.K., 2016. Nature of glutamate alterations in schizophrenia. A meta-analysis of proton magnetic resonance spectroscopy studies. *JAMA Psychiatry* 73, 665–674. <https://doi.org/10.1001/jamapsychiatry.2016.0442>
- Middleton, F.A., Strick, P.L., 1994. Anatomical evidence for cerebellar and basal ganglia involvement in higher cognitive function. *Science (80-. )*. 266, 458–461. <https://doi.org/10.1126/science.7939688>
- Miller, O.H., Yang, L., Wang, C.C., Hargroder, E.A., Zhang, Y., Delpire, E., Hall, B.J., 2014. GluN2B-containing NMDA receptors regulate depression-like behavior and are critical for the rapid antidepressant actions of ketamine. *Elife* 3, e03581. <https://doi.org/10.7554/eLife.03581>
- Mineur, Y.S., Fote, G.M., Blakeman, S., Cahuzac, E.L.M., Newbold, S.A., Picciotto, M.R., 2016. Multiple nicotinic acetylcholine receptor subtypes in the mouse amygdala regulate affective behaviors and response to social stress. *Neuropsychopharmacology* 41, 1579–1587. <https://doi.org/10.1038/npp.2015.316>

- Mineur, Y.S., Somenzi, O., Picciotto, M.R., 2007. Cytisine, a partial agonist of high-affinity nicotinic acetylcholine receptors, has antidepressant-like properties in male C57BL/6J mice. *Neuropharmacology* 52, 1256–1262.  
<https://doi.org/10.1016/j.neuropharm.2007.01.006>
- Mirza, F.J., Zahid, S., 2018. The Role of Synapsins in Neurological Disorders. *Neurosci. Bull.* 34, 349–358. <https://doi.org/10.1007/s12264-017-0201-7>
- Miyamoto, S., Duncan, G.E., Marx, C.E., Lieberman, J.A., 2005. Treatments for schizophrenia: A critical review of pharmacology and mechanisms of action of antipsychotic drugs. *Mol. Psychiatry* 10, 79–104.  
<https://doi.org/10.1038/sj.mp.4001556>
- Mizoguchi, T., Hara, H., Shimazawa, M., 2019. VGF has Roles in the Pathogenesis of Major Depressive Disorder and Schizophrenia: Evidence from Transgenic Mouse Models. *Cell. Mol. Neurobiol.* 39, 721–727.  
<https://doi.org/10.1007/s10571-019-00681-9>
- Moers-Hornikx, V.M.P., Vles, J.S.H., Tan, S.K.H., Cox, K., Hoogland, G., Steinbusch, W.M.H., Temel, Y., 2011. Cerebellar nuclei are activated by high-frequency stimulation of the subthalamic nucleus. *Neurosci. Lett.* 496, 111–115.  
<https://doi.org/10.1016/j.neulet.2011.03.094>
- Moghaddam, B., Adams, B.W., 1998. Reversal of phencyclidine effects by a group II metabotropic glutamate receptor agonist in rats. *Science* (80-. ). 281, 1349–1352. <https://doi.org/10.1126/science.281.5381.1349>
- Moghaddam, B., Adams, B.W., Verma, A., Daly, D., 1997. Activation of glutamatergic neurotransmission by ketamine: a novel step in the pathway from NMDA receptor blockade to dopaminergic and cognitive disruptions associated with the prefrontal cortex. *J. Neurosci.* 17, 2921–2927.  
[https://doi.org/10.1016/0091-3057\(93\)90217-H](https://doi.org/10.1016/0091-3057(93)90217-H)
- Moghaddam, B., Jackson, M.E., 2003. Glutamatergic Animal Models of Schizophrenia. *Ann. N. Y. Acad. Sci.* 1003, 131–137.  
<https://doi.org/10.1196/annals.1300.065>
- Mogil, J.S., 2016. Equality need not be painful. *Nature* 535, S7.
- Monyer, H., Burnashev, N., Laurie, D.J., Sakmann, B., Seeburg, P.H., 1994. Developmental and regional expression in the rat brain and functional properties of four NMDA receptors. *Neuron* 12, 529–540.  
[https://doi.org/10.1016/0896-6273\(94\)90210-0](https://doi.org/10.1016/0896-6273(94)90210-0)
- Mosconi, M.W., Wang, Z., Schmitt, L.M., Tsai, P., Sweeney, J.A., 2015. The role of cerebellar circuitry alterations in the pathophysiology of autism spectrum disorders. *Front. Neurosci.* 9, 296. <https://doi.org/10.3389/fnins.2015.00296>
- Na, J., Kakei, S., Shinoda, Y., 1997. Cerebellar input to corticothalamic neurons in layers V and VI in the motor cortex. *Neurosci. Res.* 28, 77–91.  
[https://doi.org/10.1016/S0168-0102\(97\)00031-X](https://doi.org/10.1016/S0168-0102(97)00031-X)

- Nakao, S., Miyamoto, E., Masuzawa, M., Kambara, T., Shingu, K., 2002. Ketamine-induced c-Fos expression in the mouse posterior cingulate and retrosplenial cortices is mediated not only via NMDA receptors but also via sigma receptors. *Brain Res.* 926, 191–196. [https://doi.org/10.1016/S0006-8993\(01\)03338-8](https://doi.org/10.1016/S0006-8993(01)03338-8)
- Neill, J.C., Barnes, S., Cook, S., Grayson, B., Idris, N.F., McLean, S.L., Snigdha, S., Rajagopal, L., Harte, M.K., 2010. Animal models of cognitive dysfunction and negative symptoms of schizophrenia: Focus on NMDA receptor antagonism. *Pharmacol. Ther.* 128, 419–432. <https://doi.org/10.1016/j.pharmthera.2010.07.004>
- Nguyen, L., Matsumoto, R.R., 2015. Involvement of AMPA receptors in the antidepressant-like effects of dextromethorphan in mice. *Behav. Brain Res.* 295, 26–34. <https://doi.org/10.1016/j.bbr.2015.03.024>
- Nilsson, M., Markinhuhta, K.R., Carlsson, M.L., 2006. Differential effects of classical neuroleptics and a newer generation antipsychotics on the MK-801 induced behavioural primitivization in mouse. *Prog. Neuro-Psychopharmacology Biol. Psychiatry* 30, 521–530. <https://doi.org/10.1016/j.pnpbp.2005.11.010>
- Nilsson, M., Waters, S., Waters, N., Carlsson, A., Carlsson, M.L., 2001. A behavioural pattern analysis of hypoglutamatergic mice - Effects of four different antipsychotic agents. *J. Neural Transm.* 108, 1181–1196. <https://doi.org/10.1007/s007020170008>
- Nishi, M., Hinds, H., Lu, H.P., Kawata, M., Hayashi, Y., 2001. Motoneuron-specific expression of NR3B, a novel NMDA-type glutamate receptor subunit that works in a dominant-negative manner. *J. Neurosci.* 21, 1–6.
- Nishimura, M., Sato, K., Okada, T., Yoshiya, I., Schloss, P., Shimada, S., Tohyama, M., 1998. Ketamine inhibits monoamine transporters expressed in human embryonic kidney 293 cells. *Anesthesiology* 88, 768–774.
- Nishizawa, N., Nakao, S.I., Nagata, A., Hirose, T., Masuzawa, M., Shingu, K., 2000. The effect of ketamine isomers on both mice behavioral responses and c-Fos expression in the posterior cingulate and retrosplenial cortices. *Brain Res.* 857, 188–192. [https://doi.org/10.1016/S0006-8993\(99\)02426-9](https://doi.org/10.1016/S0006-8993(99)02426-9)
- Nowak, L., Bregestovski, P., Ascher, P., Herbet, A., Prochiantz, A., 1984. Magnesium gates glutamate-activated channels in mouse central neurones. *Nature* 307, 462–465. <https://doi.org/10.1109/APS.2008.4619642>
- Olney, J.W., Labruyere, J., Price, M.T., 1989. Pathological changes induced in cerebrocortical neurons by phencyclidine and related drugs. *Science* (80-. ). 244, 1360–1362. <https://doi.org/10.1126/science.2660263>
- Ouagazzal, A. mouttalib, Nieoullon, A., Amalric, M., 1994. Locomotor activation induced by MK-801 in the rat: postsynaptic interactions with dopamine receptors in the ventral striatum. *Eur. J. Pharmacol.* 251, 229–236. [https://doi.org/10.1016/0014-2999\(94\)90404-9](https://doi.org/10.1016/0014-2999(94)90404-9)

- Pachernegg, S., Strutz-Seebohm, N., Hollmann, M., 2012. GluN3 subunit-containing NMDA receptors: Not just one-trick ponies. *Trends Neurosci.* 35, 240–249. <https://doi.org/10.1016/j.tins.2011.11.010>
- Perälä, J., Suvisaari, J., Saarni, S.I., Kuoppasalmi, K., Isometsä, E., Pirkola, S., Partonen, T., Tuulio-Henriksson, A., Hintikka, J., Kieseppä, T., Härkänen, T., Koskinen, S., Lönnqvist, J., 2007. Lifetime prevalence of psychotic and bipolar I disorders in a general population. *Arch. Gen. Psychiatry* 64, 19–28. <https://doi.org/10.1111/j.0022-3646.1983.00387>
- Percheron, G., François, C., Talbi, B., Yelnik, J., Ffnelon, G., 1996. The primate motor thalamus. *Brain Res. Rev.* 22, 93–181.
- Pérez-Otaño, I., Larsen, R.S., Wesseling, J.F., 2016. Emerging roles of GluN3-containing NMDA receptors in the CNS. *Nat. Rev. Neurosci.* 17, 623–635. <https://doi.org/10.1038/nrn.2016.92>
- Petrenko, A.B., Yamakura, T., Kohno, T., Sakimura, K., Baba, H., 2013. Increased brain monoaminergic tone after the NMDA receptor GluN2A subunit gene knockout is responsible for resistance to the hypnotic effect of nitrous oxide. *Eur. J. Pharmacol.* 698, 200–205. <https://doi.org/10.1016/j.ejphar.2012.10.034>
- Pham, Thu Ha, Defaix, C., Xu, X., Deng, S.X., Fabresse, N., Alvarez, J.C., Landry, D.W., Brachman, R.A., Denny, C.A., Gardier, A.M., 2017. Common Neurotransmission Recruited in (R,S)-Ketamine and (2R,6R)-Hydroxynorketamine-Induced Sustained Antidepressant-like Effects. *Biol. Psychiatry* 84. <https://doi.org/10.1016/j.biopsych.2017.10.020>
- Pham, T. H., Mendez-David, I., Defaix, C., Guiard, B.P., Tritschler, L., David, D.J., Gardier, A.M., 2017. Ketamine treatment involves medial prefrontal cortex serotonin to induce a rapid antidepressant-like activity in BALB/cJ mice. *Neuropharmacology* 112, 198–209. <https://doi.org/10.1016/j.neuropharm.2016.05.010>
- Picard, H., Amado, I., Mouchet-Mages, S., Olié, J.P., Krebs, M.O., 2008. The role of the cerebellum in schizophrenia: An update of clinical, cognitive, and functional evidences. *Schizophr. Bull.* 34, 155–172. <https://doi.org/10.1093/schbul/sbm049>
- Pillinger, T., Rogdaki, M., McCutcheon, R.A., Hathway, P., Egerton, A., Howes, O.D., 2019. Altered glutamatergic response and functional connectivity in treatment resistant schizophrenia: the effect of riluzole and therapeutic implications. *Psychopharmacology (Berl)*. 236, 1985–1997. <https://doi.org/10.1007/s00213-019-5188-5>
- Porsolt, R.D., Bertin, A., Jalfre, M., 1978. “Behavioural despair” in rats and mice: Strain differences and the effects of imipramine. *Eur. J. Pharmacol.* 51, 291–294. [https://doi.org/10.1016/0014-2999\(78\)90414-4](https://doi.org/10.1016/0014-2999(78)90414-4)
- Powell, S.B., Weber, M., Geyer, M.A., 2012. Genetic Models of Sensorimotor Gating: Relevance to Neuropsychiatric Disorders. *Curr. Top. Behav. Neurosci.* 12,

251–318. <https://doi.org/10.1007/7854>

Prendergast, B.J., Onishi, K.G., Zucker, I., 2014. Female mice liberated for inclusion in neuroscience and biomedical research. *Neurosci. Biobehav. Rev.* 40, 1–5. <https://doi.org/10.1016/j.neubiorev.2014.01.001>

Preskorn, S.H., Baker, B., Kolluri, S., Menniti, F.S., Krams, M., Landen, J.W., 2008. An Innovative design to establish proof of concept of the antidepressant effects of the NR2B subunit selective n-methyl-d-aspartate antagonist, CP-101,606, in patients with treatment-refractory major depressive disorder. *J. Clin. Psychopharmacol.* 28, 631–637. <https://doi.org/10.1097/JCP.0b013e31818a6cea>

Quirk, M.C., Sosulski, D.L., Feierstein, C.E., Uchida, N., Mainen, Z.F., 2009. A defined network of fast-spiking interneurons in orbitofrontal cortex: Responses to behavioral contingencies and ketamine administration. *Front. Syst. Neurosci.* 3, 1–13. <https://doi.org/10.3389/neuro.06.013.2009>

Ramsey, A.J., 2009. NR1 knockdown mice as a representative model of the glutamate hypothesis of schizophrenia, *Progress in Brain Research*. Elsevier. [https://doi.org/10.1016/S0079-6123\(09\)17906-2](https://doi.org/10.1016/S0079-6123(09)17906-2)

Ramsey, A.J., Milenkovic, M., Oliveira, A.F., Escobedo-Lozoya, Y., Seshadri, S., Salahpour, A., Sawa, A., Yasuda, R., Caron, M.G., 2011. Impaired NMDA receptor transmission alters striatal synapses and DISC1 protein in an age-dependent manner. *Proc. Natl. Acad. Sci. U. S. A.* 108, 5795–5800. <https://doi.org/10.1073/pnas.1012621108>

Ravikrishnan, A., Gandhi, P.J., Shelkar, G.P., Liu, J., Pavuluri, R., Dravid, S.M., 2018. Region-specific Expression of NMDA Receptor GluN2C Subunit in Parvalbumin-Positive Neurons and Astrocytes: Analysis of GluN2C Expression using a Novel Reporter Model. *Neuroscience* 380, 49–62. <https://doi.org/10.1016/j.neuroscience.2018.03.011>

Redrobe, J.P., Elster, L., Frederiksen, K., Bundgaard, C., De Jong, I.E.M., Smith, G.P., Bruun, A.T., Larsen, P.H., Didriksen, M., 2012. Negative modulation of GABA A  $\alpha 5$  receptors by RO4938581 attenuates discrete sub-chronic and early postnatal phencyclidine (PCP)-induced cognitive deficits in rats. *Psychopharmacology (Berl.)* 221, 451–468. <https://doi.org/10.1007/s00213-011-2593-9>

Réus, G.Z., Abelaira, H.M., Tuon, T., Titus, S.E., Ignácio, Z.M., Rodrigues, A.L.S., Quevedo, J., 2016. Glutamatergic NMDA Receptor as Therapeutic Target for Depression. *Adv. Protein Chem. Struct. Biol.* 103, 169–202. <https://doi.org/10.1016/bs.apcsb.2015.10.003>

Rogóz, Z., Kamińska, K., 2016. The effect of combined treatment with escitalopram and risperidone on the MK-801-induced changes in the object recognition test in mice. *Pharmacol. Reports* 68, 116–120. <https://doi.org/10.1016/j.pharep.2015.07.004>

Romeo, B., Choucha, W., Fossati, P., Rotge, J.Y., 2015. Meta-analysis of short-

and mid-term efficacy of ketamine in unipolar and bipolar depression. *Psychiatry Res.* 230, 682–688. <https://doi.org/10.1016/j.psychres.2015.10.032>

Rosa, A.O., Lin, J., Calixto, J.B., Santos, A.R.S., Rodrigues, A.L.S., 2003. Involvement of NMDA receptors and L-arginine-nitric oxide pathway in the antidepressant-like effects of zinc in mice. *Behav. Brain Res.* 144, 87–93. [https://doi.org/10.1016/S0166-4328\(03\)00069-X](https://doi.org/10.1016/S0166-4328(03)00069-X)

Rothstein, J.D., Dykes-Hoberg, M., Pardo, C.A., Bristol, L.A., Jin, L., Kuncl, R.W., Kanai, Y., Hediger, M.A., Wang, Y., Schielke, J.P., Welty, D.F., 1996. Knockout of glutamate transporters reveals a major role for astroglial transport in excitotoxicity and clearance of glutamate. *Neuron* 16, 675–686. [https://doi.org/10.1016/S0896-6273\(00\)80086-0](https://doi.org/10.1016/S0896-6273(00)80086-0)

Rung, J.P., Carlsson, A., Markinhuhta, K.R., Carlsson, M.L., 2005. (+)-MK-801 induced social withdrawal in rats; A model for negative symptoms of schizophrenia. *Prog. Neuro-Psychopharmacology Biol. Psychiatry* 29, 827–832. <https://doi.org/10.1016/j.pnpbp.2005.03.004>

Sambataro, F., Thomann, P.A., Nolte, H.M., Hasenkamp, J.H., Hirjak, D., Kubera, K.M., Hofer, S., Seidl, U., Depping, M.S., Stieltje, B., Maier-Hein, K., Wolf, R.C., 2019. Transdiagnostic modulation of brain networks by electroconvulsive therapy in schizophrenia and major depression. *Eur. Neuropsychopharmacol.* 1–11. <https://doi.org/10.1016/j.euroneuro.2019.06.002>

Santana, N., Bortolozzi, A., Serrats, J., Mengod, G., Artigas, F., 2004. Expression of serotonin1A and serotonin2A receptors in pyramidal and GABAergic neurons of the rat prefrontal cortex. *Cereb. Cortex* 14, 1100–1109. <https://doi.org/10.1093/cercor/bhh070>

Santana, N., Troyano-Rodríguez, E., Mengod, G., Celada, P., Artigas, F., 2011. Activation of thalamocortical networks by the N-methyl-D-aspartate receptor antagonist phencyclidine: Reversal by clozapine. *Biol. Psychiatry* 69, 918–927. <https://doi.org/10.1016/j.biopsych.2010.10.030>

Santuy, A., Rodríguez, J.R., DeFelipe, J., Merchán-Pérez, A., 2018. Study of the size and shape of synapses in the juvenile rat somatosensory cortex with 3D electron microscopy. *eNeuro* 5, e0377-17.2017. <https://doi.org/10.1523/ENEURO.0377-17.2017>

Sanz-Clemente, A., Nicoll, R.A., Roche, K.W., 2013. Diversity in NMDA receptor composition: many regulators, many consequences. *Neuroscientist* 19, 62–75. <https://doi.org/10.1177/1073858411435129>

Sapkota, K., Mao, Z., Synowicki, P., Lieber, D., Liu, M., Ikezu, T., Gautam, V., Monaghan, D.T., 2016. GluN2D N-methyl-D-aspartate receptor subunit contribution to the stimulation of brain activity and gamma oscillations by ketamine: Implications for schizophrenia. *J. Pharmacol. Exp. Ther.* 356, 702–711. <https://doi.org/10.1124/jpet.115.230391>

Sarkar, A., Kabbaj, M., 2016. Sex differences in effects of ketamine on behavior,

spine density, and synaptic proteins in socially isolated rats. *Biol. Psychiatry*, 80, 448-456.

Sato, Y., Kobayashi, E., Hakamata, Y., Kobahashi, M., Wainai, T., Murayama, T., Mishina, M., Seo, N., 2004. Chronopharmacological studies of ketamine in normal and NMDA E1 receptor knockout mice. *Br. J. Anaesth.* 92, 859–864. <https://doi.org/10.1093/bja/ae144>

Sawyer, S.F., Martone, M.E., Groves, P.M., 1991. A GABA immunocytochemical study of rat motor thalamus: Light and electron microscopic observations. *Neuroscience* 42, 103–124. [https://doi.org/10.1016/0306-4522\(91\)90152-E](https://doi.org/10.1016/0306-4522(91)90152-E)

Scherzer, C.R., Landwehrmeyer, G.B., Kerner, J.A., Standaert, D.G., Hollingsworth, Z.R., Daggett, L.P., Veliçelebi, G., Penney, J.B., Young, A.B., 1997. Cellular distribution of NMDA glutamate receptor subunit mRNAs in the human cerebellum. *Neurobiol. Dis.* 4, 35–46. <https://doi.org/10.1006/nbdi.1997.0136>

Scorza, M.C., Castañé, A., Bortolozzi, A., Artigas, F., 2010. Clozapine does not require 5-HT1A receptors to block the locomotor hyperactivity induced by MK-801. Clz and MK-801 in KO1A mice. *Neuropharmacology* 59, 112–120. <https://doi.org/10.1016/j.neuropharm.2010.04.012>

Scorza, M.C., Meikle, M.N., Hill, X.L., Richeri, A., Lorenzo, D., Artigas, F., 2008. Prefrontal cortex lesions cause only minor effects on the hyperlocomotion induced by MK-801 and its reversal by clozapine. *Int. J. Neuropsychopharmacol.* 11, 519–532. <https://doi.org/10.1017/S1461145708008432>

Shelkar, G.P., Pavuluri, R., Gandhi, P.J., Ravikrishnan, A., Gawande, D.Y., Liu, J., Stairs, D.J., Ugale, R.R., Dravid, S.M., 2019. Differential effect of NMDA receptor GluN2C and GluN2D subunit ablation on behavior and channel blocker-induced schizophrenia phenotypes. *Sci. Rep.* 9, 7572. <https://doi.org/10.1038/s41598-019-43957-2>

Shepherd, A.M., Laurens, K.R., Matheson, S.L., Carr, V.J., Green, M.J., 2012. Systematic meta-review and quality assessment of the structural brain alterations in schizophrenia. *Neurosci. Biobehav. Rev.* 36, 1342–1356. <https://doi.org/10.1016/j.neubiorev.2011.12.015>

Shi, Q., Guo, L., Patterson, T.A., Dial, S., Li, Q., Sadovova, N., Zhang, X., Hanig, J.P., Paule, M.G., Slikker Jr, W., Wang, C., 2010. Gene expression profiling in the developing rat brain exposed to ketamine. *Neuroscience* 166, 852–863. <https://doi.org/10.1111/j.1432-0436.2008.00274>

Shigematsu, N., Ueta, Y., Mohamed, A.A., Hatada, S., Fukuda, T., Kubota, Y., Kawaguchi, Y., 2016. Selective Thalamic Innervation of Rat Frontal Cortical Neurons. *Cereb. Cortex* 26, 2689–2704. <https://doi.org/10.1093/cercor/bhv124>

Shirai, Y., Fujita, Y., Hashimoto, K., 2012. Effects of the antioxidant sulforaphane on hyperlocomotion and prepulse inhibition deficits in mice after phencyclidine administration. *Clin. Psychopharmacol. Neurosci.* 10, 94–98.

Sillitoe, R. V., Joyner, A.L., 2007. Morphology, Molecular Codes, and Circuitry



- Produce the Three-Dimensional Complexity of the Cerebellum. *Annu. Rev. Cell Dev. Biol.* 23, 549–577.  
<https://doi.org/10.1146/annurev.cellbio.23.090506.123237>
- Simon, M.M., Greenaway, S., White, J.K., Fuchs, H., Gailus-Durner, V., Wells, S., Sorg, T., Wong, K., Bedu, E., Cartwright, E.J., Dacquin, R., Djebali, S., Estabel, J., Graw, J., Ingham, N.J., Jackson, I.J., Lengeling, A., Mandillo, S., Marve, J., Meziane, H., Preitner, F., Puk, O., Roux, M., Adams, D.J., Atkins, S., Ayadi, A., Becker, L., Blake, A., Brooker, D., Cater, H., Champy, M.F., Combe, R., Danecek, P., Di Fenza, A., Gates, H., Gerdin, A.K., Golini, E., Hancock, J.M., Hans, W., Hölter, S.M., Hough, T., Jurdic, P., Keane, T.M., Morgan, H., Müller, W., Neff, F., Nicholson, G., Pasche, B., Roberson, L.A., Rozman, J., Sanderson, M., Santos, L., Selloum, M., Shannon, C., Southwel, A., Tocchini-Valentini, G.P., Vancollie, V.E., Westerberg, H., Wurst, W., Zi, M., Yalcin, B., Ramirez-Solis, R., Steel, K.P., Mallon, A.M., De Angelis, M.H., Herault, Y., Brown, S.D.M., 2013. A comparative phenotypic and genomic analysis of C57BL/6J and C57BL/6N mouse strains. *Genome Biol.* 14, R82. <https://doi.org/10.1186/gb-2013-14-7-r82>
- Skolnick, P., Kos, T., Czekaj, J., Popik, P., 2015. Effect of NMDAR antagonists in the tetrabenazine test for antidepressants: Comparison with the tail suspension test. *Acta Neuropsychiatr.* 27, 228–234. <https://doi.org/10.1017/neu.2015.14>
- Slattery, D.A., Cryan, J.F., 2012. Using the rat forced swim test to assess antidepressant-like activity in rodents. *Nat. Protoc.* 7, 1009–1014.  
<https://doi.org/10.1038/nprot.2012.044>
- Snyder, M.A., Gao, W.J., 2013. NMDA hypofunction as a convergence point for progression and symptoms of schizophrenia. *Front. Cell. Neurosci.* 7, 1–12.  
<https://doi.org/10.3389/fncel.2013.00031>
- Sokolov, A.A., Miall, R.C., Ivry, R.B., 2017. The Cerebellum: Adaptive Prediction for Movement and Cognition. *Trends Cogn. Sci.* 21, 313–332.  
<https://doi.org/10.1016/j.tics.2017.02.005>
- Song, S.H., Augustine, G.J., 2015. Synapsin isoforms and synaptic vesicle trafficking. *Mol. Cells* 38, 936–940. <https://doi.org/10.14348/molcells.2015.0233>
- Spanos, L.J., Yamamoto, B.K., 1989. Acute and subchronic effects of methylenedioxymethamphetamine [(+/-)MDMA] on locomotion and serotonin syndrome behavior in the rat. *Pharmacol. Biochem. Behav.* 32, 835–840.
- Spooren, W., Mombereau, C., Maco, M., Gill, R., Kemp, J.A., Ozmen, L., Nakanishi, S., Higgins, G.A., 2004. Pharmacological and genetic evidence indicates that combined inhibition of NR2A and NR2B subunit containing NMDA receptors is required to disrupt prepulse inhibition. *Psychopharmacology (Berl)*. 175, 99–105. <https://doi.org/10.1007/s00213-004-1785-y>
- Steinpreis, R.E., Salamone, J.D., 1993. The role of nucleus accumbens dopamine in the neurochemical and behavioral effects of phencyclidine: a microdialysis and behavioral study. *Brain Res.* 612, 263–270. [https://doi.org/10.1016/0006-8993\(93\)91671-E](https://doi.org/10.1016/0006-8993(93)91671-E)

- Suryavanshi, P.S., Ugale, R.R., Yilmazer-Hanke, D., Stairs, D.J., Dravid, S.M., 2014. GluN2C/GluN2D subunit-selective NMDA receptor potentiator CIQ reverses MK-801-induced impairment in prepulse inhibition and working memory in Y-maze test in mice. *Br. J. Pharmacol.* 171, 799–809. <https://doi.org/10.1111/bph.12518>
- Swerdlow, N.R., Geyer, M.A., Braff, D.L., 2001. Neural circuit regulation of prepulse inhibition of startle in the rat: current knowledge and future challenges. *Psychopharmacology (Berl.)* 156, 194–215.
- Szlachta, M., Pabian, P., Kuśmider, M., Solich, J., Kolasa, M., Żurawek, D., Dziedzicka-Wasylewska, M., Faron-Górecka, A., 2017. Effect of clozapine on ketamine-induced deficits in attentional set shift task in mice. *Psychopharmacology (Berl.)* 234, 2103–2112. <https://doi.org/10.1007/s00213-017-4613-x>
- Tabone, C.J., Ramaswami, M., 2012. Is NMDA Receptor-Coincidence Detection Required for Learning and Memory? *Neuron* 74, 767–769. <https://doi.org/10.1016/j.neuron.2012.05.008>
- Tanaka, Y.H., Tanaka, Y.R., Kondo, M., Terada, S.I., Kawaguchi, Y., Matsuzaki, M., 2018. Thalamocortical Axonal Activity in Motor Cortex Exhibits Layer-Specific Dynamics during Motor Learning. *Neuron* 100, 244–258. <https://doi.org/10.1016/j.neuron.2018.08.016>
- Tavares, M.R., Pavan, I.C.B., Amaral, C.L., Meneguello, L., Luchessi, A.D., Simabuco, F.M., 2015. The S6K protein family in health and disease. *Life Sci.* 131, 1–10. <https://doi.org/10.1016/j.lfs.2015.03.001>
- Temme, L., Schepmann, D., Schreiber, J.A., Frehland, B., Wünsch, B., 2018. Comparative Pharmacological Study of Common NMDA Receptor Open Channel Blockers Regarding Their Affinity and Functional Activity toward GluN2A and GluN2B NMDA Receptors. *ChemMedChem* 13, 446–452. <https://doi.org/10.1002/cmdc.201700810>
- Thelen, C., Sens, J., Mauch, J., Pandit, R., Pitychoutis, P.M., 2016. Repeated ketamine treatment induces sex-specific behavioral and neurochemical effects in mice. *Behav. Brain Res.* 312, 305–312. <https://doi.org/10.1016/j.bbr.2016.06.041>
- Tizabi, Y., Bhatti, B., Manaye, K., Das, J., Akinfiresoye, L., 2012. Antidepressant-like effects of low ketamine dose is associated with increased hippocampal AMPA/NMDA receptor density ratio in female Wistar-Kyoto rats. *Neuroscience* 213, 72–80. <https://doi.org/10.1016/j.neuroscience.2012.03.052>
- Tlamsa, A.P., Brumberg, J.C., 2010. Organization and morphology of thalamocortical neurons of mouse ventral lateral thalamus. *Somatosens. Mot. Res.* 27, 34–43. <https://doi.org/10.3109/08990221003646736>
- Tomitaka, S., Tomitaka, M., Tolliver, B.K., Sharp, F.R., 2000. Bilateral blockade of NMDA receptors in anterior thalamus by dizocilpine (MK-801) injures pyramidal neurons in rat retrosplenial cortex. *Eur. J. Neurosci.* 12, 1420–1430.

<https://doi.org/10.1046/j.1460-9568.2000.00018>

Trautmann, S., Rehm, J., Wittchen, H., 2016. The economic costs of mental disorders: Do our societies react appropriately to the burden of mental disorders? *EMBO Rep.* 17, 1245–1249.

<https://doi.org/10.15252/embr.201642951>

Traynelis, S.F., Wollmuth, L.P., McBain, C.J., Menniti, F.S., Vance, K.M., Ogden, K.K., Hansen, K.B., Yuan, H., Myers, S.J., Dingledine, R., 2010. Glutamate Receptor Ion Channels: Structure, Regulation, and Function. *Pharmacol. Rev.* 62, 405–496. <https://doi.org/10.1124/pr.109.002451>

Tricklebank, M.D., Singh, L., Oles, R.J., Preston, C., Iversen, S.D., 1989. The behavioural effects of MK-801: a comparison with antagonists acting non-competitively and competitively at the NMDA receptor. *Eur. J. Pharmacol.* 167, 127–135. [https://doi.org/10.1016/0014-2999\(89\)90754-1](https://doi.org/10.1016/0014-2999(89)90754-1)

Troyano-Rodriguez, E., Lladó-Pelfort, L., Santana, N., Teruel-Martí, V., Celada, P., Artigas, F., 2014. Phencyclidine inhibits the activity of thalamic reticular gamma-aminobutyric acidergic neurons in rat brain. *Biol. Psychiatry* 76, 937–945.

<https://doi.org/10.1016/j.biopsych.2014.05.019>

Tsai, G., Coyle, J.T., 2002. Glutamatergic mechanisms in schizophrenia. *Annu. Rev. Pharmacol. Toxicol.* 42, 165–179.

Tsukada, H., Harada, N., Nishiyama, S., Ohba, H., Sato, K., Fukumoto, D., Kakiuchi, T., 2000. Ketamine decreased striatal [<sup>11</sup>C]raclopride binding with no alterations in static dopamine concentrations in the striatal extracellular fluid in the monkey brain: Multiparametric pet studies combined with microdialysis analysis. *Synapse* 37, 95–103.

Tu, P.-C., Bai, Y.M., Li, C.-T., Chen, M.-H., Lin, W.-C., Chang, W.-C., Su, T.-P., 2018. Identification of Common Thalamocortical Dysconnectivity in Four Major Psychiatric Disorders. *Schizophr. Bull.* 45, 1143–1151.

<https://doi.org/10.1093/schbul/sby166>

Turgeon, S.M., Lin, T., Subramanian, M., 2007. Subchronic phencyclidine exposure potentiates the behavioral and c-Fos response to stressful stimuli in rats. *Pharmacol. Biochem. Behav.* 88, 73–81.

<https://doi.org/10.1016/j.pbb.2007.07.005>

Ulbrich, M.H., Isacoff, E.Y., 2008. Rules of engagement for NMDA receptor subunits. *Proc. Natl. Acad. Sci.* 105, 14163–14168.

<https://doi.org/10.1073/pnas.0802075105>

Unal, G., Ates, A., Aricioglu, F., 2018. Agmatine-attenuated cognitive and social deficits in subchronic MK-801 model of schizophrenia in rats. *Psychiatry Clin. Psychopharmacol.* 28, 245–253.

<https://doi.org/10.1080/24750573.2018.1426696>

Uno, Y., Coyle, J.T., 2019. Glutamate hypothesis in schizophrenia. *Psychiatry Clin. Neurosci.* 73, 204–215. <https://doi.org/10.1111/pcn.12823>

- van Beugen, B.J., Gao, Z., Boele, H.J., Hoebeek, F., De Zeeuw, C.I., 2013. High frequency burst firing of granule cells ensures transmission at the parallel fiber to purkinje cell synapse at the cost of temporal coding. *Front. Neural Circuits* 7, 95. <https://doi.org/10.3389/fncir.2013.00095>
- Volianskis, A., France, G., Jensen, M.S., Bortolotto, Z.A., Jane, D.E., Collingridge, G.L., 2015. Long-term potentiation and the role of N-methyl-D-aspartate receptors. *Brain Res.* 1621, 5–16. <https://doi.org/10.1016/j.brainres.2015.01.016>
- Vrajová, M., Šťastný, F., Horáček, J., Lochman, J., Šerý, O., Peková, S., Klaschka, J., Höschl, C., 2010. Expression of the hippocampal NMDA receptor GluN1 subunit and its splicing isoforms in schizophrenia: Postmortem study. *Neurochem. Res.* 35, 994–1002. <https://doi.org/10.1007/s11064-010-0145-z>
- Wagner, M.J., Kim, T.H., Savall, J., Schnitzer, M.J., Luo, L., 2017. Cerebellar granule cells encode the expectation of reward. *Nature* 544, 96–100. <https://doi.org/10.1038/nature21726>
- Wang, C., McInnis, J., Ross-Sanchez, M., Shinnick-Gallagher, P., Wiley, J.L., Johnson, K.M., 2001. Long-term behavioral and neurodegenerative effects of perinatal phencyclidine administration: Implications for schizophrenia. *Neuroscience* 107, 535–550. [https://doi.org/10.1016/S0306-4522\(01\)00384-0](https://doi.org/10.1016/S0306-4522(01)00384-0)
- Wang, C.C., Held, R.G., Chang, S.C., Yang, L., Delpire, E., Ghosh, A., Hall, B.J., 2011. A critical role for gluN2B-containing NMDA receptors in cortical development and function. *Neuron* 72, 789–805. <https://doi.org/10.1016/j.neuron.2011.09.023>
- Wang, C.C., Held, R.G., Hall, B.J., 2013. SynGAP regulates protein synthesis and homeostatic synaptic plasticity in developing cortical networks. *PLoS One* 8, e83941. <https://doi.org/10.1371/journal.pone.0083941>
- Wang, N., Zhang, G.F., Liu, X.Y., Sun, H.L., Wang, X.M., Qiu, L.L., Yang, C., Yang, J.J., 2014. Downregulation of Neuregulin 1-ErbB4 Signaling in Parvalbumin Interneurons in the Rat Brain May Contribute to the Antidepressant Properties of Ketamine. *J. Mol. Neurosci.* 54, 211–218. <https://doi.org/10.1007/s12031-014-0277-8>
- Wang, X., Yang, Y., Zhou, X., Wu, J., Li, J., Jiang, X., Qu, Q., Ou, C., Liu, L., Zhou, S., 2011. Propofol pretreatment increases antidepressant-like effects induced by acute administration of ketamine in rats receiving forced swimming test. *Psychiatry Res.* 185, 248–253. <https://doi.org/10.1016/j.psychres.2010.04.046>
- Watkins, J.C., Evans, R.H., 1981. Excitatory Amino Acid Transmitters. *Annu. Rev. Pharmacol. Toxicol.* 21, 165–204. <https://doi.org/10.1146/annurev.pa.21.040181.001121>
- Wee, K.S.L., Zhang, Y., Khanna, S., Low, C.M., 2008. Immunolocalization of NMDA receptor subunit NR3B in selected structures in the rat forebrain, cerebellum, and lumbar spinal cord. *J. Comp. Neurol.* 509, 118–135.

<https://doi.org/10.1002/cne.21747>

Weinberger, D.R., 1987. Implications of Normal Brain Development for the Pathogenesis of Schizophrenia. *Arch. Gen. Psychiatry* 44, 660–669.  
<https://doi.org/10.1001/archpsyc.1988.01800350089019>

Wenzel, A., Fritschy, J.M., Mohler, H., Benke, D., 1997. NMDA Receptor Heterogeneity During Postnatal Development of the Rat Brain: Differential Expression of the NR2A, NR2B, and NR2C Subunit Proteins. *J. Neurochem.* 68, 469–478. <https://doi.org/10.1046/j.1471-4159.1997.68020469>

WHO, 2017. Depression and other common mental disorders: global health estimates. *World Heal. Organ.* 1–24.

Wiescholleck, V., Manahan-Vaughan, D., 2012. PDE4 inhibition enhances hippocampal synaptic plasticity in vivo and rescues MK801-induced impairment of long-term potentiation and object recognition memory in an animal model of psychosis. *Transl. Psychiatry* 2, e89. <https://doi.org/10.1038/tp.2012.17>

Wong, D.T., Horng, J.S., Bymaster, F.P., Hauser, K.L., Molloy, B.B., 1974. A selective inhibitor of serotonin uptake: Lilly 110140, 3-(p-Trifluoromethylphenoxy)-n-methyl-3-phenylpropylamine. *Life Sci.* 15, 471–479.  
[https://doi.org/10.1016/0024-3205\(74\)90345-2](https://doi.org/10.1016/0024-3205(74)90345-2)

Wong, H.K., Liu, X.B., Matos, M.F., Chan, S.F., Pérez-Otaño, I., Boysen, M., Cui, J., Nakanishi, N., Trimmer, J.S., Jones, E.G., Lipton, S.A., Sucher, N.J., 2002. Temporal and regional expression of NMDA receptor subunit NR3A in the mammalian brain. *J. Comp. Neurol.* 450, 303–317.  
<https://doi.org/10.1002/cne.10314>

Wu, G.Y., Malinow, R., Cline, H.T., 1996. Maturation of a central glutamatergic synapse. *Science* (80- ). 274, 972–976.  
<https://doi.org/10.1126/science.274.5289.972>

Wu, J., Zou, H., Strong, J.A., Yu, J., Zhou, X., Xie, Q., Zhao, G., Jin, M., Yu, L., 2005. Bimodal effects of MK-801 on locomotion and stereotypy in C57BL/6 mice. *Psychopharmacology (Berl)*. 177, 256–263. <https://doi.org/10.1007/s00213-004-1944-1>

Xi, D., Keeler, B., Zhang, W., Houle, J.D., Gao, W.J., 2009. NMDA receptor subunit expression in GABAergic interneurons in the prefrontal cortex: Application of laser microdissection technique. *J. Neurosci. Methods* 176, 172–181.  
<https://doi.org/10.1016/j.jneumeth.2008.09.013>

Xu, K., Krystal, J.H., Ning, Y., Chen, D.C., He, H., Wang, D., Ke, X., Zhang, Xifan, Ding, Y., Liu, Y., Gueorguieva, R., Wang, Z., Limoncelli, D., Pietrzak, R.H., Petrakis, I.L., Zhang, Xiangyang, Fan, N., 2015. Preliminary analysis of positive and negative syndrome scale in ketamine-associated psychosis in comparison with schizophrenia. *J. Psychiatr. Res.* 61, 64–72.  
<https://doi.org/10.1016/j.jpsychires.2014.12.012>

Xu, Y., Hackett, M., Carter, G., Loo, C., Gálvez, V., Glozier, N., Glue, P., Lapidus,

- K., McGirr, A., Somogyi, A.A., Mitchell, P.B., Rodgers, A., 2016. Effects of Low-Dose and Very Low-Dose Ketamine among Patients with Major Depression: A Systematic Review and Meta-Analysis. *Int. J. Neuropsychopharmacol.* 19, 1–15. <https://doi.org/10.1093/ijnp/pyv124>
- Yamamoto, H., Kamegaya, E., Hagino, Y., Takamatsu, Y., Sawada, W., Matsuzawa, M., Ide, S., Yamamoto, T., Mishina, M., Ikeda, K., 2017. Loss of GluN2D subunit results in social recognition deficit, social stress, 5-HT2C receptor dysfunction, and anhedonia in mice. *Neuropharmacology* 112, 188–197. <https://doi.org/10.1016/j.neuropharm.2016.07.036>
- Yamamoto, H., Kamegaya, E., Sawada, W., Hasegawa, R., Yamamoto, T., Hagino, Y., Takamatsu, Y., Imai, K., Koga, H., Mishina, M., Ikeda, K., 2013. Involvement of the N-methyl-d-aspartate receptor GluN2D subunit in phencyclidine-induced motor impairment, gene expression, and increased Fos immunoreactivity. *Mol. Brain* 6, 56. <https://doi.org/10.1186/1756-6606-6-56>
- Yamamoto, T., Nakayama, T., Yamaguchi, J., Matsuzawa, M., Mishina, M., Ikeda, K., Yamamoto, H., 2016. Role of the NMDA receptor GluN2D subunit in the expression of ketamine-induced behavioral sensitization and region-specific activation of neuronal nitric oxide synthase. *Neurosci. Lett.* 610, 48–53. <https://doi.org/10.1016/j.neulet.2015.10.049>
- Yang, B., Zhang, J. chun, Han, M., Yao, W., Yang, C., Ren, Q., Ma, M., Chen, Q.X., Hashimoto, K., 2016. Comparison of R-ketamine and rapastinel antidepressant effects in the social defeat stress model of depression. *Psychopharmacology (Berl.)* 233, 3647–3657. <https://doi.org/10.1007/s00213-016-4399-2>
- Yang, C., Hu, Y.M., Zhou, Z.Q., Zhang, G.F., Yang, J.J., 2013. Acute administration of ketamine in rats increases hippocampal BDNF and mTOR levels during forced swimming test. *Ups. J. Med. Sci.* 118, 3–8. <https://doi.org/10.3109/03009734.2012.724118>
- Yang, C., Shirayama, Y., Zhang, J.C., Ren, Q., Yao, W., Ma, M., Dong, C., Hashimoto, K., 2015. R-ketamine: A rapid-onset and sustained antidepressant without psychotomimetic side effects. *Transl. Psychiatry* 5, e632. <https://doi.org/10.1038/tp.2015.136>
- Yoon, S.C., Seo, M.S., Kim, S.H., Jeon, W.J., Ahn, Y.M., Kang, U.G., Kim, Y.S., 2008. The effect of MK-801 on mTOR/p70S6K and translation-related proteins in rat frontal cortex. *Neurosci. Lett.* 434, 23–28. <https://doi.org/10.1016/j.neulet.2008.01.020>
- Zanos, P., Moaddel, R., Morris, P.J., Georgiou, P., Fischell, J., Elmer, G.I., Alkondon, M., Yuan, P., Pribut, H.J., Singh, N.S., Dossou, K.S.S., Fang, Y., Huang, X.P., Mayo, C.L., Wainer, I.W., Albuquerque, E.X., Thompson, S.M., Thomas, C.J., Zarate, C.A., Gould, T.D., 2016. NMDAR inhibition-independent antidepressant actions of ketamine metabolites. *Nature* 533, 481–486. <https://doi.org/10.1038/nature17998>
- Zanos, P., Nelson, M.E., Highland, J.N., Krimmel, S.R., Georgiou, P., Gould, T.D.,

- Thompson, S.M., 2017. A negative allosteric modulator for  $\alpha 5$  subunit-containing GABA receptors exerts a rapid and persistent antidepressant-like action without the side effects of the NMDA receptor antagonist ketamine in mice. *eNeuro* 4, 1–11. <https://doi.org/10.1523/ENEURO.0285-16.2017>
- Zarate, C.A., Singh, J.B., Carlson, P., Brutsche, N., Ameli, R., Luckenbaugh, D.A., Charney, D.S., Manji, H.K., 2006a. A randomized trial of an N-methyl-D-aspartate antagonist in treatment-resistant major depression. *Arch. Gen. Psychiatry* 63, 856–864.
- Zarate, C.A., Singh, J.B., Quiroz, J.A., De Jesus, G., Denicoff, K.K., Luckenbaugh, D.A., Manji, H.K., Charney, D.S., 2006b. A double-blind, placebo-controlled study of memantine in the treatment of major depression. *Am. J. Psychiatry* 163, 153–155. <https://doi.org/10.1176/appi.ajp.163.1.153>
- Zhang, J.C., Li, S.X., Hashimoto, K., 2014. R (-)-ketamine shows greater potency and longer lasting antidepressant effects than S (+)-ketamine. *Pharmacol. Biochem. Behav.* 116, 137–141. <https://doi.org/10.1016/j.pbb.2013.11.033>
- Zhang, Y., Buonanno, A., Vertes, R.P., Hoover, W.B., Lisman, J.E., 2012. NR2C in the thalamic reticular nucleus; effects of the NR2C knockout. *PLoS One* 7, e41908. <https://doi.org/10.1371/journal.pone.0041908>
- Zhang, Y., Llinas, R.R., Lisman, J.E., 2009. Inhibition of NMDARs in the nucleus reticularis of the thalamus produces delta frequency bursting. *Front. Neural Circuits* 3, 1–9. <https://doi.org/10.3389/neuro.04.020.2009>
- Zhou, W., Wang, N., Yang, C., Li, X.M., Zhou, Z.Q., Yang, J.J., 2014. Ketamine-induced antidepressant effects are associated with AMPA receptors-mediated upregulation of mTOR and BDNF in rat hippocampus and prefrontal cortex. *Eur. Psychiatry* 29, 419–423. <https://doi.org/10.1016/j.eurpsy.2013.10.005>
- Ziółkowska, B., Gieryk, A., Solecki, W., Przewłocki, R., 2015. Temporal and anatomic patterns of immediate-early gene expression in the forebrain of C57BL/6 and DBA/2 mice after morphine administration. *Neuroscience* 284, 107–124. <https://doi.org/10.1016/j.neuroscience.2014.09.069>
- Zou, X., Patterson, T.A., Sadvovova, N., Twaddle, N.C., Doerge, D.R., Zhang, X., Fu, X., Hanig, J.P., Paule, M.G., Slikker, W., Wang, C., 2009. Potential neurotoxicity of ketamine in the developing rat brain. *Toxicol. Sci.* 108, 149–158. <https://doi.org/10.1093/toxsci/kfn270>





# **Annex**



## Article 1

### **Glial GLT-1 blockade in infralimbic cortex as a new strategy to evoke rapid antidepressant-like effects in rats**

J Gasull-Camós<sup>1,2,3</sup>, M Tarrés-Gatius<sup>1,3</sup>, F Artigas<sup>1,2,3</sup> and A Castañé<sup>1,2,3</sup>

*Translational Psychiatry* (2017). 7(2): e1038.

doi: 10.1038/tp.2017.7.

<sup>1</sup>Department of Neurochemistry and Neuropharmacology, CSIC-Institut d'Investigacions Biomèdiques de Barcelona, Barcelona, Spain

<sup>2</sup>Centro de Investigación Biomédica en Red de Salud Mental, Instituto de Salud Carlos III, Madrid, Spain

<sup>3</sup>Institut d'Investigacions Biomèdiques August Pi i Sunyer, Barcelona, Spain.

This study proposes different roles of the infralimbic (IL) and the prelimbic (PrL) cortices on mood regulation. Concretely, the present work shows that enhancing glutamatergic transmission into IL, but not PrL, evokes rapid antidepressant-like effects in rats. These effects depend on increased serotonin (5-HT) release in the mPFC, which is probably mediated by the activation of IL- dorsal raphe projection.



OPEN

Citation: *Transl Psychiatry* (2017) 7, e1038; doi:10.1038/tp.2017.7

www.nature.com/tp

## ORIGINAL ARTICLE

## Glial GLT-1 blockade in infralimbic cortex as a new strategy to evoke rapid antidepressant-like effects in rats

J Gasull-Camós<sup>1,2,3</sup>, M Tarrés-Gatius<sup>1,3</sup>, F Artigas<sup>1,2,3</sup> and A Castañé<sup>1,2,3</sup>

Ketamine and deep brain stimulation produce rapid antidepressant effects in humans and rodents. An increased AMPA receptor (AMPA-R) signaling in medial prefrontal cortex (mPFC) has been suggested to mediate these responses. However, little research has addressed the direct effects of enhancing glutamate tone or AMPA-R stimulation in mPFC subdivisions. The current study investigates the behavioral and neurochemical consequences of glutamate transporter-1 (GLT-1) blockade or s-AMPA microinfusion in the infralimbic (IL) and prelimbic (PrL) cortex. Owing to the connectivity between the mPFC and raphe nuclei, the role of serotonin is also explored. The bilateral microinfusion of the depolarizing agent veratridine into IL—but not PrL—of rats evoked immediate antidepressant-like responses. The same regional selectivity was observed after microinfusion of dihydrokainic acid (DHK), a selective inhibitor of GLT-1, present in astrocytes. The DHK-evoked antidepressant-like responses appear to be mediated by an AMPA-R-driven enhancement of serotonergic activity, as (i) they were prevented by NBQX 2,3-dioxo-6-nitro-1,2,3,4-tetrahydrobenzof[quinoxaline]-7-sulfonamide disodium salt) and mimicked by s-AMPA; (ii) DHK and s-AMPA elevated similarly extracellular glutamate in IL and PrL, although extracellular 5-HT and *c-fos* expression in the midbrain dorsal raphe increased only when these agents were applied in IL; and (iii) DHK antidepressant-like responses were prevented by 5-HT synthesis inhibition and mimicked by citalopram microinfusion in IL. These results indicate that an acute increase of glutamatergic neurotransmission selectively in IL triggers immediate antidepressant-like responses in rats, likely mediated by the activation of IL–raphe pathways, which then results in a fast increase of serotonergic activity.

*Translational Psychiatry* (2017) 7, e1038; doi:10.1038/tp.2017.7; published online 21 February 2017

## INTRODUCTION

Major depressive disorder is a leading cause of disability worldwide with a high socioeconomic impact.<sup>1</sup> Standard treatments, based on serotonin (5-HT) and/or norepinephrine reuptake inhibition, show slow onset of clinical action and limited efficacy, which results in a high percentage of chronic or recurrent patients.<sup>2,3</sup> The non-competitive *N*-methyl-D-aspartate receptor antagonist ketamine and deep brain stimulation (DBS) overcome some of these limitations and evoke a rapid and long-lasting clinical improvement in treatment-resistant patients.<sup>4–7</sup> Currently, research efforts are focused on identifying the mechanism procuring these rapid antidepressant actions.

The prefrontal cortex (PFC) has a crucial role in the pathophysiology and treatment of major depressive disorder. Early neuroimaging studies reported on a reduced energy metabolism in the subgenual anterior cingulate cortex of major depressive disorder patients, associated with a glial loss.<sup>8,9</sup> Further studies indicated an increased activity of the adjacent Brodmann area 25, which was normalized after effective treatment including DBS.<sup>4,10–13</sup> In some contrast to the latter observations, sub-anesthetic doses of ketamine increased glucose metabolism in this area in healthy volunteers.<sup>14–16</sup>

In rats, the most ventral part of the medial PFC (mPFC), namely the infralimbic cortex (IL), has emerged as an important hub for emotional control.<sup>17–19</sup> Indeed, DBS of the IL but not prelimbic cortex (PrL) induced robust antidepressant-like responses in rats.<sup>20</sup> Likewise, local IL ketamine infusion evoked rapid and long-lasting

effects, which were mimicked by the optogenetic stimulation of IL<sup>21</sup> suggesting that ketamine's antidepressant action is mediated by an increased excitatory neurotransmission in this area. In agreement, ketamine has been shown to increase glutamate release in rat PFC.<sup>22</sup> Moreover, ketamine and DBS induce antidepressant-like responses that require the activation of AMPA-R.<sup>20,23</sup>

Here we further assess the role of excitatory neurotransmission in dorsal (PrL) and ventral (IL) mPFC subdivisions in the control of emotional states. For this purpose, we investigated the behavioral and neurochemical consequences of blocking the glutamate transporter-1 (GLT-1), mainly localized in astrocytes and mainly responsible for cortical glutamate reuptake.<sup>24,25</sup> Moreover, owing to the reciprocal connectivity and mutual control between mPFC and the raphe nuclei,<sup>26–28</sup> we investigated the contribution of serotonin neurotransmission on these effects.

## MATERIALS AND METHODS

## Subjects

Male Wistar rats (Charles River, Lyon, France) weighing 280–330 g at the time of surgery were used. The rats were maintained in a controlled environment (12 h light/dark, 22 ± 1 °C) with *ad libitum* access to food and water. Before surgery, the rats were acclimatized to the housing conditions for at least 7 days and were daily handled. After surgery, the rats were singly housed and randomly assigned to treatment. All the experimental procedures were conducted in accordance with national (Royal Decree 53/2013) and European legislation (Directive 2010/63/EU, on the

<sup>1</sup>Department of Neurochemistry and Neuropharmacology, CSIC-Institut d'Investigacions Biomèdiques de Barcelona, Barcelona, Spain; <sup>2</sup>Centro de Investigación Biomédica en Red de Salud Mental, Instituto de Salud Carlos III, Madrid, Spain and <sup>3</sup>Institut d'Investigacions Biomèdiques August Pi i Sunyer, Barcelona, Spain. Correspondence: Dr A Castañé, Department of Neurochemistry and Neuropharmacology, CSIC-Institut d'Investigacions Biomèdiques de Barcelona, Rosselló 161, 6th Floor, Barcelona 08036, Spain. E-mail: acfnq@libb.csic.es.

Received 7 October 2016; revised 2 December 2016; accepted 22 December 2016

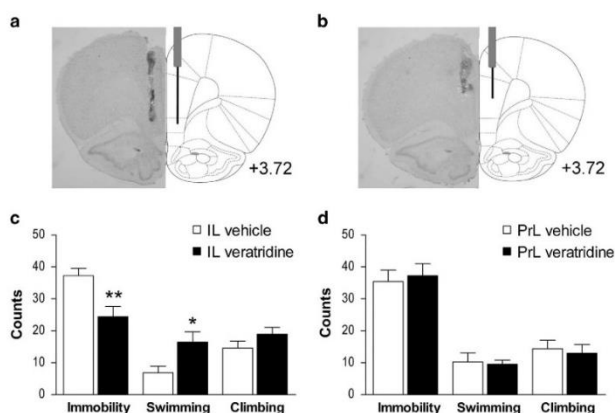


**Figure 1.** Bilateral microinfusion sites and antidepressant-like action of veratridine on the FST. Neutral red staining of mPFC brain sections at anteroposterior +3.72 from bregma (left) and schematic representation of guide cannula and infusion cannula placement (right) in the (a) infralimbic cortex (IL) and (b) prelimbic cortex (PrL). (c) Bilateral microinfusion of veratridine (50 pmoles) into IL produced a rapid antidepressant-like response, as shown by decreased immobility counts and increased swimming (IL vehicle,  $n = 7$ ; IL veratridine,  $n = 9$ ). (d) Veratridine infusion into PrL produced no behavioral change on the FST (PrL vehicle,  $n = 5$ ; PrL veratridine,  $n = 7$ ). The values are expressed as mean  $\pm$  s.e.m. \* $P < 0.05$  and \*\* $P < 0.01$  versus vehicle-treated rats (Student's *t*-test). FST, forced swimming test; mPFC, medial prefrontal cortex.

protection of animals used for scientific purposes, 22 September 2010), and were approved by the Institutional Animal Care and Use Committee of the University of Barcelona.

#### Drugs

Veratridine, dihydrokainic acid (DHK), 2,3-dioxo-6-nitro-1,2,3,4-tetrahydrobenzo[*f*]quinoline-7-sulfonamide disodium salt (NBQX), (S)- $\alpha$ -Amino-3-hydroxy-5-methyl-4-isoxazolepropionic acid (s-AMPA) and citalopram hydrobromide were purchased from Tocris (Bristol, UK). 4-chloro-*o*-phenylalanine methyl ester hydrochloride (pCPA) was purchased from Sigma-Aldrich (Tres Cantos, Spain).

For intracerebral microinfusion, veratridine was dissolved in 12.5% dimethyl sulfoxide in artificial cerebrospinal fluid and pH adjusted to 6.5; DHK and s-AMPA were dissolved in PBS 10 $\times$  as previously reported;<sup>29</sup> NBQX and citalopram were dissolved in artificial cerebrospinal fluid. The microinfusion volume was 0.5  $\mu$ l per side in all cases. pCPA was administered intraperitoneally, was daily prepared by dissolving in saline and pH was adjusted to 6.0 with 0.1 M NaOH.<sup>30</sup>

#### Surgery and microinfusions

Anesthetized rats (sodium pentobarbital, 60 mg kg<sup>-1</sup>, intraperitoneally) were implanted with stainless steel 22-gauge bilateral guide cannulae (Plastics One, Roanoke, VA, USA) in the cingulate cortex: anteroposterior +3.2; mediolateral  $\pm$  0.75; dorsoventral -2.4.<sup>31</sup> The coordinates in mm were taken from bregma and the skull surface. Guide cannulae were fixed with stainless steel screws using dental acrylic. To prevent occlusion, a dummy cannula was inserted into the guide cannula and manipulated daily. This handling decreased the stress associated with the infusion on the testing day.<sup>32</sup> The rats were allowed 7 days to recover after surgery.

The microinfusion cannulae (28 gauge) extended 1.5 or 3 mm beyond the guide cannulae for PrL or IL local administration (dorsoventral: -3.9 or -5.4, respectively). Previous to the tests, three mock infusions were performed. On the testing day, drug or vehicle solutions were bilaterally administered over 1 min through two 50  $\mu$ l Hamilton syringes connected to the microinfusion cannulae via 0.28 mm ID polyethylene tubing, using an infusion/withdrawal pump (Harvard Apparatus, Holliston, MA, USA). Microinfusion cannulae were left in place for 3 min to allow drug diffusion. Behavioral tests were performed 10 min after drug local administration. In double microinfusion procedures (NBQX and DHK), the second

administration occurred 5 min after the first. Figure 1 shows an example of IL (a) and PrL (b) microinfusion sites.

#### Behavioral studies

The forced swimming test (FST) was conducted as described previously.<sup>33</sup> Briefly, a clear methacrylate cylinder (46  $\times$  20 cm) filled with water (24  $\pm$  1  $^{\circ}$ C) to a depth of 30 cm was used. Each rat was placed into the cylinder for 15 min in a pretest session where no scoring of behavior was needed. Twenty-four hours later, the rats were exposed to the same conditions during a 5 min test and behavior was video recorded. In a posterior analysis, test recordings were divided into periods of 5 s and the predominant behavior was rated as immobility, swimming or climbing by an experimenter blind to the treatment.

The novelty-suppressed feeding test (NSFT) assesses the rat's aversion to eat in a novel environment. Before the test rats were food restricted (18 g per day, 3 days + 24 h deprivation). On the test day, rats were placed into a novel arena (90  $\times$  90  $\times$  40 cm) for 10 min containing two food pellets in the highly illuminated center (600 lx) and latency to eat was measured, only sniffing was not considered. As a control, homecage food consumption was measured at 5 min and 24 h after test.

Locomotor activity was assessed to ensure that responses on the FST were due to depression-related effects rather than changes in general activity. Measurements were performed in a dimly lighted black open field (35  $\times$  35 cm) and video recorded during 15 min. The distance moved was calculated for each animal using the VideoTrack View Point software (Lyon, France).

#### *In vivo* microdialysis studies and tissue 5-HT assessment

Microdialysis experiments were conducted as previously described.<sup>20,34</sup> Concentric dialysis probes (1.5 mm membrane length) were implanted in anesthetized rats (sodium pentobarbital, 60 mg kg<sup>-1</sup>, intraperitoneally) unilaterally in the PrL (anteroposterior +3.2; mediolateral -0.6; dorsoventral -4.3) or IL (anteroposterior +3.2; mediolateral -0.6; dorsoventral -5.7). The coordinates were taken from bregma and the skull.<sup>31</sup> The rats were continuously perfused with artificial cerebrospinal fluid containing 1  $\mu$ M citalopram at a rate of 1.65  $\mu$ l/min. A stabilization period of 3 h was used. The effects of vehicle perfusion (10% PBS 10 $\times$  in artificial cerebrospinal fluid) and increasing doses of DHK (3 and 10  $\mu$ M) or s-AMPA (100  $\mu$ M) were tested at 24 and 48 h after surgery, respectively. Dialysate samples were

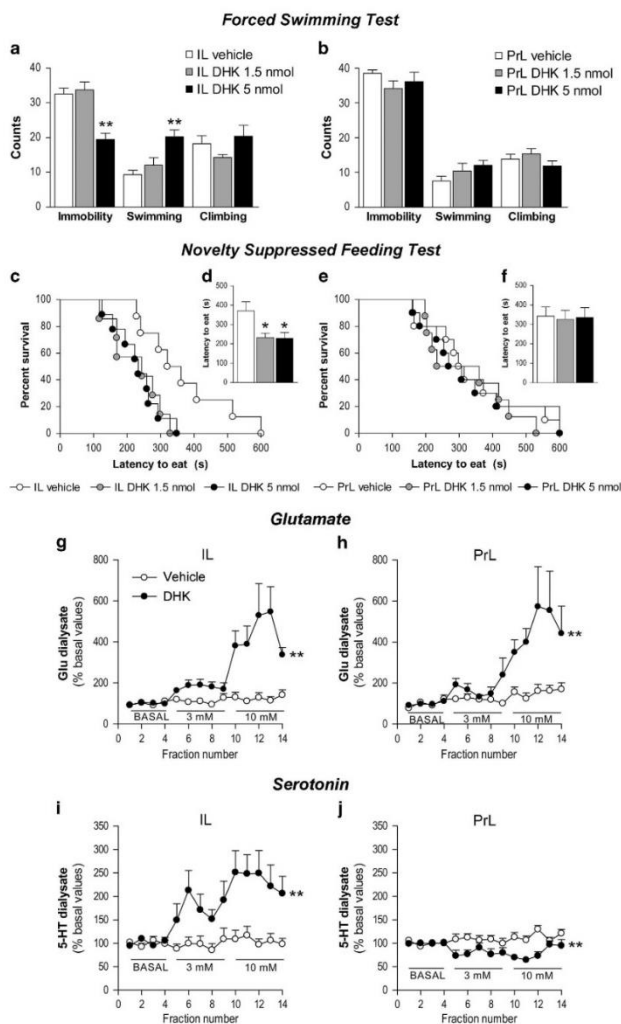


**Figure 2.** Antidepressant-like action of DHK on the FST and NSFT and neurochemical effects over glutamate and serotonin output. **(a)** Bilateral microinfusion of DHK (5 nmol) into the IL produced a rapid antidepressant-like response on the FST, as shown by decreased immobility and increased swimming (IL vehicle,  $n = 10$ ; IL DHK 1.5 nmol,  $n = 7$ ; IL DHK 5 nmol,  $n = 9$ ). **(b)** PrL DHK infusion produced no behavioral change on the FST (PrL vehicle,  $n = 6$ ; PrL DHK 1.5 nmol,  $n = 5$ ; PrL DHK 5 nmol,  $n = 6$ ). IL DHK (1.5 and 5 nmol) also produced an antidepressant-like response on the NSFT, as shown by **(c)** increased percentage of animals that have eaten in the cumulative survival curve and **(d)** reduced latency to eat (IL vehicle,  $n = 8$ ; IL DHK 1.5 nmol,  $n = 9$ ; IL DHK 5 nmol,  $n = 7$ ), whereas **(e)** and **(f)** PrL DHK produced no behavioral change on the NSFT (PrL vehicle,  $n = 10$ ; PrL DHK 1.5 nmol,  $n = 8$ ; PrL DHK 10 nmol,  $n = 10$ ). In microdialysis experiments, DHK dose-dependently increased the extracellular glutamate (Glu) concentration both in **(g)** IL (vehicle; DHK,  $n = 10$ ) and **(h)** PrL (vehicle,  $n = 10$ ; DHK,  $n = 7$ ). Extracellular serotonin (5-HT) concentration **(i)** increased in IL during DHK perfusion (vehicle,  $n = 8$ ; DHK,  $n = 7$ ), **(j)** whereas small 5-HT decreases were observed during DHK perfusion in PrL (vehicle; DHK,  $n = 7$ ). The values are expressed as mean  $\pm$  s.e.m. \* $P < 0.05$  and \*\* $P < 0.01$  versus vehicle-treated rats (Bonferroni *post hoc* test). Microdialysis data are expressed as percentages of four basal values. DHK, dihydrokainic acid; FST, forced swimming test; IL, infralimbic cortex; mPFC, medial prefrontal cortex; NSFT, novelty-suppressed feeding test; PrL, prelimbic cortex.

collected every 25 (DHK) or 35 min (*s*-AMPA). Neurotransmitter concentrations were determined by high performance liquid chromatography with electrochemical (5-HT) or fluorimetric (glutamate) detection.

The 5-HT depletion was assessed as reported earlier.<sup>35</sup> Briefly, the mPFC (25–50 mg) and dorsal raphe (DR) (10–15 mg) brain samples were homogenized adding a buffer solution (0.4 M perchloric acid, 0.1% sodium metabisulphite, 0.01% EDTA and 0.1% cysteine; 100 µl buffer per 10 mg of wet tissue). The homogenates were centrifuged (4 °C, 30 min, 12 000 r.p.m.) and the supernatants were filtered (Millex 0.45 µm filters, Merck Millipore, Madrid, Spain) and analyzed by high performance liquid chromatography with electrochemical detection.

#### *In situ* hybridization studies

The effects of IL and PrL DHK and *s*-AMPA on brain *c-fos* mRNA expression were examined by *in situ* hybridization 1 h after treatment, as described previously.<sup>36</sup> The brain sections (14 µm) were thaw-mounted onto APTS (3-aminopropyltriethoxysilane, Sigma, St Louis, MO, USA)-coated slides and kept at –30 °C. The *c-fos* oligonucleotide probe was complementary to bases 131–178 (GenBank ID: NM\_022197) and was labeled with [<sup>32</sup>P]-dATP (>2500 Ci mmol<sup>-1</sup>; DuPont-NEN, Boston, MA, USA) with terminal deoxynucleotidyltransferase (TdT, Calbiochem, La Jolla, CA, USA) and purified with ProbeQuant G-50 Micro Columns (GE Healthcare UK Limited, Buckinghamshire, UK). Hybridized sections were exposed to Biomax MR film (Kodak, Sigma-Aldrich, Madrid, Spain) for 7 days with intensifying screens. Relative optical densities were measured with a computer-assisted image analyzer (MCID, Mering, Germany). Three consecutive brain sections at any level of interest were analyzed for each rat and averaged to obtain individual values.

#### Histological verification

At the end of the studies, the rats were killed by sodium pentobarbital overdose and the brains were removed to proceed with the histological verification of the cannulae and probes placement. The brain sections (30 µm) were mounted onto slides and posteriorly stained with neutral red. Rats infused outside PrL or IL were excluded from all analyses.

#### Statistical analysis

The number of animals used for each test is reported in the figure legends. The sample sizes were determined based on power analysis and common practice in behavioral, neurochemical (~10 animals per group) and *in situ* hybridization studies (~5 animals per group). The data are expressed as mean ± s.e.m. Statistical analysis was carried out using unpaired Student's *t*-test, one-way analysis of variance (ANOVA) followed by Bonferroni *post hoc* comparisons and two-way repeated-measures ANOVA. In the NSFT, we also used nonparametric statistics, the Kaplan–Meier estimator as described previously.<sup>37</sup> In all cases, the level of significance was set at  $P < 0.05$ .

## RESULTS

Veratridine microinfusion in IL, but not PrL, induces antidepressant responses on the FST

The bilateral microinfusion of the depolarizing drug veratridine (50 pmoles per side) into IL produced an antidepressant-like

response on the FST (Figure 1), reducing immobility ( $t_{(14)} = 3.120$ ;  $P < 0.01$ ) and increasing swimming behavior ( $t_{(14)} = 2.323$ ;  $P < 0.05$ ; Figure 1c). On the contrary, veratridine microinfusion into the PrL produced no significant behavioral responses (Figure 1d).

DHK microinfusion in IL, but not PrL, induces antidepressant responses on the FST and NSFT

The microinfusion of the GLT-1 inhibitor DHK into IL produced an antidepressant-like response on the FST (Figure 2), reducing the immobility ( $F_{(2,25)} = 16.917$ ;  $P < 0.0001$ ) and increasing swimming behavior ( $F_{(2,25)} = 9.990$ ;  $P < 0.001$ ). *Post hoc* comparisons revealed significant differences versus controls at 5 but not 1.5 nmoles of DHK ( $P < 0.01$ , in all cases; Figure 2a). A dose of 0.15 nmoles of DHK was also tested with no changes in the immobility time ( $s$ ) ( $147.27 \pm 12.12$ ) compared with controls ( $153.45 \pm 16.49$ ;  $t_{(16)} = 0.302$ ; not significant (NS)). The bilateral IL DHK microinfusion produced an antidepressant-like response on the NSFT (Figure 2). Thus, Kaplan–Meier survival analysis showed an effect of treatment (log-rank test,  $P < 0.05$ ) and a significant difference between 1.5 and 5 nmoles versus vehicle ( $P < 0.05$ ,  $P < 0.01$ , respectively; Figure 2c). Moreover, one-way ANOVA showed a significant effect of treatment on the latency to eat ( $F_{(2,23)} = 5.605$ ;  $P < 0.05$ ; Figure 2d). *Post hoc* comparisons showed that both doses of DHK reduced the latency to eat compared with vehicle ( $P < 0.05$ , all cases). Homecage food intake was similar between IL DHK and vehicle groups for the 5 min test (data in grams; vehicle:  $0.68 \pm 0.12$ ; 1.5 nmoles:  $0.84 \pm 0.16$ ; 5 nmoles:  $0.62 \pm 0.13$ ;  $F_{(2,23)} = 0.710$ ; NS) and for the 24 h test data (vehicle:  $32.91 \pm 0.89$ ; 1.5 nmoles:  $32.08 \pm 1.32$ ; 5 nmoles:  $32.79 \pm 1.36$ ;  $F_{(2,23)} = 0.145$ ; NS).

However, DHK microinfusion into the PrL produced no significant behavioral responses on the FST (Figure 2b) and NSFT (Figures 2e and f).

#### IL and PrL DHK effects on glutamate and 5-HT output

Baseline concentrations of glutamate (pmol per fraction) in IL and PrL were  $11.2 \pm 1.3$  ( $n = 20$ ) and  $13.2 \pm 1.7$  ( $n = 17$ ), respectively (NS). DHK perfusion dose-dependently enhanced extracellular glutamate in IL and PrL, with significant effects of the treatment ( $F_{(1,18)} = 14.021$ ;  $P < 0.01$ ), fraction ( $F_{(13,234)} = 8.721$ ;  $P < 0.0001$ ) and treatment × fraction interaction ( $F_{(13,234)} = 7.057$ ;  $P < 0.0001$ ; IL data; Figure 2g, Supplementary Figure S1a) and significant effect of treatment ( $F_{(1,15)} = 12.980$ ;  $P < 0.01$ ), fraction ( $F_{(13,195)} = 7.793$ ;  $P < 0.0001$ ) and treatment × fraction interaction ( $F_{(13,195)} = 4.575$ ;  $P < 0.0001$ ; PrL data; Figure 2h, Supplementary Figure S1b).

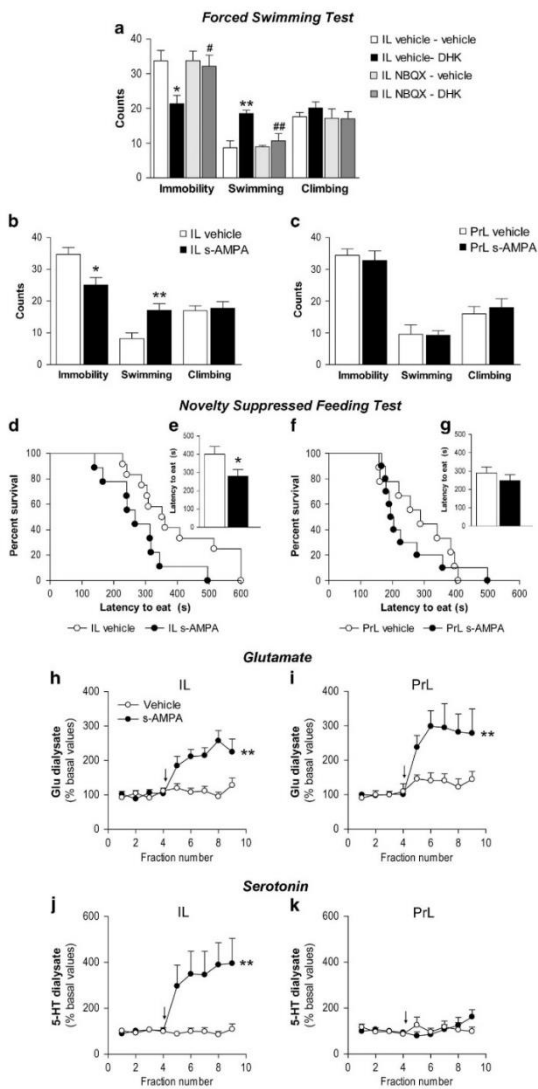
Baseline concentrations of 5-HT (fmol per fraction) in IL and PrL were  $5.8 \pm 1.1$  ( $n = 14$ ) and  $4.4 \pm 0.3$  ( $n = 14$ ), respectively (NS).

**Figure 3.** AMPA-R mediates DHK-induced antidepressant-like actions and *s*-AMPA mimics DHK behavioral and neurochemical effects. (a) Effects of NBQX (10 nmoles) and DHK (5 nmoles) double microinfusion into the IL cortex on the FST. The reduction in immobility and increase in swimming counts observed in VEH/DHK group ( $n = 6$ ) compared with control (VEH/VEH;  $n = 6$ ) was prevented by previous local microinfusion of NBQX (NBQX/DHK;  $n = 7$ ). NBQX/VEH group ( $n = 5$ ) was similar to controls. (b) The bilateral microinfusion of *s*-AMPA (50 pmoles) into IL produced a rapid antidepressant-like response, as shown by decreased immobility and increased swimming counts (IL vehicle,  $n = 7$ ; IL *s*-AMPA,  $n = 9$ ). (c) *s*-AMPA microinfusion into PrL produced no behavioral change on the FST (PrL vehicle,  $n = 5$ ; PrL *s*-AMPA,  $n = 5$ ). (d) IL *s*-AMPA also produced an antidepressant-like response on the NSFT, as shown by increased percentage of animals that have eaten in the cumulative survival curve and (e) reduced latency to eat (IL vehicle,  $n = 12$ ; IL *s*-AMPA,  $n = 9$ ), whereas (f and g) PrL DHK produced no behavioral change on the NSFT (PrL vehicle,  $n = 9$ ; PrL *s*-AMPA,  $n = 10$ ). In microdialysis experiments, *s*-AMPA increased extracellular glutamate (Glu) concentration both in (h) IL (vehicle,  $n = 10$ ; *s*-AMPA,  $n = 11$ ) and (i) PrL (vehicle,  $n = 6$ ; *s*-AMPA,  $n = 9$ ). (j) IL *s*-AMPA increased extracellular serotonin concentration (vehicle,  $n = 8$ ; *s*-AMPA,  $n = 7$ ), whereas (k) no change was observed in PrL *s*-AMPA microdialysis (vehicle  $n = 7$ ; *s*-AMPA,  $n = 9$ ). The values are expressed as mean ± s.e.m. \* $P < 0.05$ , \*\* $P < 0.01$  versus vehicle–vehicle or vehicle; and # $P < 0.05$ , ## $P < 0.01$  versus vehicle–DHK (Bonferroni *post hoc* test). Microdialysis data are expressed as percentages of four basal values. The arrow represents the start of the microinfusion with vehicle or *s*-AMPA (h–k). AMPA-R, AMPA receptor; DHK, dihydrokaïnacid; FST, forced swimming test; IL, infralimbic cortex; NBQX, 2,3-dioxo-6-nitro-1,2,3,4-tetrahydrobenzo[*f*]quinoxaline-7-sulfonamide disodium salt; NSFT, novelty-suppressed feeding test; PrL, prelimbic cortex; VEH, vehicle.



DHK perfusion into IL markedly increased 5-HT release, with a significant effect of treatment ( $F_{1,13} = 10.041$ ;  $P < 0.01$ ), fraction ( $F_{13,169} = 4.852$ ;  $P < 0.0001$ ) and treatment  $\times$  fraction interaction ( $F_{13,169} = 3.952$ ;  $P < 0.0001$ ; Figure 2i, Supplementary Figure S1c).

Conversely, PrL DHK perfusion decreased extracellular 5-HT, with a significant effect of treatment ( $F_{1,12} = 13.382$ ;  $P < 0.01$ ) and treatment  $\times$  fraction interaction ( $F_{13,156} = 3.388$ ;  $P < 0.001$ ; Figure 2j, Supplementary Figure S1d).



## Prevention of the antidepressant responses of IL DHK by NBQX pretreatment

Pretreatment with IL NBQX (10 nmoles) prevented the antidepressant-like response of IL DHK on the FST (Figure 3a). One-way ANOVA showed a significant effect of treatment on immobility ( $F_{3,23}=4.117$ ;  $P < 0.05$ ) and swimming behavior ( $F_{3,23}=7.448$ ;  $P < 0.01$ ). *Post hoc* comparisons showed that IL NBQX prevented the reduction of immobility ( $P < 0.05$ ) and the increased swimming behavior ( $P < 0.01$ ) of IL DHK (5 nmoles). Nonsignificant responses were observed for the control and NBQX groups.

## s-AMPA microinfusion in IL, but not PrL, induces antidepressant responses on the FST and NSFT

IL s-AMPA (50 pmoles per side) microinfusion produced an antidepressant-like response on the FST, with a significant decrease of immobility ( $t_{(14)}=2.900$ ;  $P < 0.05$ ) and increased swimming behavior ( $t_{(14)}=3.123$ ;  $P < 0.01$ ; Figure 3b). IL s-AMPA also evoked an antidepressant-like response on the NSFT (Figure 3). Thus, Kaplan–Meier survival analysis showed a significant difference between s-AMPA and vehicle groups ( $t_{(19)}=2.127$ ;  $P < 0.05$ ). Likewise, IL s-AMPA reduced the latency to eat compared with vehicle ( $P < 0.05$ , unpaired *t*-test; Figure 3e). There were no differences in homecage food intake between IL s-AMPA and vehicle groups neither in the 5 min test (data in grams; vehicle:  $0.65 \pm 0.08$ , s-AMPA:  $0.43 \pm 0.09$ ;  $t_{(19)}=1.824$ ; NS) nor in the 24 h test (vehicle:  $28.20 \pm 0.62$ , s-AMPA:  $26.38 \pm 2.28$ ;  $t_{(17)}=0.807$ ; NS).

In contrast, PrL s-AMPA produced no significant behavioral response on the FST (Figure 3c) and NSFT (Figures 3f and g).

## IL and PrL s-AMPA effects on glutamate and 5-HT output

Baseline extracellular glutamate concentrations (pmol per fraction) in IL and PrL were  $9.8 \pm 0.9$  ( $n=20$ ) and  $10.0 \pm 0.9$  ( $n=14$ ), respectively (NS). s-AMPA perfusion enhanced the extracellular glutamate similarly in IL and PrL, with a significant effect of treatment ( $F_{1,19}=19.480$ ;  $P < 0.001$ ), fraction ( $F_{8,152}=9.750$ ;  $P < 0.0001$ ) and treatment  $\times$  fraction interaction ( $F_{8,152}=7.389$ ;  $P < 0.0001$ ; IL data; Figure 3h, Supplementary Figure S2a). For PrL data, there was a significant effect of treatment ( $F_{1,13}=11.590$ ;  $P < 0.01$ ), fraction ( $F_{8,104}=4.961$ ;  $P < 0.0001$ ) and treatment  $\times$  fraction interaction ( $F_{8,104}=2.151$ ;  $P < 0.05$ ; Figure 3i, Supplementary Figure S2b).

Baseline extracellular 5-HT concentrations (fmol per fraction) in IL and PrL were  $5.0 \pm 1.1$  ( $n=15$ ) and  $3.3 \pm 0.5$  ( $n=12$ ), respectively (NS). The perfusion of DHK into IL markedly increased 5-HT release, with a significant effect of treatment ( $F_{1,13}=10.560$ ;  $P < 0.01$ ), fraction ( $F_{8,104}=5.416$ ;  $P < 0.0001$ ) and treatment  $\times$  fraction interaction ( $F_{8,104}=5.638$ ;  $P < 0.0001$ ; Figure 3j, Supplementary Figure S2c). Conversely, s-AMPA into PrL cortex did not change extracellular 5-HT with no significant effect of treatment, fraction or interaction in the two-way ANOVA (Figure 3k, Supplementary Figure S2d).

## Prevention of antidepressant responses of IL DHK by pCPA

5-HT depletion by pCPA ( $86 \text{ mg kg}^{-1}$ , 4 days, intraperitoneally) prevented the antidepressant-like responses of IL DHK on the FST (Figure 4a). One-way ANOVA showed a significant effect of treatment for immobility ( $F_{3,30}=6.380$ ;  $P < 0.01$ ) and swimming behavior ( $F_{3,30}=9.981$ ;  $P < 0.01$ ) with significant *post hoc* differences in immobility ( $P < 0.01$ ) and swimming behavior ( $P < 0.05$ ) between pCPA-pretreated and saline-pretreated rats infused with IL DHK, indicating a full suppression of DHK effects in 5-HT-depleted rats. Nonsignificant differences were observed between the control and pCPA-treated rats.

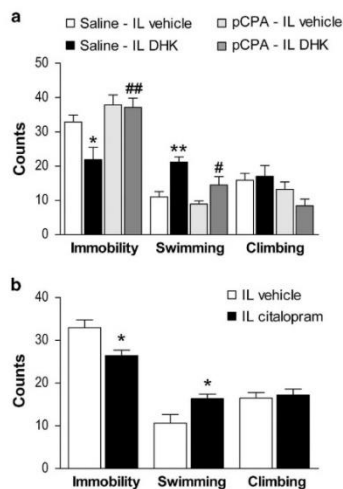


**Figure 4.** Serotonin is necessary for the DHK-induced antidepressant-like actions. (a) Effect of systemic pCPA ( $86 \text{ mg kg}^{-1}$ , 4 days) and IL DHK (5 nmoles) microinfusion on the FST. The reduction in immobility and increase in swimming counts observed in saline–IL DHK group compared with saline–IL vehicle ( $n=7$ , both groups) was prevented by previous intraperitoneal treatment with pCPA (pCPA–IL DHK;  $n=8$ ). pCPA–IL vehicle group ( $n=9$ ) was similar to controls. (b) The bilateral microinfusion of citalopram (15 pmoles) into IL produced a rapid antidepressant-like response, as shown by decreased immobility and increased swimming counts (IL vehicle,  $n=10$ ; IL s-AMPA,  $n=9$ ). The values are expressed as mean  $\pm$  s.e.m. \* $P < 0.05$ , \*\* $P < 0.01$  versus saline–vehicle or vehicle; and # $P < 0.05$ , ## $P < 0.01$  versus saline–DHK (Bonferroni *post hoc* test). DHK, dihydrokainic acid; FST, forced swimming test; IL, infralimbic cortex; pCPA, 4-chloro-*D,L*-phenylalanine methyl ester hydrochloride.

Detection of neurotransmitter concentration in tissue samples showed that pretreatment with pCPA significantly decreased the concentration of 5-HT and its metabolite 5-hydroxyindoleacetic acid (5-HIAA) by 95% and 98% in the mPFC; and by 83% and 80% in the DR, respectively ( $P < 0.01$ , all cases, data not shown).

## IL citalopram produces antidepressant responses on the FST

As results with pCPA indicated an involvement of serotonin in the antidepressant-like effects of DHK microinfusion, we examined the effects of IL microinfusion of the selective serotonin reuptake inhibitor citalopram. Thus, IL citalopram (15 pmoles per side) produced an antidepressant-like response on the FST (Figure 4b). Unpaired *t*-test showed that IL citalopram produced a significant decrease in immobility ( $t_{(17)}=2.803$ ;  $P < 0.05$ ) and an increase in swimming behavior ( $t_{(17)}=2.377$ ;  $P < 0.05$ ).

## c-fos mRNA expression after IL and PrL DHK or s-AMPA

As in previous studies,<sup>36,38,39</sup> we used *c-fos* mRNA expression as a surrogate marker of neuronal activation to examine brain areas engaged in the antidepressant-like effects of DHK and s-AMPA microinfusion in IL.

IL DHK significantly increased *c-fos* expression in the nucleus accumbens and lateral septum ( $P < 0.05$ ), and in the CA3 and dentate gyrus region of the hippocampus, the centromedial,

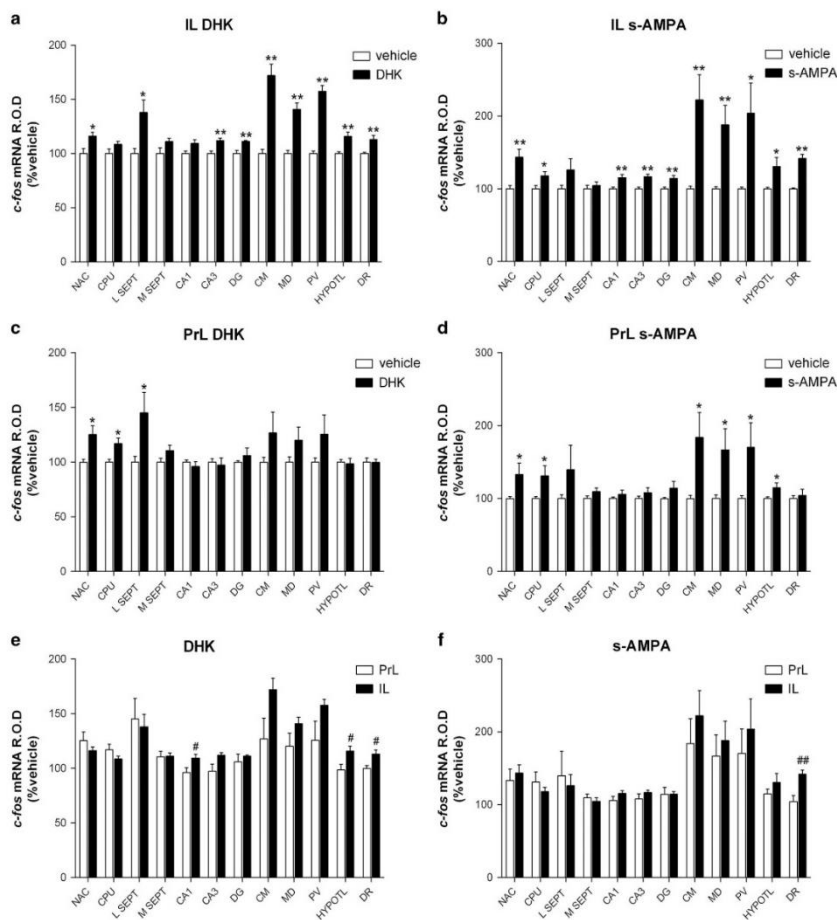


**Figure 5.** *c-fos* mRNA expression after bilateral IL and PrL DHK (5 nmoles) and s-AMPA (50 pmoles) microinfusion. Rats were killed 1 h after drug or vehicle microinfusion. (a–f) Bar graphs showing mean  $\pm$  s.e.m. of optical activity (arbitrary units) after treatments ( $n=6$  per group), in different brain areas: CA1 and CA3, CA regions of the hippocampus; CM, centromedial nucleus of thalamus; CPU, caudate-putamen nucleus; DG, dentate gyrus; DHK, dihydrokainic acid; DR, dorsal raphe; HYPOTL, hypothalamus; IL, infralimbic cortex; L SEPT, lateral septum; MD, mediodorsal nucleus of the thalamus; M SEPT, medial septum; NAC, nucleus accumbens; PrL, prelimbic cortex; PV, paraventricular nucleus. \* $P < 0.05$ , \*\* $P < 0.01$  versus vehicle; # $P < 0.05$ , ## $P < 0.01$  versus PrL (Student's *t*-test).

mediodorsal and paraventricular nuclei of the thalamus, the hypothalamus and the DR ( $P < 0.01$ ; Figure 5a). PrL DHK increased *c-fos* expression in the nucleus accumbens, caudate-putamen and lateral septum ( $P < 0.05$ ; Figure 5c). Significant differences between IL and PrL DHK were found in the CA1, hypothalamus and DR ( $P < 0.05$ ; Figure 5e). Likewise, IL s-AMPA significantly increased *c-fos* expression in the caudate-putamen, paraventricular and hypothalamus ( $P < 0.05$ ), and in the nucleus accumbens, CA1, CA3, dentate gyrus, centromedial, mediodorsal

and DR ( $P < 0.01$ ; Figure 5b). PrL s-AMPA increased *c-fos* expression in the nucleus accumbens, caudate-putamen, centromedial, mediodorsal and paraventricular ( $P < 0.05$ ; Figure 5d). Significant differences between IL and PrL s-AMPA were found in the DR ( $P < 0.01$ ; Figure 5f).

IL veratridine, DHK and s-AMPA effects on locomotor activity Behavioral changes observed on the FST were not due to a drug-induced increase in general locomotor activity. On the contrary,

unpaired *t*-test showed that IL veratridine (50 pmoles) reduced distance moved compared with vehicle group. No changes in locomotor activity were observed after IL DHK or s-AMPA microinfusion (Supplementary Figure S3).

## DISCUSSION

The present study shows that the regionally selective enhancement of glutamatergic neurotransmission in the IL -but not PrL- induces robust antidepressant-like responses in rats. This effect appears to involve the activation of IL AMPA-R and the subsequent enhancement of serotonergic activity, as suggested by the large increase of 5-HT release associated to DHK and s-AMPA infusion in IL and by the prevention of antidepressant-like effects by 5-HT depletion with pCPA. Likewise, the involvement of 5-HT is also supported by the antidepressant-like response evoked by IL citalopram. Overall, our data emphasize the relevance of excitatory and serotonergic neurotransmission in ventral mPFC on mood regulation.

First, we observed that veratridine, which is a non-selective depolarizing agent, evoked antidepressant-like responses when microinfused specifically into IL. Although veratridine is not neurotransmitter-selective, more than 80% of PFC neurons are excitatory and the PFC contains a dense network of afferent and efferent glutamatergic fibers that would release glutamate after veratridine microinfusion. In agreement, the optogenetic activation of IL pyramidal neurons evoked rapid antidepressant-like responses in rats.<sup>21</sup> Then, we used a glutamate transporter inhibitor (DHK) to increase PFC glutamate. DHK selectively blocks the GLT-1, mainly localized in astrocytes and responsible for more than the 90% of the cortical glutamate uptake.<sup>24,25</sup> Similar to veratridine, IL -but not PrL- DHK induced antidepressant-like responses on the FST at the dose of 5 nmoles, whereas lower doses (1.5 nmoles) were ineffective. In addition, a 10-fold lower dose of DHK (0.15 nmoles) resulted without consequences on the FST. Although the present data suggest that antidepressant-like effects are mediated by an increase of excitatory neurotransmission, we cannot rule out that the excess glutamate may actually inhibit excitatory neurotransmission through depolarization blockade. Interestingly, IL DHK also evoked antidepressant-like responses on the NSFT. This test is sensitive to chronic, but not acute, classic antidepressants,<sup>37</sup> as well as to systemic or IL ketamine.<sup>21,40</sup> Thus, the local administration of DHK into IL mimics the rapid effects of ketamine in this test.

Our results are consistent with the distinct -sometimes opposed- roles that IL and PrL have in the control of emotional signals.<sup>17,19,41</sup> Recently, the intra-PFC infusion of DHK induced an anhedonic behavior in rats.<sup>42</sup> However, it remains to be determined whether IL and PrL contribute differently to this phenotype.

The regional selectivity observed in the present study is in agreement with recent data indicating that DBS and ketamine exert antidepressant effects via their actions into the IL.<sup>20,21,43</sup> Moreover, both treatments increase glutamate release in PFC<sup>20,22</sup> and involve the AMPA-R in their antidepressant effects.<sup>20,23</sup> Conversely, decreased levels of prefrontal AMPA-R subunits were observed in subjects with mood disorders<sup>44</sup> and in rats after repeated stress.<sup>45</sup> In line with these observations, we show that (i) the IL microinfusion of the AMPA-R antagonist NBQX blocked the antidepressant-like responses of IL DHK and (ii) IL s-AMPA evoked antidepressant-like responses. To our knowledge, this is the first study directly investigating the role of AMPA-R activation selectively in IL and PrL on depressive behaviors and provides further support for a crucial role of IL AMPA-R activation in the resilience to stress.

DHK and s-AMPA increased extracellular glutamate similarly in the IL and PrL, indicating that the behavioral differences were not due to a differential enhancement of glutamatergic

neurotransmission in both regions. Interestingly, local DHK and s-AMPA elevated extracellular 5-HT when applied in IL, and slightly reduced it or left it unaffected when applied in PrL. Thus, we hypothesized that 5-HT could be involved in the antidepressant-like responses after enhancing IL glutamate. In support of this view, 5-HT depletion with pCPA prevented the antidepressant effects of IL DHK. Conversely, serotonin transporter blockade with citalopram in IL evoked antidepressant-like effects. This is the first observation that an intracerebral selective serotonin reuptake inhibitor application can evoke antidepressant effects similar to a systemic selective serotonin reuptake inhibitor. These observations are in line with the positive role that 5-HT had in the control of stress and suggest that the enhanced 5-HT release contributes to DHK-induced effects. Moreover, the increased swimming behavior observed in the FST is consistent with an antidepressant-mediated increase in serotonergic neurotransmission as previously reported.<sup>33,46</sup> This view is also supported by previous observations showing an association between enhanced 5-HT release and antidepressant-like responses after reducing the expression of 5-HT<sub>1A</sub> autoreceptors,<sup>47</sup> DBS<sup>48,49</sup> and ketamine administration.<sup>50</sup>

Although we cannot exclude a local effect of glutamate on 5-HT terminals in the mPFC, there are more data supporting the circuitry-based hypothesis. There is compelling evidence of reciprocal connectivity between PFC and DR.<sup>27,51–53</sup> Pyramidal neurons in the mPFC exert a tight control over brainstem monoaminergic neurons, including raphe 5-HT neurons.<sup>26,54</sup> The latter pathway controls animal response to behavioral challenges, as shown by the antidepressant-like responses after optogenetic stimulation of mPFC-DR projection.<sup>55</sup> Hence, Fukumoto *et al.*<sup>50</sup> showed that the antidepressant effects of PFC microinfusion of ketamine and mGlu2/3 receptor antagonism require the activation of raphe 5-HT neurons. Reciprocally, raphe 5-HT neurons control the activity of PFC pyramidal neurons.<sup>26,56</sup> Therefore, the differential 5-HT response in IL and PrL to the similar enhancement of glutamate in both mPFC subdivisions likely reflects a differential control of raphe 5-HT neurons by IL and PrL. Supporting this view, we have observed a differential expression of *c-fos* in the DR after DHK and s-AMPA infusion in IL and PrL, suggesting an increased activity in DR after IL drug treatments. Anatomical studies may support our results,<sup>27</sup> yet it remains to be established by electrophysiological and imaging techniques. Hence, previous electrophysiological studies had shown that mPFC pyramidal neurons may activate or inhibit DR serotonin neurons.<sup>26</sup> Excitations are monosynaptic and involve the activation of AMPA-R and *N*-methyl-D-aspartate receptor on serotonin neurons, whereas inhibitions are mediated by two different processes, (i) a local negative feedback involving 5-HT<sub>1A</sub> autoreceptors and (ii) the activation of GABA interneurons in the midbrain raphe by mPFC inputs and the subsequent inhibition of serotonin neurons.<sup>26,57</sup> However, to date, it is uncertain whether IL and PrL inputs to the midbrain raphe may elicit selective responses, as suggested by the present data. In addition, IL and PrL are reciprocally connected and IL exerts an inhibitory control over PrL activity, which adds an additional element of complexity.<sup>58</sup> Recent findings suggest that the activation of neuronal population in IL and its descending axons is implicated on the antidepressant-like responses of IL DBS, leading to an increased firing of raphe 5-HT neurons.<sup>43</sup> Thus, an enhanced excitatory transmission in mPFC-raphe descending pathways<sup>55</sup> could be a common feature of different fast-acting antidepressant strategies.

Finally, it has been described that an increase of presynaptic neuronal activity in the cerebral cortex slows the clearance of glutamate by astrocytes, increasing the persistence of glutamate in the extracellular space, which may facilitate receptor activation. This physiological mechanism represents a novel form of neuronal-astrocyte communication, challenging the previous view

that glutamate transport by EAATs has solely a housekeeping function.<sup>59</sup> In our studies with DHK, the reduction in glutamate transport facilitates glutamate availability and AMPA-R activation, which produce an antidepressant phenotype. Thus, given the role of glial cells in synaptic transmission,<sup>60,61</sup> further work is necessary to elucidate the role of the tripartite glutamate synapse in the pathophysiology of major depressive disorder.<sup>62</sup>

Overall, we show that the increase of glutamatergic tone in IL—but not PrL—exerts immediate antidepressant-like responses in rats. These effects are dependent on stimulation of AMPA-R and involve an increased serotonergic function. This adds to recent studies in the field supporting an important role of IL mPFC subdivision in the mechanism of action of fast-acting antidepressant strategies.

#### CONFLICT OF INTEREST

FA has received consulting honoraria from Lundbeck A/S and has been PI of a grant from Lundbeck A/S. He is also a member of the scientific advisory board of Neurolix and a co-inventor of two patents on conjugated oligonucleotide sequences. The remaining authors declare no conflict of interest.

#### ACKNOWLEDGMENTS

This work was supported by the Spanish Ministry of Economy and Competitiveness (grant numbers SAF2012-35183; SAF2015-68346; and BES2013-063241 to JG-C), co-financed by European Regional Development Fund (ERDF); Generalitat de Catalunya (grant number 2014-SGR798 and 2016FI-B00285 to MT-G) and Centro de Investigación Biomédica en Red de Salud Mental (CIBERSAM). We thank Leticia Campa and Verónica Paz for technical support on high performance liquid chromatography and *in situ* hybridization experiments, respectively, and Paloma Bravo for technical support on behavioral studies and histology.

#### REFERENCES

- Global Burden of Disease Study 2013 Collaborators. Global, regional, and national incidence, prevalence, and years lived with disability for 301 acute and chronic diseases and injuries in 188 countries, 1990-2013: a systematic analysis for the Global Burden of Disease Study 2013. *Lancet* 2015; **386**: 743-800.
- Rush AJ, Trivedi MH, Wisniewski SR, Nierenberg AA, Stewart JW, Warden D *et al*. Acute and longer-term outcomes in depressed outpatients requiring one or several treatment steps: a STAR\*D report. *Am J Psychiatry* 2006; **163**: 1905-1917.
- Trivedi MH, Rush AJ, Wisniewski SR, Nierenberg AA, Warden D, Ritz L *et al*. Evaluation of outcomes with citalopram for depression using measurement-based care in STAR\*D: Implications for clinical practice. *Am J Psychiatry* 2006; **163**: 28-40.
- Mayberg HS, Lozano AM, Voon V, McNeely HE, Seminowicz D, Hamani C *et al*. Deep brain stimulation for treatment-resistant depression. *Neuron* 2005; **45**: 651-660.
- Zarate CA Jr, Singh JB, Carlson PJ, Brutsche NE, Ameli R, Luckenbaugh DA *et al*. A randomized trial of an N-methyl-D-aspartate antagonist in treatment-resistant major depression. *Arch Gen Psychiatry* 2006; **63**: 856-864.
- Holtzheimer PE, Kelley ME, Gross RE, Filkowski MM, Garlow SJ, Barocas A *et al*. Subcallosal cingulate deep brain stimulation for treatment-resistant unipolar and bipolar depression. *Arch Gen Psychiatry* 2012; **69**: 150-158.
- Zarate CA Jr, Brutsche NE, Ibrahim L, Franco-Chaves J, Diazgranados N, Cravchik A *et al*. Replication of ketamine's antidepressant efficacy in bipolar depression: a randomized controlled add-on trial. *Biol Psychiatry* 2012; **71**: 939-946.
- Drevets WC, Price JL, Simpson JR Jr, Todd RD, Reich T, Vannier M *et al*. Subgenual prefrontal cortex abnormalities in mood disorders. *Nature* 1997; **386**: 824-827.
- Öngür D, Drevets WC, Price JL. Glial reduction in the subgenual prefrontal cortex in mood disorders. *Proc Natl Acad Sci USA* 1998; **95**: 13290-13295.
- Mayberg HS, Brannan SK, Tekell JL, Silva JA, Mahurin RK, McGinnis S *et al*. Regional metabolic effects of fluoxetine in major depression: serial changes and relationship to clinical response. *Biol Psychiatry* 2000; **48**: 830-843.
- Nobler MS, Quendo MA, Kegeles LS, Malone KM, Campbell CC, Sackeim HA *et al*. Decreased regional brain metabolism after ect. *Am J Psychiatry* 2001; **158**: 305-308.
- Dougherty DD, Weiss AP, Cosgrove GR, Alpert NM, Cassem EH, Nierenberg AA *et al*. Cerebral metabolic correlates as potential predictors of response to anterior cingulotomy for treatment of major depression. *J Neurosurg* 2003; **99**: 1010-1017.

- Seminowicz DA, Mayberg HS, McIntosh AR, Goldapple K, Kennedy S, Segal Z *et al*. Limbic-frontal circuitry in major depression: a path modeling metaanalysis. *NeuroImage* 2004; **22**: 409-418.
- Långsjö JW, Kaisti KK, Aalto S, Hinkka S, Aantaa R, Oikonen V *et al*. Effects of subanesthetic doses of ketamine on regional cerebral blood flow, oxygen consumption, and blood volume in humans. *Anesthesiology* 2003; **99**: 614-623.
- Långsjö JW, Salmi E, Kaisti KK, Aalto S, Hinkka S, Aantaa R *et al*. Effects of sub-anesthetic ketamine on regional cerebral glucose metabolism in humans. *Anesthesiology* 2004; **100**: 1065-1071.
- Vollenweider FX, Kometer M. The neurobiology of psychedelic drugs: implications for the treatment of mood disorders. *Nat Rev Neurosci* 2010; **11**: 642-651.
- Killcross S, Coutureau E. Coordination of actions and habits in the medial prefrontal cortex of rats. *Cereb Cortex* 2003; **13**: 400-408.
- Vidal-Gonzalez I, Vidal-Gonzalez B, Rauch SL, Quirk GJ. Microstimulation reveals opposing influences of prelimbic and infralimbic cortex on the expression of conditioned fear. *Learn Mem* 2006; **13**: 728-733.
- Sierra-Mercado D, Padilla-Coreano N, Quirk GJ. Dissociable roles of prelimbic and infralimbic cortices, ventral hippocampus, and basolateral amygdala in the expression and extinction of conditioned fear. *Neuropsychopharmacology* 2011; **36**: 529-538.
- Jiménez-Sánchez L, Castañé A, Pérez-Caballero L, Grifoll-Escoda M, López-Gil X, Campa L *et al*. Activation of AMPA receptors mediates the antidepressant action of deep brain stimulation of the infralimbic prefrontal cortex. *Cereb Cortex* 2016; **26**: 2778-2789.
- Fuchikami M, Thomas A, Liu R, Wohleb ES, Land BB, Dileone RJ *et al*. Optogenetic stimulation of infralimbic PFC reproduces ketamine's rapid and sustained antidepressant actions. *Proc Natl Acad Sci USA* 2015; **112**: 8106-8111.
- Moghaddam B, Adams B, Verma A, Daly D. Activation of glutamatergic neurotransmission by ketamine: a novel step in the pathway from NMDA receptor blockade to dopaminergic and cognitive disruptions associated with the prefrontal cortex. *J Neurosci* 1997; **17**: 2921-2927.
- Maeng S, Zarate CA Jr, Du J, Schloesser RJ, McCammon J, Chen G *et al*. Cellular mechanisms underlying the antidepressant effects of ketamine: role of alpha-amino-3-hydroxy-5-methylisoxazole-4-propionic acid receptors. *Biol Psychiatry* 2008; **63**: 349-352.
- Danbolt NC, Storm-Mathisen J, Kanner BI. An [Na<sup>+</sup>+K<sup>+</sup>]-coupled L-glutamate transporter purified from rat brain is located in glial cell processes. *Neuroscience* 1992; **51**: 295-310.
- Petr GT, Sun Y, Frederick NM, Zhou Y, Dhamme SC, Hameed MQ *et al*. Conditional deletion of the glutamate transporter GLT-1 reveals that astrocytic GLT-1 protects against fatal epilepsy while neuronal GLT-1 contributes significantly to glutamate uptake into synaptosomes. *J Neurosci* 2015; **35**: 5187-5201.
- Celada P, Puig MV, Casanovas JM, Guillazo G, Artigas F. Control of dorsal raphe serotonergic neurons by the medial prefrontal cortex: Involvement of serotonin-1A, GABA(A), and glutamate receptors. *J Neurosci* 2001; **21**: 9917-9929.
- Vertes RP. Differential projections of the infralimbic and prelimbic cortex in the rat. *Synapse* 2004; **51**: 32-58.
- Puig MV, Artigas F, Celada P. Modulation of the activity of pyramidal neurons in rat prefrontal cortex by raphe stimulation *in vivo*: involvement of serotonin and GABA. *Cereb Cortex* 2005; **15**: 1-14.
- Lee Y, Gaskins D, Anand A, Shekhar A. Glia mechanisms in mood regulation: a novel model of mood disorders. *Psychopharmacol* 2007; **191**: 55-65.
- Jensen JB, du Jardin KG, Song D, Budac D, Smagin G, Sanchez C *et al*. Vortioxetine, but not escitalopram or duloxetine, reverses memory impairment induced by central 5-HT depletion in rats: evidence for direct 5-HT receptor modulation. *Eur Neuropsychopharmacol* 2014; **24**: 148-159.
- Paxinos C, Watson D. *The Rat Brain in Stereotaxic Coordinates*. Elsevier/Academic Press: Amsterdam, The Netherlands, 2005.
- Slattery DA, Neumann ID, Cryan JF. Transient inactivation of the infralimbic cortex induces antidepressant-like effects in the rat. *J Psychopharmacol* 2011; **25**: 1295-1303.
- Slattery DA, Cryan JF. Using the rat forced swim test to assess antidepressant-like activity in rodents. *Nat Protoc* 2012; **7**: 1009-1014.
- López-Gil X, Babot Z, Amargós-Bosch M, Suñol C, Artigas F, Adell A. Clozapine and haloperidol differentially suppress the MK-801-increased glutamatergic and serotonergic transmission in the medial prefrontal cortex of the rat. *Neuropsychopharmacology* 2007; **32**: 2087-2097.
- Adell A, Sarna GS, Hutson PH, Curzon G. *An in vivo* dialysis and behavioural study of the release of 5-HT by p-chloroamphetamine in reserpine-treated rats. *Br J Pharmacol* 1989; **97**: 206-212.
- Kargieman L, Santana N, Mengod G, Celada P, Artigas F. Antipsychotic drugs reverse the disruption in prefrontal cortex function produced by NMDA receptor blockade with phencyclidine. *Proc Natl Acad Sci USA* 2007; **104**: 14843-14848.

- 37 Samuels BA, Hen R. Novelty-suppressed feeding in the mouse. In: Gould TD (ed). *Mood and Anxiety Related Phenotypes in Mice: Characterization Using Behavioral Tests*, Volume II. Humana Press: Totowa, NJ, USA, 2011, pp 107–121.
- 38 Santana N, Troyano-Rodríguez E, Mengod G, Celada P, Artigas F. Activation of thalamocortical networks by the N-methyl-D-aspartate receptor antagonist phencyclidine: reversal by clozapine. *Biol Psychiatry* 2011; **69**: 918–927.
- 39 Liadó-Pelfort L, Santana N, Ghisi V, Artigas F, Celada P. 5-HT1A receptor agonists enhance pyramidal cell firing in prefrontal cortex through a preferential action on GABA interneurons. *Cereb Cortex* 2012; **22**: 1487–1497.
- 40 Li N, Lee B, Liu RJ, Banas M, Dwyer JM, Iwata M *et al*. mTOR-dependent synapse formation underlies the rapid antidepressant effects of NMDA antagonists. *Science* 2010; **329**: 959–964.
- 41 Adhikari A, Lerner TN, Finkelstein J, Pak S, Jennings JH, Davidson TJ *et al*. Basomedial amygdala mediates top-down control of anxiety and fear. *Nature* 2015; **527**: 179–185.
- 42 John CS, Sypek EI, Carlezon WA, Cohen BM, Öngür D, Bechtholt AJ. Blockade of the GLT-1 transporter in the central nucleus of the amygdala induces both anxiety and depressive-like symptoms. *Neuropsychopharmacology* 2014; **40**: 1700–1708.
- 43 Etiévant A, Oosterhof C, Bétry C, Abrial E, Novo-Perez M, Rovera R *et al*. Astroglial control of the antidepressant-like effects of prefrontal cortex deep brain stimulation. *EBioMedicine* 2015; **2**: 896–906.
- 44 Zarate CA Jr, Machado-Vieira R, Henter I, Ibrahim L, Diazgranados N, Salvatore G. Glutamatergic modulators: the future of treating mood disorders? *Harv Rev Psychiatry* 2010; **18**: 293–303.
- 45 Yuen EY, Wei J, Liu W, Zhong P, Li X, Yan Z. Repeated stress causes cognitive impairment by suppressing glutamate receptor expression and function in prefrontal cortex. *Neuron* 2012; **73**: 962–977.
- 46 Detke MJ, Lucki I. Detection of serotonergic and noradrenergic antidepressants in the rat forced swimming test: the effects of water depth. *Behav Brain Res* 1996; **73**: 43–46.
- 47 Ferrés-Coy A, Pilar-Cuellar F, Vidal R, Paz V, Masana M, Cortés R *et al*. RNAi-mediated serotonin transporter suppression rapidly increases serotonergic neurotransmission and hippocampal neurogenesis. *Transl Psychiatry* 2013; **15**: e211.
- 48 Hamani C, Diwan M, Macedo CE, Brandão ML, Shumake J, Gonzalez-Lima F *et al*. Antidepressant-like effects of medial prefrontal cortex deep brain stimulation in rats. *Biol Psychiatry* 2010; **67**: 117–124.
- 49 Veerakumar A, Challis C, Gupta P, Da J, Upadhyay A, Beck SG *et al*. Antidepressant-like effects of cortical deep brain stimulation coincide with pro-neuroplastic adaptations of serotonin systems. *Biol Psychiatry* 2014; **76**: 203–212.
- 50 Fukumoto K, Iijima M, Chaki S. The antidepressant effects of an mGlu2/3 receptor antagonist and ketamine require AMPA receptor stimulation in the mPFC and subsequent activation of the 5-HT neurons in the DRN. *Neuropsychopharmacology* 2016; **41**: 1046–1056.
- 51 Azmitia EC, Segal M. An autoradiographic analysis of the differential ascending projections of the dorsal and median raphe nuclei in the rat. *J Comp Neurol* 1978; **179**: 641–667.
- 52 Groenewegen HJ, Uylings HB. The prefrontal cortex and the integration of sensory, limbic and autonomic information. *Prog Brain Res* 2000; **126**: 3–28.
- 53 Gabbott PL, Warner TA, Jays PR, Salway P, Busby SJ. Prefrontal cortex in the rat: projections to subcortical autonomic, motor, and limbic centers. *J Comp Neurol* 2005; **492**: 145–177.
- 54 Hajós M, Richards CD, Székely AD, Sharp T. An electrophysiological and neuroanatomical study of the medial prefrontal cortex projection to the midbrain raphe nuclei in the rat. *Neuroscience* 1998; **87**: 95–108.
- 55 Warden MR, Selimbeyoglu A, Mirzabekov JJ, Lo M, Thompson KR, Kim SY *et al*. A prefrontal cortex-brainstem neuronal projection that controls response to behavioural challenge. *Nature* 2012; **492**: 428–432.
- 56 Amargós-Bosch M, Bortolozzi A, Puig MV, Serrats J, Adell A, Celada P *et al*. Co-expression and *in vivo* interaction of serotonin1A and serotonin2A receptors in pyramidal neurons of prefrontal cortex. *Cereb Cortex* 2004; **14**: 281–299.
- 57 Varga V, Székely AD, Csillag A, Sharp T, Hajós M. Evidence for a role of GABA interneurons in the cortical modulation of midbrain 5-hydroxytryptamine neurons. *Neuroscience* 2001; **106**: 783–792.
- 58 Ji G, Neugebauer V. Modulation of medial prefrontal cortical activity using *in vivo* recordings and optogenetics. *Mol Brain* 2012; **5**: 36.
- 59 Armbruster M, Hanson E, Dulla CG. Glutamate clearance is locally modulated by presynaptic neuronal activity in the cerebral cortex. *J Neurosci* 2016; **36**: 10404–10415.
- 60 Perea G, Araque A. Astrocytes potentiate transmitter release at single hippocampal synapses. *Science* 2007; **317**: 1083–1086.
- 61 Perea G, Sur M, Araque A. Neuron-glia networks: integral gear of brain function. *Front Cell Neurosci* 2014; **8**: 378.
- 62 de Sousa RT, Loch AA, Carvalho AF, Brunoni AR, Haddad MR, Henter ID *et al*. Genetic studies on the tripartite glutamate synapse in the pathophysiology and therapeutics of mood disorders. *Neuropsychopharmacology* 2016, epub ahead of print 28 September; doi: 10.1038/npp.2016.149.



This work is licensed under a Creative Commons Attribution 4.0 International License. The images or other third party material in this article are included in the article's Creative Commons license, unless indicated otherwise in the credit line; if the material is not included under the Creative Commons license, users will need to obtain permission from the license holder to reproduce the material. To view a copy of this license, visit <http://creativecommons.org/licenses/by/4.0/>

© The Author(s) 2017

Supplementary Information accompanies the paper on the Translational Psychiatry website (<http://www.nature.com/tp>)

## Article 2

### **Serotonergic mechanisms involved in antidepressant-like responses induced by GLT-1 blockade in rat infralimbic cortex**

J Gasull-Camós<sup>1,2,3</sup>, S Martínez-Torres<sup>4</sup>, M Tarrés-Gatius<sup>1,3</sup>, A Ozaita<sup>4</sup>,  
F Artigas<sup>1,2,3</sup> and A Castañé<sup>1,2,3</sup>

*Neuropharmacology* (2018). 139: 41-51

doi: 10.1016/j.neuropharm.2018.06.029.

<sup>1</sup>Department of Neurochemistry and Neuropharmacology, CSIC-Institut d'Investigacions Biomèdiques de Barcelona, Barcelona, Spain

<sup>2</sup>Centro de Investigación Biomédica en Red de Salud Mental, Instituto de Salud Carlos III, Madrid, Spain

<sup>3</sup>Institut d'Investigacions Biomèdiques August Pi i Sunyer, Barcelona, Spain.

<sup>4</sup>Laboratory of Neuropharmacology, Department of Experimental and Health Sciences, University Pompeu Fabra, Barcelona, Spain.

This study further supports the implication of the infralimbic (IL)-dorsal raphe projection in the antidepressant effects evoked by increasing glutamate transmission into the IL cortex. Moreover, the present work demonstrates the opposite roles played by presynaptic (dorsal raphe) and post-synaptic (IL) 5-HT<sub>1A</sub> receptors in preventing or facilitating, respectively, the antidepressant response.







Contents lists available at ScienceDirect

Neuropharmacology

journal homepage: [www.elsevier.com/locate/neuropharm](http://www.elsevier.com/locate/neuropharm)

## Serotonergic mechanisms involved in antidepressant-like responses evoked by GLT-1 blockade in rat infralimbic cortex



Júlia Gasull-Camós<sup>a, b, c, d</sup>, Sara Martínez-Torres<sup>e, f</sup>, Mireia Tarrés-Gatius<sup>a, b, d</sup>,  
Andrés Ozaita<sup>e, f, g</sup>, Francesc Artigas<sup>a, b, c</sup>, Anna Castañé<sup>a, b, c, \*</sup>

<sup>a</sup> Departament de Neuroquímica i Neurofarmacologia, CSIC-Institut d'Investigacions Biomèdiques de Barcelona, Barcelona, Spain

<sup>b</sup> Institut d'Investigacions Biomèdiques August Pi i Sunyer, Barcelona, Spain

<sup>c</sup> Centro de Investigación Biomédica en Red de Salud Mental, Instituto de Salud Carlos III, Madrid, Spain

<sup>d</sup> Universitat de Barcelona, Barcelona, Spain

<sup>e</sup> Departament de Ciències Experimentals i de la Salut, Universitat Pompeu Fabra, Barcelona, Spain

<sup>f</sup> Red de Trastornos Adictivos, Instituto de Salud Carlos III, Madrid, Spain

<sup>g</sup> Institut Hospital del Mar d'Investigacions Mèdiques, Barcelona, Spain

### ARTICLE INFO

#### Article history:

Received 22 December 2017

Received in revised form

19 June 2018

Accepted 21 June 2018

Available online 22 June 2018

#### Keywords:

Antidepressant effects

Dihydrokainic acid

Dorsal raphe

GLT-1

Infralimbic cortex

Serotonin

### ABSTRACT

Novel fast-acting antidepressant strategies, such as ketamine and deep brain stimulation, enhance glutamatergic neurotransmission in medial prefrontal cortex (mPFC) regions via AMPA receptor (AMPA-R) activation. We recently reported that the regionally-selective blockade of the glial glutamate transporter-1 (GLT-1) by dihydrokainic acid (DHK) microinfusion in rat infralimbic cortex (IL), the most ventral part of the mPFC, evoked immediate (10 min) antidepressant-like responses, which involved AMPA-R activation and were associated to increased serotonin (5-hydroxytryptamine, 5-HT) release. Given the reciprocal connectivity between the mPFC and the serotonergic dorsal raphe nucleus (DR), here we examined the serotonergic mechanisms involved in the reported antidepressant-like responses of DHK microinfusion. First, we show that antidepressant-like responses evoked by IL application of DHK and citalopram are mediated by local 5-HT<sub>1A</sub> receptors (5-HT<sub>1A</sub>-R), since they are cancelled by previous IL WAY100635 microinfusion. Second, IL DHK microinfusion increases excitatory inputs onto DR, as shown by an increased glutamate and 5-HT release in DR and by a selective increase of c-Fos expression in DR 5-HT neurons, not occurring in putative GABAergic neurons. This view is also supported by an increased 5-HT release in ventral hippocampus following IL DHK microinfusion. Interestingly, antidepressant-like responses evoked by IL DHK lasted for 2 h and could be prolonged for up to 24 h by attenuating self-inhibitory effects via 5-HT<sub>1A</sub> autoreceptors. In contrast, the antidepressant-like effects of S-AMPA microinfusion in IL were short-lasting. Together, our results further support a prominent role of the IL–DR pathway and of ascending 5-HT pathways in mediating antidepressant-like responses evoked by glutamatergic mechanisms.

© 2018 Elsevier Ltd. All rights reserved.

### 1. Introduction

Major depressive disorder (MDD) is a severe psychiatric syndrome with very high socioeconomic impact worldwide (Global Burden of Disease Study, 2013 Collaborators, 2015). This is attributable to the elevated prevalence of MDD, the emergence of depressive episodes during active periods of life and the slow clinical action and limited efficacy of monoamine antidepressants (Rush et al., 2006). During the last decades, the development of novel antidepressant

strategies based on the modulation of glutamatergic neurotransmission has opened new venues for the improvement of MDD treatment. Hence, the non-competitive N-methyl-D-aspartate receptor (NMDA-R) antagonist ketamine and deep brain stimulation (DBS) overcome some of these limitations and evoke rapid and long-lasting clinical improvements in MDD patients, including those presenting treatment resistant depression (Mayberg et al., 2005; Zarate et al., 2012, 2006). Thus, research efforts in the field are focused on the identification of the neurobiological mechanisms underlying these rapid antidepressant actions.

MDD has been associated to astrocyte dysfunction in frontostriatal structures (Peng et al., 2015) and to alterations in the

\* Corresponding author. c/Roselló 161, 6th floor, 08036, Barcelona, Spain.

E-mail address: [acfnq@iibb.csic.es](mailto:acfnq@iibb.csic.es) (A. Castañé).

number, morphology and function of astrocytes (Rajkowska and Stockmeier, 2013; Sanacora and Banasr, 2013). Astrocytes play a key role in the regulation of glutamatergic neurotransmission (Perea et al., 2014; Perea and Araque, 2007) and in modulating complex behaviors (Halassa and Haydon, 2010; Oliveira et al., 2015). Upon release, glutamate is cleared from the synaptic cleft by excitatory amino acid transporters (EAATs), from which EAAT1 and EAAT2 are located in astrocytes and show altered expression in MDD patients (Choudary et al., 2005). In the rat brain, the glutamate transporter-1 (GLT-1) is the homologous of the human EAAT2 and is the main responsible for cortical glutamate reuptake (Danbolt et al., 1992; Rothstein et al., 1994). We recently reported that GLT-1 blockade in the infralimbic area (IL) of the medial prefrontal cortex (mPFC) evoked fast (10 min) and robust antidepressant-like responses in rats, which depended on AMPA receptor (AMPA-R) activation and were associated to an increased serotonin (5-hydroxytryptamine, 5-HT) release in IL (Gasull-Camós et al., 2017a). None of these effects occurred when GLT-1 was blocked in the adjacent prelimbic cortex (PrL), indicating a key role of IL in mediating fast antidepressant-like effects, as also observed with ketamine and DBS (Fuchikami et al., 2015; Jiménez-Sánchez et al., 2015). Likewise, in common with ketamine (Amargós-Bosch et al., 2006; du Jardin et al., 2016; Pham et al., 2017), antidepressant responses evoked by GLT-1 blockade are associated to an increase in 5-HT release (Gasull-Camós et al., 2017a).

Behavioral differences evoked by GLT-1 blockade in IL and PrL likely involve the recruitment of different brain circuits, as assessed with microPET scan in rats (Gasull-Camós et al., 2017b). The mPFC and the serotonergic dorsal raphe nucleus (DR) are reciprocally connected (Azmitia and Segal, 1978; Gabbott et al., 2005; Groenewegen and Uylings, 2000; Vertes, 2004) and exert mutual control of their activity (Celada et al., 2013, 2001; Hajós et al., 1998; Puig et al., 2005). In view of this reciprocal interaction and given the relevance of the mPFC-DR pathway in mediating responses to behavioral challenges (Warden et al., 2012), here we confirm and extend our previous observations (Gasull-Camós et al., 2017a; b) to examine the potential serotonergic mechanisms involved in the antidepressant-like responses induced by GLT-1 blockade in IL.

## 2. Materials and methods

### 2.1. Subjects

Male Wistar rats (Charles River, Lyon, France) weighing between 275 and 325 g at the time of surgery were used. Rats had free access to food and water and were maintained in a controlled environment ( $22 \pm 1^\circ\text{C}$ ; 12 h light/dark, lights on at 7 a.m.). Rats were acclimatized to the housing conditions for at least 7 days and were daily handled. After surgery, all rats were singly housed and randomly assigned to treatment. Animal care followed the national (Royal Decree 53/2013) and European Union regulation (Directive 2010/63/EU, on the protection of animals used for scientific purposes, 22 September 2010), and was approved by the Institutional Animal Care and Use Committee of the University of Barcelona.

### 2.2. Drugs

Dihydrokainic acid (DHK), (S)- $\alpha$ -Amino-3-hydroxy-5-methyl-4-isoxazolepropionic acid (S-AMPA) and citalopram hydrobromide were purchased from Tocris (Bristol, UK). WAY100635 maleate was purchased from Sigma-Aldrich (Tres Cantos, Spain).

For intracerebral microinfusion, DHK (5 nmoles) and S-AMPA (50 pmoles) were dissolved in PBS 10X as previously reported (Gasull-Camós et al., 2017a; Lee et al., 2007); citalopram (15 pmoles) and WAY100635 (50 pmoles) were dissolved in artificial

cerebrospinal fluid (aCSF). The microinfusion volume was 0.5  $\mu\text{l}$  per side in all instances. For intraperitoneal (i.p.) systemic administration, WAY100635 (0.3 mg/kg) maleate was dissolved in saline and injected at 1 ml/kg.

### 2.3. Behavioral studies

#### 2.3.1. Surgery

Rats were anaesthetized with sodium pentobarbital (60 mg/kg, i.p.) and implanted with stainless steel 22-gauge bilateral guide cannulae (Plastics One, Roanoke, VA, USA) in the cingulate cortex: AP +3.2; L  $\pm$  0.75; DV -2.4 (Paxinos and Watson, 2005). The coordinates -in mm- were taken from bregma and the skull surface. Guide cannulae were fixed with stainless steel screws using dental acrylic. To prevent occlusion, a dummy cannula was inserted into the guide cannula and removed and reinserted daily. This procedure reduced stress associated with the microinfusion on the testing day (Slattery et al., 2011). Rats were allowed 7 days to recover after surgery.

#### 2.3.2. Microinfusions

Microinfusions were performed as described (Gasull-Camós et al., 2017a). The microinfusion cannulae (28 gauges) extended 3 mm beyond the guide cannulae aiming the IL cortex (DV -5.4). Prior to the tests, three mock infusions were performed. Drug or vehicle solutions were bilaterally administered over 1 min through two 50  $\mu\text{l}$  Hamilton syringes connected to the microinfusion cannulae via 0.28 mm ID polyethylene tubing, using an infusion/withdrawal pump (Harvard Apparatus, Holliston, MA, USA). Microinfusion cannulae were left in place for 3 min to allow drug diffusion. Behavioral tests were performed 10 min, 2 h or 24 h after drug local administration. In double microinfusion procedures (WAY100635/DHK or WAY100635/citalopram), the second administration was performed 5 min after the first one. For 24 h measurements, microinfusions of the drug took place 15 min after the pretest session.

#### 2.3.3. Forced swimming test (FST)

We conducted the modified FST protocol as previously described (Slattery and Cryan, 2012). Briefly, rats were individually placed into a clear methacrylate cylinder (46 cm  $\times$  20 cm) filled with water ( $24 \pm 1^\circ\text{C}$ ) to a depth of 30 cm, in a 15 min pretest session. Then, rats were dried and returned to their home cages. The swim cylinders were filled with fresh water for every single rat. No behavioral score was performed during the pretest session. 24 h later (testing day), rats were exposed to the same conditions during a 5 min test and behavior was video recorded. Subsequently, the 5 min test was divided into 5 s periods where the predominant behavior was rated as immobility, swimming or climbing by an experimenter blind to the treatment.

#### 2.3.4. Locomotor activity test

The effect of local drug administration on locomotor activity was assessed during a 15 min trial. Briefly, under the same microinfusion timings, rats were placed in the corner of a dimly lighted black open field (35 cm  $\times$  35 cm) and movement was monitored with a video camera. The distance moved (in cm) was calculated for each rat using the VideoTrack View Point software (Lyon, France).

### 2.4. Microdialysis studies

Microdialysis experiments were conducted as previously described (Jiménez-Sánchez et al., 2015). Concentric dialysis probes with 2 mm or 4 mm membrane length were implanted under sodium pentobarbital anesthesia (60 mg/kg, i.p.) in the DR (AP -7.8; L

-3.1; DV -7.5; angle 30°) or in the ventral hippocampus (vHPC; AP -5.3; L +4.8; DV -8.8), respectively. Likewise, bilateral guide cannulae were implanted in the cingulate cortex, as described above (AP +3.2; L ±0.75; DV -2.4). Coordinates were taken from bregma and the skull surface (Paxinos and Watson, 2005). Freely moving rats were continuously perfused with aCSF (125 mM NaCl, 2.5 mM KCl, 1.26 mM CaCl<sub>2</sub>, 1.18 mM MgCl<sub>2</sub>) containing 1 μM citalopram at a rate of 1.65 μl/min. A period of stabilization of 3 h was used to ensure stable 5-HT and glutamate levels. Four dialysate basal fractions were collected (25 min/each) before the microinfusion of the drug or vehicle into the IL (see microinfusions section for details). After microinfusion, six fractions (25 min/each) were collected. Neurotransmitter concentrations in the DR or vHPC samples were determined by high performance liquid chromatography with electrochemical (5-HT) or fluorimetric (glutamate) detection.

## 2.5. Immunohistochemistry

### 2.5.1. Tissue processing

Rats received a bilateral microinfusion of vehicle or DHK (5 nmoles/0.5 μl/side) into the IL 90 min before perfusion. Administration time was selected based on findings of previous studies (Fukumoto et al., 2016). Rats were anesthetized with sodium pentobarbital and transcardially perfused with ice-cold 4% paraformaldehyde in 0.1 M phosphate buffer (pH 7.4). Then, brains were removed, post-fixed during 24 h, cryoprotected in a 30% sucrose solution (in PB 0.1 M) and stored at 4 °C until they sank. Coronal frozen sections (30 μm) throughout the DR were obtained on a freezing microtome and stored in a 5% sucrose solution until used.

### 2.5.2. Immunofluorescence

The expression of c-Fos in DR 5-HT neurons was studied by triple immunofluorescence. Free-floating brain sections were washed three times with PB 0.1 M and blocked with 3% normal donkey serum, 0.3% Triton X-100 in PB (NDS-T-PB) at room temperature for 2 h. Slices were incubated in the NDS-T-PB with primary antibodies to c-Fos (rabbit, 1:500, sc-72, Santa Cruz Biotechnology), anti-neuronal nuclei (NeuN) (mouse, 1:500, MAB-377, Chemicon) and tryptophan hydroxylase 2 (TPH2) (sheep, 1:2500, AB-1541, Millipore). The next day, sections were rinsed three times in PB 0.1 M and incubated at room temperature with the secondary antibody to rabbit (Alexa 488, 1:500, Jackson ImmunoResearch, West Grove, USA), mouse (Alexa 647 IR, 1:500, Life Technologies, Carlsbad, CA, USA) or sheep (Alexa 555, 1:500, Jackson ImmunoResearch) in NDS-T-PB for 2 h. After incubation, sections were rinsed and mounted onto glass slides coated with gelatin. Mowiol was used as mounting medium.

### 2.5.3. Image processing

DR sections were assessed for the number of single NeuN-positive and TPH2-negative cells (putative GABAergic neurons), NeuN-positive and TPH2-positive cells (5-HT neurons), double-labeled cells for NeuN and c-Fos (putative GABAergic neurons expressing c-Fos) and triple-labeled cells for NeuN, TPH2 and c-Fos (5-HT neurons expressing c-Fos). Images were collected using a confocal microscope at a magnification of 40× (Leica TCS SP5, Leica Microsystems Heidelberg GmbH, Mannheim, Germany) and cells were counted using the ImageJ software (National Institutes of Health, Bethesda, MD).

## 2.6. Histological verification

At the completion of experiments, rats were killed by sodium pentobarbital overdose. Brains were rapidly removed and stored

at -80 °C. For histological verification of the cannulae and probes placement, brain sections (30 μm) were mounted onto slides and posteriorly stained with neutral red (Supplementary Fig. 1). Rats infused outside target region (IL, vHPC or DR) were excluded from all analyses.

## 2.7. Statistical analysis

Data are expressed as mean ± S.E.M. Statistical analysis was carried out using unpaired Student's t-test, one- or two-way analysis of variance (ANOVA), as appropriate, followed by Bonferroni *post hoc*. The level of significance was set at  $p < 0.05$ , in all cases.

## 3. Results

### 3.1. 5-HT<sub>1A</sub>-R in IL mediate DHK- and citalopram-induced immediate antidepressant-like responses

Post-synaptic 5-HT<sub>1A</sub>-R activation has been associated to antidepressant responses (reviewed in Celada et al., 2013). Given the expression of 5-HT<sub>1A</sub>-R in a large proportion of IL neurons (Santana et al., 2004), we examined their putative involvement in mediating antidepressant-like responses evoked by IL DHK microinfusion. In agreement with our previous observations (Gasull-Camós et al., 2017a) the bilateral microinfusion of DHK (5 nmoles/0.5 μl/side) into IL evoked an immediate (10 min) antidepressant-like response in the FST. This effect was prevented by the previous local microinfusion of WAY100635 (50 pmoles/0.5 μl/side) into the IL (Fig. 1a). One-way ANOVA showed a significant effect of the treatment on immobility ( $F_{3,33} = 4.656$ ;  $p < 0.01$ ) and swimming behaviors ( $F_{3,33} = 6.769$ ;  $p < 0.01$ ) (Fig. 1a). *Post hoc* comparisons showed that WAY100635 prevented the effect of DHK on immobility ( $p < 0.05$ ) and swimming behaviors ( $p < 0.01$ ).

Likewise, the bilateral microinfusion of citalopram (15 pmoles/0.5 μl/side) into the IL induced an antidepressant-like response, as previously reported (Gasull-Camós et al., 2017a), which was also prevented by the prior microinfusion of WAY100635 (50 pmoles/0.5 μl/side) in IL. One-way ANOVA showed a significant effect of treatment on immobility ( $F_{3,28} = 5.175$ ;  $p < 0.01$ ) and swimming ( $F_{3,28} = 6.185$ ;  $p < 0.01$ ) behavior (Fig. 1b). *Post hoc* comparisons showed that WAY100635 prevented the reduced immobility ( $p < 0.05$ ) and the increased swimming behavior ( $p < 0.05$ ) induced by citalopram.

### 3.2. DHK microinfusion in IL stimulates glutamate and 5-HT release in the DR

The extracellular concentrations of glutamate and 5-HT in the DR were used as surrogate neurochemical markers of the activity of IL-descending excitatory inputs, and of 5-HT neuron activity, respectively. The bilateral microinfusion of DHK (5 nmoles/0.5 μl/side) in IL increased glutamate and 5-HT output in the DR, as assessed by *in vivo* microdialysis. Baseline extracellular concentrations of glutamate and 5-HT in DR were  $18 \pm 3$  pmol/fraction ( $n = 15$ ) and  $27 \pm 5$  fmol/fraction ( $n = 15$ ), respectively. Two-way repeated measures ANOVA showed that DHK microinfusion in IL enhanced extracellular glutamate concentration in the DR, with a significant effect of treatment ( $F_{1,17} = 6.730$ ;  $p < 0.05$ ), fraction ( $F_{9,153} = 2.718$ ;  $p < 0.001$ ) and treatment × fraction interaction ( $F_{9,153} = 2.370$ ;  $p < 0.05$ ) (Fig. 2a). Likewise, DHK microinfusion in IL increased 5-HT concentration in the DR, with a significant effect of treatment ( $F_{1,17} = 8.871$ ;  $p < 0.01$ ), fraction ( $F_{9,153} = 8.402$ ;  $p < 0.0001$ ) and treatment × fraction interaction ( $F_{9,153} = 5.277$ ;  $p < 0.0001$ ) (Fig. 2b). Bonferroni *post hoc* analysis revealed that glutamate concentration was increased in fractions 6 and 8 ( $p < 0.05$ , DHK vs. vehicle) and 5-HT concentration remained

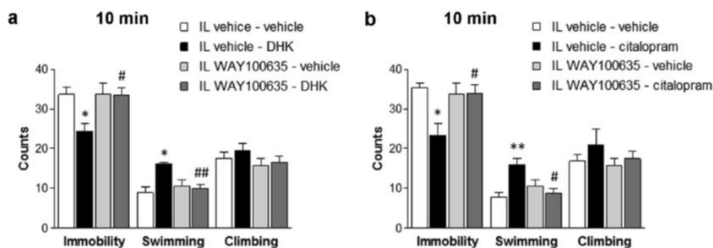


**Fig. 1.** IL 5-HT<sub>1A</sub>-R are necessary for the DHK and citalopram-induced antidepressant-like actions. (a) Effects of WAY100635 (50 pmoles/0.5  $\mu$ l/side) double microinjection into the IL cortex on the FST. The reduction in immobility and increase in swimming counts observed in vehicle/DHK group ( $n = 8$ ) compared to control (vehicle/vehicle;  $n = 9$ ) was prevented by previous local microinjection of the 5-HT<sub>1A</sub>-R antagonist WAY100635 (WAY100635/DHK;  $n = 9$ ). WAY100635/vehicle group ( $n = 8$ ) was similar to controls. (b) Effects of WAY100635 (50 pmoles/0.5  $\mu$ l/side) and citalopram (15 pmoles/0.5  $\mu$ l/side) double microinjection into IL. Reduced immobility and increased swimming counts observed in vehicle/citalopram group ( $n = 7$ ) compared to control (vehicle/vehicle;  $n = 7$ ) was also prevented by previous IL microinjection of 5-HT<sub>1A</sub> antagonist (WAY100635/citalopram;  $n = 7$ ). WAY100635/vehicle group ( $n = 8$ ) did not differ from control group. The values are expressed as mean  $\pm$  S.E.M. \* $p < 0.05$ , \*\* $p < 0.01$  vs. vehicle/vehicle; # $p < 0.05$ , ## $p < 0.01$  vs. vehicle/DHK or vehicle/citalopram (Bonferroni *post hoc* test).

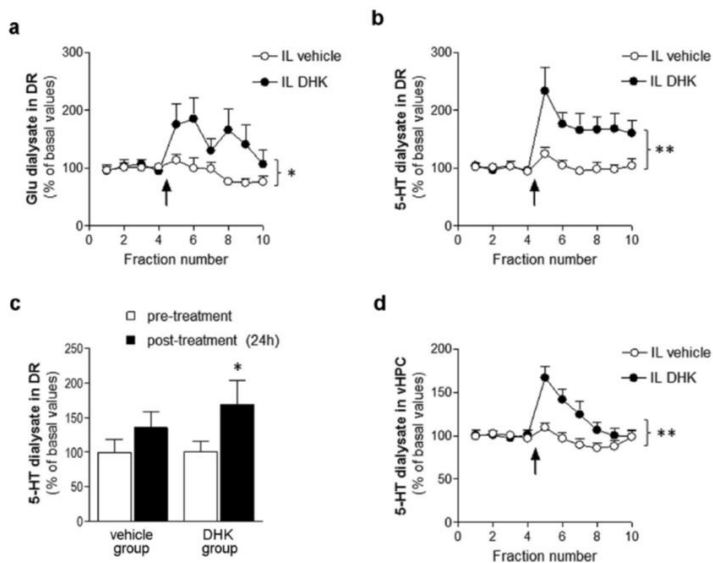


**Fig. 2.** IL blockade of GLT-1 transporter activates serotonergic neurotransmission in DR and evokes 5-HT release in vHPC. The bilateral microinjection of DHK (5 nmoles/0.5  $\mu$ l/side) into the IL cortex (a) increases glutamate (Bonferroni *post hoc* analysis revealed that glutamate concentration was increased in fractions 6 and 8;  $p < 0.05$  in both cases, DHK vs. vehicle;  $n = 10$ /group) and (b) serotonin (5-HT) release (Bonferroni *post hoc* analysis revealed that 5-HT concentration remained significantly elevated for up to 2 h after IL DHK microinjection;  $p < 0.01$  in fraction 5,  $p < 0.05$  for fractions 6 to 9; DHK vs. vehicle;  $n = 10$ /group) in the DR. (c) DR 5-HT increased extracellular concentration remains increased 24 h after IL DHK microinjection (pre-treatment vehicle,  $n = 7$ ; pre-treatment DHK,  $n = 8$ ; post-treatment vehicle,  $n = 7$ ; post-treatment DHK,  $n = 8$ ). (d) IL DHK microinjection transiently increases 5-HT release in the vHPC (Bonferroni *post hoc* analysis revealed that 5-HT was significantly increased in dialysate fractions 5 to 7 ( $p < 0.01$  in fractions 5 and 6,  $p < 0.05$  in fraction 7; DHK vs. vehicle;  $n = 9$ /group), which receives important afferents from DR. Microdialysis data are expressed as percentages of four basal values. The values are expressed as mean  $\pm$  S.E.M. \* $p < 0.05$  and \*\* $p < 0.01$  (significant main effect of treatment in the two-way ANOVA; pre-treatment vs. post-treatment Student's *t*-test). The arrow represents the start of the IL microinjection with vehicle or DHK. Dialysate fractions were 25 min each.

significantly elevated for up to 2 h after IL DHK microinjection ( $p < 0.01$  in fraction 5,  $p < 0.05$  for fractions 6 to 9; DHK vs. vehicle).

On the following day (24 h after IL DHK microinjection) the basal 5-HT concentration in the DR remained significantly elevated. Two-

way repeated measures ANOVA revealed a significant effect of time ( $F_{1,13} = 9.780$ ;  $p < 0.01$ ) and Bonferroni *post hoc* showed a significant difference between pre- and post-treatment measures in the DHK group ( $p < 0.05$ ) (Fig. 2c).

### 3.3. DHK microinfusion in IL stimulates 5-HT release in vHPC

We next examined whether DHK microinfusion in IL increased 5-HT release in the vHPC, a forebrain area involved in MDD treatment, innervated by the DR and devoid of descending inputs from mPFC. Baseline extracellular concentration of 5-HT in vHPC was  $47 \pm 4$  fmol/fraction ( $n = 18$ ). DHK (5 nmoles/0.5  $\mu$ l/side) microinfusion in IL elevated the 5-HT output in vHPC to a maximum of  $166 \pm 13\%$  of baseline, an effect that was followed by a faster decline than that observed in DR (Fig. 2d). Two-way repeated measures ANOVA revealed a significant effect of treatment ( $F_{1,16} = 8.838$ ;  $p < 0.01$ ), fraction ( $F_{9,144} = 8.047$ ;  $p < 0.0001$ ) and treatment  $\times$  fraction interaction ( $F_{9,144} = 5.145$ ;  $p < 0.0001$ ). Bonferroni *post hoc* analysis revealed that 5-HT was significantly increased in dialysate fractions 5 to 7 ( $p < 0.01$ , fractions 5 and 6;  $p < 0.05$  fraction 7) in the DHK group vs. the vehicle group.

### 3.4. DHK microinfusion in IL stimulates c-Fos expression in DR 5-HT neurons

The bilateral microinfusion of DHK (5 nmoles/0.5  $\mu$ l/side) into IL stimulated c-Fos expression specifically in DR 5-HT neurons. Unpaired *t*-test showed that NeuN-positive/TPH2-positive cells (serotonergic) presented a significant increase in c-Fos immunoreactivity in DHK-treated rats compared to vehicle ( $t_{(11)} = 2.927$ ,  $p < 0.05$ ), while NeuN-positive/TPH2-negative cells –mostly GABAergic neurons (Day et al., 2004)– presented similar expression of c-Fos in the two treatment groups ( $t_{(11)} = 0.773$ ; n.s.) (Fig. 3). The total number of 5-HT and putative GABAergic cells were similar in the DR sections studied (5-HT:  $346.15 \pm 33.08$ , putative GABA:  $317.69 \pm 18.33$ ;  $t_{(24)} = 0.752$ ; n.s.). As expected, the number of 5-HT (vehicle:  $382.83 \pm 47.79$ , DHK:  $314.71 \pm 45.55$ ;  $t_{(11)} = 0.325$ ; n.s.) and putative GABAergic cells (vehicle:  $341.83 \pm 33.98$ , DHK:  $297.00 \pm 16.39$ ;  $t_{(11)} = 0.238$ ; n.s.) did not differ between groups.

### 3.5. IL DHK evoked antidepressant responses are crucially modulated by 5-HT<sub>1A</sub> autoreceptors

The antidepressant-like response evoked by DHK microinfusion into the IL (5 nmoles/0.5  $\mu$ l/side) was still present 2 h after drug microinfusion (Fig. 4a), with a significant decrease in immobility ( $t_{(14)} = 3.630$ ;  $p < 0.001$ ) and increase in swimming behaviors ( $t_{(14)} = 3.011$ ;  $p < 0.001$ ; unpaired *t*-test). These changes were not associated to changes in locomotor activity as assessed by the distance traveled (cm) in an open field (mean  $\pm$  S.E.M in vehicle:  $1831 \pm 172$ , DHK:  $1979 \pm 266$ ;  $t_{(10)} = 0.4671$ , n.s.;  $n = 6$  rats/group). However, DHK microinfusion in IL did not evoke any antidepressant-like response in the FST 24 h after drug application (Fig. 4b).

The lack of an antidepressant-like response 24 h after DHK microinfusion was somehow discordant with the elevated serotonergic activity at this time, as suggested by the increase in DR 5-HT output (Fig. 2c). Given the crucial role of somatodendritic 5-HT<sub>1A</sub> autoreceptors in controlling ascending serotonergic activity and in presenting antidepressant-like responses (Artigas, 2013), we then examined whether 5-HT<sub>1A</sub> autoreceptor blockade could disinhibit serotonergic activity and bring about an antidepressant-like response at 24 h.

Thus, the systemic administration of WAY100635 (0.3 mg/kg, i.p.) 40 min before FST reduced the immobility time in rats microinfused with DHK in IL 24 h before (15 min after the pretest session), but not in control rats microinfused with vehicle. One-way ANOVA showed a significant effect of treatment on immobility ( $F_{(3,27)} = 3.419$ ;  $p < 0.05$ ) and swimming behaviors ( $F_{(3,27)} = 3.680$ ;  $p < 0.05$ ) (Fig. 4c). Bonferroni *post hoc* comparisons indicated a

significant decrease in immobility and increase in swimming behavior ( $p < 0.05$ , in both cases) in the DHK/WAY100635 group compared to vehicle/saline. WAY100635 alone was ineffective in rats treated with vehicle on the preceding day.

The antidepressant-like behavior seen in the FST was not associated to changes in locomotor activity, as assessed by the similar distance travelled (cm) in the open field by both experimental groups (mean  $\pm$  S.E.M in DHK/WAY100635:  $6300 \pm 408$ , vehicle/WAY100635:  $7302 \pm 303$ ;  $t_{(10)} = 1.973$ , n.s.;  $n = 6$  rats/group).

### 3.6. S-AMPA microinfusion in IL produces a different temporal response pattern

We previously showed that the fast (10 min) antidepressant-like effects of GLT-1 blockade in IL were prevented by AMPA-R blockade and mimicked by S-AMPA microinfusion (Gasull-Camós et al., 2017a). We therefore examined the effect of the bilateral microinfusion of S-AMPA (50 pmoles/0.5  $\mu$ l/side) into IL on glutamate and 5-HT output in the DR. Baseline extracellular glutamate and 5-HT concentrations in DR were  $15 \pm 1$  pmol/fraction ( $n = 16$ ) and  $64 \pm 13$  fmol/fraction ( $n = 17$ ), respectively. Two-way repeated measures ANOVA showed that IL S-AMPA microinfusion significantly heightened DR extracellular glutamate concentration, with a significant effect of treatment ( $F_{1,18} = 7.055$ ;  $p < 0.05$ ), fraction ( $F_{9,162} = 4.485$ ;  $p < 0.0001$ ) and treatment  $\times$  fraction interaction ( $F_{9,162} = 4.588$ ;  $p < 0.0001$ ) (Fig. 5a). Subsequent *post hoc* comparisons showed that glutamate was significantly enhanced during the first and second fractions collected after S-AMPA microinfusion (fraction 5,  $p < 0.05$ ; and fraction 6,  $p < 0.01$ ). IL S-AMPA increased DR 5-HT concentration, as shown by significant effect of treatment ( $F_{1,18} = 6.428$ ;  $p < 0.05$ ), fraction ( $F_{9,162} = 3.480$ ;  $p < 0.001$ ) and treatment  $\times$  fraction interaction ( $F_{9,162} = 3.288$ ;  $p < 0.001$ ) (Fig. 5b), and *post hoc* comparisons showed that 5-HT was significantly elevated only during the second fraction collected after S-AMPA microinfusion (fraction 6;  $p < 0.01$ ).

S-AMPA did not evoke any antidepressant-like response 2 h after drug microinfusion in IL (Fig. 5c). Unpaired *t*-test showed no significant difference in immobility ( $t_{(16)} = 0.954$ ; n.s.), swimming ( $t_{(16)} = 0.352$ ; n.s.) nor climbing behaviors ( $t_{(16)} = 1.070$ ; n.s.).

## 4. Discussion

The present study shows that antidepressant-like responses evoked by the enhancement of glutamatergic neurotransmission in IL are associated to an activation of descending excitatory pathways to the DR and the subsequent enhancement of serotonergic neurotransmission. Thus, a single bilateral microinfusion of DHK into IL activates DR 5-HT neurons, as observed by an increased 5-HT release in DR, with a time course parallel to that of antidepressant-like responses; and by an increased c-Fos expression in DR 5-HT neurons, but not in putative GABAergic neurons. Moreover pre- and post-synaptic 5-HT<sub>1A</sub>-R appear to play opposite roles in modulating these antidepressant-like responses, as post-synaptic 5-HT<sub>1A</sub>-R in IL are required for the immediate (10 min) antidepressant-like responses, while pre-synaptic 5-HT<sub>1A</sub>-R prevent a larger duration of the antidepressant response (24 h), possibly due to self-inhibitory actions on 5-HT neurons.

### 4.1. Post-synaptic 5-HT<sub>1A</sub>-R located in IL are necessary for the immediate antidepressant-like responses of DHK and citalopram

We previously reported that the enhancement of glutamatergic neurotransmission in IL following GLT-1 blockade with DHK evoked antidepressant-like responses 10 min after drug

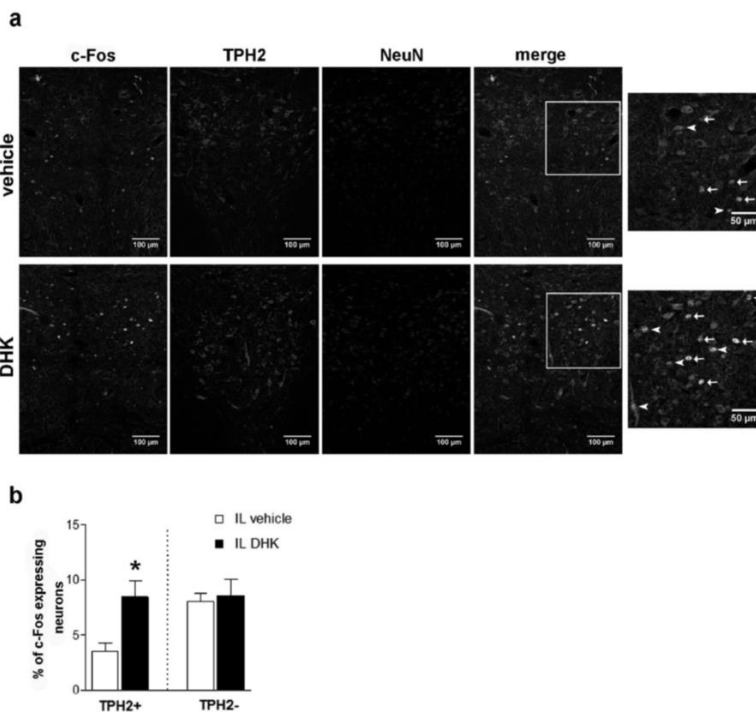


**Fig. 3.** IL blockade of GLT-1 increases c-Fos expression specifically in DR serotonergic neurons. (a) Confocal images of c-Fos expressing cells (green), 5-HT neurons (NeuN-positive/TPH2-positive cells; red) and putative GABA interneurons (NeuN-positive/TPH2-negative cells; blue) in vehicle- and DHK-treated rats. Arrowheads show 5-HT neurons expressing c-Fos (triple c-Fos, NeuN and TPH2 positive), tailed arrows show putative GABAergic neurons expressing c-Fos (double c-Fos and NeuN positive). (b) Percentages of colocalization 90 min after IL microinfusion of vehicle ( $n = 6$ ) or DHK (5 nmol/0.5  $\mu$ l/site;  $n = 7$ ) in 5-HT or GABA neurons. No differences in the number of 5-HT or GABA neurons in the DR were observed between groups. Values indicate the mean  $\pm$  S.E.M. \* $p < 0.05$  vs. vehicle (Student's *t*-test). (For interpretation of the references to colour in this figure legend, the reader is referred to the Web version of this article.)

microinfusion, which were associated to an enhancement of 5-HT release in IL and were prevented by prior 5-HT depletion with pCPA (Gasull-Camós et al., 2017a). Given the role of post-synaptic 5-HT<sub>1A</sub>-R in mediating antidepressant responses (Celada et al., 2013), we first investigated whether they were involved in this immediate antidepressant response. The mPFC is enriched in 5-HT<sub>1A</sub>-R and 5-HT<sub>2A</sub>-R (Pompeiano et al., 1994, 1992), with varying proportions of neurons expressing both receptors in PrL and IL. The former subdivision contains a roughly similar proportion of pyramidal neurons expressing the mRNAs encoding inhibitory 5-HT<sub>1A</sub>-R and excitatory 5-HT<sub>2A</sub>-R ( $61 \pm 2$  vs.  $51 \pm 3\%$ , respectively) (Santana et al., 2004). In contrast, the IL subdivision contains a significantly greater proportion of pyramidal neurons expressing 5-HT<sub>1A</sub>-R vs 5-HT<sub>2A</sub>-R mRNAs ( $40 \pm 4$  vs.  $12 \pm 1\%$ , respectively). The proportion of GABA interneurons expressing one or other receptor in both subdivisions varies in a non-significant manner, between  $20 \pm 1$  and  $32 \pm 1\%$ . This suggests that the antidepressant-like effects resulting from an enhanced serotonergic neurotransmission in IL would be most likely mediated by the activation of post-synaptic 5-HT<sub>1A</sub>-R. In agreement, here we

show that the local application of the selective 5-HT<sub>1A</sub>-R antagonist WAY100635 in IL prevented the antidepressant-like responses induced by DHK and citalopram. Remarkably, the similarity of the antidepressant-like effect of local (in IL) and systemic citalopram administrations supports a key role of IL in SSRI-induced antidepressant-like responses.

Since the activation of 5-HT<sub>1A</sub>-R inhibits the activity of mPFC pyramidal neurons (Amargós-Bosch et al., 2004; Puig et al., 2003), the present results seem in apparent controversy with the previously reported role of IL AMPA-R in DHK-evoked antidepressant-like responses (Gasull-Camós et al., 2017a) and the increased metabolic activity in IL after DHK microinfusion (Gasull-Camós et al., 2017b). One possible explanation is that 5-HT<sub>1A</sub>-R mediating immediate antidepressant-like responses may be expressed by pyramidal neuron populations different from those projecting to the DR. In this regard, the IL subdivision contains a large number of pyramidal neurons projecting to subcortical structures involved in MDD, such as the amygdala, the lateral hypothalamus, the septum or the periaqueductal gray matter (Gabbott et al., 2005). Hence, activation of AMPA-R in midbrain-projecting pyramidal neurons

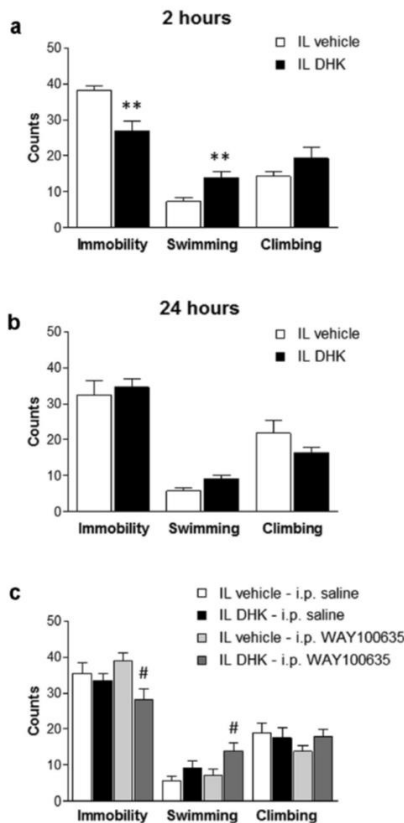


**Fig. 4.** IL blockade of GLT-1 evokes fast antidepressant-like responses that can be prolonged by blockade of pre-synaptic 5-HT<sub>1A</sub>-R. (a) DHK (5 nmol/0.5 µl/side) produced antidepressant-like responses 2 h after IL bilateral microinfusion, as shown by reduced immobility and increased swimming counts (vehicle; DHK,  $n = 8$ ). (b) 24 h after IL DHK microinfusion there was no behavioral response on the FST (vehicle; DHK,  $n = 7$ ). (c) Systemic administration of WAY100635 (0.3 mg/kg, i.p.) 40 min before the FST in combination with IL DHK microinfusion on the previous day evoked antidepressant-like responses (vehicle/saline,  $n = 6$ ; DHK/saline,  $n = 6$ ; vehicle/WAY100635,  $n = 9$ ; DHK/WAY100635,  $n = 7$ ). Values are expressed as mean  $\pm$  S.E.M. \*\* $p < 0.01$  compared to vehicle (Student's  $t$ -test); # $p < 0.05$  compared to vehicle/WAY100635 (Bonferroni *post hoc* test).

would enhance the activity of ascending 5-HT neurons, leading to an increased 5-HT release in IL which would then inhibit pyramidal neurons projecting to MDD-related areas, thus evoking an antidepressant-like phenotype. An alternative –yet less likely– explanation relies on the presence of 5-HT<sub>1A</sub>-R in GABAergic interneurons. The exogenous administration of selective 5-HT<sub>1A</sub>-R agonists increases pyramidal neuron activity and c-fos expression in PFC (Hajós et al., 1998; Llado-Pelfort et al., 2010). This effect is mediated by the preferential activation of 5-HT<sub>1A</sub>-R in fast-spiking

GABAergic interneurons, resulting in the disinhibition and subsequent excitation of pyramidal neurons (Llado-Pelfort et al., 2012). The reasons for the preferential action on fast-spiking GABA interneurons remain unknown.

#### 4.2. DHK microinfusion in IL stimulates the IL-DR pathway

Given that the increased 5-HT in the IL was apparently due to enhanced activity of the mPFC–DR pathway (Gasull-Camós et al., 2017b), we then studied the consequences of IL GLT-1 blockade on DR neurochemistry. *In vivo* microdialysis studies revealed that IL DHK microinfusion increased glutamate and 5-HT release in the DR. The increased glutamate release in DR likely results from the increased activity of pyramidal axons reaching the DR. Similarly, IL DBS also increases glutamate release in DR (Jiménez-Sánchez et al., 2015). Moreover, optogenetic activation of the mPFC–raphe evokes fast antidepressant-like responses, which depend on the glutamatergic synaptic input onto the DR, as microinfusion of the AMPA-R antagonist NBQX into the DR blocks the stimulation driven antidepressant-like response (Warden et al., 2012).

Glutamate release by pyramidal axons in the DR can activate or inhibit 5-HT neurons, depending on the final cellular target in the midbrain. Hence, mPFC-driven excitations of 5-HT neurons are monosynaptic and involve the activation of local AMPA-R and NMDA-R, whereas inhibitions are driven by (i) local negative feedback through 5-HT<sub>1A</sub> autoreceptors and/or (ii) activation of local GABA interneurons and the subsequent inhibition of 5-HT neurons (Celada et al., 2001; Varga et al., 2001). Our results show a simultaneous increase of glutamate and 5-HT release in the DR and a significant increase of c-Fos expression specifically in DR 5-HT neurons, but not in putative GABAergic neurons (TPH2- neurons) after IL DHK microinfusion. This suggests that –despite the simultaneous innervation of 5-HT and GABA neurons– activation of IL descending pathways by DHK enhances direct glutamatergic inputs onto 5-HT neurons more markedly than those on GABA neurons. Moreover, our results indicate a predominant activation of DR GABAergic neurons under basal conditions, as c-Fos expression was greater in TPH2- than in TPH2+ neurons in control rats. In agreement, others have reported that both systemic and intramPFC ketamine administration increase c-Fos expression in DR 5-HT neurons (Fukumoto et al., 2016), yet they did not examine the effect on TPH2- neurons.

The activation of DR 5-HT neurons induced by DHK microinfusion in IL is also supported by increased 5-HT release in IL (Gasull-Camós et al., 2017a) and in vHPC (present study). The latter effect cannot be mediated by a direct descending mPFC–vHPC pathway, since the PFC does not project to the hippocampal formation in rats (Gabbott et al., 2005). More convincingly, and given the increased c-Fos expression in DR after DHK microinfusion in IL, this effect possibly results from the excitation of raphe 5-HT neurons, leading to an increased 5-HT release in vHPC, an area innervated by both DR and median raphe nuclei (McQuade and Sharp, 1997). In line with the present results, DBS of the mPFC also increased 5-HT release in the HPC (Hamani et al., 2010) and hippocampal plasticity related to DBS depends on 5-HT release into the HPC (Etiévant et al., 2015).

It is important to note that 5-HT release in DR remained stable for 2 h and slightly elevated until 24 h later, suggesting that plastic changes may occur in the DR after the stimulation of descending IL afferents. In line with the former observation, a 20 min electrical stimulation of mPFC neurons at moderate –yet physiological– frequencies, such as 20 Hz, increased 5-HT release in the DR for at least 1 h after the cessation of the stimulation (Celada et al., 2001). Moreover, it has also been reported that DBS of the vmPFC induces neuroplastic changes in DR 5-HT neurons, associated to increased

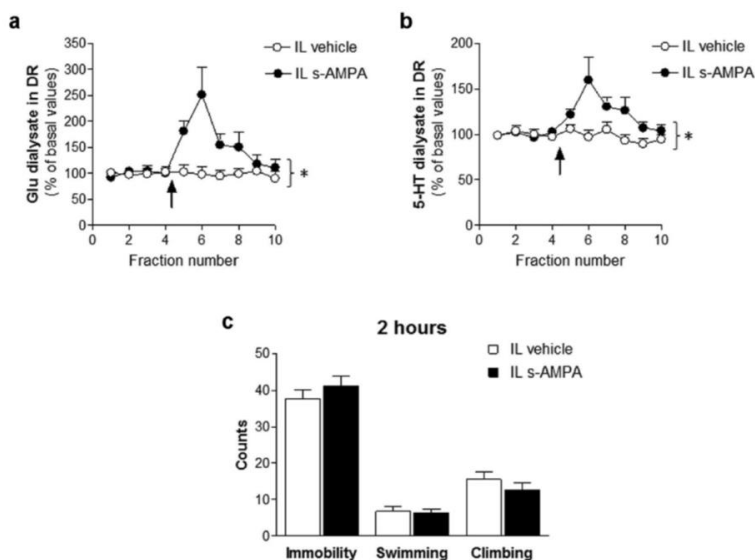


**Fig. 5.** Direct activation of AMPA-R in IL cortex evokes a transient increase in DR 5-HT and glutamate release and does not maintain its antidepressant effect 2 h after microinfusion. The bilateral microinfusion of S-AMPA (50 pmol/0.5  $\mu$ l/site) into the IL cortex transiently increases (a) glutamate (*Post hoc* comparisons showed that glutamate was significantly enhanced during the first and second fractions collected after S-AMPA microinfusion;  $p < 0.05$  in fraction 5; and  $p < 0.01$  in fraction 6; S-AMPA vs. vehicle,  $n = 10$ /group) and (b) serotonin (5-HT) release (*Post hoc* comparisons showed that 5-HT was significantly enhanced only during the second fraction collected after S-AMPA microinfusion;  $p < 0.01$  in fraction 6; S-AMPA vs. vehicle;  $n = 10$ /group) in the DR. (c) IL S-AMPA produced no behavioral response on the FST 2 h after drug microinfusion (vehicle; S-AMPA,  $n = 9$ /group). The values are expressed as mean  $\pm$  S.E.M. \* $p < 0.05$  (significant main effect of treatment in the two-way ANOVA). The arrow represents the start of the IL microinfusion with vehicle or S-AMPA. Dialysate fractions were 25 min each.

5-HT excitability and antidepressant-like responses (Etiévant et al., 2015; Veerakumar et al., 2014).

#### 4.3. Sustained antidepressant-like responses after IL stimulation

We then studied the time course of the IL DHK-evoked antidepressant-like responses by testing the effects of IL DHK in the FST at 2 h and 24 h after drug microinfusion. The antidepressant-like responses found at 2 h after IL DHK are consistent with the DR 5-HT elevation observed. However, behavioral responses disappeared 24 h after IL DHK microinfusion despite the presence of a moderate (yet statistically significant) elevation in DR 5-HT release. In an attempt to potentiate subthreshold responses, we systemically administered the 5-HT<sub>1A</sub>-R antagonist WAY100635, under the hypothesis that this receptor was inducing a 5-HT-mediated negative feedback on 5-HT neurons, and consequently preventing the emergence of the antidepressant response. WAY100635 on its own did not affect behavior, probably due to the lack of a tonic activation of 5-HT<sub>1A</sub> autoreceptors in control rats. However, systemic administration of WAY100635 allowed the appearance of an antidepressant effect 24 h after IL DHK microinfusion. This suggests that 24 h after IL DHK a moderate enhancement of serotonergic neurotransmission is still present, yet attenuated by self-inhibition through 5-HT<sub>1A</sub> autoreceptors activation. Unlike the blockade of post-synaptic 5-HT<sub>1A</sub>-R in IL by a higher local dose (see above), the systemic dose of WAY100635

used did not prevent the antidepressant-like effects of boosting serotonergic activity via 5-HT<sub>1A</sub> autoreceptor blockade, suggesting a different contribution of pre- and post-synaptic 5-HT<sub>1A</sub>-R in both experimental situations. These results are consistent with the key role of pre-synaptic 5-HT<sub>1A</sub>-R in the control of serotonergic activity and in antidepressant responses (Albert and Le François, 2010; Artigas et al., 2001, 1996; Blier and de Montigny, 1994). However, a limitation of the present experiments lies in the systemic administration of WAY100635. Hence, unlike local (IL) WAY100635 administration, which enabled to clearly identify the population of post-synaptic receptors involved in antidepressant-like effects of DHK and citalopram, the present experiments cannot discard the involvement of 5-HT<sub>1A</sub>-R receptor populations other than somatodendritic autoreceptors. Fig. 6 shows a scheme of DHK effects on the IL-DR pathway at the different times examined.

Finally DHK and S-AMPA microinfusion in IL evoked similar antidepressant-like effects in the FST at 10 min post-administration (Gasull-Camós et al., 2017a), thus adding further evidence to the role of AMPA-R activation in fast-acting antidepressant responses (Jiménez-Sánchez et al., 2015; Maeng et al., 2008). However, unlike DHK, S-AMPA did not evoke a behavioral response nor enhanced glutamate and 5-HT release in the DR 2 h after administration, suggesting that other ionotropic or metabotropic glutamate receptors may contribute to sustained DHK-induced antidepressant-like effects.



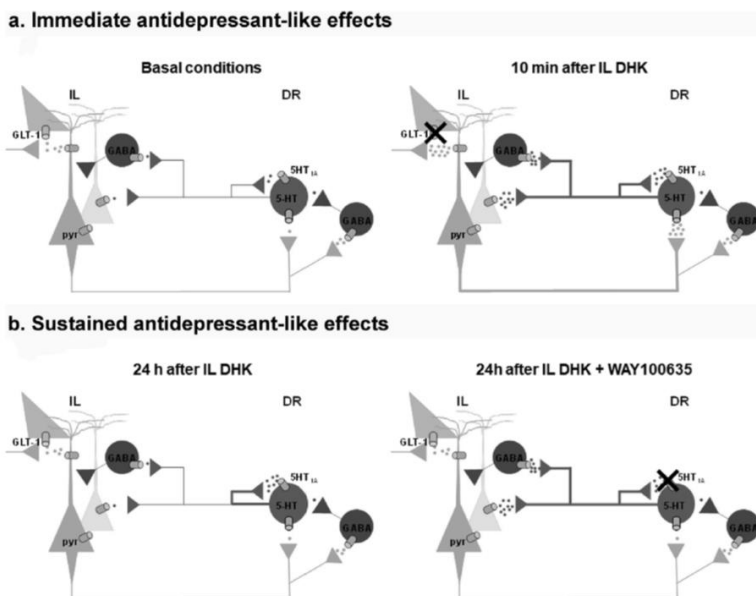


**Fig. 6.** Schematic diagram of serotonergic mechanism involved in the antidepressant-like responses evoked by IL DHK application. (a) Immediate antidepressant-like effects. Blockade of the glial GLT-1 transporter in the infralimbic cortex (IL) evokes an immediate local increase in glutamate, which then activates pyramidal neurons projecting –among other areas– to midbrain, thus increasing extracellular glutamate and 5-HT concentrations in the DR. The increased activity of serotonergic neurons is then translated into an increased 5-HT release in forebrain, including the IL and vHPC (not shown here, see Fig. 2). The activation of 5-HT neurons bypasses self-inhibitory actions of 5-HT<sub>1A</sub> autoreceptors, this allowing the appearance of the antidepressant response. Thick lines indicate enhanced activity of glutamatergic or serotonergic axons. (b) Sustained antidepressant-like effects. 24 h after IL DHK microinfusion, 5-HT remains elevated in the DR. In this condition, 5-HT may activate 5-HT<sub>1A</sub> pre-synaptic receptors and attenuates forebrain 5-HT release. Removal of the self-inhibitory action through the administration of the 5-HT<sub>1A</sub>-R antagonist WAY100635 allows the activation of the ascending 5-HT pathways and the emergence of the antidepressant-like response.

## 5. Conclusions

In summary, the present study shows that antidepressant-like responses induced by enhancing glutamatergic neurotransmission in IL are mediated essentially by serotonergic mechanisms (Fig. 6). The blockade of the glial glutamate transporter GLT-1 with DHK evoked antidepressant-like responses at 10 min and 2 h post-administration, which were paralleled by an increased 5-HT release in the IL-DR pathway. Moreover, post-synaptic 5-HT<sub>1A</sub>-R in IL appear to be relevant for the immediate antidepressant-like effects. The antidepressant-like responses could also be evoked 24 h post-administration by removing pre-synaptic 5-HT<sub>1A</sub> autoreceptors-mediated self-inhibition of serotonergic activity. The temporal differences between the effects of DHK and 5-AMPA suggest the involvement of glutamatergic receptors other than AMPA-R in the persistence of antidepressant-like responses. Overall, the present results indicate that boosting serotonergic neurotransmission by enhancing glutamatergic inputs onto 5-HT neurons may be a more efficient way than blocking SERT, a process triggering a series of pre- and post-synaptic negative feed-back mechanisms (Artigas et al., 1996, 2001; Riga et al., 2016). This view is also supported by the efficacy of a single DHK administration in IL to reduce the latency to feed in the novelty-suppressed feeding test, which is typically

sensitive to chronic –but not acute– SSRI treatment. In addition, the present study contributes to a better understanding of neural mechanisms involved in fast-acting antidepressant responses and may help to identify new antidepressant targets.

## Conflict of interests or disclosure

FA has received consulting honoraria from Lundbeck A/S and has been PI of a grant from Lundbeck A/S. He is also a member of the scientific advisory board of Neurolix and a co-inventor of two patents on conjugated oligonucleotide sequences. The remaining authors declare no conflict of interest.

## Acknowledgments

We thank Leticia Campa and Lluís Miquel Rio for their technical support on high performance liquid chromatography and microdialysis experiments.

This work was supported by the Spanish Ministry of Economy and Competitiveness (SAF2015-68346 and BES2013-063241 to J.G.-C; BFU2015-68568-P to A.O.) co-financed by European Regional Development Fund; Generalitat de Catalunya (CERCA Programme; 2014-SGR798, 2016FI-B00285 to M.T.-G, 2016 FI-B00531 to S.M.-T

and ICREA Acadèmia to A.O.); Instituto de Salud Carlos III, Centro de Investigación Biomédica en Red de Salud Mental (CIBERSAM).

#### Appendix A. Supplementary data

Supplementary data related to this article can be found at <https://doi.org/10.1016/j.neuropharm.2018.06.029>.

#### References

- Albert, P.R., Le François, B., 2010. Modifying 5-HT1A receptor gene expression as a new target for antidepressant therapy. *Front. Neurosci.* 4, 1–7. <https://doi.org/10.3389/fnins.2010.00035>.
- Amargós-Bosch, M., Bortolozzi, A., Puig, M.V., Serrats, J., Adell, A., Celada, P., Toth, M., Mengod, G., Artigas, F., 2004. Co-expression and in vivo interaction of Serotonin1A and Serotonin2A receptors in pyramidal neurons of pre-frontal cortex. *Cereb. Cortex* 14, 281–299. <https://doi.org/10.1093/cercor/bbh128>.
- Amargós-Bosch, M., López-Gil, X., Artigas, F., Adell, A., 2006. Clozapine and olanzapine, but not haloperidol, suppress serotonin efflux in the medial prefrontal cortex elicited by phencyclidine and ketamine. *Int. J. Neuropsychopharmacol.* 9, 565–573. <https://doi.org/10.1017/S1461145705005900>.
- Artigas, F., 2013. Future directions for serotonin and antidepressants. *ACS Chem Neurosci.* 4, 5–8.
- Artigas, F., Celada, P., Laruette, M., Adell, A., 2001. How does pindolol improve antidepressant action? *Trends Pharmacol. Sci.* 22, 224–228. [https://doi.org/10.1016/S0165-6147\(00\)01682-5](https://doi.org/10.1016/S0165-6147(00)01682-5).
- Artigas, F., Romero, L., De Montigny, C., Blier, P., 1996. Acceleration of the effect of selected antidepressants drugs in major depression by 5-HT<sub>1A</sub> antagonists. *Trends Neurosci.* 19, 378–383. [https://doi.org/10.1016/S0166-2236\(96\)10037-0](https://doi.org/10.1016/S0166-2236(96)10037-0).
- Azmitia, E.C., Segal, M., 1978. An autoradiographic analysis of the differential ascending projections of the dorsal and median raphe nuclei in the rat. *J. Comp. Neurol.* 179, 641–667. <https://doi.org/10.1002/cne.91790311>.
- Blier, P., de Montigny, C., 1994. Current advances and trends in the treatment of depression. *Trends Pharmacol. Sci.* 15, 220–226. [https://doi.org/10.1016/0165-6147\(94\)90315-8](https://doi.org/10.1016/0165-6147(94)90315-8).
- Celada, P., Puig, M.V., Artigas, F., 2013. Serotonin modulation of cortical neurons and networks. *Front. Integr. Neurosci.* 7 (25). <https://doi.org/10.3389/fnint.2013.00025>.
- Celada, P., Puig, M.V., Casanovas, J.M., Guillozo, G., Artigas, F., 2001. Control of dorsal raphe serotonergic neurons by the medial prefrontal cortex: involvement of Serotonin-1A, GABA<sub>A</sub>, and glutamate receptors. *J. Neurosci.* 21, 9917–9929.
- Choudary, P.V., Molnar, M., Evans, S.J., Tomita, H., Li, J.Z., Vawter, M.P., Myers, R.M., Bunney, W.E., Akil, H., Watson, S.J., Jones, E.G., 2005. Altered cortical glutamatergic and GABAergic signal transmission with glial involvement in depression. *Proc. Natl. Acad. Sci. U. S. A.* 102, 15653–15658. <https://doi.org/10.1073/pnas.0507901102>.
- Danbolt, N.C., Storm-Mathisen, J., Kanner, B.J., 1992. An [Na<sup>+</sup> + K<sup>+</sup>]-coupled L-glutamate transporter purified from rat brain is located in glial cell processes. *Neuroscience* 51, 295–310. [https://doi.org/10.1016/0304-5222\(92\)90316-7](https://doi.org/10.1016/0304-5222(92)90316-7).
- Day, H.E.W., Greenwood, B.N., Hammack, S.E., Watkins, L.R., Flesher, M., Maier, S.F., Campeau, S., 2004. Differential expression of 5HT-1A, alpha 1b adrenergic, CRF-1, and CRF-2 receptor mRNA in serotonergic, gamma-aminobutyric acidergic, and catecholaminergic cells of the rat dorsal raphe nucleus. *J. Comp. Neurol.* 474, 364–378. <https://doi.org/10.1002/cne.20138>.
- du Jardin, K.G., Liebenberg, N., Müller, H.K., Elfving, B., Sanchez, C., Wegener, G., 2016. Differential interaction with the serotonin system by 5-ketamine, vortioxetine, and fluoxetine in a genetic rat model of depression. *Psychopharmacology (Berl)* 233, 2813–2825. <https://doi.org/10.1007/s00213-016-4327-5>.
- Étiévant, A., Oosterhof, C., Bétry, C., Abrial, E., Novo-Perez, M., Rovera, R., Scama, H., Devader, C., Mazella, J., Wegener, G., Sánchez, C., Dkhissi-Benyahya, O., Gronfier, C., Cozic, V., Beaulieu, J.M., Blier, P., Lucas, G., Haddjeri, N., 2015. Astroglial control of the antidepressant-like effects of prefrontal cortex deep brain stimulation. *EBioMedicine* 2, 898–908. <https://doi.org/10.1016/j.ebiom.2015.06.023>.
- Fuchikami, M., Thomas, A., Liu, R., Wohltet, E.S., Land, B.R., DiLeone, R.J., Aghajanian, G.K., Duman, R.S., 2015. Optogenetic stimulation of infralimbic PFC reproduces ketamine's rapid and sustained antidepressant actions. *Proc. Natl. Acad. Sci. U. S. A.* 112, 8106–8111. <https://doi.org/10.1073/pnas.1414728112>.
- Fukumoto, K., Iijima, M., Chaki, S., 2016. The antidepressant effects of an mGlu2/3 receptor antagonist and ketamine require AMPA receptor stimulation in the mPFC and subsequent activation of the 5-HT neurons in the DRN. *Neuropsychopharmacology* 41, 1046–1056. <https://doi.org/10.1038/npp.2015.233>.
- Gabbott, P.L.A., Warner, T.A., Jays, P.R.L., Salway, P., Busby, S.J., 2005. Prefrontal cortex in the rat: projections to subcortical autonomic, motor, and limbic centers. *J. Comp. Neurol.* 492, 145–177. <https://doi.org/10.1002/cne.20738>.
- Gasull-Camós, J., Soto-Montenegro, M., Casquero-Veiga, M., Descò, M., Artigas, F., Castañé, A., 2017a. Differential patterns of subcortical activity evoked by glial GLT-1 blockade in prelimbic and infralimbic cortex: relationship to antidepressant-like effects in rats. *Int. J. Neuropsychopharmacol.* 20, 988–993. <https://doi.org/10.1093/ijnp/nyy087>.
- Gasull-Camós, J., Tarrés-Gatusas, M., Artigas, F., Castañé, A., 2017b. Glial GLT-1 blockade in infralimbic cortex as a new strategy to evoke rapid antidepressant-like effects in rats. *Transl. Psychiatry* 7 e1038. <https://doi.org/10.1038/tp.2017.7>.
- Global Burden of Disease Study 2013 Collaborators, 2015. Global, regional, and national incidence, prevalence, and years lived with disability for 301 acute and chronic diseases and injuries in 188 countries, 1990–2013: a systematic analysis for the Global Burden of Disease Study 2013. *Lancet* 386, 743–800. [https://doi.org/10.1016/S0140-6736\(15\)90692-4](https://doi.org/10.1016/S0140-6736(15)90692-4).
- Groenewegen, H.J., Uylings, H.B.M., 2000. The prefrontal cortex and the integration of sensory, limbic and autonomic information. *Prog. Brain Res.* 3, 2–38. [https://doi.org/10.1016/S0079-6123\(00\)26003-2](https://doi.org/10.1016/S0079-6123(00)26003-2).
- Hajós, M., Richards, C.D., Székely, A.D., Sharp, T., 1998. An electrophysiological and neuroanatomical study of the medial prefrontal cortical projection to the midbrain raphe nuclei in the rat. *Neuroscience* 87, 95–108. [https://doi.org/10.1016/S0304-5222\(98\)00157-2](https://doi.org/10.1016/S0304-5222(98)00157-2).
- Halassa, M.M., Haydon, P.G., 2010. Integrated brain circuits: astrocytic networks modulate neuronal activity and behavior. *Annu. Rev. Physiol.* 72, 335–355. <https://doi.org/10.1146/annurev-physiol-021909-135843>.
- Hamami, C., Diwan, M., Macedo, C.E., Brandão, M.L., Shumake, J., Gonzalez-Lima, F., Raymond, R., Lozano, A.M., Fletcher, P.J., Nobrega, J.N., 2010. Antidepressant-like effects of medial prefrontal cortex deep brain stimulation in rats. *Biol. Psychiatry* 67, 117–124. <https://doi.org/10.1016/j.biopsych.2008.08.025>.
- Jiménez-Sánchez, L., Castañé, A., Pérez-Caballero, L., Grifoll-Escoda, M., López-Gil, X., Campa, L., Galofré, M., Berrocoso, E., Adell, A., 2015. Activation of AMPA receptors mediates the antidepressant action of deep brain stimulation of the infralimbic prefrontal cortex. *Cereb. Cortex* 26, 2778–2789. <https://doi.org/10.1093/cercor/bhv133>.
- Lee, Y., Gaskins, D., Anand, A., Shekhar, A., 2007. Glia mechanisms in mood regulation: a novel model of mood disorders. *Psychopharmacology (Berl)* 191, 55–66. <https://doi.org/10.1007/s00213-006-0852-4>.
- Lladó-Pelfort, L., Assié, M.B., Newman-Tancredi, A., Artigas, F., Celada, P., 2010. Preferential in vivo action of F15599, a novel 5-HT<sub>1A</sub> receptor agonist, at postsynaptic 5-HT<sub>1A</sub> receptors. *Br. J. Pharmacol.* 160, 1929–1940. <https://doi.org/10.1111/j.1476-5381.2010.00738.x>.
- Lladó-Pelfort, L., Santana, N., Ghisi, V., Artigas, F., Celada, P., 2012. 5-HT<sub>1A</sub> Receptor agonists enhance pyramidal cell firing in prefrontal cortex through a preferential action on GABA interneurons. *Cereb. Cortex* 22, 1487–1497. <https://doi.org/10.1093/cercor/bhr230>.
- Maeng, S., Zarate, C., Du, J., Schloesser, R.J., McCammon, J., Chen, G., Manji, H.K., 2008. Cellular mechanisms underlying the antidepressant effects of ketamine: role of alpha-amino-3-hydroxy-5-methylisoxazole-4-propionic acid receptors. *Biol. Psychiatry* 63, 349–352. <https://doi.org/10.1016/j.biopsych.2007.05.028>.
- Mayberg, H.S., Lozano, A.M., Voon, V., McNeely, H.E., Seminowicz, D., Hamani, C., Schwab, J.M., Kennedy, S.H., 2005. Deep brain stimulation for treatment-resistant depression. *Neuron* 45, 651–660. <https://doi.org/10.1016/j.neuron.2005.02.014>.
- McQuade, R., Sharp, T., 1997. Functional mapping of dorsal and median raphe 5-hydroxytryptamine pathways in forebrain of the rat using microdialysis. *J. Neurochem.* 69, 791–796. <https://doi.org/10.1046/j.1471-4159.1997.69.791.x>.
- Oliveira, J.F., Sardinha, V.M., Guerra-Gomes, S., Araque, A., Sousa, N., 2015. Do stars govern our actions? Astrocyte involvement in rodent behavior. *Trends Neurosci.* 38, 535–549. <https://doi.org/10.1016/j.tins.2015.07.006>.
- Paxinos, G., Watson, C., 2005. *The Rat Brain in Stereotaxic Coordinates*. English.
- Peng, L., Verkhatsky, A., Gu, L., Li, B., 2015. Targeting astrocytes in major depression. Targeting astrocytes in major depression. *Expert Rev. Neurother.* 15, 1299–1306. <https://doi.org/10.1586/14737175.2015.1095094>.
- Perea, G., Araque, A., 2007. Astrocytes potentiate transmitter release at single hippocampal synapses. *Science (80- )* 317, 1083–1086. <https://doi.org/10.1126/science.1144640>.
- Perea, G., Sur, M., Araque, A., 2014. Neuron-glia networks: integral gear of brain function. *Front. Cell. Neurosci.* 8, 1–8. <https://doi.org/10.3389/fnecel.2014.00378>.
- Pham, T.H., Mendez-David, I., Defaix, C., Guiard, B.P., Tritschler, L., David, D.J., Gardier, A.M., 2017. Ketamine treatment involves medial prefrontal cortex serotonin to induce a rapid antidepressant-like activity in BALB/c mice. *Neuropharmacology* 112, 198–209. <https://doi.org/10.1016/j.neuropharm.2016.05.010>.
- Pompeiano, M., Palacios, J.M., Mengod, G., 1994. Distribution of the serotonin 5-HT<sub>2</sub> receptor family mRNAs: comparison between 5-HT<sub>2A</sub> and 5-HT<sub>2C</sub> receptors. *Mol. Brain Res.* 23, 163–178. [https://doi.org/10.1016/0169-328X\(94\)90223-2](https://doi.org/10.1016/0169-328X(94)90223-2).
- Pompeiano, M., Palacios, J.M., Mengod, G., 1992. Distribution and cellular localization of mRNA coding for 5-HT<sub>1A</sub> receptor in the rat brain: correlation with receptor binding. *J. Neurosci.* 12, 440–453.
- Puig, M.V., Artigas, F., Celada, P., 2005. Modulation of the activity of pyramidal neurons in rat prefrontal cortex by raphe stimulation in vivo: involvement of serotonin and GABA. *Cereb. Cortex* 15, 1–14. <https://doi.org/10.1093/cercor/bhh104>.
- Puig, M.V., Celada, P., Diaz-Mataix, L., Artigas, F., 2003. In vivo modulation of the activity of pyramidal neurons in the rat medial prefrontal cortex by 5-HT<sub>2A</sub> receptors: relationship to thalamocortical afferents. *Cereb. Cortex* 13, 870–882. <https://doi.org/10.1093/cercor/13.8.870>.
- Rajkowska, G., Stockmeier, C.A., 2013. Astrocyte pathology in major depressive disorder: insights from human postmortem brain tissue. *Curr. Drug Targets* 14, 1225–1236. <https://doi.org/10.2174/1389450113149990156>.
- Riga, M.S., Sanchez, C., Celada, P., Artigas, F., 2016. Involvement of 5-HT<sub>3</sub> receptors in the action of vortioxetine in rat brain: focus on glutamatergic and GABAergic neurotransmission. *Neuropharmacology* 108, 73–81.
- Rothstein, J.D., Martin, L., Levey, A.I., Dykes-Hoberg, M., Jin, L., Wu, D., Nash, N., Kuncl, R.W., 1994. Localization of neuronal and glial glutamate transporters. *Neuron* 13, 713–725. [https://doi.org/10.1016/0896-6273\(94\)90038-8](https://doi.org/10.1016/0896-6273(94)90038-8).

- Rush, A.J., Trivedi, M.H., Wisniewski, S.R., Nierenberg, A.A., Stewart, J.W., Warden, D., Niederehe, G., Thase, M.E., Lavori, P.W., Lebowitz, B.D., McGrath, P.J., Rosenbaum, J.F., Sackeim, H.A., Kupfer, D.J., Luther, J., Fava, M., 2006. Acute and longer-term outcomes in depressed outpatients requiring one or several treatment steps: a STAR\*D report. *Am. J. Psychiatr.* 163, 1905–1917. <https://doi.org/10.1176/appi.ajp.163.11.1905>.
- Sanacora, G., Banas, M., 2013. From pathophysiology to novel antidepressant drugs: glial contributions to the pathology and treatment of mood disorders. *Biol. Psychiatr.* 73, 1172–1179. <https://doi.org/10.1016/j.biopsych.2013.03.032>.
- Santana, N., Bortolozzi, A., Serrats, J., Mengod, G., Artigas, F., 2004. Expression of serotonin1A and serotonin2A receptors in pyramidal and GABAergic neurons of the rat prefrontal cortex. *Cerebr. Cortex* 14, 1100–1109. <https://doi.org/10.1093/cercor/bbh070>.
- Slattery, D. a, Cryan, J.F., 2012. Using the rat forced swim test to assess antidepressant-like activity in rodents. *Nat. Protoc.* 7, 1009–1014. <https://doi.org/10.1038/nprot.2012.044>.
- Slattery, D. a, Neumann, I.D., Cryan, J.F., 2011. Transient inactivation of the infralimbic cortex induces antidepressant-like effects in the rat. *J. Psychopharmacol.* 25, 1295–1303. <https://doi.org/10.1177/0269881110368873>.
- Varga, V., Székely, A.D., Csillag, A., Sharp, T., Hajós, M., 2001. Evidence for a role of GABA interneurons in the cortical modulation of midbrain 5-hydroxytryptamine neurones. *Neuroscience* 106, 783–792. [https://doi.org/10.1016/S0306-4522\(01\)00294-9](https://doi.org/10.1016/S0306-4522(01)00294-9).
- Veerakumar, A., Challis, C., Gupta, P., Da, J., Upadhyay, A., Beck, S.G., Berton, O., 2014. Antidepressant-like effects of cortical deep brain stimulation coincide with neuroplastic adaptations of serotonin systems. *Biol. Psychiatr.* 76, 203–212. <https://doi.org/10.1016/j.biopsych.2013.12.009>.
- Vertes, R.P., 2004. Differential projections of the infralimbic and prelimbic cortex in the rat. *Synapse* 51, 32–58. <https://doi.org/10.1002/syn.10279>.
- Warden, M.R., Selimbeyoglu, A., Mirzabekov, J.J., Lo, M., Thompson, K.R., Kim, S.-Y., Adhikari, A., Tye, K.M., Frank, L.M., Deisseroth, K., 2012. A prefrontal cortex-brainstem neuronal projection that controls response to behavioural challenge. *Nature* 492, 428–432. <https://doi.org/10.1038/nature11617>.
- Zarate, C.A., Brutsche, N.E., Ibrahim, L., Franco-Chaves, J., Diazgranados, N., Cravchik, A., Selter, J., Marquardt, C.A., Liberty, V., Luckenbaugh, D.A., 2012. Replication of ketamine's antidepressant efficacy in bipolar depression: a randomized controlled add-on trial. *Biol. Psychiatr.* 71, 939–946. <https://doi.org/10.1016/j.biopsych.2011.12.010>.
- Zarate, C.A., Singh, J.B., Carlson, P.J., Brutsche, N.E., Ameli, R., Luckenbaugh, D.A., Charney, D.S., Manji, H.K., 2006. A Randomized Trial of an NMDA antagonist in treatment-resistant major depression. *Arch. Gen. Psychiatr.* 63, 856–864. <https://doi.org/10.1001/archpsyc.63.8.856>.



---

## Article 3

### **Astrocyte control of glutamatergic activity: Downstream effects on serotonergic function and emotional behavior**

N Fullana<sup>1,2,3</sup>, J Gasull-Camós<sup>1,2,3</sup>, M Tarrés-Gatius<sup>1,2,3</sup>, A Bortolozzi<sup>1,2,3</sup>,  
A Castañé<sup>1,2,3</sup> and F Artigas<sup>1,2,3</sup>

*Neuropharmacology* (invited review, submitted)

<sup>1</sup>Department of Neurochemistry and Neuropharmacology, CSIC-Institut d'Investigacions Biomèdiques de Barcelona, Barcelona, Spain

<sup>2</sup>Centro de Investigación Biomédica en Red de Salud Mental, Instituto de Salud Carlos III, Madrid, Spain

<sup>3</sup>Institut d'Investigacions Biomèdiques August Pi i Sunyer, Barcelona, Spain.

This review focuses on the pathophysiological causes of major depressive disorder (MDD), paying a special attention to three important and interrelated factors: 1) the ventral anterior cingulate cortex (vACC) hyperactivity seen in untreated and treatment-resistant MDD patients, 2) the tight control of serotonergic neurotransmission by vACC, and 3) the role of astrocytes in glutamatergic neurotransmission, mainly via astrocyte glutamate transporters. Along these lines, we also review recent studies from our group testing the working hypothesis that astrocyte-induced alterations of excitatory neurotransmission in the infralimbic cortex (IL) (rodent equivalent of vACC) may alter the activity of raphe 5-HT neurons via descending afferents from IL and evoke depressive-like or antidepressant-like effects in rodents.



Elsevier Editorial System(tm) for  
Neuropharmacology  
Manuscript Draft

Manuscript Number:

Title: Astrocyte control of glutamatergic activity: Downstream effects on serotonergic function and emotional behavior

Article Type: VSI: Serotonin Research

Keywords: antidepressant effects; astrocytes; emotional behavior; GLAST; GLT-1; infralimbic cortex

Corresponding Author: Professor Francesc Artigas,

Corresponding Author's Institution: Instituto de Investigaciones Biomedicas

First Author: Neus Fullana

Order of Authors: Neus Fullana; Júlia Gasull-Camós; Mireia Tarrés-Gatius; Analia Bortolozzi; Anna Castañé; Francesc Artigas

Abstract: Major depressive disorder (MDD) is a leading cause of disability worldwide, with a poorly known pathophysiology and sub-optimal treatment, based on serotonin (5-hydroxytryptamine, 5-HT) reuptake inhibitors. We review existing theories on MDD, paying special attention to the role played by the ventral anterior cingulate cortex (vACC) or its rodent equivalent, infralimbic cortex (IL), which tightly control the activity of brainstem monoamine neurons (including raphe 5-HT neurons) via descending afferents. Further, astrocytes regulate excitatory synapse activity via glutamate reuptake through astrocytic transporters EAAT1 and EAAT2 (GLAST and GLT-1 in rodents), and alterations of astrocyte number/function have been reported in MDD patients and suicide victims. We recently assessed the impact of reducing GLAST/GLT 1 function in IL on emotional behavior and serotonergic function in rodents. The acute pharmacological blockade of GLT-1 with dihydrokainate (DHK) in rat IL evoked an antidepressant-like effect mediated by local AMPA-R activation and a subsequent enhancement of serotonergic function. No effects were produced by DHK microinfusion in prelimbic cortex (PrL). In the second model, a moderate small interfering RNAs (siRNA)-induced reduction of GLAST and GLT-1 expression in mouse IL markedly increased local glutamatergic neurotransmission and evoked a depressive-like phenotype (reversed by citalopram and ketamine), and reduced serotonergic function and BDNF expression in cortical/hippocampal areas. As for DHK, siRNA microinfusion in PrL did not evoke behavioral/neurochemical effects. Overall, both studies support a critical role of the astrocyte-neuron communication in the control of excitatory neurotransmission in IL, and subsequently, on emotional behavior, via the downstream associated changes on serotonergic function.







Vestibular  
Subunit

Ves  
Subu

Vestibular  
Subunit